

School of Doctoral Studies in Biological Sciences
University of South Bohemia in České Budějovice, Faculty of Science

***Borrelia* – host interactions:
zoom in on the big picture**

Ph.D. Thesis

Martin Strnad, MSc.

Supervisor: Ryan O. M. Rego, Ph.D.
Co-supervisor: Marie Vancová, Ph.D.

University of South Bohemia in České Budějovice, Faculty of Science,
Czech Republic

&

Biology Centre CAS, Institute of Parasitology,
Czech Republic

České Budějovice 2021

This thesis should be cited as:

Strnad, M., 2021: *Borrelia* – host interactions: zoom in on the big picture. Ph.D. Thesis. University of South Bohemia, Faculty of Science, School of Doctoral Studies in Biological Sciences, České Budějovice, Czech Republic, 122 pp.

Annotation

The thesis was written with the intention to bring together cutting-edge imaging methods and applications in order to illustrate how imaging can answer pathogenesis-related questions in Lyme disease at various resolution scale. Correlative light and electron microscopy, atomic force microscopy-based single-molecule force spectroscopy and solution nuclear magnetic resonance have been used to shed light on the underlying mechanisms associated with Lyme disease *Borrelia* infection. Specifically, the key molecular players and interactions responsible for the variance in the pathogenicity and disease outcome of *Borrelia* species have been studied. The rationale behind such studies was highlighted by review articles, which are part of the thesis.

Declaration

I hereby declare that I am the author of this dissertation and that I have used only those sources and literature detailed in the list of references.

V Českých Budějovicích, 12. 7. 2021

.....
Martin Strnad, MSc.

This thesis originated from a partnership of Faculty of Science, University of South Bohemia, and Institute of Parasitology, Biology Centre CAS, supporting doctoral studies in the Molecular and Cell Biology and Genetics study program.



Přírodovědecká
fakulta
Faculty
of Science

Jihočeská univerzita
v Českých Budějovicích
University of South Bohemia
in České Budějovice



Parazitologický ústav,
Biologické centrum AV ČR

Institute of Parasitology
Biology Centre, AS CR

Financial support

This work was supported by the Grant Agency of the Czech Republic (17-21244S), the Technology Agency of the Czech Republic (TE01020118, TG02010034), ANTIDotE (EU-7FP; 602272-2), ANTIGONE (EU-7FP; 278976), the Grant Agency of the University of South Bohemia (04-026/2015/P), Czech Ministry of Education, Youth and Sports (8J19AT009), the MEYS CR (Czech BioImaging LM2015062 and CZ.02.1.01/0.0/0.0/16_013/0001775), and Czechoslovak Microscopy Society.

Acknowledgements

The work presented in this dissertation would not have been possible without the support and guidance of many people. Without their help, I would not have been able to put it together and finish this dissertation.

First, I would like to thank my supervisors Maruška and Ryan. They gave me plenty space for self-realization while providing me with crucial incentives, motivation and feedbacks. Many thanks go to Patti Rosa and Vivian Kjelland, who hosted me generously during my research stays in US and Norway, respectively. They allowed me to grasp new ideas, learn from their vast experience and, most importantly, meet new great friends (yes, I mean you Chad Hillman, Phil Stewart, and many others). Thank you also to Jana Nebesářová, Libor Grubhoffer, Peter Hinterdorfer, YooJin Oh, who have served as a great source of knowledge and support.

Most importantly, I would like to thank my family, my partner Lenka, and our kids Ella and Jakub. Ellčo, Jakube, although you have made my night's sleep much shorter, the income of your unlimited positive energy make it up to me more than sufficiently.

And thank you to all of you who were not mentioned above but who think they should have been.

Thank you! ☺

List of papers and author's contribution

The thesis is based on the following papers (listed chronologically and according to aims of the thesis):

AIM 1 (3 manuscripts) :

Strnad, M., Hönig, V., Růžek, D., Grubhoffer, L., Rego, R. O. M. (2017) Europe-wide meta-analysis of *Borrelia burgdorferi* sensu lato prevalence in questing *Ixodes ricinus* ticks. *Applied and Environmental Microbiology* 83: e00609-17. **IF: 4.792 (2017)**

- Martin Strnad is the corresponding author, conceived the study, searched the literature and together with Václav Hönig wrote the manuscript. Estimated student's share: 70%

Strnad, M., Grubhoffer, L., Rego, R. O. M. (2020) Novel targets and strategies to combat borreliosis. *Applied Microbiology and Biotechnology* 104: 1915-1925. **IF: 4.813 (2020)**

- Martin Strnad is the corresponding author, conceived the study, searched the literature and wrote the manuscript. Estimated student's share: 90%

Strnad, M., Rego, R. O. M. (2020) The need to unravel the twisted nature of the *Borrelia burgdorferi* sensu lato complex across Europe. *Microbiology* 166: 428–435. **IF: 2.777 (2020)**

- Martin Strnad conceived the study, searched the literature and co-wrote the manuscript. Estimated student's share: 60%

AIM 2 (4 manuscripts):

Strnad, M., Elsterová, J., Schrenková, J., Vancová, M., Rego, R. O. M., Grubhoffer, L., Nebesářová, J. (2015) Correlative cryo-fluorescence and cryo-scanning electron microscopy as a straightforward tool to study host-pathogen interactions. *Sci. Rep.* 5, 18029. **IF: 5.228 (2015)**

- Martin Strnad is the corresponding author, conceived the study, performed the experiments and wrote the manuscript. Estimated student's share: 80%

Hillman, C., Stewart, P.E., **Strnad, M.**, Stone, H., Starr, T., Carmody, A., Evans, T.J., Carracoi, V., Wachter, J., Rosa, P. (2019) Visualization of spirochetes by labeling membrane proteins with fluorescent biarsenical dyes. *Frontiers in Cellular and Infection Microbiology* 9: 287. **IF: 4.123 (2019)**

- Martin Strnad contributed to the design and conducted the FLAsH dye experiments, and revision of the manuscript. Estimated student's share: 15%

Strnad, M., Oh, Y.J., Vancová, M., Hain, L., Salo, J., Grubhoffer, L., Nebesářová, J., Hytönen, J., Hinterdorfer, P., Rego, R. O. M. (2021) Nanomechanical mechanisms of Lyme disease spirochete motility enhancement in extracellular matrix. *Communications Biology* 4: 268. **IF: 6.268 (2020)**

- Martin Strnad is the corresponding author, conceived the study, performed the experiments excluding those associated with atomic force microscopy and together with YooJin Oh wrote the manuscript. Estimated student's share: 50%

Hejduk, L., Rathner, P., **Strnad, M.**, Grubhoffer, L., Sterba, J., Rego, R. O. M., Müller, N., Rathner, A. (accepted with minor revisions) Resonance assignment and secondary structure of DbpA protein from the European species, *Borrelia afzelii*. *Biomol NMR Assign.* **IF: 0.746 (2020)**

- Martin Strnad was involved in recombinant protein preparation and revision of the manuscript. Estimated student's share: 15%

Agreement of the co-authors

I, as a corresponding/senior co-author, agree with the estimated student's share in the publication.

- **Strnad, M.**, Hönig, V., Růžek, D., Grubhoffer, L., Rego, R. O. M. (2017) Europe-wide meta-analysis of *Borrelia burgdorferi* sensu lato prevalence in questing *Ixodes ricinus* ticks. *Applied and Environmental Microbiology* 83: e00609-17
- **Strnad, M.**, Grubhoffer, L., Rego, R. O. M. (2020) Novel targets and strategies to combat borreliosis. *Applied Microbiology and Biotechnology* 104: 1915-1925.
- **Strnad, M.**, Rego, R. O. M. (2020) The need to unravel the twisted nature of the *Borrelia burgdorferi* sensu lato complex across Europe. *Microbiology* 166: 428–435.
- **Strnad, M.**, Elsterová, J., Schrenková, J., Vancová, M., Rego, R. O. M., Grubhoffer, L., Nebesářová, J. (2015) Correlative cryo-fluorescence and cryo-scanning electron microscopy as a straightforward tool to study host-pathogen interactions. *Sci. Rep.* 5, 18029.
- **Strnad, M.**, Oh, Y.J., Vancová, M., Hain, L., Salo, J., Grubhoffer, L., Nebesářová, J., Hytönen, J., Hinterdorfer, P., Rego, R. O. M. (2021) Nanomechanical mechanisms of Lyme disease spirochete motility enhancement in extracellular matrix. *Commun. Biol.* 4:268

Ryan OM Rego, Ph.D.

- Hillman, C., Stewart, P.E., **Strnad, M.**, Stone, H., Starr, T., Carmody, A., Evans, T.J., Carracoi, V., Wachter, J., Rosa, P. (2019) Visualization of spirochetes by labeling membrane proteins with fluorescent biarsenical dyes. *Frontiers in Cellular and Infection Microbiology* 9: 287.

Patricia Rosa, Ph.D.

- Hejduk, L., Rathner, P., **Strnad, M.**, Grubhoffer, L., Sterba, J., Rego, R. O. M., Müller, N., Rathner, A. (accepted with minor revisions) Resonance assignment and secondary structure of DbpA protein from the European species, *Borrelia afzelii*. *Biomol NMR Assign.*

Adriana Rathner, Ph.D.

Table of Contents

1	Aims and objectives	1
2	Introduction	2
2.1	Spirochetes: Importance of studying the diversity at all taxonomy levels	2
2.2	Complexity of <i>Borrelia burgdorferi</i> sensu lato	3
2.3	Clinical presentation of Lyme disease	4
2.4	Seeing is believing: Multiscale imaging approach for studying the adhesion mechanisms of <i>B. burgdorferi</i>	6
2.4.1	Imaging at the cellular level: Correlative light electron microscopy	10
2.5	Molecular players behind differential pathogenicity of <i>Borrelia</i> genospecies	14
2.5.1	Imaging at the molecule level: Single-molecule studies of DbpA and DbpB by atomic force microscopy	16
2.5.2	Sub-molecular imaging of DbpA by nuclear magnetic resonance	18
3	Manuscripts	21
3.1	Europe-wide meta-analysis of <i>Borrelia burgdorferi</i> sensu lato prevalence in questing <i>Ixodes ricinus</i> ticks	21
3.2	Novel targets and strategies to combat borreliosis	38
3.3	The need to unravel the twisted nature of the <i>Borrelia burgdorferi</i> sensu lato complex across Europe	50
3.4	Correlative cryo-fluorescence and cryo-scanning electron microscopy as a straightforward tool to study host-pathogen interactions	59
3.5	Visualization of spirochetes by labeling membrane proteins with fluorescent biarsenical dyes	68
3.6	Nanomechanical mechanisms of Lyme disease spirochete motility enhancement in extracellular matrix	83

3.7	Resonance assignment and secondary structure of DbpA protein from the European species, <i>Borrelia afzelii</i>	93
4	Conclusion and future perspectives	106
5	References	110
6	List of abbreviations	118
7	Curriculum vitae	119

1 Aims and objectives

AIM 1: To estimate Europe-wide patterns of Lyme disease *Borrelia* infection in ticks, highlight the need to undertake independent studies of genospecies within Europe, given their varying genetic content and pathogenic potential, and differences in clinical manifestation, and summarize the potential countermeasures and strategies against Lyme disease in general (**3 manuscripts**)

AIM 2: To delineate the underlying structure-functional mechanisms defining the delicate *Borrelia*-host interactions in order to better understand the pathogenic process at multiscale resolution using various imaging techniques (**4 manuscripts**)

2 Introduction

2.1 Spirochetes: Importance of studying the diversity at all taxonomy levels

Spirochetes are a diverse group of bacteria found in soil, in a liquid environment, as commensals in the gut of arthropods, or obligate parasites of vertebrates. Spirochetes from the genera *Leptospira*, *Treponema*, and *Borrelia* are highly invasive pathogens that pose public health problems of global dimensions. Because of its double-membrane structure, these spirochetes are often described as Gram-negative bacteria. However, this analogy is biochemically and structurally inaccurate as they share features of both Gram-positive and -negative bacteria [1,2]. *Borrelia* is unique among diderm bacteria in their abundance of surface-exposed lipoproteins that are often directly responsible for borreliac pathogenicity. *Treponema* expresses abundant lipoproteins but these molecules reside predominantly below the surface. Both *Borrelia* and *Treponema*, in contrast to *Leptospira*, lack outer membrane lipopolysaccharides [2–4].

Although the pathogenic genera of the class *Spirochaetes* are bound together by similar morphological features, many differences exist in their life cycles, environmental adaptations, size of the genome, and the diseases they cause [3–5]. *Borrelia* includes the causative agent of Lyme disease (e.g. *Borrelia burgdorferi*) and relapsing fever (e.g. *Borrelia hermsii*), whereas the related spirochete *Treponema* causes the sexually transmitted syphilis (*Treponema pallidum*) or periodontal disease (*Treponema denticola*). *Borrelia* species are transmitted to humans by ticks and lice. For *Treponema* it is usually directly from human to human by contact with skin lesions, body fluids, and secretions. *Leptospira* causes leptospirosis (*Leptospira interrogans*), which is a blood infection transmitted by

animals. It is spread mainly by contact with water or soil contaminated by the urine of infected animals, especially from dogs, rodents, and farm animals [6].

Lyme disease (LD) (or Lyme borreliosis) is a disease of humans caused by tick-transmitted bacteria belonging to the *Borrelia burgdorferi* sensu lato (s.l.) species complex. The bacteria are maintained in natural transmission cycles between their vertebrate reservoir hosts and vector ticks of the genus *Ixodes* [7]. Due to the intensive research that has been carried out over the past years, we now know that the substantial heterogeneity is not only between the genera of spirochetes, but a great amount of diversity stems between the LD *Borrelia* species as well.

2.2 Complexity of *Borrelia burgdorferi* sensu lato

B. burgdorferi s.l. complex is a diverse group of worldwide distributed bacteria. The complex includes more than 20 genospecies known to vary in their geographical distribution, host associations, and human pathogenicity [8]. At least 9 genospecies are commonly found in Europe (Table 1), whose geographic distribution and prevalence in ticks vary greatly across the Old Continent. We systematically reviewed the literature and collected the data from the epidemiological studies of *Ixodes ricinus* ticks infected with *B. burgdorferi* s.l. in Europe to evaluate the overall rate of infection of *I. ricinus* and regional distributions within Europe [9] (**Manuscript 1**).

B. burgdorferi sensu stricto (s.s.) is the primary cause of the disease in the United States. All three traditional pathogenic species, *B. burgdorferi* s.s., *Borrelia afzelii*, and *Borrelia garinii*, occur in Europe. Other species that have been found in humans include *B. mayonii*, *B. spielmanii*, *B. bavariensis*, *B. bissettii*, *B. lusitaniae*, and *B. valaisiana*. Although a number of wild vertebrates can act as hosts for the *B. burgdorferi* s.l.,

most *B. burgdorferi* s.l. species can utilize only a subset of hosts to support their life cycle. As an example, mammals are recognized as reservoir hosts of *B. burgdorferi* s.s. and *B.afzelii*, birds of *B. garinii* and *B. valaisiana*, and lizards of *B. lusitaniae* [10].

Table 1. The *Borrelia burgdorferi* sensu lato species present in Europe.

Genospecies	Reservoir host	Human pathogenicity	Clinical manifestation
<i>B. afzelii</i>	Mammals	Yes	Skin lesion, ACA
<i>B. bavariensis</i>	Mammals	Yes	Lyme oligoarthritis, neuroborreliosis
<i>B. bissetii</i>	Mammals	Probably yes [11]	Endocarditis and aortic valve stenosis
<i>B. burgdorferi</i> s.s.	Mammals, birds	Yes	Lyme arthritis
<i>B. garinii</i>	Birds	Yes	Neuroborreliosis
<i>B. lusitaniae</i>	Lizards	Potentially [12]	Mostly unknown, chronic skin lesion
<i>B. spielmanii</i>	Mammals	Yes	Skin lesion
<i>B. turdi</i>	Birds	Unknown	Unknown
<i>B. valaisiana</i>	Birds	Probably no [13]	Unknown

2.3 Clinical presentation of Lyme disease

LD is generally divided into three partially overlapping stages (early localized, early disseminated, and late disseminated), reflecting the duration of the infection and the severity of the disease [14]. This disease usually begins with an expanding skin lesion at the site of the tick-bite, erythema migrans, which is often accompanied by nonspecific flu-like

symptoms, such as headache, fatigue, and muscle-aches. Depending on the disease manifestation at the early stage, the infection can usually be treated successfully with 2–4 weeks of oral antibiotic therapy. If not treated properly or undetected, this infection can disseminate to the nervous system, heart, and joints, but the hallmark clinical manifestation of late LD is acrodermatitis chronica atrophicans (ACA) [15]. Despite numerous efforts, a vaccine for human use is not currently available. A review of new promising vaccine candidates and strategies that are targeted against LD was summarized in **Manuscript 2**.

Different species of Lyme borrelia have propensities to cause different clinical manifestations [16]. In the United States, *B. burgdorferi* s.s. is the most dominant agent of LD, with Lyme arthritis as the main clinical presentation. In Europe, the most common cause of the disease is *B. afzelii*, which usually remains localized to the skin tissue. The next one in Europe is *B. garinii*, which is usually associated with a disorder of the central nervous system [14]. *B. burgdorferi* s.s. infections are quite rare in Europe and not much is known about the clinical course. For all three species, the first sign of infection is often erythema migrans. *B. burgdorferi* s.s. infection in the United States is frequently associated with a greater number of clinical signs and hematogenous dissemination than *B. afzelii* or *B. garinii* infection in Europe [17]. However, despite numerous attempts, the various manifestations of LD cannot be conclusively attributed to infections with one specific genospecies.

Apart from these clear-cut manifestations, patients occasionally suffer from non-characteristic persistent complaints of unknown cause such as myalgia, fatigue, musculoskeletal pain, and cognitive complaints. This condition is termed Post-Treatment Lyme Disease Syndrome (PTLDS) and it is often long-lasting, disabling, and debilitating. Notably, there is more than one PTLDS, each with a distinct pathogenesis caused by maladaptive host

responses [18]. Consequently, it is often difficult to determine whether the patients still have active infection or any postinfectious syndrome. It is already known that different genospecies of *B. burgdorferi* are associated with distinct clinical manifestations of LD [16] and that different genospecies and different members within a genospecies differ in their propensity to cause erythema migrans [19] but no data are available about PTLDS and *Borrelia* genospecies association.

2.4 Seeing is believing: Multiscale imaging approach for studying the adhesion mechanisms of *B. burgdorferi*

Imaging techniques include a palette of options one might exploit, spanning from whole animal imaging (bioluminescent imaging [20]) to techniques able to reach subatomic resolution (X-ray crystallography, NMR) (Fig. 1). The methodologies are highly varied, so is the scale of the resulting data that are gained. Whole animal imaging allows visualization of *B. burgdorferi* infection in an entire animal. The important advantage of whole animal imaging is the ability to follow the infection of *Borrelia* in a living animal over time and observe the dissemination patterns by non-invasive means in a physiologically relevant environment [20]. Another technique used to study *Borrelia* pathogenesis including dissemination and colonization of the host is intravital microscopy [21]. Intravital imaging allows the direct visualization of a pathogen in a living host at specific locations in real-time. In contrast to whole animal imaging which uses bioluminescent spirochetes, an important advantage of this methodology is being able to discriminate between the pathogen and the tissues of the infected animal. This is typically accomplished by fluorescent labeling of the pathogen, preferably by expression of a fluorescent fusion protein such as GFP. Using intravital microscopy, the details of LD *Borrelia* - endothelial interactions and vascular transmigration were disclosed by Moriarty et al. [21]. This work shows that the bacterium engages in multi-

stage interactions with the endothelial cells, including transient tethering and dragging interactions, and stationary adhesion to the vasculature.

For many years, the conventional diffraction-limited light (optical) microscopy (LM) has been the prime tool to study and image the structural components of *Borrelia* and follow their virulence mechanisms in contact with host cells or tissues. The primary and by far the most important limitation is the resolution power of the optical microscopes. These microscopes utilize visible light and an arrangement of glass lenses to magnify a field of view. The magnitude of diffraction and the resolving power of an optical microscope depends on the light wavelength and the numerical aperture of the objective lens. For the microscopes using light sources within the range of visible optical wavelength, their spatial resolution is limited to about 0.2 μm . Fluorescence microscopy (FM) is a special form of light microscopy that exploits the ability of fluorochromes to emit light after being excited with light of a certain wavelength. This provides significantly greater contrast compared with brightfield microscopy alone and allows to simultaneously detect multiple color-labeled molecules of interest. Super-resolution microscopy techniques bypass the diffraction limit imposed by the diffraction of light and the typically achieved spatial resolutions are tens of nanometers [22].

Electron microscopy (EM) is an imaging technique widely used in the characterization of fine structural details, as the electron wavelength is orders of magnitude lower than that of photons. This allows one to achieve much better sub-nanometer resolution as EM uses a beam of electrons focused onto the surface of the sample by various electromagnetic lenses. This technique is not able to study live specimens as the samples must be analyzed in a vacuum. Environmental modes with limited resolution are available but not commonly employed. The spatial resolution

of environmental SEM is limited by the scattering experienced by the electrons as they collide with gas molecules and vapours present in the specimen chamber [23]. EM produces low-contrast images and labeling multiple structures in one sample is problematic. However, when combined with FM techniques, new technology, termed correlative light electron microscopy (CLEM), holds the promise of giving much deeper understanding of the host-pathogen interplay [24].

CLEM combines the advantages of possible live-cell imaging, allowing highest temporal analysis, with the nanometric resolution of EM. While LM might provide insights in dynamic cellular processes, ultrastructural analysis by EM can be performed at a selected time point. CLEM enables to benefit from the labeling power of FM allowing scientists to spot cellular structures and processes of interest in whole cell images. FM is unable to visualize the unlabeled cellular context, however, this deficit is compensated by transmission electron microscopy (TEM) or scanning electron microscopy (SEM). Specifically, analyses of dynamic adhesion and invasion of host cells by pathogens can benefit from combining FM with EM. The examination of the object of interest provided by CLEM offers important complementary and unique information [25]. The primary challenge of CLEM is the relocation of the region of interest in the electron microscope previously identified by LM.

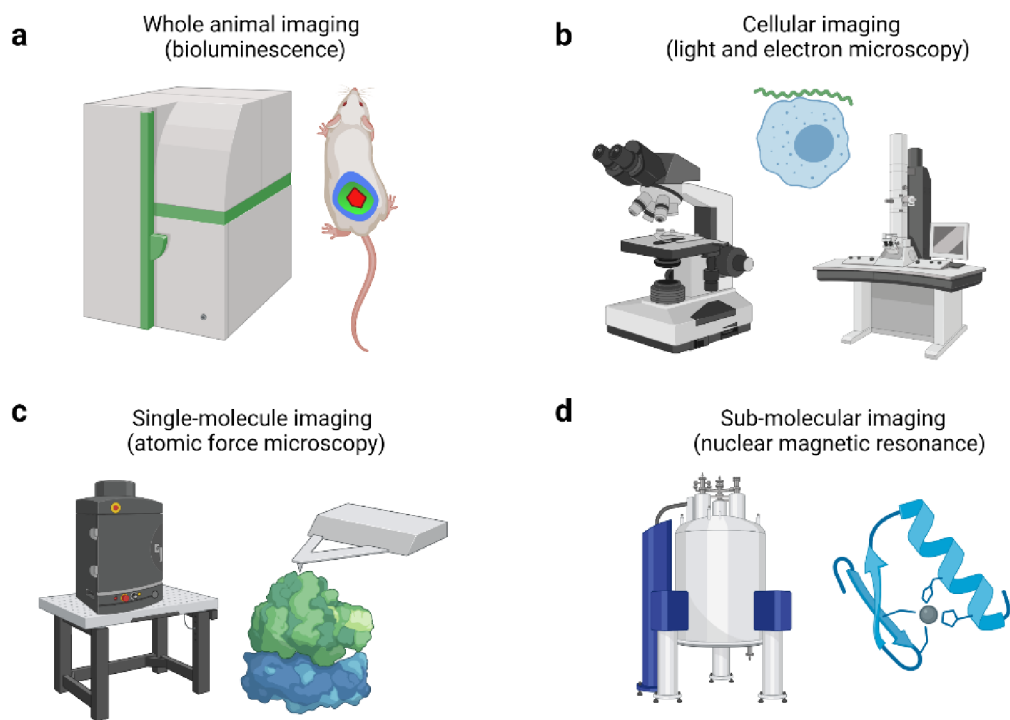


Figure 1. The dynamic nature of life starts at the subatomic level and ends at the organismal level. The rapid development of imaging technologies has revolutionised our ability to visualize the delicate intricacies of host-pathogen interactions at very different scales. Bioluminescent imaging enables to follow the infection of *Borrelia* in a living animal over time (a). Light and electron microscopy are used to provide a cellular-level understanding of borreliac infection mechanisms (e.g. adhesion) (b). Atomic force microscopy-based techniques enable to study the protein-protein interactions at the single-molecule level (c) and nuclear magnetic resonance-based techniques can determine the location of the binding site with amino acid precision (d). In the thesis, the modalities depicted in (b - d) were used to study the adhesion mechanisms of *B. burgdorferi*.

2.4.1 Imaging at the cellular level: Correlative light electron microscopy

One of the questions within the *Borrelia* community, that is still a matter of debate, is whether *B. burgdorferi* is an obligate extracellular pathogen, or if the spirochete is capable of living, and possibly reproducing, inside the host cells, when the conditions outside the cells are not favorable (for instance due to presence of strong immunity or antibiotics). Although *Borrelia* is considered extracellular, a number of studies reported the intracellular localization of the bacteria inside non-phagocytic cells, especially fibroblasts [26–28]. The studies exploring the intricacies of *B. burgdorferi* internalization by mammalian cells *in vitro* have utilized either immunofluorescence microscopy [26,29] or solely TEM without specific labeling [30] for determining the extracellular or intracellular location of the spirochetes. Immunofluorescence techniques might be sometimes misleading since the relative mutual positioning of a cell and a pathogen is hard to be reliably discerned without ultrastructural information. On the other hand, to scan through large sample areas using EM can take many hours due to borrelial size. One can see many structures or artifacts that can resemble *Borrelia* by their shape and without specific labeling these structures can be falsely identified. So that no ambiguity can arise, it is fundamental to use the correlative approach.

In **Manuscript 4**, we have established a novel correlative cryo-fluorescence microscopy and cryo-scanning electron microscopy workflow, which enables imaging of the studied object of interest very close to its natural state, devoid of artifacts caused for instance by slow chemical fixation, dehydration, and drying. Using this system, the interaction of *B. burgdorferi* with two mammalian cell lines of neural origin was investigated in order to broaden our knowledge about the cell-association mechanisms and the possible invasion of the non-phagocytic

host cells. We have shown that *B. burgdorferi* associates with mammalian non-phagocytic cells, but is not able to invade them within three hours of co-incubation. If *Borrelia* has an intracellular niche in some of the non-phagocytic host cells, as suggested by the aforementioned studies, the neuroblastoma cells apparently do not belong among them. The method appears to be an unprecedentedly fast (<3 hours), straightforward and reliable solution to study the fine details of pathogen-host cell interactions and provides important insights into the complex and dynamic relationship between a pathogen and a host.

CLEM is especially convenient for visualization of rare events, which cannot be tracked down by EM on its own. The main trick with CLEM is to label the object of interest in a manner suitable for detection by both FM and EM. In **Manuscript 4**, we used GFP-tagged *B. burgdorferi* for the experiments. As the goal was to localize whole bacterial cells, no special probes for CLEM were needed. The location of the object of interest (borrelia) was enabled by the coordination system that was created on the sapphire discs (Fig. 2) on which the mammalian cells were grown. TEM finder grids were placed on the sapphire discs and carbon-coated to facilitate the retrieval of the previously visualized cell-borrelia interactions. Carbon coating also prevents the charging of the specimen during observation in the SEM.

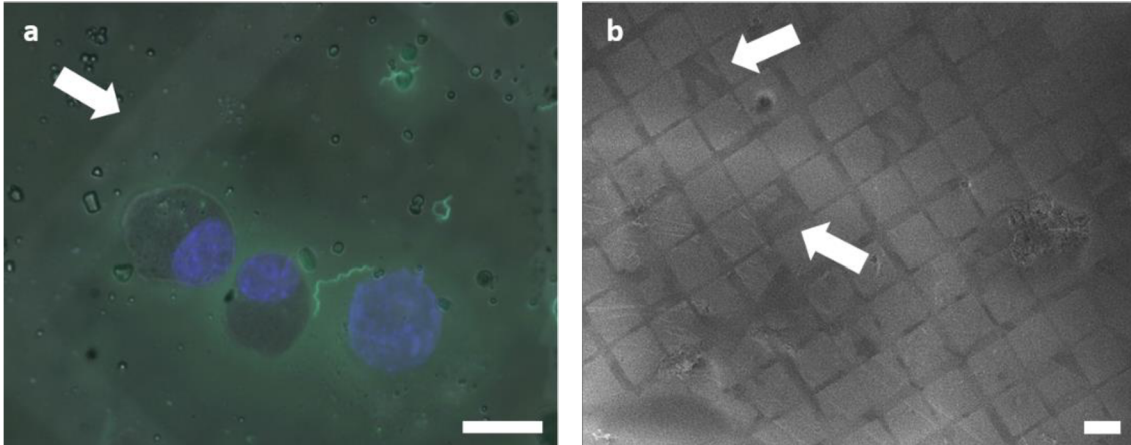


Figure 2. TEM finder grid pattern was created on the sapphire discs to facilitate the retrieval of the cell-borrelia interactions previously visualized by FM. The arrows point to the graphical landmarks in the FM (a) and SEM images (b). Scale bar: 25 μm (a), 100 μm (b).

Very often, however, scientists need to locate objects that are much smaller than cells. Proteins are commonly the favourite targets of microscopy studies as they perform a vast array of functions within organisms. GFP-tagging is arguably one of the most common strategies for protein labeling and definitely the most used genetically-encoded fluorescent protein. Genetically-encoded fluorescent proteins are popular fluorescent probes for CLEM, especially when imaging live cells. However, the use of fluorescent protein fusions, such as GFP or RFP (red fluorescent protein), has limitations: the bulkiness of these proteins, typically around 30 kDa, can lead to atypical protein localization and irregular cellular trafficking. Additionally, these tags are not electron-dense and their fluorescence is usually quenched by osmium tetroxide postfixation and embedding methods [31]. To overcome this issue, scientists have developed a technique that involves the photo-conversion of a molecule called diaminobenzidine (DAB) by a reaction cascade triggered by the fluorescence emitted by a fluorophore such as GFP. When oxidized, DAB forms a highly insoluble product that can be made electron-dense through treatment with osmium tetroxide and the resulting precipitate can act as an EM probe. GFP was one of the first fusion proteins to be used for CLEM

[32]. While GFP is extremely bright and photostable, it is a very poor producer of reactive singlet oxygen species, necessary for DAB polymerization [33]. GFP has been occasionally used as a CLEM tag where there is high expression of GFP-tagged proteins [34].

As GFP does not seem to be the ultimate solution for CLEM, researchers have been searching and developing new ways to use LM probes to produce EM probes. The first and arguably the most successfully applied genetically encoded technology involving a small molecule label is the tetracysteine tag technology [35]. It was also the first genetically encoded system for CLEM using photo-oxidation [25]. This technique is based on the binding of a small fluorescein dye, called fluorescein arsenical hairpin binder (FAsH), to a tetracysteine motif of 6 amino acids; Cys-Cys-X-X-Cys-Cys (X denotes any amino acid). FAsH is a small, membrane-permeable fluorescent molecule, which is used as a nonfluorescent complex with ethanedithiol. It becomes fluorescent upon binding to the tetracysteine motif. In addition to FAsH, which emits green fluorescence, a set of color variants with enhanced photostability has been reported [36]. The most extensively used alternative is the red light emitting analog ReAsH (resorufin arsenical hairpin binder). Similarly to GFP, neither of these two probes are visible with EM. However, the biarsenical dyes can photo-convert DAB to form an osmiophilic precipitate distinguishable by EM. These dyes, especially ReAsH, provide about 6 times higher singlet oxygen quantum yield than GFP [33]. Importantly, the small increase in protein size conferred by the tetracysteine motif minimizes potential negative effects that may occur when targets are fused to larger fluorogenic proteins (e.g. GFP or RFP), such as steric hindrance, causing improper protein folding, trafficking to the incorrect cellular location, or inappropriate oligomerization. In particular, infectivity of the pathogens is maintained even when the tetracysteine tags are inserted into internal protein positions [37].

In **Manuscript 5**, we have adapted FIAsh/ReAsH dye for live-cell imaging of *Borrelia* and *Leptospira*, by tagging their inner or outer membrane proteins with tetracysteine motifs. We have shown by using infectious *Borrelia* that the tetracysteine motif was stably maintained *in vivo* and did not adversely affect infectivity in either the arthropod vector or murine host. The biarsenical-bound proteins could be followed over several days, indicating that this approach can be used in time-course studies. Using this method, new avenues of investigation into spirochete morphology, motility, and pathogenic mechanisms, previously inaccessible with large fluorescent proteins, can now be explored. Although the complete CLEM procedure was not performed in Manuscript 5 (based on the scope of the study), the successful adaptation of the tetracysteine motif/ReAsH technology in *Borrelia* now paves the way for future implementation of CLEM into the spirochete research [38].

2.5 Molecular players behind differential pathogenicity of *Borrelia* genospecies

The phenomenon of differential pathogenicity and tissue tropism between and within different *Borrelia* genospecies has stimulated the scientific community to study the molecular basis of this matter. The first studies worked with and confirmed the original assumption that the tissue tropism and invasiveness are affected primarily by the borrelial outer surface proteins and their heterogeneity [39,40]. Specifically, it was determined that decorin binding protein A (DbpA) mediates colonization, tissue tropism, and disease by the LD spirochete in an allele-dependent manner and contributes to the etiology of distinct clinical manifestations associated with different LD species and strains. This variance is apparently based on the different binding activity towards extracellular matrix (ECM) components among the *Borrelia* genospecies. Salo and colleagues [41]

found differences in the decorin binding activity among the three main pathogenic genospecies. Significant binding differences of DbpA to the proteoglycan decorin and to the glycosaminoglycan (GAG) dermatan sulfate were also shown at the *Borrelia* strain level [42]. DbpA sequence is highly polymorphic, with amino acid sequence identities as low as 38% between variants (Table 2).

	<i>B. valaisiana</i>	<i>B. turdi</i>	<i>B. spielmanii</i>	<i>B. mayonii</i>	<i>B. garinii</i>	<i>B. burgdorferi</i>	<i>B. bissettii</i>	<i>B. bavariensis</i>	<i>B. afzelii</i>
<i>B. valaisiana</i>		53.49%	59.04%	48.62%	48.26%	46.86%	42.31%	52.30%	56.21%
<i>B. turdi</i>	53.49%		48.24%	55.98%	69.19%	56.77%	55.28%	41.67%	46.55%
<i>B. spielmanii</i>	59.04%	48.24%		43.82%	45.29%	45.35%	40.22%	54.71%	54.49%
<i>B. mayonii</i>	48.62%	55.98%	43.82%		53.26%	66.85%	58.51%	43.09%	44.81%
<i>B. garinii</i>	48.26%	69.19%	45.29%	53.26%		53.44%	50.51%	43.89%	46.55%
<i>B. burgdorferi</i>	46.86%	56.77%	45.35%	66.85%	53.44%		65.66%	43.96%	41.81%
<i>B. bissettii</i>	42.31%	55.28%	40.22%	58.51%	50.51%	65.66%		39.68%	38.25%
<i>B. bavariensis</i>	52.30%	41.67%	54.71%	43.09%	43.89%	43.96%	39.68%		50.28%
<i>B. afzelii</i>	56.21%	46.55%	54.49%	44.81%	46.55%	41.81%	38.25%	50.28%	

Table 2. High heterogeneity (given as amino acid's % identity) of DbpA among the species (strains: *B. valaisiana* VS116, *B. spielmanii* A14S, *B. garinii* PBr, *B. burgdorferi* B31, *B. bissettii* DN127, *B. bavariensis* PBi, *B. afzelii* A91).

Given the very high variance in *dbpA*, it is apparent that the various *B. burgdorferi* s.l. species use different molecular mechanisms for their interaction with the host. The presence of decorin binding proteins is a crucial factor for the pathogenic strategy of dissemination LD *Borrelia*, enabling the bacteria to colonize various tissues and organs [43]. Decorin binding proteins A and B (DbpA and DbpB) are encoded by a bicistronic operon, which is located on the plasmid lp54. Although not absolutely essential for infection, the important role of these adhesins for the overall virulence of *B. burgdorferi* was demonstrated in a number of studies [44–48]. DbpA and DbpB mutants show significant attenuation in mice, particularly early in infection [49,50], or have significant attenuations in virulence as measured by bacterial loads in disseminated sites [39,51]. Disruption of *dbpA* and *dbpB* decrease recovery of spirochetes from tissues distant to the inoculation site [48,50]. Decorin deficient mice showed colonization defects by *B. burgdorferi* in heart, bladder, and joint [52]. The common denominator of all these defects in the context of infection is

delayed dissemination and colonization particularly of distal tissues. Up to now, the reason for this remains largely obscure as it was differently attributed to the effects of acquired immunity [49], innate immunity [50], or to the inability to adhere properly to host ECM components [50]. In **Manuscript 6**, we have shown that not only the stationary binding (anchoring) interactions are mediated by DbpA and DbpB but these surface adhesins are directly associated with borrelial translational motion and propagation within the host. By designing an in-vitro motility assay that mimics the environmental signals in the host, we observed movement-enhancing effects of DbpA/B in an ECM-like gel [53].

2.5.1 Imaging at the molecule level: Single-molecule studies of DbpA and DbpB by atomic force microscopy

Whole animal imaging and light (intravital) microscopy have been successfully used to study dissemination and movement of *Borrelia* within the host, and underscore the power of imaging to provide insights into a wide variety of virulence mechanisms [20,21]. However, the underlying molecular mechanisms driving the borrelial pathogenesis and dissemination lie much deeper, hidden in the nanoworld of single-molecule interactions. Single-molecule force spectroscopy using the atomic force microscope (AFM-SMFS) is a technique that provides molecular level insights into protein functions, allowing researchers to understand the functional mechanisms in biology. AFM-SMFS directly probes structural changes of macromolecules under the influence of mechanical force and it is well-suited to explore the specialized surface-exposed molecules of bacterial pathogens that bind to ligands on host tissues [54]. Since mechanical forces are ubiquitous in biological systems, and especially extensive during borrelial dissemination periods, data obtained from AFM-SMFS experiments may provide important information about the molecular players and forces that govern the host infection [55].

Single-molecule techniques overcome the averaging effects inherent in ensemble measurements and enable characterization of the enormous heterogeneity that exists in biomolecular systems, complementing the information that is impossible to observe using traditional bulk ensemble methods. In single-molecule studies, molecular properties are measured one molecule at a time. Hence, in contrast with conventional ensemble experiments, distributions in molecular properties are more directly measured and distributions of folding states can be directly observed. In addition, rare states can be discovered in single-molecule experiments, which would be averaged in an ensemble measurement [56]. Single-molecule imaging can also provide new insights on weak transient biomolecular interactions with micromolar to millimolar affinity that usually remains hidden in ensemble-averaged measurements. Interestingly, some adhesins of bacterial pathogens are adapted for strong mechanical attachment to their target, rather than high affinity [54].

In **Manuscript 6**, we have shown that DbpA and DbpB, the borrelial surface adhesins, which are known to contribute to tissue tropism of different Lyme disease spirochete species, are directly associated with borrelial motility and propagation within the host-associated structures. As atomic force microscopy (AFM) makes it possible to force probe single adhesins, we took the opportunity to exploit AFM-SMFS in order to disentangle the mechanistic details of DbpA/B and decorin/laminin interactions at the single-molecule level. Our results show that spirochetes are able to leverage a wide variety of adhesion strategies to adopt distinct motility states and transition between them. *Borrelia* makes it through force-tuning transient molecular binding to ECM components, which concertedly enhance spirochetal dissemination through the host [53]. The data presented in Manuscript 6 were obtained from measurements on DbpA and DbpB from the most common European species *B. afzelii*. As

mentioned before, our ultimate goal was to provide a comprehensive picture of the variations of structural features and ensuing binding modes in Dbps interactions. AFM-SMFS measurements of DbpA, DbpB, and also other borrelial adhesins (BBK32) from European pathogenic species, *B. garinii* and *B. bavariensis*, are currently in progress/being analysed.

2.5.2 Sub-molecular imaging of DbpA by nuclear magnetic resonance

AFM-SMFS experiments have enabled us to study the binding interactions at the resolution of single macromolecules. However, there is still space to go deeper in our understanding. Proteins fold up into specific shapes according to the sequence of amino acid residues in the polymer, and the protein function is directly related to the resulting 3D structure. Characterization of the backbone structure and dynamics of individual protein motifs is crucial for proper understanding of the key interactions at sub-molecular level. It allows to examine the importance of individual amino acid residues in proteins. Nuclear magnetic resonance (NMR) is an essential tool for biologists and chemists in determining structure-function relationships in biomolecules and it is the only method that provides detailed 3D data at angstrom resolution of molecules both in solution and in noncrystalline solids. Recently, substantial advances in NMR have pushed the boundaries of molecular structure determination, including application of NMR to larger and larger molecules. Its high sensitivity to molecular structure is due to the ability to monitor interactions between single atoms. In addition to structural information, dynamic information can also be obtained through NMR. Time scales of both fast (picoseconds) and slow (seconds) processes can be followed [57]. Of the available NMR techniques, NMR titration analysis, such as chemical shift perturbation (CSP), is a powerful strategy used to identify substrate-binding sites of proteins at amino acid residue resolution [58]. CSP enables comprehensive analysis of interaction sites on the proposed structure of a protein without

crucial conformational change. This approach has been used previously for the analysis of Dbps from N. American strains and various GAGs molecules, including the interaction site and binding specificity [59].

With one exception, Dbps have been structurally-functionally characterized only in North American strains at the amino acid resolution scale [59,60]. The main differences in their tertiary structures have been found near the GAG-binding pocket, in the highly dynamic "linker region", indicating that the global structures and the ensuing dynamics are determining factors for the selective interaction with ligands resulting in various colonization patterns of these bacterial strains. Three structures of DbpA and DbpB proteins from different *Borrelia* strains have been solved previously by solution NMR [59–61], including DbpA from *B. burgdorferi* strain N40 and B31 and from the *B. garinii* strain PBr. In spite of a similar overall fold (5 helices with unstructured C-terminus), there are significant deviations, mainly between DbpA from European *B. garinii* PBr and North American *B. burgdorferi* N40/B31. In PBr-DbpA, the flexible linker between helices 1 and 2 is less disordered. It retracts from the binding pocket increasing the affinity of this strain's DbpA towards GAG ligands. The sequence variations between the Dbps of different *Borrelia* strains are relatively high. Even though their secondary structures are widely homologous, the atomic-level details of the DbpA/DbpB-GAG interactions differ between borreliac species/strains [60].

In **Manuscript 6**, we have measured in-detail the interaction landscape between DbpA and DbpB with two common ECM components (decorin and laminin) that are known to be important ligands for *Borrelia* during host colonization. Decorin and laminin are glycoproteins, which consist of a core protein and one or more covalently linked GAG chains [62]. GAGs are long-repeating disaccharides that can be divided into different classes, such as chondroitin sulfate, dermatan sulfate and heparan sulfate,

depending upon the sugar composition [62]. Several lines of evidence have indicated that, not the core protein, but GAG side chains are the primary points of contact that mediate the interaction between ECM glycoproteins and borrelial virulence-associated proteins such as Dbps, OspC, and BBK32 [40,63].

To shed even more light into the structure-function relationships in borrelia-host interactions and to probe the etiology of distinct clinical manifestations associated with different LD species (it has been documented that *Borrelia* species vary in GAGs recognition [64]), we have recently characterized DbpA from the most common European species *B. afzelii* by solution NMR (**Manuscript 7**). Backbone and side chain resonance assignments were performed as they provide a crucial starting point for the comparative studies of interactions between DbpA variants and various ECM components. Secondary structure estimates provide important first insight into structural differences among DbpA homologues and bring us closer to creation of 3D structural models that will enable to understand the differential structure-activity relationships of Dbps-GAGs interactions. Establishing an amino acid residue-level model of the structure and dynamics of the GAG-Dbps complexes based on experimental data is a requirement to apprehend the molecular mechanisms involved in the borrelial pathogenesis. As our ultimate goal is to provide a comprehensive picture of the variations of structural features and ensuing binding modes in Dbps-ligand interactions, works on other European pathogenic species *B. garinii* and *B. bavariensis* are currently ongoing.

3 Manuscripts

3.1 Manuscript 1:

Strnad, M., Hönig, V., Růžek, D., Grubhoffer, L., Rego, R. O. M. (2017) Europe-wide meta-analysis of *Borrelia burgdorferi* sensu lato prevalence in questing *Ixodes ricinus* ticks. *Applied and Environmental Microbiology* 83: e00609-17.

Annotation

Lyme disease, caused by the bacterium *Borrelia burgdorferi*, is the most common zoonotic disease transmitted by ticks in Europe and North America. Although *Borrelia* prevalence is considered an important predictor of infection risk and national/regional prevalence studies are performed frequently, solitary isolated data have only limited value. In this study, the primary focus was to evaluate the infection rate of Lyme disease *Borrelia* in ticks, accounting for tick stage, adult tick gender, region and detection method, as well as to investigate any changes in prevalence over time in European region. We have evaluated the spatio-temporal trends in the prevalence of *B. burgdorferi* sensu lato and its different genospecies. As no such meta-analysis discerning the Europe-wide tick prevalence patterns has been done in the 21st century, this study serves as a topical source of data for public health surveillance.



Europe-Wide Meta-Analysis of *Borrelia burgdorferi Sensu Lato* Prevalence in Questing *Ixodes ricinus* Ticks

Martin Strnad,^{a,b} Václav Hönig,^{a,c} Daniel Růžek,^{a,c} Libor Grubhoffer,^{a,b} Ryan O. M. Rego^{a,b}

Institute of Parasitology, Biology Centre of the Czech Academy of Sciences, České Budějovice, Czech Republic; Faculty of Science, University of South Bohemia in České Budějovice, České Budějovice, Czech Republic; Department of Virology, Veterinary Research Institute, Brno, Czech Republic

ABSTRACT Lyme borreliosis is the most common zoonotic disease transmitted by ticks in Europe and North America. Despite having multiple tick vectors, the causative agent, *Borrelia burgdorferi sensu lato*, is vectored mainly by *Ixodes ricinus* in Europe. In the present study, we aimed to review and summarize the existing data published from 2010 to 2016 concerning the prevalence of *B. burgdorferi sensu lato* spirochetes in questing *I. ricinus* ticks. The primary focus was to evaluate the infection rate of these bacteria in ticks, accounting for tick stage, adult tick gender, region, and detection method, as well as to investigate any changes in prevalence over time. The data obtained were compared to the findings of a previous metastudy. The literature search identified data from 23 countries, with 115,028 ticks, in total, inspected for infection with *B. burgdorferi sensu lato*. We showed that the infection rate was significantly higher in adults than in nymphs and in females than in males. We found significant differences between European regions, with the highest infection rates in Central Europe. The most common genospecies were *B. afzelii* and *B. garinii*, despite a negative correlation of their prevalence rates. No statistically significant differences were found among the prevalence rates determined by conventional PCR, nested PCR, and real-time PCR.

IMPORTANCE *Borrelia burgdorferi sensu lato* is a pathogenic bacterium whose clinical manifestations are associated with Lyme borreliosis. This vector-borne disease is a major public health concern in Europe and North America and may lead to severe arthritic, cardiovascular, and neurological complications if left untreated. Although pathogen prevalence is considered an important predictor of infection risk, solitary isolated data have only limited value. Here we provide summarized information about the prevalence of *B. burgdorferi sensu lato* spirochetes among host-seeking *Ixodes ricinus* ticks, the principal tick vector of borreliae in Europe. We compare the new results with previously published data in order to evaluate any changing trends in tick infection.

KEYWORDS *Borrelia burgdorferi sensu lato*, tick, *Ixodes ricinus*, genospecies, meta-analysis, Lyme borreliosis, Lyme disease

The *Borrelia burgdorferi sensu lato* group includes the causative agents of Lyme borreliosis (LB), the most prevalent human tick-borne disease in the Northern Hemisphere (1). The bacterium is maintained in a horizontal transmission cycle between its vector, ticks of the genus *Ixodes*, and vertebrate reservoir host species. In Europe, there are a number of different *B. burgdorferi sensu lato* genospecies, many of them directly associated with human LB. The disease is caused predominantly by *Borrelia burgdorferi sensu stricto*, *B. afzelii*, *B. garinii*, and *B. bavariensis* (previously known as *B. garinii* OspA serotype 4) (2). In addition, four other genospecies are occasionally

Received 15 March 2017 Accepted 16 May 2017

Accepted manuscript posted online 26 May 2017

Citation Strnad M, Hönig V, Růžek D, Grubhoffer L, Rego ROM. 2017. Europe-wide meta-analysis of *Borrelia burgdorferi sensu lato* prevalence in questing *Ixodes ricinus* ticks. Appl Environ Microbiol 83:e00609-17. <https://doi.org/10.1128/AEM.00609-17>.

Editor Eric V. Stabb, University of Georgia

Copyright © 2017 American Society for Microbiology. All Rights Reserved.

Address correspondence to Martin Strnad, martin.strnad.cze@gmail.com.

M.S. and V.H. contributed equally to this article.

detected in humans: *B. bissettae* (3, 4), *B. lusitaniae* (5, 6), *B. spielmanii* (7), and *B. valaisiana* (8); however, their pathogenicity is still unclear (9).

The principal tick vector for *Borrelia* species in Europe is the castor bean tick, *Ixodes ricinus*. To date, *B. burgdorferi sensu stricto*, *B. afzelii*, *B. garinii*, *B. valaisiana*, *B. lusitaniae*, *B. spielmanii*, *B. bavariensis*, *B. bissettae*, *B. finlandensis*, and *B. carolinensis* have been detected in *I. ricinus* ticks (10, 11). Different genospecies display different patterns of host specialization and tissue tropism and are associated with overlapping but distinct spectra of clinical manifestations: *B. burgdorferi sensu stricto* is most often associated with arthritis and neuroborreliosis, *B. garinii* with neuroborreliosis, and *B. afzelii* with chronic skin conditions such as acrodermatitis chronica atrophicans (12). Apart from spirochetes associated with LB, *I. ricinus* is well recognized as a vector of many other pathogens of veterinary and human medical importance, particularly tick-borne encephalitis virus (TBEV), *Babesia* spp., spotted fever group rickettsiae, *Anaplasma phagocytophilum*, and *Bartonella* spp. (13).

A number of field studies have already pointed to increases in average densities and activities of questing ticks in parts of Europe with long-documented *I. ricinus* populations (14, 15). Moreover, the distributional area of *I. ricinus* appears to be steadily shifting toward higher altitudes and latitudes, increasing the total surface area of tick-suitable habitats in many European countries (16–18). However, several studies have identified a strong negative association of tick density with altitude, associated mainly with local climatic conditions (19, 20). Climate changes and their direct effects on vertebrate host distribution, population dynamics, and vegetation are associated with the altitudinal and latitudinal changes in the distribution of *I. ricinus* (16, 17).

In the present study, we aimed to systematically analyze the existing literature covering the prevalence of *B. burgdorferi sensu lato* and its different genospecies in host-seeking *I. ricinus* ticks in Europe. We focused on the evaluation of the prevalence rate in ticks according to tick developmental stage, adult tick gender, region of sampling, and method of detection, as well as investigating any changes in prevalence over time. The work represents a follow-up of the meta-analysis done by Rauter and Hartung (21) in order to reevaluate the spatiotemporal trends in *B. burgdorferi sensu lato* prevalence after another decade of data accumulation.

RESULTS

Prevalences of *Borrelia burgdorferi sensu lato* in ticks at different developmental stages. Reports published between 2010 and 2016 on the prevalence of *B. burgdorferi sensu lato* in questing *I. ricinus* ticks in Europe were reviewed and analyzed (Table 1). Of all 115,028 ticks tested, 14,134 (12.3%) were determined to be positive for the presence of *B. burgdorferi sensu lato*. The average prevalence per study reached 15.6%.

In some studies, only adult or only nymphal ticks were analyzed, or it was not possible to assign the prevalence rate to a specific tick developmental stage. In order to provide a direct comparison of *B. burgdorferi sensu lato* prevalence among adult and nymphal ticks, we analyzed only those entries ($n = 65$) where the prevalence rates for both adult and nymphal ticks were reported. In this subset, the prevalence of LB spirochetes reached significantly higher average values for adult (14.9% [3,784/25,377]) than for nymphal (11.8% [6,670/56,401]) ticks ($P, <0.001$ by the χ^2 test). The average prevalence per study reached 17.8% for adult and 14.2% for nymphal *I. ricinus* ticks. When individual results paired for each study were compared, the difference in the prevalence of *B. burgdorferi sensu lato* between the tick developmental stages was also statistically significant ($P, <0.01$ by a paired t test) (Fig. 1). In 61.5% (40/65) of individual entries with both developmental stages analyzed and numbers specified, the prevalence of *B. burgdorferi sensu lato* in adult ticks surpassed that in nymphs. Considering only entries with more than 100 adult samples analyzed, the prevalence in adults was higher than that in nymphs in 73.2% (30/41) of the entries. A moderate linear correlation was found between the *B. burgdorferi sensu lato* prevalence rates in adult and nymphal *I. ricinus* ticks ($R^2 = 0.30$; Pearson's $r = 0.5518$; $P < 0.001$) (Fig. 2).

TABLE 1 Studies used for the analysis of rates of *B. burgdorferi sensu lato* infection in *I. ricinus* ticks in Europe

Country	Reference(s)
Austria	46–48
Belarus	50
Belgium	55
Bosnia and Herzegovina	62
Czech Republic	75–78
Denmark	51
Estonia	83
Finland	87, 88
France	11, 51, 75, 92–98
Germany	14, 23, 75, 95, 100–106
Hungary	111, 112
Italy	22, 46, 119–124
Luxembourg	49
The Netherlands	51–54
Norway	56–61, 127, 128
Poland	63–75
Portugal	75, 79, 80
Romania	24, 81, 82
Serbia	84–86
Slovakia	89–91
Spain	99
Switzerland	10, 107–110, 125, 126
United Kingdom	113–118

In 37 entries, the adult ticks were included and the prevalence of *B. burgdorferi sensu lato* was reported for each sex separately. The overall prevalence in females (13.9% [1,271/9,164]) surpassed the prevalence rate in males (11.1% [960/8,664]) (P , <0.001 by the χ^2 test). The average prevalence per entry reached 18.4% for females and 15.7% for males. The differences were also statistically significant when paired values for each study were compared (P , <0.05 by a paired Student t test) (Fig. 3). For females, higher prevalence rates were reached in 67.6% (25/37) of the individual studies. When only entries with at least 50 samples of each sex tested were taken into account, the proportion increased to 78.9% (15/19).

Notably, some studies included in the data set reported the detection of *B. burgdorferi sensu lato* spirochetes in larval *I. ricinus* (22–24). The overall prevalence among larvae reported in these papers reached 1.5% (17/1,147 [range, 0.4% to 25.8%]).

Prevalence of *Borrelia burgdorferi sensu lato* in ticks according to the method of detection. Although lower mean prevalence rates were determined using simple conventional PCR than using nested PCR or quantitative PCR (qPCR) for the detection of *B. burgdorferi sensu lato* in all tick samples, adults only, and nymphs only (Table 2),

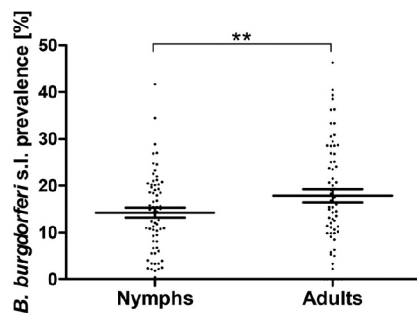


FIG 1 Comparison of *B. burgdorferi sensu lato* prevalences in nymphal and adult *I. ricinus* ticks in Europe. Each dot represents a single entry (locality). Data were extracted from 65 entries where the prevalence rates for both developmental stages were reported. The middle lines represent the means; error bars, standard errors of the means. **, P < 0.01.

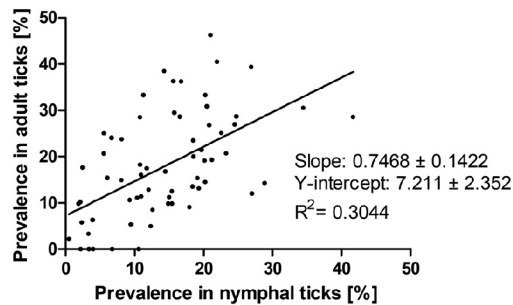


FIG 2 Linear correlation analysis for the prevalence of *B. burgdorferi sensu lato* in adult and nymphal *I. ricinus* ticks in Europe. Each dot represents a single entry (locality). Data were extracted from 65 entries where the prevalence rates for both developmental stages were reported.

no statistically significant differences were found. Only in two studies were microscopy-based detection techniques (dark-field and phase-contrast) used. In 15 of 78 entries on prevalence in nymphal ticks, pooling was used (usually 10 individuals per pool). Significantly lower mean prevalence rates were found in studies using pooled samples (from which uncorrected minimum infection rates were calculated) than in studies testing individual ticks (6.0% and 15.2%, respectively) ($P, <0.001$ by a t test with Welch's correction).

Prevalence of *Borrelia burgdorferi sensu lato* in ticks according to the year of tick sampling. In order to compare the infection rates in all ticks over the years, the data were divided into 2-year cycles (2002–2003 up to 2012–2013) according to the year of tick sampling. Data for 2001 and 2015 consisted only of a single entry each and therefore were not included in the analysis. If the collection period was longer or did not fit exactly into the given 2-year time frame, the data were excluded (resulting in 66 separate entries). Because of big differences in the numbers of entries available for particular years, the 2-year cycles were used in order to get comparable numbers of entries per time period. No trend was observed when the mean prevalence rates in 2-year cycles were analyzed by linear regression, no significant differences were found among the 2-year periods (Fig. 4), and no statistically significant difference was found when the 2002–2007 group (mean prevalences in adults and nymphs, 18.2% and 14.5%, respectively) was compared to the 2008–2014 group (16.7% and 13.1%, respectively).

In contrast, the mean *B. burgdorferi sensu lato* prevalence rate in our whole data set (2002 to 2014 for nymphs and 2001 to 2015 for adults) was statistically significantly lower for adult ticks (14.9%), but significantly higher for nymphal ticks (11.8%), than those determined from the data collected by Rauter and Hartung (21) for 1985 to 2004

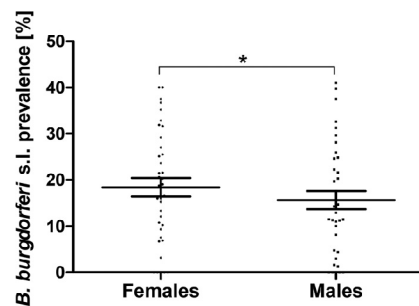


FIG 3 Comparison of *B. burgdorferi sensu lato* prevalence rates between female and male *I. ricinus* ticks in Europe. Each dot represents a single entry (locality). Data were extracted from 37 entries where the prevalence rate for each sex was reported. The middle lines represent the means; error bars, standard errors of the means. *, $P < 0.05$.

TABLE 2 Mean prevalence rates of *B. burgdorferi sensu lato* determined by different molecular methods of detection

Detection method	Prevalence (%) ^a		
	All ticks	Adults	Nymphs
PCR	14.0 ± 1.5 (42)	15.4 ± 1.9 (36)	12.3 ± 1.5 (29)
Nested PCR	17.3 ± 2.2 (18)	20.4 ± 3.0 (16)	14.6 ± 2.1 (13)
qPCR	17.9 ± 1.7 (35)	21.0 ± 2.3 (29)	15.4 ± 1.7 (31)

^aValues are means ± standard errors of the means (number of records).

(18.6% and 10.1%, respectively) (P , <0.001 by the χ^2 test). The numbers of samples analyzed were comparable.

Geographical differences in the prevalence of *Borrelia burgdorferi sensu lato* in ticks. Statistically significant differences in the prevalence of *B. burgdorferi sensu lato* were observed among individual countries (P , <0.05 by the Kruskal-Wallis test), but no significant differences were found in the paired comparison. Therefore, the data were stratified by area, and countries were merged into bigger regional units based on geographical proximity and environmental/climate similarity. The European regions in which the tick infection rate was calculated are defined as follows: British Isles (England, Scotland, and Wales), Iberian Peninsula (Portugal and Spain), Western Europe (Belgium, France, Luxembourg, and the Netherlands), Scandinavia (Belarus, Denmark, Estonia, Finland, and Norway), Central Europe (Austria, Czech Republic, Germany, Hungary, Poland, Slovakia, and Switzerland), Southern Europe (Italy), and the Balkan Peninsula (Romania, Serbia, and Bosnia and Herzegovina). In each region, at least 3 independent entries were available for all ticks as well as for each of the developmental stages.

The mean prevalence rates of *B. burgdorferi sensu lato* in *I. ricinus* ticks differed among the regions (P , <0.01 by analysis of variance [ANOVA]) (Table 3). The highest prevalence for all ticks was found in Central Europe (19.3%). The lowest prevalence was observed in the British Isles (3.6%). The difference in infection rates between these two regions and that between Central Europe (19.3%) and Western Europe (10.2%) were the only statistically significant differences in paired-region comparisons (P , <0.05 by Bonferroni's multiple-comparison test) (Fig. 5). Similarly, the nymphal infection rate differed significantly among the regions (P , <0.001 by ANOVA). In paired comparisons of prevalence among nymphs, significant differences were found not only between Central Europe (16.7%) and the British Isles (3.6%) and between Central Europe (16.7%) and Western Europe (5.7%) but also between the Balkan Peninsula (22.1%) and the British Isles (3.6%) and between the Balkan Peninsula (22.1%) and Western Europe (5.7%) (P , <0.05 by Bonferroni's multiple-comparison test) (Fig. 5). No significant differences in the infection rate of adult *I. ricinus* ticks were found among the regions.

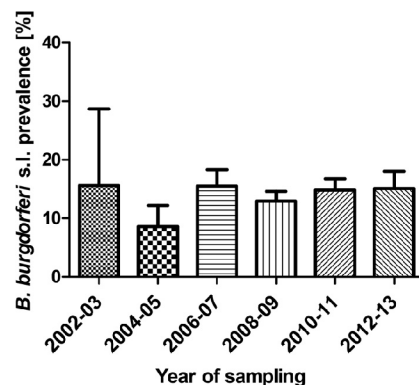


FIG 4 Mean prevalences of *B. burgdorferi sensu lato* in *I. ricinus* ticks in Europe in 2-year cycles. Each bar represents the mean prevalence reached in a particular 2-year cycle. Error bars, standard errors of the means.

TABLE 3 Mean prevalence rates of *B. burgdorferi sensu lato* in *I. ricinus* ticks in defined regions of Europe

Region	Prevalence (%) of <i>B. burgdorferi sensu lato</i> in <i>I. ricinus</i> ticks ^a		
	Nymphs	Adults	Total
Iberian Peninsula	9.4 (2.8)	11.4 (6.6)	9.5 (5.0)
British Isles	3.6 (0.6)	3.2 (1.8)	3.6 (0.6)
Western Europe	5.7 (1.1)	14.6 (3.0)	10.2 (2.0)
Central Europe	16.7 (1.4)	21.6 (1.9)	19.3 (1.3)
Scandinavia	12.9 (2.2)	21.0 (4.0)	15.5 (2.5)
Southern Europe	14.0 (2.5)	14.7 (3.4)	15.3 (2.6)
Balkan Peninsula	22.1 (8.6)	19.1 (7.0)	18.5 (6.8)

^aValues are means (standard errors of the means).

The prevalence rate of *B. burgdorferi sensu lato* in nymphal ticks rises with increasing longitude (linear regression; $R^2 = 0.0927$; $P < 0.05$) (Fig. 6). A similar tendency, but one that was not statistically significant, was observed for infection of adult ticks. The relationship between the *B. burgdorferi sensu lato* prevalence rate and latitude was not found significant for either nymphal, adult, or all ticks. Nevertheless, special attention was paid to the northern distribution limit of *I. ricinus*, which is reported to be steadily shifting in latitudes above 60°N (25). In our data set, 5 studies contained ticks sampled at localities above this limit (61 to 65°N). Altogether, 5,574 ticks (4,797 nymphs and 777 adults) were analyzed in this subset, reaching an average *B. burgdorferi sensu lato* prevalence of 15.9% in nymphal ticks and 23.2% in adult ticks, values statistically significantly higher than those in localities south of the limit (13.2% for nymphs and 19.3% for adults) ($P, < 0.01$ by a χ^2 test with the Yates correction).

Representation of individual *Borrelia burgdorferi sensu lato* genospecies. For the analysis of genospecies composition, the proportion of each genospecies was expressed as a percentage of all identified samples of *B. burgdorferi sensu lato* for each study. The data were extracted from a total of 69 entries. To minimize the impact of sample size per study, the overall proportions were calculated as averages of the percentages from individual papers (not from the sums of numbers). For each genospecies, the proportion was calculated by including only studies that employed a method that could safely identify that particular genospecies.

Statistically significant differences in the representation of the nine genospecies analyzed were observed. *B. afzelii* (46.6%; 69 values) and *B. garinii* (23.8%; 69 values) were the most frequently detected genospecies ($P, < 0.001$ for differences from all other genospecies and from each other by Bonferroni's multiple-comparison test), followed

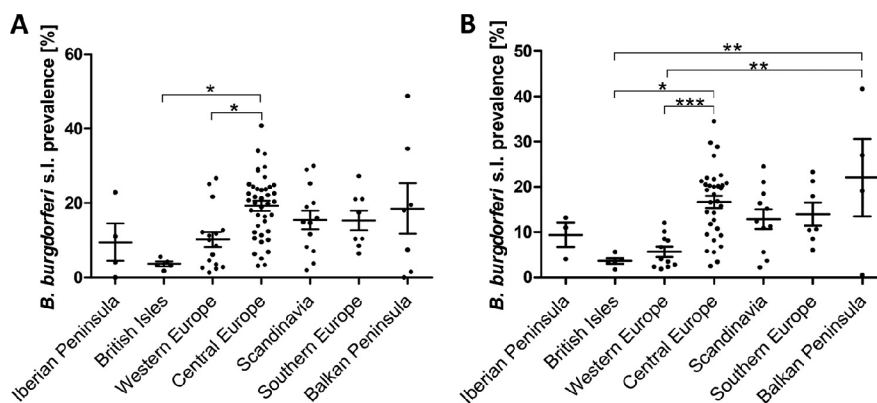


FIG 5 Prevalence of *B. burgdorferi sensu lato* in *I. ricinus* ticks in defined regions of Europe. Each dot represents a single entry (locality). The middle lines represent the means; error bars, standard errors of the means. Results were compared by ANOVA, followed by Bonferroni's multiple-comparison test. *, $P < 0.05$; **, $P < 0.01$; ***, $P < 0.001$. (A) Comparison of all ticks; (B) comparison of nymphal *I. ricinus* ticks.

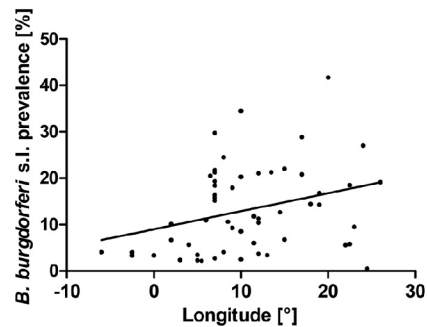


FIG 6 Regression analysis of the prevalence of *B. burgdorferi sensu lato* in nymphal *I. ricinus* ticks in Europe with longitude (linear regression; $R^2 = 0.0927$; $P < 0.05$). Each dot represents a single entry (locality).

by *B. valaisiana* (11.4%; 65 values), *B. burgdorferi sensu stricto* (10.2%; 68 values), and *B. lusitaniae* (7.0%; 58 values) ($P, < 0.05$ for differences from all other genospecies but not from each other). *B. bavariensis* (2.0%; 44 values), *B. spielmanii* (1.7%; 54 values), *B. finlandensis* (0.2%; 35 values), and *B. bissettiae* (0.06%; 51 values), were rarely detected ($P, < 0.05$ for differences from all other genospecies except *B. lusitaniae*; not significantly different from each other) (Fig. 7).

Negative correlations were found by the Spearman rank test between the proportions of *B. afzelii* and *B. garinii* ($r = -0.46$; $P < 0.001$), *B. afzelii* and *B. burgdorferi sensu stricto* ($r = -0.37$; $P < 0.01$), *B. afzelii* and *B. valaisiana* ($r = -0.52$; $P < 0.001$), and *B. afzelii* and *B. lusitaniae* ($r = -0.29$; $P < 0.05$). The proportions of *B. garinii* and *B. lusitaniae* also correlated negatively ($r = -0.263$; $P < 0.05$).

The relationships of the proportional representation of the individual genospecies with latitude and longitude were examined using linear regression. The proportion of *B. afzelii* among *B. burgdorferi sensu lato*-infected ticks increases from the south of Europe to the north ($r^2 = 0.1119$; $P < 0.05$), whereas the prevalence of *B. lusitaniae* decreases in the same direction ($r^2 = 0.1949$; $P < 0.01$) (Fig. 8). Similarly, the proportion of *B. afzelii* increases toward the east ($r^2 = 0.0994$; $P < 0.05$), whereas the prevalence of *B. valaisiana* decreases significantly in the same direction ($r^2 = 0.1633$; $P < 0.001$) (Fig. 9).

The data on the proportional representation of individual genospecies were grouped according to the geographic region of tick sampling (Table 4). The distribution of individual genospecies among different geographic regions was analyzed (Fig. 10).

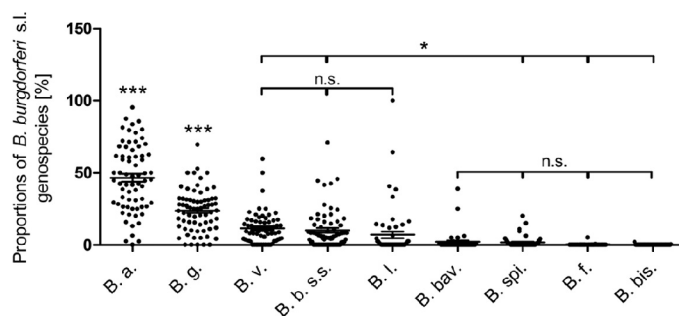


FIG 7 Proportions of *B. burgdorferi sensu lato* genospecies in *I. ricinus* ticks in Europe. Each dot represents a single entry (locality). The middle lines represent the means; error bars, standard errors of the means. Results were compared by ANOVA, followed by Bonferroni's multiple-comparison test. B. a., *B. afzelii*; B. g., *B. garinii*; B. v., *B. valaisiana*; B. b. s.s., *B. burgdorferi sensu stricto*; B. l., *B. lusitaniae*; B. bav., *B. bavariensis*; B. spi., *B. spielmanii*; B. f., *B. finlandensis*; B. bis., *B. bissettiae*. *, $P < 0.05$; ***, $P < 0.001$; n.s., not statistically significant.

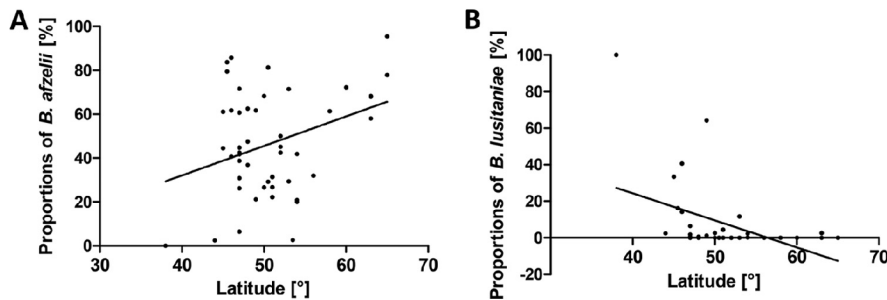


FIG 8 Regression analyses of *B. afzelii* (A) and *B. lusitaniae* (B) infection rates in *I. ricinus* ticks in Europe with latitude.

The impact of the region was not found to be statistically significant, whereas the *B. burgdorferi sensu lato* genospecies and the interaction of region and genospecies were found to contribute statistically significantly to the total variation (P , <0.01 and <0.001 , respectively, by two-way ANOVA). Significant differences were found in the representation of *B. afzelii* between the British Isles and Scandinavia as well as between Central Europe and Scandinavia (P , <0.05 by Bonferroni's multiple-comparison test). The prevalence of *B. lusitaniae* was statistically significantly different between Western Europe and the Balkan Peninsula as well as between Scandinavia and the Balkan Peninsula (P , <0.05 by Bonferroni's multiple-comparison test). Because there was only a single entry for genospecies composition from the Iberian Peninsula (100% *B. lusitaniae*), this region was not included in the analysis.

The presence of the relapsing fever spirochete *Borrelia miyamotoi* in *I. ricinus* ticks was reported by several studies (26). In our study, we did not specifically search for the prevalence of *B. miyamotoi* in *I. ricinus* ticks, but if this information was present in the screened studies, the value was noted. The prevalence rate of this spirochete reached an average of 1.27%, ranging from 0 to 3.85%. Records of the presence of *B. miyamotoi* were reported from all regions as defined in this study except the Iberian Peninsula, where no records of *B. miyamotoi* detection attempts were available in our data set.

DISCUSSION

As vectors of many disease-causing parasites, ticks pose a serious threat to human health and a considerable economic burden to public health systems. *I. ricinus*, the most common European tick, is the principal vector of *B. burgdorferi sensu lato*, the agent causing the most prevalent human tick-borne disease in Europe, Lyme borreliosis. A meta-analysis of data was performed with the aim of obtaining an all encompassing picture of *B. burgdorferi sensu lato* and its genospecies distribution in European *I. ricinus* ticks.

The prevalence of *B. burgdorferi sensu lato* spirochetes in ticks has been considered one of the most crucial elements of risk assessment for LB (21). Nevertheless, local

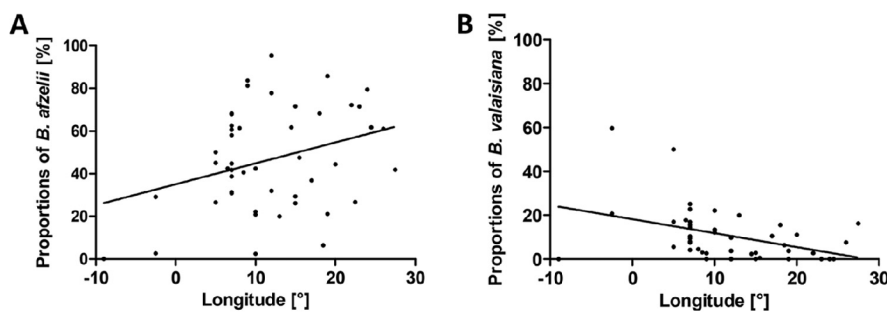


FIG 9 Regression analyses of *B. afzelii* (A) and *B. valaisiana* (B) infection rates in *I. ricinus* ticks in Europe with longitude.

TABLE 4 Proportional representation of *B. burgdorferi sensu lato* genospecies in *I. ricinus* ticks in Europe

Region	% prevalence of the indicated genospecies ^a									
	<i>B. afzelii</i>	<i>B. garinii</i>	<i>B. burgdorferi</i>			<i>B. lusitaniae</i>	<i>B. spielmanii</i>	<i>B. bissettae</i>	<i>B. bavariensis</i>	<i>B. finlandensis</i>
Iberian Peninsula	0 ± 0 (1)	0 ± 0 (1)	0 ± 0 (1)	0 ± 0 (1)	100 ± 0 (1)	0 ± 0 (1)	0 ± 0 (1)	0 ± 0 (1)	0 ± 0 (1)	0 ± 0 (1)
British Isles	33 ± 11 (4)	39 ± 4 (4)	2 ± 2 (3)	30 ± 16 (3)	0 ± 0 (3)	0 ± 0 (3)	0 ± 0 (3)	0 ± 0 (3)	0 ± 0 (3)	0 ± 0 (2)
Western Europe	45 ± 5 (10)	29 ± 5 (10)	6 ± 2 (10)	17 ± 4 (10)	0.1 ± 0.1 (9)	3 ± 1 (8)	0 ± 0 (7)	0 ± 0 (4)	0 ± 0 (4)	0 ± 0 (4)
Scandinavia	61 ± 7 (10)	24 ± 6 (10)	6 ± 2 (10)	8 ± 2 (10)	0.3 ± 0.3 (9)	1 ± 1 (9)	0 ± 0 (9)	0.1 ± 0.1 (7)	0 ± 0 (7)	0 ± 0 (7)
Central Europe	44 ± 4 (34)	23 ± 2 (34)	15 ± 3 (34)	11 ± 2 (31)	6 ± 2 (29)	2 ± 1 (27)	0.1 ± 0.1 (25)	2 ± 1 (23)	0.4 ± 0.4 (14)	0 ± 0 (4)
Southern Europe	54 ± 20 (4)	15 ± 9 (4)	2 ± 1 (4)	5 ± 3 (4)	15 ± 9 (4)	0 ± 0 (4)	0 ± 0 (4)	10 ± 10 (4)	0 ± 0 (4)	0 ± 0 (4)
Balkan Peninsula	52 ± 11 (5)	21 ± 5 (5)	7 ± 5 (5)	5 ± 2 (5)	36 ± 3 (2)	0 ± 0 (1)	0 ± 0 (1)	0 ± 0 (1)	0 ± 0 (1)	0 ± 0 (1)

^aValues are means ± standard errors of the means (number of records).

prevalence studies have a very limited value in terms of epidemiological risk assessment. In contrast, integration of the data from studies based on similar methodologies allows for the analysis of spatial and temporal variations and trends and may even reveal potential methodological pitfalls in detection or disease diagnostics. This work is a successor to a previous Europe-wide study done by Rauter and Hartung (21), which was based on data collected from 1984 to 2003. We attempted to use the same methodology, where possible, in order to be able to perform direct comparisons. The analysis showed that the overall mean prevalence of *B. burgdorferi sensu lato* in *I. ricinus* ticks reached 12.3%. The prevalence in adult ticks (14.9%) was higher than that in nymphal ticks (11.8%), a finding in accordance with data presented by others (21, 27). Since the minimum infection rate was used in case of pooled samples of nymphal ticks (a single positive tick per pool is expected), the calculated values for nymphs may slightly underestimate the real prevalence. Although transovarial transfer of *B. burgdorferi sensu lato* is considered dubious (28), some studies from our data set reported the infection of larvae with *B. burgdorferi sensu lato*. An alternative means of infection of larvae may be interrupted feeding. It has been shown previously that ixodid ticks are able to complete feeding on a second host after interruption (29); thus, partially fed ticks may be sampled as seemingly unfed larvae. This finding, together with the recent findings that *I. ricinus* larvae are able to transmit *B. afzelii* to laboratory mice (30), suggests the potential role of larvae in spreading human LB (30).

In contrast to earlier data reviews, where microscopic techniques were the main tools for determining *Borrelia* prevalence (21, 27), the current values were obtained almost exclusively by using PCR-based methods. Microscopic techniques, used as a standard procedure in the past, do not allow one to distinguish between genospecies, and if not used properly, they may lead to an underestimation of *Borrelia* infection rates (27). On the other hand, the prevalences of LB spirochetes in *I. ricinus* ticks reported in

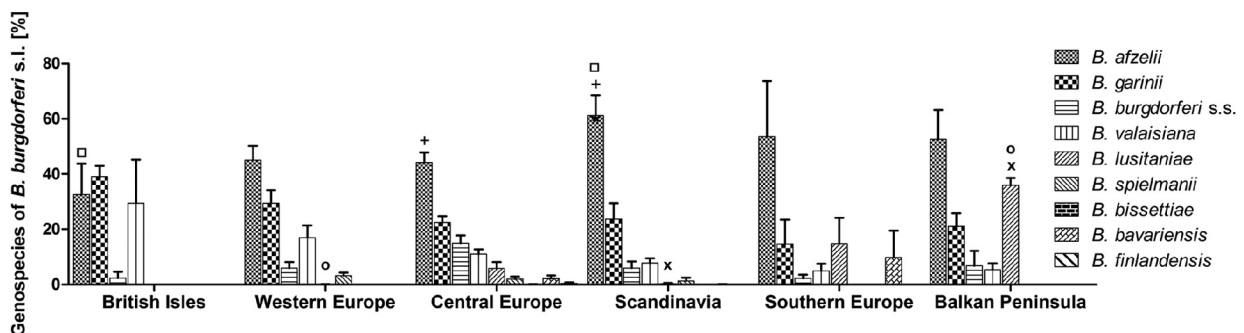


FIG 10 Proportional representation of *B. burgdorferi sensu lato* genospecies in *I. ricinus* ticks in Europe in different geographic regions. Each bar represents the mean proportion of a particular genospecies in a region; error bars, standard errors of the means. Each symbol (\square , \circ , $+$, \times) indicates a statistically significant difference ($P < 0.05$) in the proportional representation of a particular genospecies between two different regions, as determined by two-way ANOVA followed by Bonferroni's multiple-comparison test. s.s., *sensu stricto*.

the past could be also overestimated due to the misidentification of the relapsing fever spirochete *B. miyamotoi* by microscopy.

The PCR-based techniques are considered the most sensitive (27) and can detect a *Borrelia* load as low as a single spirochete (31). However, single-cell sensitivity may be superfluous in view of data suggesting that a minimum of 300 spirochetes may be required in order for a host-seeking nymphal tick to be able to transmit infection (32). In our study, we observed no significant differences in the prevalences estimated by the various PCR methods—conventional PCR, nested PCR, and qPCR—although qPCR is generally considered the most sensitive of the three (33). With regard to changes in prevalence over time, no trends in infection rates were observed over the course of 10 years in our study or in the earlier study of Rauter and Hartung (21). On the other hand, direct comparison of our data set to that of the earlier metastudy (21) indicates significant changes in overall prevalence. Numerically, the mean infection rates in all ticks and adults decreased by 1.4% and 3.7%, respectively, whereas the infection rate in nymphs increased by 1.7% relative to the data given by Rauter and Hartung (21). We may hypothesize that this difference between the results of the metastudies could be caused by the recently increased involvement of ungulates (like deer or moose), which are generally considered transmission-incompetent hosts for *B. burgdorferi sensu lato* (34, 35) but are frequent hosts of nymphal rather than larval *I. ricinus* ticks (36, 37). An increase in the total abundance of *I. ricinus* ticks was associated with the abundance of large ungulates previously (15, 25, 38).

As in the study of Rauter and Hartung (21), the correlation of *B. burgdorferi sensu lato* prevalence in ticks with the tick collection area showed a significant trend, with the rates increasing from the west to the east of Europe. The same effect was seen for nymphal ticks (in contrast to the study of Rauter and Hartung [21]) and adult ticks separately. The west-to-east trend is probably associated with the high prevalence of ticks in Central Europe. Regression analysis of the prevalence rate and latitude was not significant for *B. burgdorferi sensu lato* in nymphal, adult, or all ticks. Nevertheless, the prevalence rate in ticks sampled near their northern distribution limit reached values significantly higher than those in the rest of Europe. We hypothesize that this might be due to the lower host species diversity available for these newly established *I. ricinus* populations, making it possible to feed mostly on *B. burgdorferi sensu lato* transmission-competent hosts.

The prevalence of *B. burgdorferi sensu lato* in females surpassed the prevalence rate in males, and the difference was statistically significant when paired values were compared. Rauter and Hartung (21) also observed a higher infection rate for females (by 1.8%). Another study demonstrated a relationship between the weights of engorged nymphal ixodid ticks and their resultant sexes, revealing that the mean body weight of engorged nymphs that molted to females was significantly greater than that of nymphs that became males (39). A larger bloodmeal might result directly in a higher probability of infection and might be associated with prolonged feeding, resulting, again, in a higher chance of ingestion of the spirochetes.

Since different genospecies are involved in distinct clinical manifestations, it is important to know accurate numbers for the prevalence of a particular species with regard to risk assessment. The data show that *B. afzelii* is the most common genospecies, followed by *B. garinii* and *B. valaisiana*, findings consistent with data provided earlier. Interestingly, *B. burgdorferi sensu stricto* is the fourth most common species, despite the described dominant behavior of *B. burgdorferi sensu stricto* over some other genospecies (40).

Genospecies that were differentiated more recently are likely underrepresented in the data set, even though zero prevalence values were included only if they were generated in studies that used an identification method allowing the differentiation of the particular genospecies. In a number of reviewed studies, only the “major” genospecies were differentiated and the designation “NPD” (not possible to determine) was assigned to the other, “unidentified” genospecies (see Materials and Methods). However, during the analysis of those studies, we occasionally checked the specificity of the

primers used and found that more than one genospecies could be detected with a given set of primers (e.g., the primer set distinguished between *B. afzelii*, *B. garinii*, and *B. burgdorferi sensu stricto* but could not distinguish, for instance, between *B. burgdorferi sensu stricto* and *B. bissettae*).

The data showed that *B. valaisiana* is the third most common genospecies in Europe. Intriguingly, this species is only very rarely associated with human infection (8). It was demonstrated *in vitro* that *B. burgdorferi sensu lato* genospecies showed different patterns of resistance or sensitivity to the complement systems of different vertebrates (41). Therefore, higher sensitivity to some of the components of the human immune system might be the reason for efficient clearance of *B. valaisiana*.

Over recent decades, our planet has gone through an apparent climate change that has resulted, among other trends, in a shift toward milder winters in Europe (42). As a consequence, ticks have spread into higher latitudes (43) and altitudes (44). Interestingly, the data presented here, together with the previously published data (21, 27), covering a period of about 30 years, indicate that the prevalence of *B. burgdorferi sensu lato* in questing *I. ricinus* ticks remains reasonably constant since the beginning of investigations into this issue. Therefore, there seems to be no general effect of climate change on the prevalence rates of this pathogen. This hypothesis can also be supported by the outcomes of the analysis on the dependence of *Borrelia* prevalence on latitude and longitude. In our data set, analysis of the prevalence rate and latitude did not find a significant correlation for *B. burgdorferi sensu lato* in nymphal, adult, or all ticks (as in the study of Rauter and Hartung [21]), whereas a significant effect of longitude on prevalence was found. In light of these findings, it may also be debatable how much, in terms of resources, should be invested in future studies determining the infection rates in host-seeking ticks if no fundamental change in infection rates has been seen in the past 30 years of apparent climate change.

Monitoring changes in the prevalences of different *B. burgdorferi sensu lato* genospecies in ticks might produce an important indicator of host adaptation, which, in turn, has been suggested to contribute to differences in pathogenicity in humans (45). Nevertheless, although we have reported statistically significant changes in the overall prevalence of *B. burgdorferi sensu lato* and relatively high geographical variability, these differences have only a limited effect on the total infection risk compared with differences in total tick abundance. Therefore, we conclude that detailed monitoring of *B. burgdorferi sensu lato* prevalence is important mainly in areas undergoing current dynamic changes in tick/pathogen distribution (at the latitudinal and altitudinal limits of distribution), whereas in areas with stable vector populations, regular examination of long-term trends, including habitat-specific distribution patterns of vector/pathogen occurrence, seems more reasonable. Concerning the variable pathogenicity of *B. burgdorferi sensu lato* genospecies, information on genospecies variability may be valuable in risk estimation, especially in areas with large proportions of nonpathogenic/conditionally pathogenic genospecies.

MATERIALS AND METHODS

A systematic literature search (using the keywords "*Borrelia* AND prevalence AND *Ixodes ricinus*" and "*Borrelia* AND *Ixodes*") was carried out on the electronic database PubMed, and reports on the prevalence of *B. burgdorferi sensu lato* in *I. ricinus* ticks that were published in English between January 2010 and December 2016 were extracted. Reports identified by the database search (>900) were first assessed for eligibility by their titles and abstracts, followed by an in-depth analysis for relevant data regarding *B. burgdorferi sensu lato* prevalence in ticks.

Only data on questing nymphs and adults were used. Larvae were not included, since only a few studies included larvae in the prevalence analysis. Publications were not included in the analysis if (i) it was not possible to subtract/exclude the rate of infection with the relapsing fever spirochete (*B. miyamotoi*), (ii) it was not possible to subtract/exclude data on larvae, (iii) data were incomplete, or serious discrepancies or errors in numbers/calculations were noticed, or (iv) samples were collected earlier than the year 2000. If the number of infected *I. ricinus* ticks was not given, it was calculated, if possible, based on the reported tick infection rate and the number of ticks examined. Cleaning the data set by removing incomplete, inaccurate, or confusing data resulted in a set of 101 individual entries on *B. burgdorferi sensu lato* prevalence and 69 entries on *B. burgdorferi sensu lato* genospecies identification. When the ticks were collected over more years, the study, if possible, was divided into separate entries. When the sampling in a single study was done in several countries, the data were again separated into

several entries according to the country of sampling. In some studies, the nymphal ticks were analyzed as pooled samples from multiple individuals. In those cases, the minimum infection rate was calculated for the purpose of our study (on the assumption of a single positive tick per positive pool).

Data regarding the area (country), its global positioning system (GPS) coordinates, if available (range, 38 to 65°N, 9°W to 27.5°E), the year of tick sampling (range, 2001 to 2015), the number of ticks according to developmental stage, gender, infection with *B. burgdorferi sensu lato* (and *B. miyamotoi* when available), and specific *B. burgdorferi sensu lato* genospecies were extracted and documented. GPS coordinates were either stated by the authors or inferred from the description of the sampling site. The coordinates were rounded off to whole degrees. In case of multiple sampling points per entry, the range of coordinates was recorded, and the mean value was calculated. Furthermore, the methods used for *B. burgdorferi sensu lato* detection and genospecies identification were recorded.

In order to maximize the accuracy of the calculated infection rates of *B. burgdorferi sensu lato* genospecies, the method used to distinguish between genospecies was inspected and assessed with regard to how many genospecies the particular method could distinguish. If the method was not able to determine certain genospecies, the designation "NPD" (not possible to determine) was assigned to a particular genotype, and it was left out of the calculation. For the calculation of genospecies prevalence, if a tick was multiply infected, each genospecies found was added to the corresponding single-infection category. The proportional representation of genospecies was calculated as a percentage of all successful identifications.

Statistical analysis. Statistical analyses were done using GraphPad Prism, version 5.04 (GraphPad Software, Inc., CA, USA). A paired *t* test or an unpaired *t* test (with Welch's correction) was used for the comparison of two groups. To assess the statistical significance of differences among more than two groups, ANOVA with Bonferroni's multiple-comparison *post hoc* test was used. Nonparametric alternatives (the Mann-Whitney *U* test, the Kruskal-Wallis test) were used for data lacking normality. Relationships among quantitative variables were examined using linear regression or correlation analysis (the Pearson regression coefficient, the Spearman rank test). The χ^2 test was employed for comparing prevalences between two or more groups. *P* values of <0.05 were considered statistically significant. In scatter plots, points represent individual values, middle lines represent means, and error bars represent standard errors of the means, unless stated otherwise in the figure legend.

ACKNOWLEDGMENTS

This study was supported by the Technology Agency of the Czech Republic (grant TG02010034), ANTIGONE (grant EU-7FP 278976), and ANTIDotE (grant EU-7FP 602272–2). M.S. was supported by the Grant Agency of the University of South Bohemia (grant 04-026/2015/P). V.H. and D.R. were supported by project LO1218 of the Ministry of Education, Youth and Sports of the Czech Republic under the NPU I program. The funders had no role in study design, data collection and interpretation, or the decision to submit the work for publication. We declare no competing financial interests.

REFERENCES

1. Stanek G, Wormser GP, Gray J, Strle F. 2012. Lyme borreliosis. *Lancet* 379:461–473. [https://doi.org/10.1016/S0140-6736\(11\)60103-7](https://doi.org/10.1016/S0140-6736(11)60103-7).
2. Margos G, Vollmer SA, Cornet M, Garnier M, Fingerle V, Wilske B, Bormane A, Vitorino L, Collares-Pereira M, Drancourt M, Kurtenbach K. 2009. A new *Borrelia* species defined by multilocus sequence analysis of housekeeping genes. *Appl Environ Microbiol* 75:5410–5416. <https://doi.org/10.1128/AEM.00116-09>.
3. Strle F, Picken RN, Cheng Y, Cimperman J, Maraspin V, Lotric-Furlan S, Ruzic-Sabljić E, Picken MM. 1997. Clinical findings for patients with Lyme borreliosis caused by *Borrelia burgdorferi sensu lato* with genotypic and phenotypic similarities to strain 25015. *Clin Infect Dis* 25: 273–280. <https://doi.org/10.1086/514551>.
4. Rudenko N, Golovchenko M, Růžek D, Piskunova N, Málátová N, Grubhoffer L. 2009. Molecular detection of *Borrelia bisetii* DNA in serum samples from patients in the Czech Republic with suspected borreliosis. *FEMS Microbiol Lett* 292:274–281. <https://doi.org/10.1111/j.1574-6968.2009.01498.x>.
5. Collares-Pereira M, Couceiro S, Franca I, Kurtenbach K, Schäfer SM, Vitorino L, Gonçalves L, Baptista S, Vieira ML, Cunha C. 2004. First isolation of *Borrelia lusitaniae* from a human patient. *J Clin Microbiol* 42:1316–1318. <https://doi.org/10.1128/JCM.42.3.1316-1318.2004>.
6. da Franca I, Santos L, Mesquita T, Collares-Pereira M, Baptista S, Vieira L, Viana I, Vale E, Prates C. 2005. Lyme borreliosis in Portugal caused by *Borrelia lusitaniae*? Clinical report on the first patient with a positive skin isolate. *Wien Klin Wochenschr* 117:429–432.
7. Fingerle V, Schulte-Spechtel UC, Ruzic-Sabljić E, Leonhard S, Hofmann H, Weber K, Pfister K, Strle F, Wilske B. 2008. Epidemiological aspects and molecular characterization of *Borrelia burgdorferi* s.l. from southern Germany with special respect to the new species *Borrelia spielmanii* sp. nov. *Int J Med Microbiol* 298:279–290. <https://doi.org/10.1016/j.ijmm.2007.05.002>.
8. Diza E, Papa A, Vezyri E, Tsounis S, Milonas I, Antoniadis A. 2004. *Borrelia valaisiana* in cerebrospinal fluid. *Emerg Infect Dis* 10: 1692–1693. <https://doi.org/10.3201/eid1009.030439>.
9. Stanek G, Reiter M. 2011. The expanding Lyme *Borrelia* complex—clinical significance of genomic species? *Clin Microbiol Infect* 17: 487–493. <https://doi.org/10.1111/j.1469-0691.2011.03492.x>.
10. Lommano E, Bertaiola L, Dupasquier C, Gern L. 2012. Infections and coinfections of questing *Ixodes ricinus* ticks by emerging zoonotic pathogens in Western Switzerland. *Appl Environ Microbiol* 78: 4606–4612. <https://doi.org/10.1128/AEM.07961-11>.
11. Cotté V, Bonnet S, Cote M, Vayssier-Taussat M. 2010. Prevalence of five pathogenic agents in questing *Ixodes ricinus* ticks from western France. *Vector Borne Zoonotic Dis* 10:723–730. <https://doi.org/10.1089/vbz.2009.0066>.
12. Ornstein K, Berglund J, Nilsson I, Norrby R, Bergström S. 2001. Characterization of Lyme borreliosis isolates from patients with erythema migrans and neuroborreliosis in southern Sweden. *J Clin Microbiol* 39:1294–1298. <https://doi.org/10.1128/JCM.39.4.1294-1298.2001>.
13. Schorn S, Pfister K, Reulen H, Mahling M, Silaghi C. 2011. Occurrence of *Babesia* spp., *Rickettsia* spp. and *Bartonella* spp. in *Ixodes ricinus* in Bavarian public parks, Germany. *Parasit Vectors* 4:135. <https://doi.org/10.1186/1756-3305-4-135>.
14. Schwarz A, Hönig V, Vavrušková Z, Grubhoffer L, Balczun C, Albring A, Schaub GA. 2012. Abundance of *Ixodes ricinus* and prevalence of *Borrelia burgdorferi* s.l. in the nature reserve Siebengebirge, Germany,

117. James MC, Gilbert L, Bowman AS, Forbes KJ. 2014. The heterogeneity, distribution, and environmental associations of *Borrelia burgdorferi* sensu lato, the agent of Lyme borreliosis, in Scotland. *Front Public Health* 2:129. <https://doi.org/10.3389/fpubh.2014.00129>.
118. James MC, Bowman AS, Forbes KJ, Lewis F, McLeod JE, Gilbert L. 2013. Environmental determinants of *Ixodes ricinus* ticks and the incidence of *Borrelia burgdorferi* sensu lato, the agent of Lyme borreliosis, in Scotland. *Parasitology* 140:237–246. <https://doi.org/10.1017/S003118201200145X>.
119. Ragagli C, Mannelli A, Ambrogi C, Bisanzio D, Ceballos LA, Grego E, Martello E, Selmi M, Tomassone L. 2016. Presence of host-seeking *Ixodes ricinus* and their infection with *Borrelia burgdorferi* sensu lato in the Northern Apennines, Italy. *Exp Appl Acarol* 69:167–178. <https://doi.org/10.1007/s10493-016-0030-9>.
120. Aureli S, Galuppi R, Ostanello F, Foley JE, Bonoli C, Rejmanek D, Rocchi G, Orlandi E, Tampieri MP. 2015. Abundance of questing ticks and molecular evidence for pathogens in ticks in three parks of Emilia-Romagna region of Northern Italy. *Ann Agric Environ Med* 22:459–466. <https://doi.org/10.5604/12321966.1167714>.
121. Mancini F, Di Luca M, Toma L, Vescio F, Bianchi R, Khoury C, Marini L, Rezza G, Ciervo A. 2014. Prevalence of tick-borne pathogens in an urban park in Rome, Italy. *Ann Agric Environ Med* 21:723–727. <https://doi.org/10.5604/12321966.1129922>.
122. Pintore MD, Ceballos L, Iulini B, Tomassone L, Pautasso A, Corbellini D, Rizzo F, Mandola ML, Bardelli M, Peletto S, Acutis PL, Mannelli A, Casalone C. 2015. Detection of invasive *Borrelia burgdorferi* strains in north-eastern Piedmont, Italy. *Zoonoses Public Health* 62:365–374. <https://doi.org/10.1111/zph.12156>.
123. Corrain R, Drigo M, Fenati M, Menandro ML, Mondin A, Pasotto D, Martini M. 2012. Study on ticks and tick-borne zoonoses in public parks in Italy. *Zoonoses Public Health* 59:468–476. <https://doi.org/10.1111/j.1863-2378.2012.01490.x>.
124. Pistone D, Pajoro M, Fabbri M, Vicari N, Marone P, Genchi C, Novati S, Sasserà D, Epis S, Bandi C. 2010. Lyme borreliosis, Po River Valley, Italy. *Emerg Infect Dis* 16:1289–1291. <https://doi.org/10.3201/eid1608.100152>.
125. Herrmann C, Voordouw MJ, Gern L. 2013. *Ixodes ricinus* ticks infected with the causative agent of Lyme disease, *Borrelia burgdorferi* sensu lato, have higher energy reserves. *Int J Parasitol* 43:477–483. <https://doi.org/10.1016/j.ijpara.2012.12.010>.
126. Herrmann C, Gern L. 2010. Survival of *Ixodes ricinus* (Acari: Ixodidae) under challenging conditions of temperature and humidity is influenced by *Borrelia burgdorferi* sensu lato infection. *J Med Entomol* 47:1196–1204. <https://doi.org/10.1603/ME10111>.
127. Tveten A-K. 2014. Exploring diversity among Norwegian *Borrelia* strains originating from *Ixodes ricinus* ticks. *Int J Microbiol* 2014:397143. <https://doi.org/10.1155/2014/397143>.
128. Granquist EG, Kristiansson M, Lindgren P-E, Matussek A, Nødtvedt A, Okstad W, Stuen S. 2014. Evaluation of microbial communities and symbionts in *Ixodes ricinus* and ungulate hosts (*Cervus elaphus* and *Ovis aries*) from shared habitats on the west coast of Norway. *Ticks Tick Borne Dis* 5:780–784. <https://doi.org/10.1016/j.ttbdis.2014.05.005>.

3.2 Manuscript 2:

Strnad, M., Grubhoffer, L., Rego, R. O. M. (2020) Novel targets and strategies to combat borreliosis. *Applied Microbiology and Biotechnology* 104: 1915-1925.

Annotation

The number of human cases of Lyme disease is continuously increasing and suspected to be in the hundreds of thousands both in the US and Europe. In Europe, there are about 65,000-85,000 documented cases every year. In the US, it is estimated that the number of cases per year surpasses 300,000. Despite concerted efforts of scientists, researchers and pharmaceutical industry all around the world, a vaccine for Lyme disease is not currently available. This review provides a digest of the history of vaccine development up to new promising vaccine candidates and strategies that are targeted against Lyme disease, including elements of the tick vector, the reservoir hosts, and the *Borrelia* pathogen itself.



Novel targets and strategies to combat borreliosis

Martin Strnad^{1,2} · Libor Grubhoffer^{1,2} · Ryan O.M. Rego¹

Received: 18 November 2019 / Revised: 5 January 2020 / Accepted: 12 January 2020
© Springer-Verlag GmbH Germany, part of Springer Nature 2020

Abstract

Lyme borreliosis is a bacterial infection that can be spread to humans by infected ticks and may severely affect many organs and tissues. Nearly four decades have elapsed since the discovery of the disease agent called *Borrelia burgdorferi*. Although there is a plethora of knowledge on the infectious agent and thousands of scientific publications, an effective way on how to combat and prevent Lyme borreliosis has not been found yet. There is no vaccine for humans available, and only one active vaccine program in clinical development is currently running. A spirited search for possible disease interventions is of high public interest as surveillance data indicates that the number of cases of Lyme borreliosis is steadily increasing in Europe and North America. This review provides a condensed digest of the history of vaccine development up to new promising vaccine candidates and strategies that are targeted against Lyme borreliosis, including elements of the tick vector, the reservoir hosts, and the *Borrelia* pathogen itself.

Keywords Lyme borreliosis · Vaccine candidates · Anti-tick strategies · Human pathogen · Public health

Introduction

Lyme borreliosis, or Lyme disease, is the most common tick-transmitted disease worldwide and is known to infect humans as well as domestic animals including cattle, cats, and dogs (Krupka and Straubinger 2010). Since the discovery of Lyme borreliosis in 1975 (Steere et al. 1977), a great deal of effort has been dedicated to the goal of preventing the detrimental effects of this disease. Despite improvements in diagnostic tests and public awareness of Lyme borreliosis, up to 300,000 cases in the USA (Kuehn 2013) and 65,000 cases in Europe (Hubálek 2009) are reported. However, the number of infections in Europe is likely to be an underestimation, as not all countries have made Lyme borreliosis a mandatorily notifiable disease (Smith and Takkinen 2006). The agents responsible for Lyme borreliosis are a diverse group of spirochetal bacteria within the *Borrelia* genus. *Borrelia burgdorferi*

sensu lato complex comprises at least 20 named species (Margos et al. 2019), with most human Lyme cases being caused by *B. burgdorferi* sensu stricto, *B. afzelii*, *B. garinii*, and *B. bavariensis* (Stanek et al. 2012).

B. burgdorferi is an extracellular pathogen (Strnad et al. 2015) that can infect the skin, heart, and nervous system (Cadavid et al. 2000; Stanek and Strle 2018). Ticks of the genus *Ixodes* transmit *B. burgdorferi* between reservoir hosts such as small mammals, lizards, and birds and are the only natural agents through which humans have been shown to be infected (Steere 2001). The principal vectors are *Ixodes ricinus* in Europe, *Ixodes persulcatus* in Asia, and *Ixodes scapularis* in North America. The overall prevalence of infected ticks and *Borrelia* genospecies distribution are highly variable across geographic locations (Strnad et al. 2017).

Ticks most often acquire *Borrelia* from infected rodents during their larval feeding. After molting to the next developmental stage, the tick has to find a new host. Upon ingestion of new blood, the spirochetes migrate from the midgut to the salivary glands of an infected tick followed by entering the mammal through the bite site (Ribeiro et al. 1987). The pathogen then disseminates throughout the mammalian host to establish an infection (Moriarty et al. 2008; Norman et al. 2008). All these concerted movements in the two environments are assumed or known to involve the process of motility and adhesion to cells involving a high number of protein and carbohydrate-based interactions (Ebady et al. 2016; Vechtova

✉ Martin Strnad
martin.strnad.cze@gmail.com

¹ Biology Centre, Institute of Parasitology, Czech Academy of Sciences, Branisovska 31, 37005, Ceske Budejovice, Czech Republic

² Faculty of Science, University of South Bohemia, Branisovska 31, 37005, Ceske Budejovice, Czech Republic

et al. 2018). Infected nymphal ticks occasionally feed on humans and most likely transmit the spirochete and cause human Lyme borreliosis as they are abundant in the spring and early summer and are small and difficult to detect. Unlike *B. miyamotoi*, *B. burgdorferi* sensu lato is considered not to be transmitted transovarially from female ticks to their offspring. However, several recent studies have shown that field-collected *I. ricinus* larvae may contain borrelial DNA (Kalmár et al. 2013; Tappe et al. 2014) and are able to transmit *B. afzelii* to laboratory rodents (van Duijvendijk et al. 2016), suggesting the potential role of larvae in spreading the Lyme borreliosis agent.

In the absence of antibiotic therapy, disseminated *B. burgdorferi* can persist in an individual for months or years even in the face of strong immune response. Currently, antibiotic treatment is the only effective tool to clear the infection and fight against Lyme borreliosis as no vaccine for humans is available. There are a number of new promising vaccine candidates being currently developed and tested by the research community, representing new hopes for future victims of the disease. These direct anti-*Borrelia* strategies can be complemented with anti-tick vaccines to bring a whole new level of human protection (Fig. 1), as will be discussed in this review.

On-demand treatment strategies

Most cases of Lyme borreliosis can be easily managed if treated early using antibiotics. Post-infection treatment is usually managed with antimicrobial agents for 2 to 4 weeks. Doxycycline, amoxicillin, penicillin V, and cefuroxime are

highly effective and are the preferred antibiotics for the treatment of early localized infection (Stanek and Strle 2018). Early disseminated infection is usually treated with intravenous ceftriaxone or penicillin (Stanek and Strle 2018) or oral doxycycline (Ljøstad et al. 2008). The most common routes of antibiotic administration are oral administration and intravenous injection. As an alternative approach, the topical application of 4% azithromycin cream was tested (Piesman et al. 2014). The result of the study showed that azithromycin was highly efficient when applied topically at the sites of tick bites in mice (Piesman et al. 2014). The outcomes of the study were however not fully confirmed in human studies (Schwameis et al. 2017; Shapiro and Wormser 2017). Azithromycin is an attractive possibility because of its good safety profile, long half-life in tissues, and potency against various *B. burgdorferi* species (Lee and Wormser 2008). Topical application of antimicrobial agents is a very attractive delivery method for a number of reasons and could be potentially used to stop the progression of the disease in the early localized stage of infection. The advantages include smaller amount of drug to be used, avoidance of the metabolic processing of the drug in the liver, ease of administration especially for young children, higher concentration of the drug to the affected area, and fairly diminished effects on nontargeted body locations such as intestinal flora. The transdermal route apart from the abovementioned advantages may be more convenient also for patients who cannot use normal oral intake because of swallowing problems such as intubation, deep sedation, or concurrent diseases (Tanner and Marks 2008). However, as a very motile organism, *B. burgdorferi* spread readily and very fast all over the body from site of skin entrance. Therefore, the

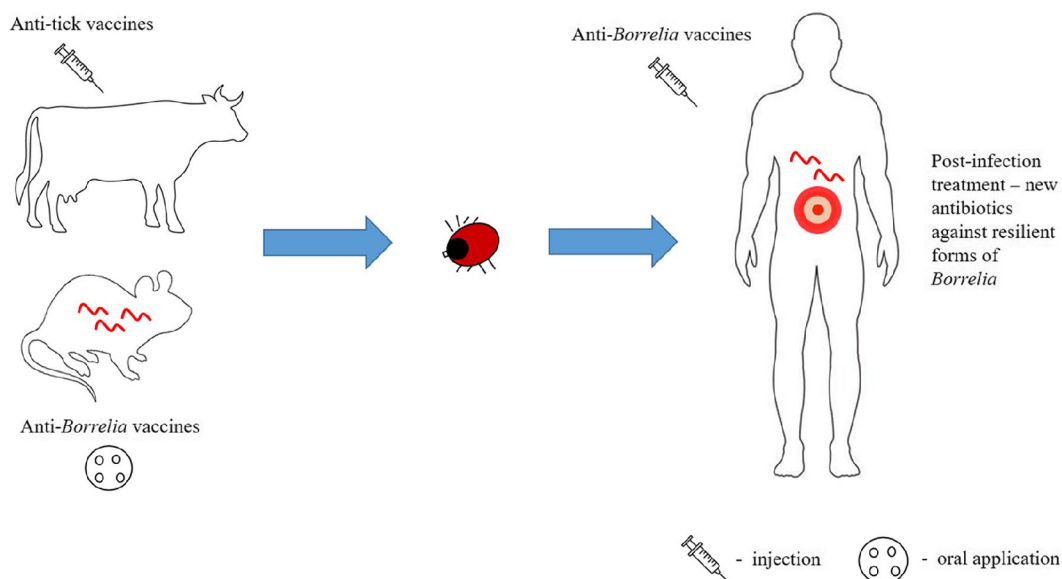


Fig. 1 The intensive research areas of current anti-*Borrelia* strategies. The focus is set on direct prophylactic anti-*Borrelia* strategies as well as on anti-tick vaccines

risk of Lyme borreliosis is substantially increased when tick bites are unrecognized, and the topical treatment of tick bite site is not managed soon enough after onset of tick feeding.

Antibiotic prophylactic treatment, or chemoprophylaxis, can be loosely defined as the administration of drug/antibiotics to prevent the development of a disease at the very beginning before the symptoms arise. This treatment strategy can also potentially play an important role as a method to prevent *B. burgdorferi* dissemination (Lascher and Goldmann 2016). Chemoprophylaxis with a single high dose of doxycycline after removal of tick from the patients within 72 h was found beneficial in the USA. During a 6-week follow-up period, 1 of 235 treated patients developed erythema migrans, whereas 8 of 247 in the placebo group developed this skin condition, showing that antibiotic prophylaxis may significantly reduce the chances of developing Lyme borreliosis (Nadelman et al. 2001; Warshafsky et al. 2010). However, the unnecessary (over)use of antibiotics may lead to accelerated antibiotic resistance and is not generally recommended.

New antibiotics against Lyme borreliosis

While still a matter of dispute (Auwaerter and Melia 2012; Baker and Wormser 2017; Wormser et al. 2017), there are several reports of antibiotic treatment unable to fully eradicate *B. burgdorferi* from blood and tissues (Rudenko et al. 2016). The phenomenon of tolerance to otherwise lethal doses of antibiotics and the antibiotic resistance is often attributed to so-called *B. burgdorferi* persisters. At least three morphological forms of persistent *B. burgdorferi* were described based on observations from experimental studies. They are capable of forming round bodies, L-forms, and biofilm-like structures. Persisters may remain viable despite antibiotic therapy and are able to reversibly convert into motile spirochetal forms under favorable conditions (Timmaraju et al. 2015; Vancová et al. 2017; Rudenko et al. 2019). The mechanism that makes the bacterium less susceptible to killing by therapeutic doses of antimicrobials is not known; however, human neutrophil calprotectin was shown to make *B. burgdorferi* more tolerant to penicillin (Montgomery et al. 2006). *B. burgdorferi* in culture can also become tolerant to antibiotics used in treating Lyme borreliosis such as ceftriaxone, doxycycline, and amoxicillin (Feng et al. 2014; Sharma et al. 2015).

If the still limited but slowly growing number of evidence supporting the existence of chronic/persistent Lyme borreliosis will end up being accepted by the Lyme community, new antibiotics or targeted designer drugs to treat the Lyme spirochetes will be needed to cope more efficiently with the outcomes of the disease (Stricker and Middelveen 2018). Some studies suggest that treatment of a borrelial infection with the currently available antimicrobial agents may suppress but not eradicate the infection (Middelveen et al. 2018). Therefore, new drug candidates have been investigated and found using

high-throughput screening of existing FDA-approved drugs in the USA (Feng et al. 2014; Feng et al. 2015; Pothineni et al. 2016), with the ultimate goal of complete microbial eradication and clinical cure. The usefulness and potential application in human medicine will have to be evaluated.

Prophylactic treatment strategies

Anti-*Borrelia* strategies: human-targeted approaches

Research efforts have long focused on ameliorating the symptoms and consequences of disease through treatment, commonly using various kinds of broad-spectrum antibiotics. However, prevention of the disease is far preferable to treating the short- and long-term often debilitating consequences of the disease. Human vaccination has greatly reduced the burden of infectious diseases and prevented more suffering than any other form of medical activity (Andre et al. 2008). Prophylactic vaccination of humans was the first choice for companies and health organizations for prevention of Lyme borreliosis. Despite a plethora of highly antigenic and immunologically accessible borrelial surface-exposed proteins (Gilmore et al. 1996; Hanson et al. 1998; Probert and Johnson 1998; Fikrig et al. 2004), the first and only licensed vaccine developed to prevent Lyme borreliosis was LYMERix, with efficacy of nearly 80% after all three doses had been administered (Nigrovic and Thompson 2007). It stayed on the market for only 4 years, and in 2002 it was withdrawn from the US market due to several reported cases of diversely serious side effects. The most common adverse events noted after receiving at least one dose included pain or reaction at the injection site, joint pain, muscle pain, and headache. It was hypothesized that the vaccine antigen, outer surface protein A (OspA), behaves as an autoantigen and therefore was arthritogenic. The adverse side effects were however never fully confirmed (Shaffer 2019).

VLA15 is the only vaccination program against Lyme borreliosis currently under clinical development. To follow in the footsteps of LYMERix, VLA15 vaccine candidate developed by Valneva is also OspA-based compound. However, it seeks to improve on efficacy and global applicability of the vaccine. LYMERix was a monovalent recombinant vaccine based on bacterial OspA serotype 1 derived from *B. burgdorferi* sensu stricto. This monovalent OspA serotype 1 vaccine had barely any potential to protect against the disease outside of North America based on the fact that OspA is antigenically very heterogeneous and at least six OspA serotypes are connected with *B. burgdorferi* sensu lato species present in Europe (Wilske et al. 1993). OspA serotype and *Borrelia* species exhibit a clear connection; *B. burgdorferi* sensu stricto represents OspA serotype 1; *B. afzelii* OspA serotype 2; *B. garinii* OspA serotypes 3, 5, and 6; and *B. bavariensis* OspA serotype 4. Since OspA protective

function is to great degree type-specific, a candidate vaccine designed to confer protection against the majority of Lyme borreliosis species has to contain at least two or three antigenic variants of OspA. VLA15 targets the six most common types of *Borrelia* (Comstedt et al. 2017).

An alternative approach is called pre-exposure prophylaxis, which is based on OspA-specific human monoclonal antibodies that are borreliacidal against a broad range of *Borrelia* genospecies. Unlike a vaccine, pre-exposure prophylaxis delivers a single defensive antibody and can prevent the transmission of the spirochetes from ticks to mice (Wang et al. 2016). Unless the vaccine is available, the passive administration of a protective human antibody could be an effective approach for borreliosis prophylaxis. The feasibility of using human monoclonal antibodies for pre-exposure prophylaxis has been already shown to be effective against respiratory virus infection (Wang et al. 2011).

OspA, expressed during the tick stage of the pathogen life cycle, is proposed to be an adhesin that binds the spirochetes to the midgut cells using the tick receptor molecule, TROSPA (Pal et al. 2004). The primary mode of action of OspA-based vaccines is to block the migration of the spirochetes from the midgut to the salivary glands of the tick. It is a rather unusual mechanism as it occurs within the tick vector rather than in the vaccinated entity. Several other surface-exposed molecules were identified during this time, and their potential suitability as vaccine candidates have been examined. These, most often lipoproteins, play important roles in various aspects of tick colonization (Fikrig et al. 2004), mammalian infection, and host immune evasion and persistent infection (Lawrenz et al. 2004). This is either through direct binding to the target tissues or by interacting with host factors to create favorable conditions for *Borrelia* survival. Decorin-binding protein A (DbpA) is an outer surface molecule that is expressed on mammalian host-adapted *B. burgdorferi*. This lipoprotein has exhibited vaccine efficacy against experimental infection in the mammalian model (Hanson et al. 1998; Cassatt et al. 1998) and was shown to be immunogenic during human Lyme borreliosis (Cinco et al. 2000). Fibronectin-binding protein BBK32 plays an important role in the attachment to the extracellular matrix. BBK32 is highly immunogenic and is present in sera of Lyme disease-infected patients (Heikkilä et al. 2002; Lahdenne et al. 2006). BBK32 antisera can interfere with borreliosis transmission at various stages of the vector-host life cycle (Fikrig et al. 2000). Outer surface protein C (OspC) is required for early mammalian infection (Grimm et al. 2004) and has been tested as vaccine candidate against *B. burgdorferi* infection with varying results (Zhong et al. 1999; Earnhart and Marconi 2007).

Vaccination trials testing various lipoprotein candidates have yielded mixed results despite the generation of robust antibody titers. In order to improve on the efficacy, vaccine cocktails containing multiple immunogens have been formulated and

tested. A DbpA/OspA combination vaccine protected against 100-fold-higher challenge doses than did either single antigen vaccine or and conferred protection against various *Borrelia* genospecies (Hanson et al. 2000). Similarly, an OspA/OspC combination showed increased vaccine efficacy compared to single component immunizations (Wallich et al. 2001). A triple combination vaccine of DbpA, BBK32, and OspC was shown to be more effective than a single or double antigen vaccine in mice. Interestingly, the ratio of each component has an impact on the overall vaccine efficacy (Brown et al. 2005). The situation is further complicated by the existence of at least five species of *B. burgdorferi* sensu lato as causes of human Lyme borreliosis: *B. burgdorferi* sensu stricto, *B. afzelii*, *B. bavariensis*, *B. mayonii* and *B. garinii*. To deal with the high degree of heterogeneity of many proteins between the *Borrelia* strains and species, some research groups have focused on the development of a combination vaccine containing multivalent chimeric vaccinogens with protective effects against diverse Lyme species. As a result, multivalent OspC-based (Earnhart et al. 2007; Earnhart and Marconi 2007) and OspA-based (Wressnigg et al. 2013) chimeric vaccines targeting a broad spectrum of *Borrelia* species have been developed for prevention of Lyme borreliosis in Europe and the USA, and possibly worldwide. Notably, certain surface proteins that fail to evoke detectable antibody response in the mammalian host during the experimental infection are still able to elicit high-titer and long-term antibody response when applied in a recombinant form (Kung et al. 2016).

Not only the borreliosis (lipo)proteins but also glycolipids (Schröder et al. 2003) and polymers consisting of sugars and peptides (Jutras et al. 2019) have shown to be antigenic and could be potential vaccine candidates, or at least serve as adjuvants. The glycolipid, acylated cholesteryl galactoside (ACGal), acts as a strong immunogen as specific antibodies against this compound are frequently found during late stage of the disease (Stübs et al. 2009). Notably, all major Lyme species possess this antigen (Stübs et al. 2009). The strategy to exploit this or somewhat similar molecules is considerably appealing for the development of a single universal “pan-vaccine” to control multiple infectious agents concomitantly (Cabezas-Cruz and de la Fuente 2017). For example, galactose- α -1,3-galactose (α -Gal) epitope is highly immunogenic in humans and is present on the surface of a number of deadly pathogens causing diseases such as malaria, sleeping sickness, or Chagas disease. The practical benefits of immunization with α -Gal against pathogens with α -Gal on their surface have been already demonstrated (Cabezas-Cruz and de la Fuente 2017; de la Fuente et al. 2019).

Anti-tick strategies

Ticks are obligate hematophagous arthropods and are considered to be second only to mosquitoes as vectors of human

infectious diseases worldwide. Predominantly due to climate change, ticks have spread to altitudes and latitudes where they were not present earlier (Jore et al. 2011; Jore et al. 2014), and the pathogens transmitted by ticks represent a new health threat in these areas. At least 15 tick-borne bacterial pathogens including *Rickettsia*, *Ehrlichia*, *Francisella*, and several species of the *Borrelia burgdorferi* sensu lato complex are known to be transmitted by ticks. Viral pathogens that can cause fatal diseases in human such as tick-borne encephalitis virus (TBEV) and Powassan virus are found in ticks as are protozoan parasites of the genus *Babesia* (Parola and Raoult 2001; Shi et al. 2018). Finding an efficient way to prevent ticks from feeding and therefore transmitting multiple human pathogens would kill more than two birds with one stone and would facilitate the management of many emerging infectious diseases.

Potential vaccine candidates

The supreme solution to inhibit transmission of multiple pathogens from the tick vector to humans would be development of single universal vaccine. An alternate approach to targeting antigens that are common to many tick-borne pathogens (as discussed above) is to use tick antigens as targets of immune intervention. Recently, the identification and development of such an anti-tick vaccine has been the subject of intensive research (Sprong et al. 2014; Rego et al. 2019). Multiple factors influence the efficacy of an anti-tick vaccine. As any other vaccine candidate, the vaccinogen should firstly be highly immunogenic, be able to provide long-lasting immunity, be associated with a vital function of the tick, and preferably be able to produce cross-protective immune responses against different tick species. Additionally, the immunogen should be expressed during different stages of the tick's life cycle, allowing different tick stages to be targeted. Ideally, future anti-tick vaccine should be applicable to wildlife and domestic animals and eventually also for humans.

There are three families of ticks. The family *Ixodidae*, or “hard ticks” and the *Argasidae*, or “soft ticks” are known to transmit pathogens causing diseases to humans. The family *Nuttalliellidae*, represented by a single species confined to Southern Africa, is not known as a pathogen-associated vector (Keirans et al. 1976). Ticks from *Ixodes* genus normally take 3 to 7 days to feed, allowing the host to mount an immune response against exposed tick antigens. The pathogens exploit saliva-induced modulation of immune defense exerted by the host to promote their transmission and infection, so-called saliva-assisted transmission (SAT) (Nuttall and Labuda 2004). Tick saliva, introduced into host skin during the feeding process, contains a wide range of proteins with anti-inflammatory, anti-complement, and anti-hemostatic activity (Chmelar et al. 2011; Perner et al. 2018).

The composition of tick saliva changes during the course of tick feeding as the tick counters the dynamic response of the

host and appears to differ for different pathogens and tick vector species and possibly can even depend on the mammalian host species (Nuttall 2019). At least a few tick salivary gland proteins seem to facilitate *B. burgdorferi* transmission. Tick histamine release factor (tHRF) is upregulated in *B. burgdorferi*-infected *Ixodes scapularis* ticks. Silencing tHRF by RNA interference significantly impairs tick feeding and reduces spirochete burden in mice. Active immunization with recombinant tHRF or passive injection of tHRF antiserum decreases the efficiency of tick feeding and *B. burgdorferi* burden in mice (Dai et al. 2010). Additionally, a 15-kDa tick salivary gland protein Salp15 protects the spirochete directly from host immune responses by binding to the OspC of *B. burgdorferi* spirochetes (Ramamoorthi et al. 2005). Salp15 is also known to be able to suppress host immunity by binding to CD4 coreceptor to inhibit CD4⁺ T-cell activation, inhibiting subsequent receptor ligand-induced cell signaling, and altering the expression levels of cytokines (Anguita et al. 2002; Hovius et al. 2008). Tick salivary lectin pathway inhibitor (TSLPI) is a feeding-induced salivary protein present in *I. scapularis* (Schuijt et al. 2011) and *I. ricinus* (Wagemakers et al. 2016). Unlike Salp15, TSLPI does not adhere to *B. burgdorferi* but instead interacts with the lectin complement cascade. TSLPI-silenced ticks or ticks feeding on mice immunized with TSLPI are impaired in *B. burgdorferi* transmission. Moreover, *B. burgdorferi* acquisition and persistence in tick midguts are reduced in ticks feeding on TSLPI-immunized mice, signifying a crucial role in both *B. burgdorferi* transmission to the mammalian host as well as *B. burgdorferi* acquisition and persistence in ticks (Schuijt et al. 2011).

The design of transcriptomic and proteomic studies for conserved tick proteins involved in pathogen transmission is quite cumbersome due to the variation in transmission times for different pathogens during the tick feeding process. These complications could be avoided by targeting the niche organ where the spirochete resides before being transmitted – the tick midgut. The tick midgut protein Bm86 from *Rhipicephalus microplus* has been used as an immunogen in two licensed tick vaccines TickGARD (now discontinued) and Gavac since the 1990s (de la Fuente et al. 2007). Bm86-based vaccines have diverse efficacies reported worldwide (45–100%), with the greatest effect on the reduction of larval infestations in subsequent generations (Tabor 2018). Nevertheless, it has limited efficacy against other tick species (de la Fuente et al. 2007). Recently, it has been shown that *I. scapularis* secretes a protein, PIXR, that modulates the tick gut microbiome and interfere with the ability of *B. burgdorferi* to colonize the tick midgut (Narasimhan et al. 2017). This approach exploits the principle of rendering competent vectors incompetent and targets tick antigens that the parasites encounter during their life cycle. The tick microbiome could possibly be an additional target for the preventive strategies against the tick-borne pathogens (Rego et al. 2019).

Non-vaccine anti-tick strategies

Information campaigns are the most common policy measures to reduce the risk of tick-borne diseases. Common recommendations and prevention measures against Lyme borreliosis include avoiding tick-endemic areas, staying on trails while in high-risk areas, the usage of protective clothing, using tick repellents, and checking the body for ticks and removing them before or as soon as possible after they attach (Connally et al. 2009; Slunge and Boman 2018). Risk of Lyme borreliosis from an ecological perspective is measured in terms of density of infected nymphal ticks (Diuk-Wasser et al. 2012). Common methods for killing ticks include the application of acaricides to tick-rich areas, rodent hosts, or to the host animals (Hinckley et al. 2016). The acaricidal treatment of livestock remains the most effective way to prevent ticks from biting and feeding; however, the adverse effects for environmental and public health are more than self-evident (Walker 2014; De Meneghi et al. 2016).

Small mammals are considered the primary hosts of tick larvae and therefore form a key determinant for the abundance of questing nymphs (Perez et al. 2016). Hence, a possible but more difficult strategy to achieve could include landscape modifications and vegetation management strategies in urban and suburban areas in a way that it favors the small mammal species that can build resistance to ticks, a phenomenon in which ticks are unable to feed successfully after several tick infestations (Perez et al. 2016). As an example, repeated infestation of bank voles by larval ticks reduced the feeding success, whereas feeding on wood mice did not negatively affect the successive feeding of ticks (Humair et al. 1999). Changes and growth of agricultural landscapes also significantly affect the communities of small mammals. Wooded habitats are considered favorable for ticks because of temperature and humidity they constantly provide (Perez et al. 2016). Deforestation would definitely be negatively related to tick density because woodland areas act as habitats for ticks and their hosts but the detrimental effects of this action are obvious. Consequently, highly unconventional strategies such as building artificial wood ant nests would be elegant and eco-friendly solutions to reduce the tick density (Zingg et al. 2018), in comparison to rather drastic solutions such as eradication of some mammalian hosts of ticks (Rand et al. 2004).

Reservoir-based approaches

Oral vaccinations

The sources of the microbes that cause infectious diseases and where the pathogens can multiply or merely survive until they are transmitted are known as reservoirs. Vector ticks must acquire *B. burgdorferi* from wildlife reservoirs as there is no clear evidence of a transovarial transmission route (Rollend

et al. 2013). Disrupting *B. burgdorferi* transmission between the tick vector and reservoir hosts is regarded as a promising strategy to reduce human exposure to Lyme borreliosis (Melo et al. 2016). Rodents are a major reservoir for Lyme borreliosis and as such a very promising target to prevent them from getting infected with *B. burgdorferi*. The development of a specific, easily distributable, thermostable, and economically viable oral vaccine for wildlife reservoirs surrounding human communities could significantly reduce the incidence of Lyme borreliosis (Gomes-Solecki et al. 2006).

Oral vaccination is of high interest as a tool to prevent the spread of Lyme borreliosis as it can be used to deliver the vaccine to humans, domestic animals, and wildlife reservoirs of *B. burgdorferi*. The immunogen can be administered as a purified antigen (Luke et al. 1997) or as a genetically altered *Escherichia coli* (Fikrig et al. 1991). A number of oral vaccines based in *E. coli* expressing recombinant OspC, OspB, BBK32 from *B. burgdorferi*, and Salp25 and Salp15 from *Ixodes scapularis* were developed. Of the five immunogenic candidates, only OspC induced significant antibody response in mice when they were immunized by intragastric inoculation. Nevertheless, the antibodies did not prevent dissemination of *B. burgdorferi* as determined by the presence of spirochetes in the ear, heart, and bladder (Melo et al. 2016). Again, OspA seems to be a more promising oral vaccine candidate as oral vaccination of wild white-footed mice resulted in reductions of 23% and 76% in the nymphal infection prevalence (Richer et al. 2014). Significant decreases in tick infection were observed within 2–3 years after oral vaccine deployment. The usage of reservoir-based vaccines as part of a strategy to fight the expansion of Lyme borreliosis is also vastly dependent on the development of effective strategies for delivery of the immunogen. One of the promising approaches is the usage of *Lactobacillus plantarum* as a live vaccine delivery vehicle. These bacteria are naturally associated with the gastrointestinal tract and generally regarded as safe by the FDA. Oral administration of live *L. plantarum* expressing OspA was shown to be effective in blocking transmission of *B. burgdorferi* (del Rio et al. 2008). Not only is the deployment of borrelial immunogens in oral vaccines achievable but also the tick antigens can be used to inhibit the transmission of *B. burgdorferi*. Using the recombinant vaccinia virus, a single dose of the subolesin vaccine resulted in strong immune system response and partial protection from *B. burgdorferi* infection among vaccinated mice (Bensaci et al. 2012).

Immunization by genome editing

A novel theoretical model for prevention of tick-borne diseases, using CRISPR-based genome editing technology, has been recently suggested (Buchthal et al. 2019). Mice Against Ticks is a proof of principle project that aims to heritably immunize local wild white-footed mouse populations against

Lyme borreliosis and, potentially, against ticks using antibodies derived from natural adaptive immunity, with the ultimate goal to reduce the reservoir competence of a host for many decades. It is important to emphasize that the protective antibodies have not yet been identified, nor has heritable genome editing been ever achieved in white-footed mice.

Conclusion

Presently, the use of acaricides constitutes a major component of integrated tick control strategies and therefore indirectly acts as the first line of human-induced defense against a multitude of tick-borne pathogens. However, this is accompanied by the selection of acaricide-resistant ticks and severe pollution of the environment (Kunz and Kemp 1994). Lyme borreliosis is the most common disease spread by ticks in the Northern Hemisphere with an ever increasing incidence, and as such this disease is a major topic on the public health agenda. In order to effectively control the spread of Lyme borreliosis, a multifront battle should be seriously considered, involving environment management, wildlife and domestic animal vaccinations, and of course policymaking. New approaches and strategies that target against Lyme borreliosis, including elements of the tick vector, the reservoir hosts, and the *Borrelia* pathogen itself, are being developed. Human vaccination is the most effective means of prevention. However, there are a lot of hurdles to overcome, not just regulatory and scientific ones, but public acceptance as well. Let us hope that the challenges present today will be met and an efficient defense against Lyme borreliosis will not only be found but also publicly available in the very near future.

Author contribution MS took the lead role in manuscript preparation with direction and assistance from LG and ROMR.

Funding information This study was supported by the Czech Science Foundation grant 17-21244S and European Union FP7 project ANTIDotE (602272-2).

Compliance with ethical standards

Conflict of interest The authors declare that they have no conflict of interest.

Ethical approval This article does not contain any studies with human participants or animals performed by any of the authors.

References

- Andre F, Booy R, Bock H, Clemens J, Datta S, John T, Lee B, Lolekha S, Peltola H, Ruff T, Santosham M, Schmitt H (2008) Vaccination greatly reduces disease, disability, death and inequity worldwide. *Bull World Health Organ* 86:140–146. <https://doi.org/10.2471/BLT.07.040089>
- Anguita J, Ramamoorthi N, Hovius JWR, Das S, Thomas V, Persinski R, Conze D, Askenase PW, Rincón M, Kantor FS, Fikrig E (2002) Salp15, an *Ixodes scapularis* salivary protein, inhibits CD4(+) T cell activation. *Immunity* 16:849–859
- Auwaerter PG, Melia MT (2012) Bullying *Borrelia*: when the culture of science is under attack. *Trans Am Clin Climatol Assoc* 123:79–90
- Baker PJ, Wormser GP (2017) The clinical relevance of studies on *Borrelia burgdorferi* persists. *Am J Med* 130:1009–1010. <https://doi.org/10.1016/j.amjmed.2017.04.014>
- Bensaci M, Bhattacharya D, Clark R, Hu LT (2012) Oral vaccination with vaccinia virus expressing the tick antigen subolesin inhibits tick feeding and transmission of *Borrelia burgdorferi*. *Vaccine* 30:6040–6046. <https://doi.org/10.1016/j.vaccine.2012.07.053>
- Brown EL, Kim JH, Reisenbichler ES, Höök M (2005) Multicomponent Lyme vaccine: three is not a crowd. *Vaccine* 23:3687–3696. <https://doi.org/10.1016/j.vaccine.2005.02.006>
- Buchthal J, Evans SW, Lunshof J, Telford SR, Esvelt KM (2019) Mice against ticks: an experimental community-guided effort to prevent tick-borne disease by altering the shared environment. *Philos Trans R Soc Lond Ser B Biol Sci* 374:20180105. <https://doi.org/10.1098/rstb.2018.0105>
- Cabezas-Cruz A, de la Fuente J (2017) Immunity to α -gal: toward a single-antigen pan-vaccine to control major infectious diseases. *ACS Cent Sci* 3:1140–1142. <https://doi.org/10.1021/acscentsci.7b00517>
- Cadavid D, O'Neill T, Schaefer H, Pachner AR (2000) Localization of *Borrelia burgdorferi* in the nervous system and other organs in a nonhuman primate model of Lyme disease. *Lab Invest J Tech Methods Pathol* 80:1043–1054. <https://doi.org/10.1038/labinvest.3780109>
- Cassatt DR, Patel NK, Ulbrandt ND, Hanson MS (1998) DbpA, but not OspA, is expressed by *Borrelia burgdorferi* during spirochetemia and is a target for protective antibodies. *Infect Immun* 66:5379–5387
- Chmelar J, Oliveira CJ, Rezacova P, Francischetti IMB, Kovarova Z, Pejler G, Kopacek P, Ribeiro JMC, Mares M, Kopecky J, Kotsyfakis M (2011) A tick salivary protein targets cathepsin G and chymase and inhibits host inflammation and platelet aggregation. *Blood* 117:736–744. <https://doi.org/10.1182/blood-2010-06-293241>
- Cinco M, Ruscio M, Rapagna F (2000) Evidence of Dbps (decorin binding proteins) among European strains of *Borrelia burgdorferi* sensu lato and in the immune response of LB patient sera. *FEMS Microbiol Lett* 183:111–114. <https://doi.org/10.1111/j.1574-6968.2000.tb08942.x>
- Comstedt P, Schüler W, Meinke A, Lundberg U (2017) The novel Lyme borreliosis vaccine VLA15 shows broad protection against *Borrelia* species expressing six different OspA serotypes. *PLoS One* 12:e0184357. <https://doi.org/10.1371/journal.pone.0184357>
- Connally NP, Durante AJ, Yousey-Hindes KM, Meek JI, Nelson RS, Heimer R (2009) Peridomestic Lyme disease prevention: results of a population-based case-control study. *Am J Prev Med* 37:201–206. <https://doi.org/10.1016/j.amepre.2009.04.026>
- Dai J, Narasimhan S, Zhang L, Liu L, Wang P, Fikrig E (2010) Tick histamine release factor is critical for *Ixodes scapularis* engorgement and transmission of the Lyme disease agent. *PLoS Pathog* 6:e1001205. <https://doi.org/10.1371/journal.ppat.1001205>
- de la Fuente J, Almazán C, Canales M, Pérez de la Lastra JM, Kocan KM, Willadsen P (2007) A ten-year review of commercial vaccine performance for control of tick infestations on cattle. *Anim Health Res Rev* 8:23–28. <https://doi.org/10.1017/S1466252307001193>
- de la Fuente J, Pacheco I, Villar M, Cabezas-Cruz A (2019) The alpha-gal syndrome: new insights into the tick-host conflict and cooperation. *Parasit Vectors* 12:154. <https://doi.org/10.1186/s13071-019-3413-z>

- De Meneghi D, Stachurski F, Adakal H (2016) Experiences in tick control by acaricide in the traditional cattle sector in Zambia and Burkina Faso: possible environmental and public health implications. *Front Public Health* 4:239. <https://doi.org/10.3389/fpubh.2016.00239>
- del Rio B, Dattwyler RJ, Aroso M, Neves V, Meirelles L, Seegers JFML, Gomes-Solecki M (2008) Oral immunization with recombinant *Lactobacillus plantarum* induces a protective immune response in mice with Lyme disease. *Clin Vaccine Immunol* 15:1429–1435. <https://doi.org/10.1128/CVI.00169-08>
- Diuk-Wasser MA, Hoen AG, Cislo P, Brinkerhoff R, Hamer SA, Rowland M, Cortinas R, Voure'h G, Melton F, Hickling GJ, Tsao JI, Bunikis J, Barbour AG, Kitron U, Piesman J, Fish D (2012) Human risk of infection with *Borrelia burgdorferi*, the Lyme disease agent, in eastern United States. *Am J Trop Med Hyg* 86:320–327. <https://doi.org/10.4269/ajtmh.2012.11-0395>
- Earnhart CG, Buckles EL, Marconi RT (2007) Development of an OspC-based tetraavalent, recombinant, chimeric vaccinogen that elicits bactericidal antibody against diverse Lyme disease spirochete strains. *Vaccine* 25:466–480. <https://doi.org/10.1016/j.vaccine.2006.07.052>
- Earnhart CG, Marconi RT (2007) An octavalent Lyme disease vaccine induces antibodies that recognize all incorporated OspC type-specific sequences. *Hum Vaccin* 3:281–289. <https://doi.org/10.4161/hv.4661>
- Ebady R, Niddam AF, Boczula AE, Kim YR, Gupta N, Tang TT, Odisho T, Zhi H, Simmons CA, Skare JT, Moriarty TJ (2016) Biomechanics of *Borrelia burgdorferi* vascular interactions. *Cell Rep* 16:2593–2604. <https://doi.org/10.1016/j.celrep.2016.08.013>
- Feng J, Wang T, Shi W, Zhang S, Sullivan D, Auwaerter PG, Zhang Y (2014) Identification of novel activity against *Borrelia burgdorferi* persisters using an FDA approved drug library. *Emerg Microbes Infect* 3:e49. <https://doi.org/10.1038/emi.2014.53>
- Feng J, Weitner M, Shi W, Zhang S, Sullivan D, Zhang Y (2015) Identification of additional anti-persister activity against *Borrelia burgdorferi* from an FDA drug library. *Antibiotics* 4:397–410. <https://doi.org/10.3390/antibiotics4030397>
- Fikrig E, Barthold SW, Kantor FS, Flavell RA (1991) Protection of mice from Lyme borreliosis by oral vaccination with *Escherichia coli* expressing OspA. *J Infect Dis* 164:1224–1227. <https://doi.org/10.1093/infdis/164.6.1224>
- Fikrig E, Feng W, Barthold SW, Telford SR, Flavell RA (2000) Arthropod- and host-specific *Borrelia burgdorferi* btk32 expression and the inhibition of spirochete transmission. *J Immunol* 164:5344–5351. <https://doi.org/10.4049/jimmunol.164.10.5344>
- Fikrig E, Pal U, Chen M, Anderson JF, Flavell RA (2004) OspB antibody prevents *Borrelia burgdorferi* colonization of *Ixodes scapularis*. *Infect Immun* 72:1755–1759. <https://doi.org/10.1128/iai.72.3.1755-1759.2004>
- Gilmore RD, Kappel KJ, Dolan MC, Burkot TR, Johnson BJ (1996) Outer surface protein C (OspC), but not P39, is a protective immunogen against a tick-transmitted *Borrelia burgdorferi* challenge: evidence for a conformational protective epitope in OspC. *Infect Immun* 64:2234–2239
- Gomes-Solecki MJC, Brisson DR, Dattwyler RJ (2006) Oral vaccine that breaks the transmission cycle of the Lyme disease spirochete can be delivered via bait. *Vaccine* 24:4440–4449. <https://doi.org/10.1016/j.vaccine.2005.08.089>
- Grimm D, Tilly K, Byram R, Stewart PE, Krum JG, Bueschel DM, Schwan TG, Policastro PF, Elias AF, Rosa PA (2004) Outer-surface protein C of the Lyme disease spirochete: a protein induced in ticks for infection of mammals. *Proc Natl Acad Sci U S A* 101:3142–3147. <https://doi.org/10.1073/pnas.0306845101>
- Hanson MS, Cassatt DR, Guo BP, Patel NK, McCarthy MP, Dorward DW, Höök M (1998) Active and passive immunity against *Borrelia burgdorferi* decorin binding protein a (DbpA) protects against infection. *Infect Immun* 66:2143–2153
- Hanson MS, Patel NK, Cassatt DR, Ulbrandt ND (2000) Evidence for vaccine synergy between *Borrelia burgdorferi* decorin binding protein a and outer surface protein a in the mouse model of Lyme borreliosis. *Infect Immun* 68:6457–6460
- Heikkilä T, Seppälä I, Saxén H, Panelius J, Peltomaa M, Julin T, Carlsson S-A, Lahdenne P (2002) Recombinant BBK32 protein in serodiagnosis of early and late Lyme borreliosis. *J Clin Microbiol* 40:1174–1180. <https://doi.org/10.1128/JCM.40.4.1174-1180.2002>
- Hinckley AF, Meek JI, Ray JAE, Niesobecki SA, Connally NP, Feldman KA, Jones EH, Backenson PB, White JL, Lukacik G, Kay AB, Miranda WP, Mead PS (2016) Effectiveness of residential acaricides to prevent Lyme and other tick-borne diseases in humans. *J Infect Dis* 214:182–188. <https://doi.org/10.1093/infdis/jiv775>
- Hovius JWR, de Jong MAWP, den Dunnen J, Litjens M, Fikrig E, van der Poll T, Gringhuis SI, Geijtenbeek TBH (2008) Salp15 binding to DC-SIGN inhibits cytokine expression by impairing both nucleosome remodeling and mRNA stabilization. *PLoS Pathog* 4:e31. <https://doi.org/10.1371/journal.ppat.0040031>
- Hubálek Z (2009) Epidemiology of Lyme borreliosis. *Curr Probl Dermatol* 37:31–50. <https://doi.org/10.1159/000213069>
- Humair PF, Rais O, Gern L (1999) Transmission of *Borrelia afzelii* from *Apodemus* mice and *Clethrionomys* voles to *Ixodes ricinus* ticks: differential transmission pattern and overwintering maintenance. *Parasitology* 118(Pt 1):33–42. <https://doi.org/10.1017/s0031182098003564>
- Jore S, Vanwambeke SO, Viljugrein H, Isaksen K, Kristoffersen AB, Woldehiwet Z, Johansen B, Brun E, Brun-Hansen H, Westermann S, Larsen I-L, Ytrehus B, Hofshagen M (2014) Climate and environmental change drives *Ixodes ricinus* geographical expansion at the northern range margin. *Parasit Vectors* 7:11. <https://doi.org/10.1186/1756-3305-7-11>
- Jore S, Viljugrein H, Hofshagen M, Brun-Hansen H, Kristoffersen AB, Nygård K, Brun E, Ottesen P, Sævik BK, Ytrehus B (2011) Multi-source analysis reveals latitudinal and altitudinal shifts in range of *Ixodes ricinus* at its northern distribution limit. *Parasit Vectors* 4:84. <https://doi.org/10.1186/1756-3305-4-84>
- Jutras BL, Lochhead RB, Kloos ZA, Biboy J, Strle K, Booth CJ, Govers SK, Gray J, Schumann P, Vollmer W, Bockenstedt LK, Steere AC, Jacobs-Wagner C (2019) *Borrelia burgdorferi* peptidoglycan is a persistent antigen in patients with Lyme arthritis. *Proc Natl Acad Sci U S A* 116:13498–13507. <https://doi.org/10.1073/pnas.1904170116>
- Kalmár Z, Mihalca AD, Dumitrache MO, Gherman CM, Magdaş C, Mircean V, Oltean M, Domşa C, Matei IA, Mărcuţan DI, Sándor AD, D'Amico G, Paştui A, Györke A, Gavrea R, Marosi B, Ionică A, Burkhardt E, Toriay H, Cozma V (2013) Geographical distribution and prevalence of *Borrelia burgdorferi* genospecies in questing *Ixodes ricinus* from Romania: a countrywide study. *Ticks Tick-Borne Dis* 4:403–408. <https://doi.org/10.1016/j.ttbdis.2013.04.007>
- Keirans JE, Clifford CM, Hoogstraal H, Easton ER (1976) Discovery of *Nuttalliella namaqua* Bedford (*Acarina: Ixodoidea: Nuttalliellidae*) in Tanzania and redescription of the female based on scanning electron microscopy. *Ann Entomol Soc Am* 69:926–932. <https://doi.org/10.1093/aesa/69.5.926>
- Krupka I, Straubinger RK (2010) Lyme borreliosis in dogs and cats: background, diagnosis, treatment and prevention of infections with *Borrelia burgdorferi* sensu stricto. *Vet Clin North Am Small Anim Pract* 40:1103–1119. <https://doi.org/10.1016/j.cvsm.2010.07.011>
- Kuehn BM (2013) CDC estimates 300,000 US cases of Lyme disease annually. *JAMA* 310:1110. <https://doi.org/10.1001/jama.2013.278331>
- Kung F, Kaur S, Smith AA, Yang X, Wilder CN, Sharma K, Buyuktanir O, Pal U (2016) A *Borrelia burgdorferi* surface-exposed transmembrane protein lacking detectable immune responses supports pathogen persistence and constitutes a vaccine target. *J Infect Dis* 213:1786–1795. <https://doi.org/10.1093/infdis/jiw013>

- Kunz SE, Kemp DH (1994) Insecticides and acaricides: resistance and environmental impact. *Rev Sci Tech Int Off Epizoot* 13:1249–1286. <https://doi.org/10.20506/rst.13.4.816>
- Lahdenne P, Sarvas H, Kajanus R, Eholuoto M, Sillanpää H, Seppälä I (2006) Antigenicity of borrelial protein BBK32 fragments in early Lyme borreliosis. *J Med Microbiol* 55:1499–1504. <https://doi.org/10.1099/jmm.0.46621-0>
- Lascher S, Goldmann DR (2016) Efficacy of antibiotic prophylaxis for the prevention of Lyme disease after tick bite. *Am J Med* 129:935–937. <https://doi.org/10.1016/j.amjmed.2016.05.011>
- Lawrenz MB, Wooten RM, Norris SJ (2004) Effects of vlsE complementation on the infectivity of *Borrelia burgdorferi* lacking the linear plasmid lp28-1. *Infect Immun* 72:6577–6585. <https://doi.org/10.1128/IAI.72.11.6577-6585.2004>
- Lee J, Wormser GP (2008) Pharmacodynamics of doxycycline for chemoprophylaxis of Lyme disease: preliminary findings and possible implications for other antimicrobials. *Int J Antimicrob Agents* 31:235–239. <https://doi.org/10.1016/j.ijantimicag.2007.11.011>
- Ljøstad U, Skogvoll E, Eikeland R, Midgard R, Skarpaas T, Berg A, Mygland A (2008) Oral doxycycline versus intravenous ceftriaxone for European Lyme neuroborreliosis: a multicentre, non-inferiority, double-blind, randomised trial. *Lancet Neurol* 7:690–695. [https://doi.org/10.1016/S1474-4422\(08\)70119-4](https://doi.org/10.1016/S1474-4422(08)70119-4)
- Luke CJ, Huebner RC, Kasmiersky V, Barbour AG (1997) Oral delivery of purified lipoprotein OspA protects mice from systemic infection with *Borrelia burgdorferi*. *Vaccine* 15:739–746. [https://doi.org/10.1016/S0264-410X\(97\)00219-3](https://doi.org/10.1016/S0264-410X(97)00219-3)
- Margos G, Fingerle V, Reynolds S (2019) *Borrelia bavariensis*: vector switch, niche invasion, and geographical spread of a tick-borne bacterial parasite. *Front Ecol Evol* 7:401. <https://doi.org/10.3389/fevo.2019.00401>
- Melo R, Richer L, Johnson DL, Gomes-Solecki M (2016) Oral immunization with OspC does not prevent tick-borne *Borrelia burgdorferi* infection. *PLoS One* 11:e0151850. <https://doi.org/10.1371/journal.pone.0151850>
- Middelveen MJ, Sapi E, Burke J, Filush KR, Franco A, Fesler MC, Stricker RB (2018) Persistent *Borrelia* infection in patients with ongoing symptoms of Lyme disease. *Healthcare* 6:2. <https://doi.org/10.3390/healthcare6020033>
- Montgomery RR, Schreck K, Wang X, Malawista SE (2006) Human neutrophil calprotectin reduces the susceptibility of *Borrelia burgdorferi* to penicillin. *Infect Immun* 74:2468–2472. <https://doi.org/10.1128/IAI.74.4.2468-2472.2006>
- Moriarty TJ, Norman MU, Colarusso P, Bankhead T, Kubes P, Chaconas G (2008) Real-time high resolution 3D imaging of the Lyme disease spirochete adhering to and escaping from the vasculature of a living host. *PLoS Pathog* 4:e1000090. <https://doi.org/10.1371/journal.ppat.1000090>
- Nadelman RB, Nowakowski J, Fish D, Falco RC, Freeman K, McKenna D, Welch P, Marcus R, Agüero-Rosenfeld ME, Dennis DT, Wormser GP, Tick Bite Study Group (2001) Prophylaxis with single-dose doxycycline for the prevention of Lyme disease after an *Ixodes scapularis* tick bite. *N Engl J Med* 345:79–84. <https://doi.org/10.1056/NEJM200107123450201>
- Narasimhan S, Schuijt TJ, Abraham NM, Rajeevan N, Coumou J, Graham M, Robson A, Wu M-J, Daffre S, Hovius JW, Fikrig E (2017) Modulation of the tick gut milieu by a secreted tick protein favors *Borrelia burgdorferi* colonization. *Nat Commun* 8:184. <https://doi.org/10.1038/s41467-017-00208-0>
- Nigrovic LE, Thompson KM (2007) The Lyme vaccine: a cautionary tale. *Epidemiol Infect* 135:1–8. <https://doi.org/10.1017/S0950268806007096>
- Norman MU, Moriarty TJ, Dresser AR, Millen B, Kubes P, Chaconas G (2008) Molecular mechanisms involved in vascular interactions of the Lyme disease pathogen in a living host. *PLoS Pathog* 4:e1000169. <https://doi.org/10.1371/journal.ppat.1000169>
- Nuttall PA (2019) Tick saliva and its role in pathogen transmission. *Wien Klin Wochenschr*:1–12. <https://doi.org/10.1007/s00508-019-1500-y>
- Nuttall PA, Labuda M (2004) Tick-host interactions: saliva-activated transmission. *Parasitology* 129(Suppl):S177–S189. <https://doi.org/10.1017/s0031182004005633>
- Pal U, Li X, Wang T, Montgomery RR, Ramamoorthi N, Desilva AM, Bao F, Yang X, Pypaert M, Pradhan D, Kantor FS, Telford S, Anderson JF, Fikrig E (2004) TROSPA, an *Ixodes scapularis* receptor for *Borrelia burgdorferi*. *Cell* 119:457–468. <https://doi.org/10.1016/j.cell.2004.10.027>
- Parola P, Raoult D (2001) Ticks and tickborne bacterial diseases in humans: an emerging infectious threat. *Clin Infect Dis Off Publ Infect Dis Soc Am* 32:897–928. <https://doi.org/10.1086/319347>
- Perez G, Bastian S, Agoulon A, Bouju A, Durand A, Faille F, Lebert I, Rantier Y, Plantard O, Butet A (2016) Effect of landscape features on the relationship between *Ixodes ricinus* ticks and their small mammal hosts. *Parasit Vectors* 9:20. <https://doi.org/10.1186/s13071-016-1296-9>
- Perner J, Kropáčková S, Kopáček P, Ribeiro JMC (2018) Sialome diversity of ticks revealed by RNAseq of single tick salivary glands. *PLoS Negl Trop Dis* 12:e0006410. <https://doi.org/10.1371/journal.pntd.0006410>
- Piesman J, Hojgaard A, Ullmann AJ, Dolan MC (2014) Efficacy of an experimental azithromycin cream for prophylaxis of tick-transmitted Lyme disease spirochete infection in a murine model. *Antimicrob Agents Chemother* 58:348–351. <https://doi.org/10.1128/AAC.01932-13>
- Pothineni VR, Wagh D, Babar MM, Inayathullah M, Solow-Cordero D, Kim K-M, Samineni AV, Parekh MB, Tayebi L, Rajadas J (2016) Identification of new drug candidates against *Borrelia burgdorferi* using high-throughput screening. *Drug Des Devel Ther* 10:1307–1322. <https://doi.org/10.2147/DDDT.S101486>
- Probert WS, Johnson BJ (1998) Identification of a 47 kDa fibronectin-binding protein expressed by *Borrelia burgdorferi* isolate B31. *Mol Microbiol* 30:1003–1015
- Ramamoorthi N, Narasimhan S, Pal U, Bao F, Yang XF, Fish D, Anguita J, Norgard MV, Kantor FS, Anderson JF, Koski RA, Fikrig E (2005) The Lyme disease agent exploits a tick protein to infect the mammalian host. *Nature* 436:573–577. <https://doi.org/10.1038/nature03812>
- Rand PW, Lubelczyk C, Holman MS, Lacombe EH, Smith RP (2004) Abundance of *Ixodes scapularis* (Acari: Ixodidae) after the complete removal of deer from an isolated offshore island, endemic for Lyme disease. *J Med Entomol* 41:779–784. <https://doi.org/10.1603/0022-2585-41.4.779>
- Rego ROM, Trentelman JJA, Anguita J, Nijhof AM, Sprong H, Klempa B, Hajdusek O, Tomás-Cortázar J, Azagi T, Strnad M, Knorr S, Sima R, Jalovecka M, Fumačová Havlíková S, Ličková M, Sláviková M, Kopacek P, Grubhoffer L, Hovius JW (2019) Counterattacking the tick bite: towards a rational design of anti-tick vaccines targeting pathogen transmission. *Parasit Vectors* 12:229. <https://doi.org/10.1186/s13071-019-3468-x>
- Ribeiro JM, Mather TN, Piesman J, Spielman A (1987) Dissemination and salivary delivery of Lyme disease spirochetes in vector ticks (Acari: Ixodidae). *J Med Entomol* 24:201–205. <https://doi.org/10.1093/jmedent/24.2.201>
- Richer LM, Brisson D, Melo R, Ostfeld RS, Zeidner N, Gomes-Solecki M (2014) Reservoir targeted vaccine against *Borrelia burgdorferi*: a new strategy to prevent Lyme disease transmission. *J Infect Dis* 209:1972–1980. <https://doi.org/10.1093/infdis/jiu005>
- Rollend L, Fish D, Childs JE (2013) Transovarial transmission of *Borrelia* spirochetes by *Ixodes scapularis*: a summary of the literature and recent observations. *Ticks Tick-Borne Dis* 4:46–51. <https://doi.org/10.1016/j.ttbdis.2012.06.008>
- Rudenko N, Golovchenko M, Kybicova K, Vancova M (2019) Metamorphoses of Lyme disease spirochetes: phenomenon of

- Borrelia* persists. Parasit Vectors 12:237. <https://doi.org/10.1186/s13071-019-3495-7>
- Rudenko N, Golovchenko M, Vancova M, Clark K, Grubhoffer L, Oliver JH (2016) Isolation of live *Borrelia burgdorferi* sensu lato spirochaetes from patients with undefined disorders and symptoms not typical for Lyme borreliosis. Clin Microbiol Infect 22:267–e9–15. <https://doi.org/10.1016/j.cmi.2015.11.009>
- Schröder NWJ, Schombel U, Heine H, Göbel UB, Zähringer U, Schumann RR (2003) Acylated cholesteryl galactoside as a novel immunogenic motif in *Borrelia burgdorferi* sensu stricto. J Biol Chem 278:33645–33653. <https://doi.org/10.1074/jbc.M305799200>
- Schuijt TJ, Coumou J, Narasimhan S, Dai J, Deponte K, Wouters D, Brouwer M, Oei A, Roelofs JJTH, van Dam AP, van der Poll T, Van't Veer C, Hovius JW, Fikrig E (2011) A tick mannose-binding lectin inhibitor interferes with the vertebrate complement cascade to enhance transmission of the Lyme disease agent. Cell Host Microbe 10:136–146. <https://doi.org/10.1016/j.chom.2011.06.010>
- Schwameis M, Kündig T, Huber G, von Bidder L, Meinel L, Weisser R, Aberer E, Härter G, Weinke T, Jelinek T, Fätkenheuer G, Wollina U, Burchard G-D, Aschoff R, Nischik R, Sattler G, Popp G, Lotte W, Wiechert D, Eder G, Maus O, Staubach-Renz P, Gräfe A, Geigenberger V, Naudts I, Sebastian M, Reider N, Weber R, Heckmann M, Reisinger EC, Klein G, Wantzen J, Jilma B (2017) Topical azithromycin for the prevention of Lyme borreliosis: a randomised, placebo-controlled, phase 3 efficacy trial. Lancet Infect Dis 17:322–329. [https://doi.org/10.1016/S1473-3099\(16\)30529-1](https://doi.org/10.1016/S1473-3099(16)30529-1)
- Shaffer L (2019) Inner workings: Lyme disease vaccines face familiar challenges, both societal and scientific. Proc Natl Acad Sci U S A 116:19214–19217. <https://doi.org/10.1073/pnas.1913923116>
- Shapiro ED, Wormser GP (2017) Prophylaxis with topical azithromycin against Lyme borreliosis. Lancet Infect Dis 17:246–248. [https://doi.org/10.1016/S1473-3099\(16\)30551-5](https://doi.org/10.1016/S1473-3099(16)30551-5)
- Sharma B, Brown AV, Matluck NE, Hu LT, Lewis K (2015) *Borrelia burgdorferi*, the causative agent of Lyme disease, forms drug-tolerant persister cells. Antimicrob Agents Chemother 59:4616–4624. <https://doi.org/10.1128/AAC.00864-15>
- Shi J, Hu Z, Deng F, Shen S (2018) Tick-borne viruses. Virol Sin 33:21–43. <https://doi.org/10.1007/s12250-018-0019-0>
- Slunge D, Boman A (2018) Learning to live with ticks? The role of exposure and risk perceptions in protective behaviour against tick-borne diseases. PLoS One 13:6. <https://doi.org/10.1371/journal.pone.0198286>
- Smith R, Takkinen J (2006) Lyme borreliosis: Europe-wide coordinated surveillance and action needed? Euro Surveill Bull Eur Sur Mal Transm Eur Commun Dis Bull 11:E060622.1
- Sprong H, Trentelman J, Seemann I, Grubhoffer L, Rego RO, Hajdušek O, Kopáček P, Šima R, Nijhof AM, Anguita J, Winter P, Rotter B, Havlíková S, Klempa B, Schettters TP, Hovius JW (2014) ANTIDoT: anti-tick vaccines to prevent tick-borne diseases in Europe. Parasit Vectors 7:77. <https://doi.org/10.1186/1756-3305-7-77>
- Stanek G, Strle F (2018) Lyme borreliosis—from tick bite to diagnosis and treatment. FEMS Microbiol Rev 42:233–258. <https://doi.org/10.1093/femsre/fux047>
- Stanek G, Wormser GP, Gray J, Strle F (2012) Lyme borreliosis. Lancet Lond Engl 379:461–473. [https://doi.org/10.1016/S0140-6736\(11\)60103-7](https://doi.org/10.1016/S0140-6736(11)60103-7)
- Steere AC (2001) Lyme disease. N Engl J Med 345:115–125. <https://doi.org/10.1056/NEJM200107123450207>
- Steere AC, Malawista SE, Snyderman DR, Shope RE, Andiman WA, Ross MR, Steele FM (1977) Lyme arthritis: an epidemic of oligoarticular arthritis in children and adults in three Connecticut communities. Arthritis Rheum 20:7–17. <https://doi.org/10.1002/art.1780200102>
- Stricker RB, Middelveen MJ (2018) Better drugs for Lyme disease: focus on the spirochete. Infect Drug Resist 11:1437–1439. <https://doi.org/10.2147/IDR.S176831>
- Strnad M, Elsterová J, Schrenková J, Vancová M, Rego ROM, Grubhoffer L, Nebesářová J (2015) Correlative cryo-fluorescence and cryo-scanning electron microscopy as a straightforward tool to study host-pathogen interactions. Sci Rep 5:18029. <https://doi.org/10.1038/srep18029>
- Strnad M, Hönig V, Růžek D, Grubhoffer L, Rego ROM (2017) Europe-wide meta-analysis of *Borrelia burgdorferi* sensu lato prevalence in questing *Ixodes ricinus* ticks. Appl Environ Microbiol 83:15. <https://doi.org/10.1128/AEM.00609-17>
- Stübs G, Fingerle V, Wilske B, Göbel UB, Zähringer U, Schumann RR, Schröder NWJ (2009) Acylated cholesteryl galactosides are specific antigens of borrelia causing Lyme disease and frequently induce antibodies in late stages of disease. J Biol Chem 284:13326–13334. <https://doi.org/10.1074/jbc.M809575200>
- Tabor AE (2018) The enigma of identifying new cattle tick vaccine antigens. Ticks Tick-Borne Pathog. <https://doi.org/10.5772/intechopen.81145>
- Tanner T, Marks R (2008) Delivering drugs by the transdermal route: review and comment. Skin Res Technol Off J Int Soc Bioeng Skin ISBS Int Soc Digit Imaging Skin ISDIS Int Soc Skin Imaging ISSI 14:249–260. <https://doi.org/10.1111/j.1600-0846.2008.00316.x>
- Tappe J, Jordan D, Janecek E, Fingerle V, Strube C (2014) Revisited: *Borrelia burgdorferi* sensu lato infections in hard ticks (*Ixodes ricinus*) in the city of Hanover (Germany). Parasit Vectors 7:441. <https://doi.org/10.1186/1756-3305-7-441>
- Timmaraju VA, Theophilus PAS, Balasubramanian K, Shakih S, Luecke DF, Sapi E (2015) Biofilm formation by *Borrelia burgdorferi* sensu lato. FEMS Microbiol Lett 362:fnv120. <https://doi.org/10.1093/femsle/fnv120>
- van Duijvendijk G, Coipan C, Wagemakers A, Fonville M, Ersöz J, Oei A, Földvári G, Hovius J, Takken W, Sprong H (2016) Larvae of *Ixodes ricinus* transmit *Borrelia afzelii* and *B. miyamotoi* to vertebrate hosts. Parasit Vectors 9:97. <https://doi.org/10.1186/s13071-016-1389-5>
- Vancová M, Rudenko N, Vančček J, Golovchenko M, Strnad M, Rego ROM, Tichá L, Grubhoffer L, Nebesářová J (2017) Pleomorphism and viability of the Lyme disease pathogen *Borrelia burgdorferi* exposed to physiological stress conditions: a correlative cryo-fluorescence and cryo-scanning electron microscopy study. Front Microbiol 8:596. <https://doi.org/10.3389/fmicb.2017.00596>
- Vechtova P, Sterbova J, Sterba J, Vancova M, Rego ROM, Selinger M, Strnad M, Golovchenko M, Rudenko N, Grubhoffer L (2018) A bite so sweet: the glycobiology interface of tick-host-pathogen interactions. Parasit Vectors 11:594. <https://doi.org/10.1186/s13071-018-3062-7>
- Wagemakers A, Coumou J, Schuijt TJ, Oei A, Nijhof AM, van 't Veer C, van der Poll T, Bins AD, Hovius JWR (2016) An *Ixodes ricinus* tick salivary lectin pathway inhibitor protects *Borrelia burgdorferi* sensu lato from human complement. Vector Borne Zoonotic Dis Larchmt N 16:223–228. <https://doi.org/10.1089/vbz.2015.1901>
- Walker AR (2014) Ticks and associated diseases: a retrospective review. Med Vet Entomol 28(Suppl 1):1–5. <https://doi.org/10.1111/mve.12031>
- Wallich R, Siebers A, Jahraus O, Brenner C, Stehle T, Simon MM (2001) DNA vaccines expressing a fusion product of outer surface proteins a and C from *Borrelia burgdorferi* induce protective antibodies suitable for prophylaxis but not for resolution of Lyme disease. Infect Immun 69:2130–2136. <https://doi.org/10.1128/IAI.69.4.2130-2136.2001>
- Wang D, Bayliss S, Meads C (2011) Palivizumab for immunoprophylaxis of respiratory syncytial virus (RSV) bronchiolitis in high-risk infants and young children: a systematic review and additional economic modelling of subgroup analyses. Health Technol Assess Winch Engl 15:iii–iv–i1–124. <https://doi.org/10.3310/hta15050>
- Wang Y, Kern A, Boatright NK, Schiller ZA, Sadowski A, Ejemel M, Souders CA, Reimann KA, Hu L, Thomas WD, Klempner MS

- (2016) Pre-exposure prophylaxis with OspA-specific human monoclonal antibodies protects mice against tick transmission of Lyme disease spirochetes. *J Infect Dis* 214:205–211. <https://doi.org/10.1093/infdis/jiw151>
- Warshafsky S, Lee DH, Francois LK, Nowakowski J, Nadelman RB, Wormser GP (2010) Efficacy of antibiotic prophylaxis for the prevention of Lyme disease: an updated systematic review and meta-analysis. *J Antimicrob Chemother* 65:1137–1144. <https://doi.org/10.1093/jac/dkq097>
- Wilske B, Preac-Mursic V, Göbel UB, Graf B, Jauris S, Soutschek E, Schwab E, Zumstein G (1993) An OspA serotyping system for *Borrelia burgdorferi* based on reactivity with monoclonal antibodies and OspA sequence analysis. *J Clin Microbiol* 31:340–350
- Wormser GP, Shapiro ED, Strle F (2017) Studies that report unexpected positive blood cultures for Lyme *Borrelia*—are they valid? *Diagn Microbiol Infect Dis* 89:178–181. <https://doi.org/10.1016/j.diagmicrobio.2017.07.009>
- Wressnigg N, Pöllabauer E-M, Aichinger G, Portsmouth D, Löw-Baselli A, Fritsch S, Livey I, Crowe BA, Schwendinger M, Brühl P, Pilz A, Dvorak T, Singer J, Firth C, Luft B, Schmitt B, Zeitlinger M, Müller M, Kollaritsch H, Paulke-Korinek M, Esen M, Kreamsner PG, Ehrlich HJ, Barrett PN (2013) Safety and immunogenicity of a novel multivalent OspA vaccine against Lyme borreliosis in healthy adults: a double-blind, randomised, dose-escalation phase 1/2 trial. *Lancet Infect Dis* 13:680–689. [https://doi.org/10.1016/S1473-3099\(13\)70110-5](https://doi.org/10.1016/S1473-3099(13)70110-5)
- Zhong W, Gern L, Stehle T, Museteanu C, Kramer M, Wallich R, Simon MM (1999) Resolution of experimental and tick-borne *Borrelia burgdorferi* infection in mice by passive, but not active immunization using recombinant OspC. *Eur J Immunol* 29:946–957. [https://doi.org/10.1002/\(SICI\)1521-4141\(199903\)29:03<946::AID-IMMU946>3.0.CO;2-P](https://doi.org/10.1002/(SICI)1521-4141(199903)29:03<946::AID-IMMU946>3.0.CO;2-P)
- Zingg S, Dolle P, Voordouw MJ, Kern M (2018) The negative effect of wood ant presence on tick abundance. *Parasit Vectors* 11:164. <https://doi.org/10.1186/s13071-018-2712-0>

Publisher's note Springer Nature remains neutral with regard to jurisdictional claims in published maps and institutional affiliations.

3.3 Manuscript 3:

Strnad, M., Rego, R. O. M. (2020) The need to unravel the twisted nature of the *Borrelia burgdorferi* sensu lato complex across Europe. *Microbiology* 166: 428–435.

Annotation

In **Manuscript 1**, we have shown that the complex of Lyme disease-causing *Borrelia* is still expanding, while the geographical distribution and tick prevalences differ greatly across the European countries. It is known that different *B. burgdorferi* sensu lato genospecies are associated with overlapping but distinct spectra of clinical manifestations. *B. burgdorferi* sensu stricto is most often associated with arthritis and neuroborreliosis, *B. garinii* with neuroborreliosis, and *B. afzelii* with various skin conditions such as acrodermatitis chronica atrophicans. To date, the vast majority of data about borrelial biomolecules and their functions are from genetic studies carried out on North American strains of a single species ie., *B. burgdorferi* sensu stricto. Recent whole-genome sequences of several European species/strains makes adaptation and use of genetic techniques feasible in studying inherent differences between them. This review (**Manuscript 3**) highlights the need in undertaking independent studies of genospecies within Europe given the varying genetic content, pathogenic potential, and differences in clinical manifestation.

The need to unravel the twisted nature of the *Borrelia burgdorferi* sensu lato complex across Europe

Martin Strnad^{1,2} and Ryan O.M. Rego^{1,2,*}

Abstract

Lyme borreliosis is a vector-borne infection caused by bacteria under the *Borrelia burgdorferi* sensu lato complex, both in Europe and North America. Differential gene expression at different times throughout its infectious cycle allows the spirochete to survive very diverse environments within different mammalian hosts as well as the tick vector. To date, the vast majority of data about spirochetal proteins and their functions are from genetic studies carried out on North American strains of a single species, i.e. *B. burgdorferi sensu stricto*. The whole-genome sequences recently obtained for several European species/strains make it feasible to adapt and use genetic techniques to study inherent differences between them. This review highlights the crucial need to undertake independent studies of genospecies within Europe, given their varying genetic content and pathogenic potential, and differences in clinical manifestation.

INTRODUCTION

Understanding the roles of genetically encoded virulence factors among pathogens is critical for the development of new diagnostic and therapeutic tools. Targeted mutagenesis and complementation are important methods for studying genes of unknown function among most bacterial pathogens, including the Lyme borreliosis spirochete. Determining specific gene function has been hampered by the intractability of virulent strains of this bacterium to genetic manipulation [1]. To date, almost exclusively, *Borrelia burgdorferi sensu stricto* (ss) strains have been successfully utilized in genetic studies, since its genome was unveiled in 1997 by Fraser and colleagues [2]. As a consequence, the vast majority of data about spirochetal genes and their roles have come from studies performed on the North American species *Ixodes scapularis* (tick) and *B. burgdorferi* ss. The release of the whole-genome sequences of several European species/strains now makes the adaptation and use of genetic techniques a more feasible approach in studying the possible differences between genospecies from Europe and North America and among various European strains [3]. Differences in the plasmid/gene content of the major pathogenic *B. burgdorferi* genospecies, the ixodid tick vectors and in the clinical manifestations associated with each one, emphasize the need to undertake separate studies on the European genospecies/strains.

B. burgdorferi sensu lato complexity

B. burgdorferi sensu lato complex (referred to as *B. burgdorferi*) comprises at least 20 named species [4, 5], with most human Lyme cases in Europe being caused by *B. burgdorferi* ss, *Borrelia afzelii*, *Borrelia garinii*, *Borrelia bavariensis* and *B. spielmanii* [6]. In the USA, only *B. burgdorferi* ss and *Borrelia mayonii* [7] are commonly associated with human infection. In addition to the recognized Lyme borreliosis-causing species, at least three other species are occasionally detected in humans: *Borrelia bissettii* [8, 9], *Borrelia lusitaniae* [10] and *Borrelia valaisiana* [11]. However, the status of *B. valaisiana* as a human pathogen has recently been disputed [12]. What increases the complexity of the various species is the uniqueness of their genomic content at the species/strain levels. Their genomes contain a single chromosome and usually a range of linear and circular plasmids that are substantially variable in sequence between species and whose numbers differ among individual strains. It has been suggested that the presence of various plasmids enables the spirochetes to survive in a diverse range of mammalian hosts [13].

In Europe, there are at least 8 named species and 15 different sequenced strains of *B. burgdorferi* (Table 1), with most of them being directly associated with the human Lyme

Received 29 November 2019; Accepted 07 February 2020; Published 03 March 2020

Author affiliations: ¹Biology Centre, Institute of Parasitology, Czech Academy of Sciences, Branisovska 31, 37005, Ceske Budejovice, Czech Republic;

²Faculty of Science, University of South Bohemia, Branisovska 31, 37005, Ceske Budejovice, Czech Republic.

*Correspondence: Ryan O.M. Rego, ryanrego@paru.cas.cz

Keywords: Lyme borreliosis; Europe vs North America; tick; genetic manipulations; *Borrelia* diversity.

Abbreviations: CRASP, complement regulator-acquiring surface protein; CspA, complement regulator-acquiring surface protein 1; DbpA and B, decorin binding protein A and B; EM, erythema migrans; GFP, green fluorescent protein; OspC, outer surface protein C.

Table 1. List of European *B. burgdorferi* strains that have been sequenced and whose plasmid content is known

	Strain	Geographical origin	No. of plasmids	References/GB accession number
<i>B. afzelii</i> *	PKo	Germany	17	[92]
	K78	Austria	13	[93]
	ACA-1	Sweden	14	[92]
<i>B. garinii</i> *	PBr	Denmark	12	[92]
	Far04	Denmark	7	[92]
	20 047	France	10	GCA_003814405
<i>B. burgdorferi</i> *	ZS7	Germany	14	[94]
	BOL26	Italy	13	[94]
<i>B. bavariensis</i> *	PBi	Germany	11	[95]
<i>B. finlandensis</i>	SV1	Finland	10	[96]
<i>B. spielmanii</i> *	A14S	The Netherlands	13	[97]
<i>B. valaisiana</i>	VS116	Switzerland	11	[97]
<i>B. turdi</i>	T1990A	Portugal	10	[98]
	TPT2017	Portugal	10	[98]
	T2084	Portugal	9	[98]

*, confirmed human pathogenic species.

borreliosis. A recent European meta-analysis showed that *B. afzelii* and *B. garinii* are the most frequent and most widely distributed species in questing ticks, whereas *B. burgdorferi* ss and *B. bavariensis* are less common [14].

Clinical manifestations and epidemiological aspects

Lyme borreliosis is a spirochetal infection with diverse clinical features that is transmitted to humans by certain species of *Ixodes* ticks. It is primarily caused by *B. burgdorferi* ss and the more recently identified *B. mayonii* in North America, and by multiple species in Europe. Lyme borreliosis in Europe and the USA is very similar in its clinical presentation, but does differ between the continents to some extent, presumably due to the greater variety of species that cause the disease in Europe. The most commonly observed clinical manifestation is erythema migrans (EM), which eventually resolves, even without antibiotic treatment. In Europe, this early manifestation caused by *B. afzelii* generally expands more slowly than in the USA in patients with *B. burgdorferi* ss-caused EM [15].

The infecting pathogen can spread to other organs and tissues, causing more serious multi-system disorders with skin, neurological, cardiac and musculoskeletal manifestations [16]. Different *B. burgdorferi* sensu lato species are associated with overlapping but distinct spectra of clinical manifestations [6, 17]: *B. burgdorferi* ss is most often associated with arthritis

and neuroborreliosis, *B. garinii* with neuroborreliosis [18] and *B. afzelii* with various skin conditions, such as acrodermatitis chronica atrophicans or borreliolymphocytoma [19, 20]. Notably, even within the same species, there are clear differences in clinical presentation and invasiveness in humans. Jungnick and colleagues [21] showed that *B. burgdorferi* ss from Europe causes neuroborreliosis to a significantly greater degree than *B. burgdorferi* ss in the USA.

Lyme borreliosis is the most common vector-borne human disease in the USA and Europe [6]. Currently up to 300 000 cases in the USA [22] and 85 000 cases in Europe [23] are reported annually. However, the number of those affected in Europe is very likely to be an underestimate, since not all countries have made Lyme borreliosis a mandatorily notifiable disease [24]. Furthermore, inadequate laboratory test sensitivity is the leading cause of underreporting of infected patients [25]. Last but not least, several lines of evidence suggest symptomless infections. In the USA asymptomatic infections occur in about 10 % of infected individuals, whereas in Europe this number is reported to be much greater [26]. Although several attempts to develop an effective vaccine have been made, no vaccine for human use is currently available [27].

Transmission dynamics in North America vs Europe

B. burgdorferi is transmitted by the slow-feeding ixodid ticks *I. scapularis* [28] and *Ixodes pacificus* [29] in the USA and by *Ixodes ricinus* and *Ixodes persulcatus* in Europe [30]. The generally accepted model of Lyme borreliosis transmission, deduced based on research performed on North American species, can be outlined as follows. The tick vector becomes infected when it takes up an infected blood meal at the larval stage. It then moults to a nymph and the *B. burgdorferi* persist in a starvation mode in the midgut of the nymphal tick for months [31, 32]. After the tick finds a vertebrate host and starts to ingest blood, the spirochetes start to multiply within the midgut and traverse the gut epithelium in a highly organized manner [33]. The spirochetes finally disseminate through the haemocoel up to the tick salivary glands. *B. burgdorferi* is then transmitted in tick saliva into the mammalian host, where the extracellular matrix appears to provide a protective niche for the spirochete [34, 35]. However, recent data show that the course of spirochete transmission and especially the transmission dynamics can be markedly different in European species [36].

Transmission of *B. burgdorferi* spirochetes occurs during the process of tick feeding. A decisive factor for successful transmission is the duration of attachment of the tick to the host. In the USA the *B. burgdorferi* ss-*I. scapularis* interaction has served as an experimental model for the overwhelming majority of transmission dynamics studies. Immunofluorescence microscopy has confirmed the presence of *B. burgdorferi* in the nymphal tick midguts as early as 24 h after attachment to white-footed mice, before significant amounts of blood have been imbibed [37]. Poised to continue in its enzootic cycle, *B. burgdorferi* overcomes a long nutritional drought in

the tick midgut, waiting for the right environmental signals. With the influx of new blood, *B. burgdorferi* undergoes antigenic changes critical for its further dissemination. In the *B. burgdorferi* ss-*I. scapularis* experimental model, at least 48 h [38–41] or more [33, 42] are required to stably infect the tick salivary glands and subsequently the mammalian host.

In comparison with the work done in the USA, research on the transmission dynamics of European species has received less attention until recently. Examination of *I. ricinus* in Switzerland indicated that, unlike in *I. scapularis*, *B. burgdorferi* may cause systemic infection and occasionally reach the salivary glands even before the onset of tick feeding [43, 44]. This observation goes hand in hand with the findings noted by Kahl and colleagues [45], who revealed that *B. afzelii*-infected *I. ricinus* ticks were only able to infect the host after 16.7 h of tick attachment. This was confirmed in experiments conducted by Crippa and colleagues [46]. They showed that during the first 48 h of tick attachment, *B. burgdorferi* ss-infected ticks were not able to pass the pathogens onto the host, whereas *B. afzelii*-infected ticks infected half of the mice during this time interval. This indicated that *B. afzelii* are likely predisposed to being transmitted earlier than *B. burgdorferi* ss by *I. ricinus*. Stanek and Strle [17] noted that 14–18 % of Lyme patients who removed a tick within 6 h of noticing tick attachment still experienced EM development.

The earlier results indicating the differences in transmission times between European and North American spirochetes were further strengthened by a recent study that confirmed that *B. afzelii* requires less time to establish a permanent infection when transmitted from the tick [36]. Additionally, a striking difference between *B. afzelii*-*I. ricinus* and *B. burgdorferi* ss-*I. scapularis* was observed in spirochete numbers in the nymphal midgut during feeding, where the numbers of *B. afzelii* dramatically decrease in *I. ricinus*. This result clearly differs from the data previously observed in *B. burgdorferi* ss-*I. scapularis*, where a significant increase in spirochete load was observed [38]. Another substantial difference was discerned in the number of spirochetes after moulting. Whereas *B. burgdorferi* ss spirochetes multiply rapidly in feeding and engorged larvae, followed by a dramatic drop in the number of spirochetes during moulting [47], in *B. afzelii* the population grows rapidly in engorged *I. ricinus* larvae and also during moulting to nymphs [36]. These results concerning transmission require further investigation to understand whether they are just strain-specific or can be shown to be species-specific.

Genetic manipulation of *B. burgdorferi*

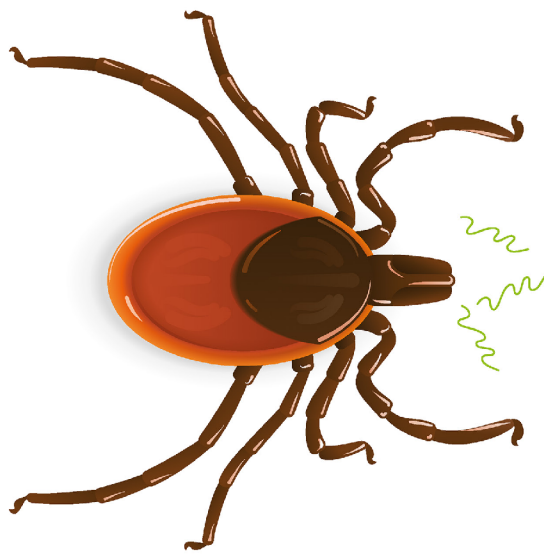
B. burgdorferi was first genetically manipulated more than two decades ago, using the electroporation method [48]. Since then, the development of diverse molecular tools has enabled investigators to probe and uncover some of the underlying pathogenic mechanisms of the spirochete on a molecular genetic level [1]. These include the use of targeted mutagenesis studies for investigating the role of genes in a tick-animal model in a high-throughput manner [49–52], the use of the cre-lox recombination system for the deletion

of a set of genes on a plasmid [53] and the use of reporter genes including *cat* gene [54], *lacZ* [55, 56], *luc* [57, 58] and GFP [33, 59]. Also published on and in use are experiments with an inducible gene expression system when the gene of interest is essential for viability and cannot be deleted. The two systems that have been used for this when studying *B. burgdorferi* strains of US origin include the tet system [60, 61] and the lac system [57, 62, 63]. Finally, in the case of gene studies where the role of the gene and the protein it encodes has been deduced by any of the above methods, gene complementation in *B. burgdorferi* includes the use of shuttle vectors and trans-complementation for the introduction of the gene back into the mutant [64–66] to see if it restores the wild-type phenotype. However, genetic manipulation of *B. burgdorferi* has been greatly hampered by a number of limiting factors, including slow growth, low transformation efficiency, loss of plasmids during laboratory cultivation, the limited number of antibiotic markers for research purposes due to the use of antibiotics such as ampicillin and tetracycline being used to treat Lyme disease patients, and the lack of a minimal defined medium [1, 67].

Genetic manipulation of European strains

The use of genetic approaches to study the factors involved in the pathogenesis of North American *B. burgdorferi* ss is now common and new techniques are still being developed [68]. Many important insights into the biology of this bacterium have been gained, giving us a better chance to cope with this malicious agent. However, only a handful of studies involving the genetic manipulation of European species have been carried out (Fig. 1).

To the best of our knowledge, very few European strains have undergone genetic modification and received mention in a scientific publication (Table 2). High-passage, non-infectious *B. garinii* strain G1 was successfully transformed with the shuttle vector pKFSS1 or its derivatives [69]. In this and subsequent studies the authors focused on exploring the mechanisms by which the pathogenic bacterium evades the host immune response, with emphasis on CRASPs [70]. Another European strain used in genetic analyses was PKo, a *B. afzelii* strain. Here, Fingerle and colleagues [71] complemented a naturally occurring outer surface protein C (*ospC*) mutant with a wild-type copy of the *ospC* gene, which led to more efficient migration of pathogens from the tick gut to the salivary glands, indicating that *OspC* is necessary for salivary gland invasion during *Borrelia* transmission. By contrast, the expression of *OspC* may not be required for accomplishing the gut-salivary gland migration in the case of their counterparts from North America [72]. Recently, two infectious European strains, *B. afzelii* BO23 and *B. garinii* CIP 103362, were evaluated as model organisms to study Eurasian Lyme borreliosis [73]. Both strains were shown to be transformable by the shuttle vector pBSV2, culturable on solid media and susceptible to antibiotic selection [73]. In our laboratory, we have been able to obtain both red and green fluorescent infectious *B. afzelii* CB43 (unpublished data), an infectious strain from the Czech Republic [36], using shuttle vectors carrying



NORTH AMERICA	EUROPE
Ticks / <i>Borrelia</i> species	
<i>I. scapularis</i> <i>I. pacificus</i> <i>B. burgdorferi</i> ss <i>B. mayonii</i> <i>B. bissettii</i>	<i>I. ricinus</i> <i>I. persulcatus</i> <i>B. afzelii</i> <i>B. garinii</i> <i>B. burgdorferi</i> ss <i>B. bavariensis</i> <i>B. lusitaniae</i> <i>B. spielmanii</i> <i>B. valaisiana</i> <i>B. finlandensis</i>
Transmission dynamics	
Midgut -> Salivary glands -> Host	Midgut -> Host ?
Genetic methods	
Mutagenesis Complementation Inducible gene expression Surrogate genetics Fluorescent reporters	Complementation Fluorescent reporters

Fig. 1. Comparison of Lyme borreliosis-associated factors and available genetic tools in North America and Europe. There are at least twice as many *B. burgdorferi* species connected with the disease in Europe compared with North America. However, the number of genetic methods successfully applied to European species is substantially smaller.

the fluorescent reporter genes dsRED and GFP, respectively. Whereas gene complementation into infectious European strains has been already successfully performed, to the best of our knowledge, targeted gene mutagenesis has yet to be achieved.

Delineation of the protein function in European *Borrelia* species

Considerable attention has been paid in the last two decades to differential gene expression by *B. burgdorferi* during their life cycle. The products of the activated genes can be sorted according to their roles during the process of tick and mammalian infection. Within the tick vector, proteins that are upregulated play a crucial role in adaptation and midgut colonization of the tick, or, after finding a new host, these antigens help the bacteria to migrate from the gut through the salivary glands and into the new host [13]. Once in the host, they can either mediate interactions with the host, or compete with the host immune system, thus facilitating survival in various tissues and organs [13, 74].

Until recently, all studies dealing with the biological function of different (lipo)proteins were performed with North American *B. burgdorferi* ss, and very little attention has been paid to the potential differences in the activity among the disease-causing European genospecies. However, a small number of studies have attempted to compare the functional roles of some infection-associated proteins present in European *Borrelia* species. A popular strategy is to use a non-infectious, easily transformable, isogenic strain, such as *B. burgdorferi* B313 or B314, and insert allelic variants of virulence genes from different borrelial strains [75–77]. An

alternative method is to use deletion mutants of the highly transformable infectious strain *B. burgdorferi* ss. Using this strategy, it was shown that *B. burgdorferi* ML23 harbouring allelic variants of virulence genes behave differently during animal infection [78]. Specifically, they have shown that decorin-binding protein (DbpA) variants alter the ability of infectious strains to bind decorin and dermatan sulfate, and therefore influence colonization functions and tissue tropism. DbpA and DbpB are surface-exposed lipoproteins of 20 and 18 kDa, respectively, that bind to the extracellular matrix proteoglycan, which ‘decorates’ collagen fibres, decorin, and also bind to dermatan sulphate. The ability of *B. burgdorferi* to bind decorin is considered to be an important factor for the disseminatory pathogenic strategy, enabling the bacteria to colonize various tissues and organs with a large quantity of decorin, e.g. the endothelium, skin, joints, bladder, etc [79].

Salo and colleagues [75] found differences in the decorin-binding activity among *B. burgdorferi* species using various binding assays. Even though *B. afzelii* is mostly associated with chronic skin disorders, such as acrodermatitis chronica atrophicans, it turned out that both DbpA and DbpB of *B. afzelii* exhibited no or only minor binding activity towards decorin, indicating that there must be another crucial binding partner, enabling *B. afzelii* to efficiently colonize skin tissue. In amino acid sequence comparison, only 40–60% similarity is seen among the Dbps of the genospecies [80]. The molecular mechanisms behind the difference in tissue tropism are not fully clear so far, but decorin-binding proteins may well play a significant role in varying tissue tropisms associated with different *Borrelia* genospecies.

Table 2. Strains of European *B. burgdorferi* species used for tick-animal model interactions (black) or for genetic manipulations (red) or both (blue)

	Strain/isolate	Geographical origin	References
<i>B. afzelii</i>	IBS-5	France	[99, 100]
	CB43	Czech Republic	[36]
	NE4049	Switzerland	[101]
	NE5046	Switzerland	[101]
	NE4053	Switzerland	[101]
	NE36	Switzerland	[101]
	NE4054	Switzerland	[101]
	NE4051	Switzerland	[101]
	P/sto	Germany	[101]
	BO23	Germany	[73]
	E61	Austria	[101, 102]
	Fin-Jyv-A3	Finland	[103]
	NE496	Switzerland	[46]
	NE2963	Switzerland	[46]
	A91	Finland	[104]
PKo	Germany	[71]	
<i>B. garinii</i>	SBK40	Finland	[104]
	CIP 103362	France	[73]
	G1	Germany	[69]
<i>B. burgdorferi</i>	NE1849	Switzerland	[53]
	BRE-13	France	[100]

The association of *B. burgdorferi* genospecies with vertebrate reservoir host species appears to be strongly affected by the polymorphism of borrelial proteins [81, 82]. The complement sensitivity or resistance of *Borrelia* genospecies is one of the crucial components governing the *Borrelia*–host relationship. The complement system is one of the major innate defence mechanisms *B. burgdorferi* has to overcome to establish a stable infection of the mammalian host. Different genospecies of *B. burgdorferi* differ in their sensitivity to human and animal sera [81, 83]. A number of borrelial polymorphic proteins may be involved in host-to-host differences in complement evasion. CspA fulfils such a role and the lack of its production results in the inability of spirochetes to bind to factor H, which, in turn, inactivates complement activation and promotes serum resistance [77]. The sequences of CspA variants among *B. burgdorferi* are highly polymorphic and binding to factor H differs significantly [77, 84], suggesting that CspA may play a role in promoting host-specific transmission of the Lyme spirochetes.

Another known polymorphic protein, OspC, displays variable binding activity to human C4b. It was shown that OspC from

B. burgdorferi and *B. garinii* restored bloodstream survival of *ospC* knock-out mutants in mice, but *B. garinii* was more susceptible than *B. burgdorferi* to killing by human serum proteins [82].

Conclusion

The genetic diversity and thus the phenotypic differences in the symptoms that the various European genospecies of *B. burgdorferi* are responsible for is on a larger scale than that seen with US species/strains [85]. This and the mode of transmission of different *B. burgdorferi* species by *I. ricinus* does not make it easy to identify new diagnostic markers or ideal vaccine candidates. Added to this is the fact that various *Borrelia* species/strains appear to have their own set of reservoir hosts because of certain genetic determinants that help them evade and persist within the mammalian host. A good example of this is *B. bavarensis*, which was designated as its own species a few years back and not part of the *B. garinii* clade [86, 87]. It is suggested that it diverged at some point from *B. garinii*, which is known to be bird-specific in terms of reservoir hosts and made a switch that enabled *B. bavarensis* to be associated with small mammals [5]. Genetic analysis is a valuable tool that has been employed extensively to determine important factors responsible for the pathogenesis of many bacterial species and could certainly answer questions regarding how genetic composition, including the identified CRASP genes, could lead to differences in reservoir host association [81, 88]. Advances in genetic manipulation [89] and the release of the complete genome of *B. burgdorferi* ss [2] has allowed investigators to identify the role of individual genes in the context of experimental Lyme borreliosis. Researchers are now in a unique position to make the next big step in order to understand the Lyme borreliosis problem in Europe by putting greater emphasis on adapting genetic tools for European *B. burgdorferi* species. This also means the use of more ‘omics’-related technologies for discerning species and strain differences. It is desirable that novel strategies against the pathogen be developed based on the findings of European genospecies and not necessarily the result of investigations on US strains. There should be a consensus on the strains that are being investigated for each European species rather than every investigative group relying on their choice of strain. Research in the USA is primarily conducted on two *B. burgdorferi* strains, B31 and N40, or variants of these two backgrounds [90]. We suggest that laboratories collaborate on working with possibly two strains for a particular European species and identify if there is strain-to-strain variation and at what level. This may help identify if the differences observed are at the strain level or only at the species level. As more recent work has shown, even transmission routes may not be the same for European and US strains [36], raising the question as to what other assumptions have been made based on studies of US strains. These could be misleading investigators working with European *B. burgdorferi* species. *B. afzelii* strain ACA-1 and other similar strains are known to cause acrodermatitis or lesions at the point of the tick bite site in 10 % of Lyme patients in Europe [91]. Why only specific strains

are capable of causing these lesions, even with knowledge of the whole genome, is something that has yet to be determined [4]. The incidence of infected ticks and their further distribution within Europe as well as the anticipated annual increase in patients with Lyme borreliosis is growing larger every year. Now is the right time for European investigators to work together to develop novel tools and animal models to improve our understanding of this pathogens' infectivity in nature. Efforts to understand mixed infections of different *Borrelia* species or of *Borrelia* with other tick-borne pathogens need to be supported. Only by combining technologies and resources will it be possible to move towards common goals for diagnosis, treatments and vaccines.

Funding information

This study was supported by the Czech Science Foundation grant 17-21244S.

Conflicts of interest

The authors declare that there are no conflicts of interest.

References

- Drecktrah D, Samuels DS. Genetic manipulation of *Borrelia* spp. *Curr Top Microbiol Immunol* 2018;415:113–140.
- Fraser CM, Casjens S, Huang WM, Sutton GG, Clayton R *et al*. Genomic sequence of a Lyme disease spirochaete, *Borrelia burgdorferi*. *Nature* 1997;390:580–586.
- Di L, Pagan PE, Packer D, Martin CL, Akther S *et al*. *BorreliaBase*: a phylogeny-centered browser of *Borrelia* genomes. *BMC Bioinformatics* 2014;15:233.
- Casjens SR, Di L, Akther S, Mongodin EF, Luft BJ *et al*. Primal origin and diversification of plasmids in Lyme disease agent bacteria. *BMC Genomics* 2018;19:218.
- Margos G, Fingerle V, Reynolds S. *Borrelia bavariensis*: vector switch, niche invasion, and geographical spread of a tick-borne bacterial parasite. *Front Ecol Evol* Epub ahead of print 2019;7.
- Stanek G, Wormser GP, Gray J, Strle F *et al*. Lyme borreliosis. *The Lancet* 2012;379:461–473.
- Pritt BS, Respicio-Kingry LB, Sloan LM, Schriefer ME, Replogle AJ *et al*. *Borrelia mayonii* sp. nov., a member of the *Borrelia burgdorferi* sensu lato complex, detected in patients and ticks in the upper midwestern United States. *Int J Syst Evol Microbiol* 2016;66:4878–4880.
- Strle F, Picken RN, Cheng Y *et al*. Clinical findings for patients with Lyme borreliosis caused by *Borrelia burgdorferi* sensu lato with genotypic and phenotypic similarities to strain 25015. *Clin Infect Dis Off Publ Infect Dis Soc Am* 1997;25:273–280.
- Margos G, Lane RS, Fedorova N, Koloczek J, Piesman J *et al*. *Borrelia bissettae* sp. nov. and *Borrelia californiensis* sp. nov. prevail in diverse enzootic transmission cycles. *Int J Syst Evol Microbiol* 2016;66:1447–1452.
- Collares-Pereira M, Couceiro S, Franca I, Kurtenbach K, Schafer SM *et al*. First isolation of *Borrelia lusitanae* from a human patient. *J Clin Microbiol* 2004;42:1316–1318.
- Diza E, Papa A, Vezyri E, Tsounis S, Milonas I *et al*. *Borrelia valaisiana* in cerebrospinal fluid. *Emerg Infect Dis* 2004;10:1692–1693.
- Margos G, Sing A, Fingerle V. Published data do not support the notion that *Borrelia valaisiana* is human pathogenic. *Infection* 2017;45:567–569.
- Tilly K, Rosa PA, Stewart PE. Biology of infection with *Borrelia burgdorferi*. *Infect Dis Clin North Am* 2008;22:217–234.
- Strnad M, Hönig V, Růžek D, Grubhoffer L, Rego ROM *et al*. Europe-Wide meta-analysis of *Borrelia burgdorferi* sensu lato prevalence in questing *Ixodes ricinus* ticks. *Appl Environ Microbiol* 2017;83.
- Stanek G, Fingerle V, Hunfeld K-P, Jaulhac B, Kaiser R *et al*. Lyme borreliosis: clinical case definitions for diagnosis and management in Europe. *Clin Microbiol Infect* 2011;17:69–79.
- Mead PS. Epidemiology of Lyme disease. *Infect Dis Clin North Am* 2015;29:187–210.
- Stanek G, Strle F. Lyme borreliosis—from tick bite to diagnosis and treatment. *FEMS Microbiol Rev* 2018;42:233–258.
- Strle F, Ružić-Sabljić E, Cimperman J, Lotric-Furlan S, Maraspin V *et al*. Comparison of findings for patients with *Borrelia garinii* and *Borrelia afzelii* isolated from cerebrospinal fluid. *Clinical Infectious Diseases* 2006;43:704–710.
- Maraspin V, Nahtigal Klevišar M, Ružić-Sabljić E, Lusa L, Strle F *et al*. Borrelial Lymphocytoma in adult patients. *Clinical Infectious Diseases* 2016;63:914–921.
- Rijkema SGT, Tazelaar DJ, Molkenboer MJCH, Noordhoek GT, Plantinga G *et al*. Detection of *Borrelia afzelii*, *Borrelia burgdorferi* sensu stricto, *Borrelia garinii* and group VS116 by PCR in skin biopsies of patients with erythema migrans and acrodermatitis chronica atrophicans. *Clinical Microbiology and Infection* 1997;3:109–116.
- Jungnick S, Margos G, Rieger M, Dzaferovic E, Bent SJ *et al*. *Borrelia burgdorferi* sensu stricto and *Borrelia afzelii*: Population structure and differential pathogenicity. *Int J Med Microbiol* 2015;305:673–681.
- Kuehn BM. CDC estimates 300 000 US cases of Lyme disease annually. *JAMA* 2013;310:1110.
- Rego ROM, Trentelman JJA, Anguita J, Nijhof AM, Sprong H *et al*. Counterattacking the tick bite: towards a rational design of anti-tick vaccines targeting pathogen transmission. *Parasit Vectors* 2019;12:229.
- Smith R, Takkinen J. Lyme borreliosis: Europe-wide coordinated surveillance and action needed? *Euro Surveill* 2006;11:E060622.1.
- Stricker RB, Johnson L. Lyme disease: call for a “Manhattan Project” to combat the epidemic. *PLoS Pathog* 2014;10:e1003796.
- 177570 CAB International W. 2011. United Kingdom, Halperin JJ 178318 (ed). Lyme disease: an evidence-based approach. <http://agris.fao.org/agris-search/search.do?recordID=XF2015037262> [accessed 29 May 2019].
- Strnad M, Grubhoffer L, Rego ROM. Novel targets and strategies to combat borreliosis. *Appl Microbiol Biotechnol* 2020;104:1915–1925.
- Burgdorfer W, Barbour A, Hayes S, Benach J, Grunwaldt E *et al*. Lyme disease—a tick-borne spirochetosis? *Science* 1982;216:1317–1319.
- Burgdorfer W, Barbour AG, Anderson JR, Lane RS, Gresbrink RA *et al*. The Western black-legged tick, *Ixodes pacificus*: a vector of *Borrelia burgdorferi*. *Am J Trop Med Hyg* 1985;34:925–930.
- Laaksonen M, Klemola T, Feuth E, Sormunen JJ, Puisto A *et al*. Tick-borne pathogens in Finland: comparison of *Ixodes ricinus* and *I. persulcatus* in sympatric and parapatric areas. *Parasit Vectors* 2018;11:556.
- Pal U, de Silva AM, Montgomery RR, Fish D, Anguita J *et al*. Attachment of *Borrelia burgdorferi* within *Ixodes scapularis* mediated by outer surface protein A. *J Clin Invest* 2000;106:561–569.
- Schwan TG, Piesman J, Golde WT, Dolan MC, Rosa PA *et al*. Induction of an outer surface protein on *Borrelia burgdorferi* during tick feeding. *Proc Natl Acad Sci U S A* 1995;92:2909–2913.
- Dunham-Ems SM, Caimano MJ, Pal U, Wolgemuth CW, Eggers CH *et al*. Live imaging reveals a biphasic mode of dissemination of *Borrelia burgdorferi* within ticks. *J Clin Invest* 2009;119:3652–3665.
- Radolf JD, Caimano MJ, Stevenson B, Hu LT *et al*. Of ticks, mice and men: understanding the dual-host lifestyle of Lyme disease spirochaetes. *Nat Rev Microbiol* 2012;10:87–99.
- Strnad M, Elsterová J, Schrenková J, Vancová M, Rego ROM *et al*. Correlative cryo-fluorescence and cryo-scanning electron

- microscopy as a straightforward tool to study host-pathogen interactions. *Sci Rep* 2015;5:18029.
36. Pospisilova T, Urbanova V, Hes O, Kopacek P, Hajdusek O *et al*. Tracking of *Borrelia afzelii* transmission from infected *Ixodes ricinus* Nymphs to Mice. *Infect Immun* 2019;87:e00896–18.
 37. Schwan TG, Piesman J. Temporal changes in outer surface proteins A and C of the Lyme disease-associated spirochete, *Borrelia burgdorferi*, during the chain of infection in ticks and mice. *J Clin Microbiol* 2000;38:382–388.
 38. de Silva AM, Fikrig E. Growth and migration of *Borrelia burgdorferi* in Ixodes ticks during blood feeding. *Am J Trop Med Hyg* 1995;53:397–404.
 39. Ohnishi J, Piesman J, de Silva AM. Antigenic and genetic heterogeneity of *Borrelia burgdorferi* populations transmitted by ticks. *Proc Natl Acad Sci U S A* 2001;98:670–675.
 40. Piesman J. Dispersal of the Lyme disease spirochete *Borrelia burgdorferi* to salivary glands of feeding nymphal *Ixodes scapularis* (Acari: Ixodidae). *J Med Entomol* 1995;32:519–521.
 41. Piesman J, Schneider BS, Zeidner NS. Use of quantitative PCR to measure density of *Borrelia burgdorferi* in the midgut and salivary glands of feeding tick vectors. *J Clin Microbiol* 2001;39:4145–4148.
 42. des Vignes F, Piesman J, Heffernan R, Schulze TL, Stafford III KC *et al*. Effect of tick removal on transmission of *Borrelia burgdorferi* and *Ehrlichia phagocytophila* by *Ixodes scapularis* nymphs. *J Infect Dis* 2001;183:773–778.
 43. Lebet N, Gern L. Histological examination of *Borrelia burgdorferi* infections in unfed *Ixodes ricinus* nymphs. *Exp Appl Acarol* 1994;18:177–183.
 44. Leuba-Garcia S, Kramer MD, Wallich R, Gern L *et al*. Characterization of *Borrelia burgdorferi* isolated from different organs of *Ixodes ricinus* ticks collected in nature. *Zentralblatt für Bakteriologie* 1994;280:468–475.
 45. Kahl O, Janetzki-Mittmann C, Gray JS, Jonas R, Stein J *et al*. Risk of infection with *Borrelia burgdorferi* sense lato for a host in relation to the duration of nymphal *Ixodes ricinus* feeding and the method of tick removal. *Zentralblatt für Bakteriologie* 1998;287:41–52.
 46. Crippa M, Rais O, Gern L. Investigations on the mode and dynamics of transmission and infectivity of *Borrelia burgdorferi* sensu stricto and *Borrelia afzelii* in *Ixodes ricinus* ticks. *Vector Borne Zoonotic Dis Larchmt N* 2002;2:3–9.
 47. Piesman J, Oliver JR, Sinsky RJ. Growth kinetics of the Lyme disease spirochete (*Borrelia burgdorferi*) in vector ticks (*Ixodes dammini*). *Am J Trop Med Hyg* 1990;42:352–357.
 48. Samuels DS, Mach KE, Garon CF. Genetic transformation of the Lyme disease agent *Borrelia burgdorferi* with coumarin-resistant *gyrB*. *J Bacteriol* 1994;176:6045–6049.
 49. Stewart PE, Hoff J, Fischer E, Krum JG, Rosa PA *et al*. Genome-wide transposon mutagenesis of *Borrelia burgdorferi* for identification of phenotypic mutants. *Appl Environ Microbiol* 2004;70:5973–5979.
 50. Lin T, Gao L, Zhang C, Odeh E, Jacobs MB *et al*. Analysis of an ordered, comprehensive STM mutant library in infectious *Borrelia burgdorferi*: insights into the genes required for mouse infectivity. *PLoS One* 2012;7:e47532.
 51. Lin TYao, Lin T *et al*. Transposon mutagenesis as an approach to improved understanding of *Borrelia* pathogenesis and biology. *Front Cell Infect Microbiol*;4.
 52. Lin T, Gao L, Zhao X, Liu J, Norris SJ *et al*. Mutations in the *Borrelia burgdorferi* flagellar type III secretion system genes *fliH* and *fliI* profoundly affect spirochete flagellar assembly, morphology, motility, structure, and cell division. *mBio* 2015;6.
 53. Bestor A, Stewart PE, Jewett MW, Sarkar A, Tilly K *et al*. Use of the cre-lox recombination system to investigate the *Ip54* gene requirement in the infectious cycle of *Borrelia burgdorferi*. *Infect Immun* 2010;78:2397–2407.
 54. Sohaskey CD, Arnold C, Barbour AG. Analysis of promoters in *Borrelia burgdorferi* by use of a transiently expressed reporter gene. *J Bacteriol* 1997;179:6837–6842.
 55. Hayes BM, Jewett MW, Rosa PA. lacZ reporter system for use in *Borrelia burgdorferi*. *Appl Environ Microbiol* 2010;76:7407–7412.
 56. Hayes BM, Dulebohn DP, Sarkar A *et al*. Regulatory protein BBD18 of the Lyme disease spirochete: essential role during tick acquisition? *mBio*;5.
 57. Blevins JS, Revel AT, Smith AH, Bachlani GN, Norgard MV *et al*. Adaptation of a luciferase gene reporter and lac expression system to *Borrelia burgdorferi*. *Appl Environ Microbiol* 2007;73:1501–1513.
 58. Skare JT, Shaw DK, Trzeciakowski JP, Hyde JA *et al*. In vivo imaging demonstrates that *Borrelia burgdorferi* ospC is uniquely expressed temporally and spatially throughout experimental infection. *PLoS One*;11:e0162501.
 59. Carroll JA, Stewart PE, Rosa P, Elias AF, Garon CF *et al*. An enhanced GFP reporter system to monitor gene expression in *Borrelia burgdorferi*. *Microbiology* 2003;149:1819–1828.
 60. Jutras BL, Bowman A, Brissette CA, Adams CA, Verma A *et al*. EbfC (YbaB) is a new type of bacterial nucleoid-associated protein and a global regulator of gene expression in the Lyme disease spirochete. *J Bacteriol* 2012;194:3395–3406.
 61. Whetstone CR, Slusser JG, Zückert WR. Development of a single-plasmid-based regulatable gene expression system for *Borrelia burgdorferi*. *Appl Environ Microbiol* 2009;75:6553–6558.
 62. Gilbert MA, Morton EA, Bundle SF, Samuels DS *et al*. Artificial regulation of *ospC* expression in *Borrelia burgdorferi*. *Mol Microbiol* 2007;63:1259–1273.
 63. Ouyang Z, Zhou J, Norgard MV. Synthesis of *rpoS* is dependent on a putative enhancer binding protein Rrp2 in *Borrelia burgdorferi*. *PLoS One* 2014;9:e96917.
 64. Stewart PE, Thalken R, Bono JL, Rosa P *et al*. Isolation of a circular plasmid region sufficient for autonomous replication and transformation of infectious *Borrelia burgdorferi*. *Mol Microbiol* 2001;39:714–721.
 65. Elias AF, Bono JL, Kupko III JJ, Stewart PE, Krum JG *et al*. New antibiotic resistance cassettes suitable for genetic studies in *Borrelia burgdorferi*. *J Mol Microbiol Biotechnol* 2003;6:29–40.
 66. Hübner A, Yang X, Nolen DM, Popova TG, Cabello FC *et al*. Expression of *Borrelia burgdorferi* OspC and DbpA is controlled by a RpoN-RpoS regulatory pathway. *Proc Natl Acad Sci U S A* 2001;98:12724–12729.
 67. Winslow C, Coburn J. Recent discoveries and advancements in research on the Lyme disease spirochete *Borrelia burgdorferi*. *F1000 Research*;8.
 68. Hillman C, Stewart PE, Strnad M, Stone H, Starr T *et al*. Visualization of spirochetes by labeling membrane proteins with fluorescent biarsenical dyes. *Front Cell Infect Microbiol*;9.
 69. Siegel C, Schreiber J, Haupt K, Skerka C, Brade V *et al*. Deciphering the ligand-binding sites in the *Borrelia burgdorferi* complement regulator-acquiring surface protein 2 required for interactions with the human immune regulators factor H and factor H-like protein 1. *J Biol Chem* 2008;283:34855–34863.
 70. Hallström T, Siegel C, Mörgelin M, Kraczyk P, Skerka C *et al*. Cspa from *Borrelia burgdorferi* inhibits the terminal complement pathway. *mBio* 2013;4.
 71. Fingerle V, Goettner G, Gern L, Wilske B, Schulte-Spechtel U *et al*. Complementation of a *Borrelia afzelii* OspC mutant highlights the crucial role of OspC for dissemination of *Borrelia afzelii* in *Ixodes ricinus*. *Int J Med Microbiol IJMM* 2007;297:97–107.
 72. Tilly K, Krum JG, Bestor A, Jewett MW, Grimm D *et al*. *Borrelia burgdorferi* OspC protein required exclusively in a crucial early stage of mammalian infection. *Infect Immun* 2006;74:3554–3564.
 73. Bontemps-Gallo S, Lawrence KA, Richards CL, Gherardini FC *et al*. Genomic and phenotypic characterization of *Borrelia afzelii* B023 and *Borrelia garinii* CIP 103362. *PLoS One* 2018;13:e0199641.

74. Vechtova P, Sterbova J, Sterba J, Vancova M, Rego ROM *et al.* A bite so sweet: the glycobiology interface of tick-host-pathogen interactions. *Parasit Vectors* 2018;11:594.
75. Salo J, Loimaranta V, Lahdenne P, Viljanen MK, Hytönen J *et al.* Decorin binding by DbpA and B of *Borrelia garinii*, *Borrelia afzelii*, and *Borrelia burgdorferi* sensu stricto. *J Infect Dis* 2011;204:65–73.
76. Salo J, Pietikäinen A, Söderström M, Auvinen K, Salmi M *et al.* Flow-Tolerant adhesion of a bacterial pathogen to human endothelial cells through interaction with biglycan. *J Infect Dis* 2016;213:1623–1631.
77. Hart T, Nguyen NTT, Nowak NA, Zhang F, Linhardt RJ *et al.* Polymorphic factor H-binding activity of CspA protects Lyme borreliae from the host complement in feeding ticks to facilitate tick-to-host transmission. *PLoS Pathog* 2018;14:e1007106.
78. Lin Y-P, Benoit V, Yang X, Martínez-Herranz R, Pal U *et al.* Strain-Specific variation of the decorin-binding adhesin DbpA influences the tissue tropism of the Lyme disease spirochete. *PLoS Pathog* 2014;10:e1004238.
79. Shi Y, Xu Q, McShan K, Liang FT *et al.* Both decorin-binding proteins A and B are critical for the overall virulence of *Borrelia burgdorferi*. *Infect Immun* 2008;76:1239–1246.
80. Heikkilä T, Seppälä I, Saxen H, Panelius J, Yrjänäinen H *et al.* Species-Specific serodiagnosis of Lyme arthritis and neuroborreliosis due to *Borrelia burgdorferi* sensu stricto, *B. afzelii*, and *B. garinii* by using decorin binding protein A. *J Clin Microbiol* 2002;40:453–460.
81. Tufts DM, Hart TM, Chen GF, Kolokotronis S-O, Diuk-Wasser MA *et al.* Outer surface protein polymorphisms linked to host-spirochete association in Lyme borreliae. *Mol Microbiol* 2019;111:868–882.
82. Caine JA, Lin Y-P, Kessler JR, Sato H, Leong JM *et al.* *Borrelia burgdorferi* outer surface protein C (OspC) binds complement component C4b and confers bloodstream survival. *Cell Microbiol* 2017;19:e12786.
83. Vancová M, Rudenko N, Vaněček J, Golovchenko M, Strnad M *et al.* Pleomorphism and viability of the Lyme disease pathogen *Borrelia burgdorferi* exposed to physiological stress conditions: a correlative Cryo-Fluorescence and Cryo-Scanning electron microscopy study. *Front Microbiol* 2017;8:596.
84. Hammerschmidt C, Koenigs A, Siegel C, Hallström T, Skerka C *et al.* Versatile roles of CspA orthologs in complement inactivation of serum-resistant Lyme disease spirochetes. *Infect Immun* 2014;82:380–392.
85. Rudenko N, Golovchenko M, Grubhoffer L, Öljiver JH *et al.* Updates on *Borrelia burgdorferi* sensu lato complex with respect to public health. *Ticks Tick Borne Dis* 2011;2:123–128.
86. Margos G, Vollmer SA, Cornet M, Garnier M, Fingerle V *et al.* A new *Borrelia* species defined by multilocus sequence analysis of housekeeping genes. *Appl Environ Microbiol* 2009;75:5410–5416.
87. Margos G, Wilske B, Sing A, Hizo-Teufel C, Cao W-C *et al.* *Borrelia bavariensis* sp. nov. is widely distributed in Europe and Asia. *Int J Syst Evol Microbiol* 2013;63:4284–4288.
88. Kraiczy P, Stevenson B. Complement regulator-acquiring surface proteins of *Borrelia burgdorferi*: structure, function and regulation of gene expression. *Ticks Tick Borne Dis* 2013;4:26–34.
89. Rosa PA, Tilly K, Stewart PE. The burgeoning molecular genetics of the Lyme disease spirochete. *Nat Rev Microbiol* 2005;3:129–143.
90. Chan K, Awan M, Barthold SW, Parveen N. Comparative molecular analyses of *Borrelia burgdorferi* sensu stricto strains B31 and N40D10/E9 and determination of their pathogenicity. *BMC Microbiol* 2012;12:157.
91. Smetanick MT, Zellis SL, Ermolovich T. Acrodermatitis chronica atrophicans: a case report and review of the literature. *Cutis* 2010;85:247–252.
92. Casjens SR, Mongodin EF, Qiu W-G, Dunn JJ, Luft BJ *et al.* Whole-Genome sequences of two *Borrelia afzelii* and two *Borrelia garinii* Lyme disease agent isolates. *J Bacteriol* 2011;193:6995–6996.
93. Schüller W, Bunikis I, Weber-Lehman J, Comstedt P, Kutschan-Bunikis S *et al.* Complete genome sequence of *Borrelia afzelii* K78 and comparative genome analysis. *PLoS One* 2015;10:e0120548.
94. Schutzer SE, Fraser-Liggett CM, Casjens SR, Qiu W-G, Dunn JJ *et al.* Whole-genome sequences of thirteen isolates of *Borrelia burgdorferi*. *J Bacteriol* 2011;193:1018–1020.
95. Margos G, Gofton A, Wibberg D, Dangel A, Marosevic D *et al.* The genus *Borrelia* reloaded. *PLoS One* 2018;13:e0208432.
96. Casjens SR, Fraser-Liggett CM, Mongodin EF, Qiu W-G, Dunn JJ *et al.* Whole genome sequence of an unusual *Borrelia burgdorferi* sensu lato isolate. *J Bacteriol* 2011;193:1489–1490.
97. Schutzer SE, Fraser-Liggett CM, Qiu W-G, Kraiczy P, Mongodin EF *et al.* Whole-Genome sequences of *Borrelia bissettii*, *Borrelia valaisiana*, and *Borrelia spielmanii*. *J Bacteriol* 2012;194:545–546.
98. Margos G, Becker NS, Fingerle V, Sing A, Ramos JA *et al.* Core genome phylogenetic analysis of the avian associated *Borrelia turdi* indicates a close relationship to *Borrelia garinii*. *Mol Phylogenet Evol* 2019;131:93–98.
99. Cotté V, Sabatier L, Schnell G, Carmi-Leroy A, Rousselle J-C *et al.* Differential expression of *Ixodes ricinus* salivary gland proteins in the presence of the *Borrelia burgdorferi* sensu lato complex. *J Proteomics* 2014;96:29–43.
100. Sertour N, Cotté V, Garnier M *et al.* Infection kinetics and tropism of *Borrelia burgdorferi* sensu lato in mouse after natural (via ticks) or artificial (needle) infection depends on the bacterial strain. *Front Microbiol* 2018;9.
101. Tonetti N, Voordouw MJ, Durand J, Monnier S, Gern L *et al.* Genetic variation in transmission success of the Lyme borreliosis pathogen *Borrelia afzelii*. *Ticks Tick Borne Dis* 2015;6:334–343.
102. Lagal V, Postic D, Ruzic-Sabljić E, Baranton G *et al.* Genetic diversity among *Borrelia* strains determined by single-strand conformation polymorphism analysis of the ospC gene and its association with invasiveness. *J Clin Microbiol* 2003;41:5059–5065.
103. Heylen DJA, Sprong H, Krawczyk A, Van Houtte N, Genné D *et al.* Inefficient co-feeding transmission of *Borrelia afzelii* in two common European songbirds. *Sci Rep* 2017;7:39596.
104. Cuellar J, Pietikäinen A, Glader O, Liljenbäck H, Söderström M *et al.* *Borrelia burgdorferi* infection in biglycan knockout mice. *J Infect Dis* 2019;220:116–126.

3.4 Manuscript 4:

Strnad, M., Elsterová, J., Schrenková, J., Vancová, M., Rego, R. O. M., Grubhoffer, L., Nebesářová, J. (2015) Correlative cryo-fluorescence and cryo-scanning electron microscopy as a straightforward tool to study host-pathogen interactions. *Sci. Rep.* 5, 18029.

Annotation

B. burgdorferi is an extracellular pathogen known to interact with distinct cell types in the host and its associated molecules, exploiting molecular and structural features to establish an infection. Conventional light microscopy techniques are often inadequate to study the fine details of spirochete-cell interplay. Immunofluorescence techniques might be misleading since the relative mutual positioning of a cell and a pathogen is hard to be reliably discerned without ultrastructural information. On the contrary, the search for spirochetes over large areas using solely electron microscopy can take hours due to their size and slender morphology. Correlative light and electron microscopy is an imaging technique that enables identification and targeting of fluorescently tagged structures with subsequent imaging at near-to-nanometer resolution. We have established a novel correlative cryo-fluorescence microscopy and cryo-scanning electron microscopy workflow, which enables imaging of the studied object of interest very close to its natural state, devoid of artifacts caused for instance by slow chemical fixation. The correlative workflow was then employed to highlight the cell-association mechanisms that accompany and guide the pathogenesis of the Lyme disease.

SCIENTIFIC REPORTS

OPEN

Correlative cryo-fluorescence and cryo-scanning electron microscopy as a straightforward tool to study host-pathogen interactions

Received: 08 June 2015
Accepted: 09 November 2015
Published: 10 December 2015

Martin Strnad^{1,2}, Jana Elsterová^{1,2,3}, Jana Schrenková^{1,2}, Marie Vancová^{1,2}, Ryan O. M. Rego¹, Libor Grubhoffer^{1,2} & Jana Nebesářová^{1,2,4}

Correlative light and electron microscopy is an imaging technique that enables identification and targeting of fluorescently tagged structures with subsequent imaging at near-to-nanometer resolution. We established a novel correlative cryo-fluorescence microscopy and cryo-scanning electron microscopy workflow, which enables imaging of the studied object of interest very close to its natural state, devoid of artifacts caused for instance by slow chemical fixation. This system was tested by investigating the interaction of the zoonotic bacterium *Borrelia burgdorferi* with two mammalian cell lines of neural origin in order to broaden our knowledge about the cell-association mechanisms that precedes the entry of the bacteria into the cell. This method appears to be an unprecedentedly fast (<3 hours), straightforward, and reliable solution to study the finer details of pathogen-host cell interactions and provides important insights into the complex and dynamic relationship between a pathogen and a host.

Borrelia burgdorferi is a pathogenic bacterium whose clinical manifestations are associated with Lyme disease. This vector-borne disease is one of the major public health concerns in Europe and North America and leads to severe arthritic, cardiovascular and neurological complications if left untreated¹. Although *B. burgdorferi* is primarily referred to as an extracellular pathogen, studies performed *in vitro* have revealed its invasive properties. It has been reported that *B. burgdorferi* is able to invade various nonphagocytic mammalian cells in order to reach an immunoprotected niche^{2,3}.

Correlative light electron microscopy (CLEM) is a method that bridges the gap between light and electron microscopy. A limitation of fluorescence microscopy (FM) rests in the lack of structural information about cellular architecture together with the impossibility of precisely identifying unlabeled structures. Besides, resolution of conventional optical microscopes is limited to approximately 200 nm due to light diffraction⁴. Electron microscopy (EM), on the other hand, is not suitable for screening larger sample areas and is not able to provide any data about cell dynamics. The examination of the object of interest provided by CLEM offers important complementary and unique information.

Preparation of biological specimens for CLEM is a time-consuming operation, especially for the most common combination strategy; correlative FM and transmission electron microscopy (TEM). After light microscopy examination at ambient temperature, the fluorescent markers have to be subsequently labeled with immunogold and the sample has to be chemically fixed, sequentially dehydrated by alcohols, embedded in resin, polymerized, and sectioned⁵. A possible alternative, depending on the size of the sample, is to vitrify the biological specimen by rapid plunging into liquid ethane/propane or by high pressure freezing with subsequent cryo-sectioning⁶. The principal benefit of the latter strategy is that the specimen remains in a hydrated state in glass-like amorphous ice, free of preparation artifacts caused by chemical fixation, dehydration, and embedding steps⁷. These artifacts can also negatively influence the precise localization of the object of interest in the electron microscope.

¹Institute of Parasitology, Biology Centre of the Czech Academy of Sciences, Branišovská 31, České Budějovice CZ-37005, Czech Republic. ²Faculty of Science, University of South Bohemia in České Budějovice, Branišovská 1760, České Budějovice CZ-37005, Czech Republic. ³Department of Virology, Veterinary Research Institute, Brno CZ-62100, Czech Republic. ⁴Faculty of Science, Charles University in Prague, Viničná 1594/7, Praha CZ-12800, Czech Republic. Correspondence and requests for materials should be addressed to M.S. (email: martin.strnad.cze@gmail.com)

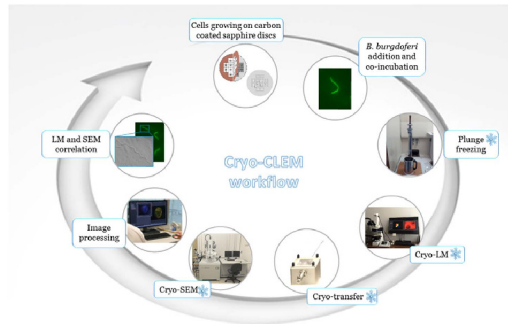


Figure 1. Schematic diagram illustrating the cryo-CLEM workflow.

A fundamental leap towards direct, fully artifact-free CLEM has been made possible by the introduction of a cryo-fluorescence microscope^{8,9}. In order to observe exactly the same instance without any minor modification in the structure when using the light microscope and the electron microscope, it is crucial to perform fluorescence microscopy after cryo-fixation¹⁰. Unlike procedures where the object of interest is studied by FM before vitrification, the all-cryo-workflow (cryo-CLEM) obviates all structural or positional changes that may occur during the period between fluorescence observation and cryo-immobilization, or during the transfer of the sample to the electron microscope¹¹.

Cryo-CLEM enables direct correlation of the sample in a native state and therefore it allows one to identify and visualize features that would otherwise remain hidden. Moving the realm of fluorescence microscopy closer to cryogenic applications, traditionally held by electron microscopy, is also motivated by the fact that the fluorescent molecules experience reduced photobleaching at very low temperatures^{8,12}. There is a dual explanation for this phenomenon; reactive molecules such as oxygen or water are frozen and cannot diffuse¹³ and transformational changes of fluorophores are reduced¹⁴. With regard to fluorescent tags, cryo-CLEM is particularly suitable for correlating membrane permeable dyes and gene fusion proteins such as green fluorescent protein (GFP)¹⁵.

The goal of this study is to provide a very fast microscopy procedure (Fig. 1) that is highly convenient for high-resolution studies of pathogen-host cell interactions in a native state. Using this novel correlative cryo-FM and cryo-SEM approach, we sought to further define the cell binding properties of *B. burgdorferi* and the suggested propensity of *B. burgdorferi* towards invasion of nonphagocytic cells.

Methods

Bacterial strain. *B. burgdorferi* Bb914, a GFP-expressing virulent derivative of strain 297¹⁶ was used. *B. burgdorferi* were grown in prepared Barbour-Stoenner-Kelly (BSK-II) medium containing 6% rabbit serum (Sigma-Aldrich) at 34 °C until mid-log phase ($\sim 1 \times 10^7$ spirochetes/ml), and enumerated with a Petroff-Hausser counting chamber using a dark-field microscope.

Mammalian cell cultures. Human neural cell line UKF-NB-4 was established from bone marrow metastasis harvested in a patient with Evans stage IV neuroblastoma¹⁷. Cells were cultured in Iscove's modified Dulbecco's Media (IMDM) supplemented with 10% fetal calf serum, 1% L-glutamine, and 1% antibiotic-antimycotic solution (Sigma-Aldrich) at 37 °C with 5% CO₂. Mouse neuroblastoma N2a cell line¹⁸ was cultured in high glucose Dulbecco's modified Eagle's medium (DMEM) containing ultraglutamine I (Lonza) supplemented with 10% fetal bovine serum and 1% antibiotic-antimycotic solution (Sigma-Aldrich) at 37 °C with 5% CO₂.

Cell viability assay. Trypan blue staining was performed to monitor the viability of mammalian cells after incubation with *B. burgdorferi*. Neural cells grown in tissue culture flasks were washed twice with PBS, trypsinized, and enumerated. Both sets of mammalian cells (1×10^6 cells) and *B. burgdorferi*, cultured to mid-log phase, were subsequently mixed in fresh cell culture medium at a multiplicity of infection (MOI) of 5, 10, and 20. After 1 and 5 hours of incubation at 34 °C, trypan blue dye (10%) was added and the viable cells were enumerated using a Bürker counting chamber. Each infection was performed in triplicate and one hundred cells were assessed for their viability. As control, cells without *Borrelia* were examined.

***B. burgdorferi* motility assay.** Approximately 1×10^7 spirochetes were centrifuged at 1500 g for 10 min at 15 °C and gently resuspended in 1 mL of either DMEM or IMDM media (with all supplements mentioned above) and maintained at 34 °C to test the motility of *B. burgdorferi* in these media. The motility was monitored for 8 hrs at 1 hr intervals on a glass slide using a dark-field microscope.

***B. burgdorferi* viability assays.** 1×10^7 spirochetes were centrifuged at 1500 g for 10 min at 15 °C and gently resuspended in 1 mL of either BSKII or DMEM media (with all supplements mentioned above) and maintained at 34 °C to test the viability of *B. burgdorferi*. Every 1.5 hrs equal diluted volumes from both media with borrelia, were separately plated in duplicate. This was done for 4 time points and the plates were then kept at 34 °C under anaerobic

Number of viable cells following <i>B. burgdorferi</i> co-incubation ^a				
Neural cell line	MOI	<i>Borrelia</i> (1 hr) ^b	<i>Borrelia</i> (5 hrs) ^b	No <i>Borrelia</i> control (5 hrs)
UKF-NB-4	5	100	99	98
	10	97	98	
	20	100	98	
N2a	5	91	90	90
	10	89	90	
	20	88	88	

Table 1. Cell viability assay. ^a100 cells counted (average out of 3 measurements; rounded value). ^bCells co-incubation time with *B. burgdorferi*.

conditions for 2 weeks. The colonies formed were then counted. In addition, the same number of spirochetes after centrifugation was also resuspended in 1 ml of BSKII or DMEM media and dead cell stain propidium iodide (PI) in DMSO was added to a final concentration of 60 μ M/mL. The viability was monitored for 6 hrs at 1 hr intervals on a glass slide using a fluorescence microscope (Olympus BX-60 with Olympus DP71 camera). Control experiments were performed to test the applicability of PI staining for GFP-expressing *Borrelia* (Supplementary Figure S1).

Mammalian cell-*B. burgdorferi* association assay. Neural cells were harvested using trypsin, enumerated and 1×10^5 cells were seeded 12 hrs before the start of experiment on 3 mm sapphire discs (Leica Microsystems) placed on a 24-well plate and allowed to attach at 37 °C with 5% CO₂. Prior to this, for orientation purposes, TEM finder grids (Electron Microscopy Sciences) were placed on the sapphire discs and carbon-coated to facilitate the cell re-localization (sapphire discs were UV-sterilized for 30 min after that). *B. burgdorferi* were centrifuged at 1500 g for 10 min at 15 °C and resuspended in IMDM or DMEM, depending on the mammalian cells being used. The spirochetes (1×10^6) were added to the mammalian cells and incubated at 34 °C for up to 3 hrs. At the same time, nuclear stain Hoechst 33342 (Sigma-Aldrich) was added in a final concentration of 10 μ g/mL. Sapphire discs with attached cells and bacteria were washed in PBS, blotted for 2 sec (each side) at room temperature and cryo-immobilized in a home-made plunge freezing device containing liquid propane.

Cryo-CLEM examination. For cryo-FM examination, the Leica EM CryoCLEM (Leica Microsystems) set with the Leica DM6000 FS was used. After cryo-fixation, remainders of propane were blotted using pre-cooled filter paper and the sapphire discs mounted on the cartridge were loaded directly into the microscope using a cryo-transfer shuttle cooled with liquid nitrogen. For imaging, Leica HXC PL APO 50x/0.9 CLEM objective and Leica DFC310FX camera were employed.

Following cryo-FM examination, the sapphire discs left mounted on the cartridge were put back into the cryo-transfer shuttle, where the whole cartridge was transferred under vacuum into the chamber of the cryo-attachment CryoALTO 2500 (Gatan, Inc.). The chamber was heated to -95 °C *in vacuo* for 5–20 min to remove the ice contamination by sublimation and subsequently the sample was sputter coated for 40 sec with Pt/Pd before observation. The specimens were observed in FESEM JEOL 7401F (JEOL Ltd.) operated at 1 kV with a working distance around 9 mm and the stage temperature of approximately -140 °C.

Image analysis and overlays of images were carried out using LAS X software (Leica Microsystems) and Adobe Photoshop CS6. Linear adjustments of brightness and contrast performed on fluorescence microscopy images did not obscure, eliminate, or misrepresent any information present in the original images. Final figures were constructed using CorelDraw 11.

Results

Cell viability assay. The cytopathic effects of *B. burgdorferi* co-culturing on the well-being of neural cell lines was investigated. For the neural cell-*B. burgdorferi* association assay, the neural cells were first seeded on the sapphire discs 12 hrs before addition of *Borrelia*. Although, the doubling times of the respective cell lines in our culture conditions were not assessed, the cell viability assay was performed at various multiplicities of infection, which should cover the whole range of potential MOIs during the mammalian cell-*B. burgdorferi* association assay. In both analysed cell lines, there were no observable adverse effects on neural cells after co-culturing with *B. burgdorferi*, when compared to the cells alone controls (Table 1). Furthermore, there were no statistically significant differences in the number of dead cells at both inspected time intervals, i.e. 1 hour and 5 hours of co-incubation. These results confirmed the ability of *B. burgdorferi* to interact and associate with neural cells without causing any observable adverse effects.

***B. burgdorferi* motility assay.** Since the association assays were carried out in cell culture media, the cytotoxic effects of DMEM and IMDM with all supplements on *B. burgdorferi* had to be determined. The motility was monitored every hour for a total of 8 hrs. During the first three examinations, the overwhelming majority of spirochetes were motile, indicating good fitness. Subsequent bacterial counts revealed a steady decrease in motility with an increasing number of nonmotile spirochetes. After 8 hrs, only *Borrelia* that formed aggregates were partially motile, the rest of spirochetes showed no such signs.

***B. burgdorferi* viability assays.** Having discerned that the antibiotic/antimycotic mixture added to both IMDM and DMEM media was the possible reason for the loss of motility, we wanted to confirm whether this

Time-point (hrs)	BSKII (No. of colonies) ^a	DMEM (No. of colonies) ^a
1.5	372	368
3	380	52
4.5	382	46
6	414	0

Table 2. *B. burgdorferi* viability assay using plating. ^aaverage of two plates.

Time-point (hrs)	BSKII (No. of dead cells) ^a	DMEM (No. of dead cells) ^a
1	0	0
2	–	1
3	0	2
4	–	6
5	–	12
6	0	14

Table 3. *B. burgdorferi* *in situ* viability assay using dead staining. –Not measured. ^a100 cells counted (average out of 3 measurements; rounded value).

motility loss was because of non-viable spirochetes. We therefore used only one of the media, DMEM for this assay. The number of colonies that grew on the plates (Table 2) indicates a significant drop in the number of viable *Borrelia* at 3 hrs compared to 1.5 hrs between the DMEM medium and the BSKII. But since it is likely that the antibiotic/antimycotic mixture may have influenced the multiplication and therefore the apparent viability of the spirochetes after antibiotic exposure, we decided to carry out one more viability assay that assessed more accurately the viability *in situ*. Fluorescence microscopy enumeration of live/dead cells revealed a significantly lower increase in the number of dead borrelia among those incubated with the DMEM media (Table 3) compared to the numbers obtained by the plating of borrelia incubated in the same media.

Mammalian cell-*B. burgdorferi* association assay. After tick transmission, *B. burgdorferi* must cope with the strong immune response of the mammalian host. One potential strategy exploited by *Borrelia* to avoid immune clearance might be to invade the host's nonphagocytic cells². To examine this assumption, the ability of *B. burgdorferi* to associate with one human and with one mouse cell line of neural origin was tested. GFP-expressing *B. burgdorferi* cells were added at MOI of 10 to the cells. On average, 1 in 5 cells was *Borrelia*-associated under this MOI. The MOI chosen was lower than in previous studies^{2,19} in order to test the applicability of the cryo-correlative workflow for studies of pathogens, which are able to cause an infection at very low numbers.

The co-incubation time of *Borrelia* with neural cells was set at 3 hrs for the following reasons. We experienced cell culture contamination without the addition of the antibiotic-antimycotic solution. The addition of the antibiotic-antimycotic solution, however, limited the time interval of possible mammalian cell-*B. burgdorferi* co-incubation. Although there was a significant drop in the number of viable *Borrelia* at 3 hrs indicated by plating, the *in situ* viability assay using dead cell staining revealed the first more significant increase in the number of dead cells only after three hours of co-incubation. Moreover, the motility assay has shown that the majority of spirochetes were still motile at 3 hrs and because it was found that motility is critical for infection of the mammalian host²⁰, we decided to work at this time point.

Following incubation, cryo-FM was used to reveal the sparsely distributed spirochetes, which were afterwards easily located in the scanning electron microscope. The whole procedure from cryo-immobilization to SEM image acquisition (Fig. 1) lasted less than three hours, which is much less than in correlative microscopic studies at ambient temperatures. *B. burgdorferi* were observed to be associated with both cell lines examined. There were no indications suggesting that *Borrelia* can penetrate either of the cell lines within the three hour time period. We assume that *Borrelia* did not have enough time to penetrate the cells. Of course, the possibility that *Borrelia* either were inhibited by antibiotics in the cell medium, or cannot invade the cells used in this study cannot be excluded. We observed that the spirochetes retained their spiral-shape during this period of time, touching the neural cells only at a few discrete sites, which might also suggest uneven distribution of outer surface proteins important for *Borrelia*-host interplay²¹. Figures 2 and 3 show representative images of both of the cell lines interacting with *Borrelia*. It is clear from the figures that the *Borrelia* actively interact with the cells and are not idly lying on the cell surface. Low-resolution overview images from a cryo-fluorescence microscope and high-resolution details of mammalian cell-*B. burgdorferi* association acquired by cryo-SEM are displayed. The hydrated specimen was coated with a layer of Pt/Pd (2–4 nm) in the cryo-attachment chamber and observed at low kV to avoid charging artifacts and decrease sensitivity to beam damage in the microscope. Interestingly, fluorescence was not lost after covering the sample surface with a metal layer when re-examined in the cryo-fluorescence microscope (Fig. 3B).

Discussion

For many decades, the primary method of choice for imaging host-parasite interactions has been light microscopy, especially fluorescence microscopy. However, the interplay between a pathogen and a host cell is characterized by

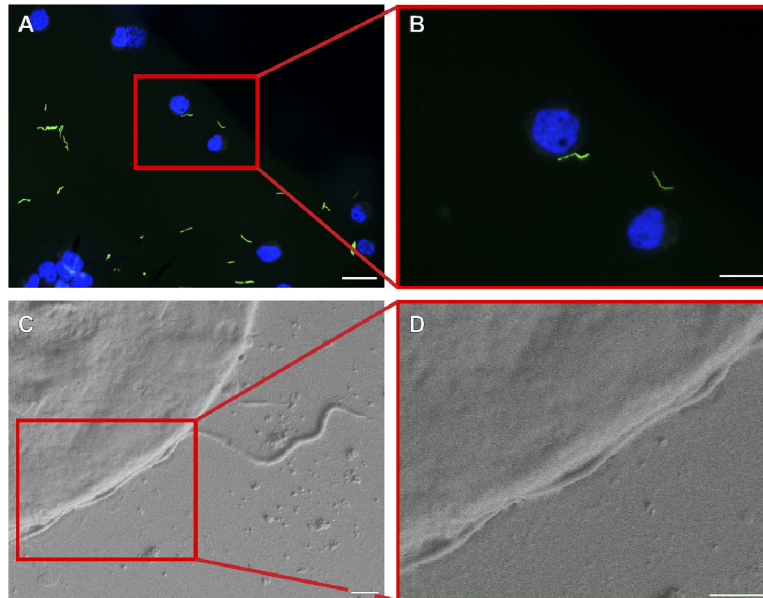


Figure 2. Correlative cryo-fluorescence (A,B) and cryo-scanning electron microscopy (C,D) of *Borrelia burgdorferi*-GFP on the surface of human neuroblastoma cells grown on carbon-coated sapphire discs. A series of images of one particular GFP-tagged spirochete (green) interacting with the cell counterstained with Hoechst 33342 (blue). Images of region of interest from low magnification FM to high magnification SEM. The cryo-SEM images were acquired after 10 minutes ice sublimation and deposition of Pt/Pd layer onto the sample surface. Scale bars: (A) 50 μm , (B) 25 μm , (C,D) 1 μm .

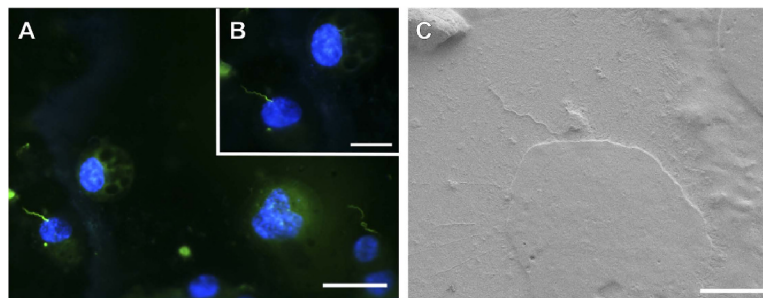


Figure 3. Demonstration of fluorescence preservation after deposition of Pt/Pd layer on the sample followed by SEM examination under cryo-conditions. Association of *B. burgdorferi*-GFP (green) with mouse neuroblastoma cells. Cells were counterstained with Hoechst 33342 (blue). Images acquired before (A) and after (B) cryo-SEM examination. (B) Image taken after 20 minutes ice sublimation and deposition of Pt/Pd layer on the sample surface. (C) Cryo-SEM micrograph of the spirochete-cell interaction shown in (A) and (B). Scale bars: (A) 50 μm , (B) 25 μm and (C) 10 μm .

a cascade of events occurring at the scale that are not resolved by conventional diffraction-limited FM. In order to obtain more informative ultrastructural data, some high-resolution microscopy techniques such as electron microscopy have to be co-applied²².

This study describes a complete cryo-correlative workflow for the localization of objects of interest by cryo-FM and their subsequent ultrastructural examination by cryo-SEM. Due to the fact that FM is performed after cryo-fixation and there are no additional procedures between cryo-FM and cryo-EM, this technique provides the ability to obtain the most precise and reliable correlative data. Using this method, one is likely to gain insight into

crucial molecular mechanisms that could potentially be exploited for innovative antimicrobial strategies when looking at pathogen-host interactions.

Cryo-CLEM is a state-of-the-art approach and only few applications have been described in literature so far. In all the setups, cryo-FM was combined with cryo-electron tomography to identify GFP-tagged microtubule bundles in mammalian cells⁸, filament bundles in migrating keratinocytes⁹, mitochondria in human endothelial cells¹⁵, cytoplasmic bundles of MreB in *V. cholerae*²³, cytoplasmic arrays in *R. spheroides*²⁴, secretion system in *M. xanthus*²⁵, and to study cell division in *Streptomyces*²⁶. To the best of our knowledge, we report the first cryo-correlation between fluorescence and scanning electron microscopy. Probably the most important advantage of our setup over correlating with TEM rests in the fact that no constraints are set on the cell's size. For TEM, cells have to grow thinner than 1 μm , better close to 500 nm, allowing them to be used for cryo-TEM without the need for cryo-sectioning²⁷. Cryo-sectioning is a difficult technique that requires higher level of expertise and specialised equipment. Furthermore, correlation with SEM is ideal for study of surface interactions, which could be only hardly followed by TEM. Moreover, after cryo-FM examination, the whole cartridge holding the sapphire disc was mounted to the SEM holder. This is generally not possible for highly sophisticated holders used in electron tomography. This option is highly convenient because we avoid the possibility of losing or damaging the sapphire disc by direct manipulation. In case of using finder grids, as it is popular practice in the cryoFM-TEM studies²⁴, the quite common scenario of bending the grid is also omitted in our setup.

In our hands, the cryo-CLEM has proven to be an extremely straightforward and efficient method. Still there are few points to keep in mind. Firstly, transferring the sample from the plunge freezer into the light microscope and later on into the electron microscope has to be precisely controlled to avoid any adverse contamination and structural damage. It is advisable to maintain sample temperature below $-135\text{ }^{\circ}\text{C}$ ¹⁰, preventing vitreous ice from crystallizing into cubic or hexagonal ice, which adversely affects the cellular ultrastructure. Secondly, what saved time during the cell of interest re-localization was keeping sapphire discs mounted on the cartridge between cryo-FM and cryo-SEM imaging, as sometimes the lettering of the finder grid pattern marked out on the sapphire discs was not clearly discernible. The cartridge clamps securing the sapphire disc from movement provided an ideal starting point for EM examination (Supplementary Figure S2). Thirdly, even with great care, slight ice contamination is usually formed on the sample surface during the sample manipulation and its transfer²⁸. This obscures the visualization of structures of interest and, moreover, it enhances the charge artifacts. In order to remove the ice contamination from the sample surface, the cryo-attachment chamber was heated to $-95\text{ }^{\circ}\text{C}$. The vacuum sublimation reduced ice contamination allowing the observation of higher structural details, but on the other hand, prolonged heating (generally $>15\text{ min}$) caused the formation of sublimation artifacts such as small pits in the sample surface.

After cryo-SEM examination under high vacuum (approximately $1 \times 10^{-5}\text{ Pa}$), it was possible to locate again the object of interest in the cryo-fluorescence microscope since fluorescence was not attenuated. The resistance to fluorescence attenuation was observed with two fluorescent molecules of different colours, namely green fluorescent protein and blue nuclear dye Hoechst 33342. The potential reduction in fluorescence intensity was not quantified since not enough data had been acquired. Of note, fluorescence was not lost even after deposition of a Pt/Pd layer on the specimens in the cryo-attachment chamber of the scanning electron microscope. Preservation of Hoechst 33342 signal can be rationalized by the fact that this nuclear dye is hidden inside the cells and shielded from the metal particles. On the other hand, the resistance of GFP to fluorescence quenching can be presumably attributed to a thin layer of ice covering the GFP-expressing *B. burgdorferi*. The GFP signal was well-detectable even after 20 minutes of ice sublimation followed by metal layer deposition. Longer times of ice sublimation were not tested since after 20 minutes the cell surface structure was impaired. The observation of fluorescence preservation can have fundamental implications for instance on sample preparation for integrated light and electron microscopes²⁹. It might also come in useful when an interesting object or phenomenon is spotted using the electron microscope and needs to be reassessed with the light microscope.

B. burgdorferi being a zoonotic pathogen finds itself in two very different environments – a mammalian host and the arthropod tick vector. Both of these environments provide enough physical/cellular barriers for the spirochete to be in motility mode or adhering to cells if not inside certain cells³⁰. In the tick the *Borrelia* migrate from the midgut to the salivary glands of an infected tick upon blood feeding followed by entrance into the mammal through the tick bite site. The spirochete also enters a tick that is feeding on a reservoir host by leaving the site of tick feeding and entering the naive tick through the bloodmeal. In a mammalian host it has to disseminate from the bite site to secondary points of infection and persist within particular niches³¹. All these concerted movements in the two environments are assumed or known to involve the process of motility and adhesion to cells³². It has been shown that *Borrelia* initially tether to a cell followed by dragging and then extravasation³³. These activities require the use of a complex of proteins that are being expressed on the surface of the *Borrelia*. Identification of most of the surface adhesins in *Borrelia* has been through *in vitro* assays³⁴. Some of these studies have made use of either light microscopy techniques or EM to look at the actual state of adhesion. Recent studies exploring the intricacies of *B. burgdorferi* internalization by mammalian cells *in vitro* have also utilized either immunofluorescence microscopy^{2,3} or solely transmission electron microscopy without *Borrelia*-specific labeling³⁵ for determining the extracellular or intracellular location of the spirochetes. Immunofluorescence techniques might be sometimes misleading since the relative mutual positioning of a cell and a pathogen is hard to be reliably discerned without ultrastructural information. On the other hand, the search for spirochetes over larger areas (e.g. over the 3 mm sapphire disc) using EM can take hours due to their size and their slender morphology. One can see many structures or artifacts that can resemble *Borrelia* by their shape and without specific labeling these structures can be falsely identified (Supplementary Figure S3). So that no ambiguity can arise, it is fundamental to use the correlative approach.

In summary, we have established a very fast, preparation-artifact-free and easily attainable correlative cryo-FM and cryo-SEM workflow with the intention to streamline the generally prolonged ambient temperature correlative procedures. Using this technique, we have shown that *B. burgdorferi* associates with mammalian nonphagocytic

cells, but is not able to invade them within three hours of co-incubation. The discussed technique is suitable for a wide array of applications ranging from single cell studies to whole tissue examination. Especially appealing for future work appears to be the combination of cryo-super resolution FM³⁶ and cryo-SEM, which could allow the organization of fluorescently labeled surface proteins to be studied with near-to-nanometer resolution.

References

1. Steere, A. C. Lyme disease. *N Engl J Med* **345**, 115–125 (2001).
2. Livengood, J. A. & Gilmore, R. D. Jr. Invasion of human neuronal and glial cells by an infectious strain of *Borrelia burgdorferi*. *Microbes Infect* **8**, 2832–2840 (2006).
3. Wu, J., Weening, E. H., Fiske, J. B., Höök, M. & Skare, J. T. Invasion of eukaryotic cells by *Borrelia burgdorferi* requires $\beta(1)$ integrins and Src kinase activity. *Infect Immun* **79**, 1338–1348, doi: 10.1128/IAI.01188-10 (2011).
4. Abbe, E. Beiträge zur Theorie des Mikroskops und der mikroskopischen Wahrnehmung. *Archiv für Mikroskopische Anatomie* **9**, 413–418 (1873).
5. Polishchuk, R. S., Polishchuk, E. V. & Luini, A. Visualizing live dynamics and ultrastructure of intracellular organelles with preembedding correlative light-electron microscopy. *Methods Cell Biol* **111**, 21–35, doi: 10.1016/B978-0-12-416026-2.00002-9 (2012).
6. Dubochet, J. et al. Cryo-electron microscopy of vitrified specimens. *Q Rev Biophys* **21**, 129–228 (1988).
7. Dubochet, J. & Sartori Blanc, N. The cell in absence of aggregation artifacts. *Micron* **32**, 91–99 (2001).
8. Schwartz, C. L., Sarbash, V. I., Ataullakhanov, F. I., McIntosh, J. R. & Nicasastro, D. Cryo-fluorescence microscopy facilitates correlations between light and cryo-electron microscopy and reduces the rate of photobleaching. *J Microsc* **227**, 98–109 (2007).
9. Sartori, A. et al. Correlative microscopy: bridging the gap between fluorescence light microscopy and cryo-electron tomography. *J Struct Biol* **160**, 135–145 (2007).
10. Rigort, A., Villa, E., Bäuerlein, F. J., Engel, B. D. & Plitzko J. M. Integrative approaches for cellular cryo-electron tomography: correlative imaging and focused ion beam micromachining. *Methods Cell Biol* **111**, 259–281, doi: 10.1016/B978-0-12-416026-2.00014-5 (2012).
11. Briegel, A. et al. Location and architecture of the *Caulobacter crescentus* chemoreceptor array. *Mol Microbiol* **69**, 30–41, doi: 10.1111/j.1365-2958.2008.06219.x (2008).
12. Li, W., Stein, S. C., Gregor, I. & Enderlein, J. Ultra-stable and versatile widefield cryo-fluorescence microscope for single-molecule localization with sub-nanometer accuracy. *Opt Express* **23**, 3770–3783, doi: 10.1364/OE.23.003770 (2015).
13. Moerner, W. E. & Orrit, M. Illuminating single molecules in condensed matter. *Science* **283**, 1670–1676 (1999).
14. Mao, B. et al. Flash photolysis and low temperature photochemistry of bovine rhodopsin with a fixed 11-ene. *Biophys J* **35**, 543–546 (1981).
15. van Driel, L. F., Valentijn, J. A., Valentijn, K. M., Koning, R. I. & Koster, A. J. Tools for correlative cryo-fluorescence microscopy and cryo-electron tomography applied to whole mitochondria in human endothelial cells. *Eur J Cell Biol* **88**, 669–684, doi: 10.1016/j.ejcb.2009.07.002 (2009).
16. Dunham-Ems, S. M. et al. Live imaging reveals a biphasic mode of dissemination of *Borrelia burgdorferi* within ticks. *J Clin Invest* **119**, 3652–3665, doi: 10.1172/JCI39401 (2009).
17. Cinatl, J. et al. Differentiation arrest in neuroblastoma cell culture. *J Cancer Res Clin Oncol (Suppl.)* **116**, 9 (1990).
18. Klebe, R. J. & Ruddle, F. H. Neuroblastoma: cell culture analysis of a differentiating stem cell system. *J Cell Biol* **43**, 69a (1969).
19. Ma, Y., Sturrock, A. & Weis, J. J. Intracellular localization of *Borrelia burgdorferi* within human endothelial cells. *Infect Immun* **59**, 671–678 (1991).
20. Sultan, S. Z. et al. Motility is crucial for the infectious life cycle of *Borrelia burgdorferi*. *Infect Immun* **81**, 2012–2021, doi: 10.1128/IAI.01228-12 (2013).
21. Lemgruber, L. et al. Nanoscopic localization of surface-exposed antigens of *Borrelia burgdorferi*. *Microsc Microanal* **21**, 680–688, doi: 10.1017/S1431927615000318 (2015).
22. Loussert, C., Forestier, C. L. & Humbel, B. M. Correlative light and electron microscopy in parasite research. *Methods Cell Biol* **111**, 59–73, doi: 10.1016/B978-0-12-416026-2.00004-2 (2012).
23. Swilius, M. T. et al. Long helical filaments are not seen encircling cells in electron cryotomograms of rod-shaped bacteria. *Biochem Biophys Res Commun* **407**, 650–655, doi: 10.1016/j.bbrc.2011.03.062 (2011).
24. Briegel, A. et al. Structure of bacterial cytoplasmic chemoreceptor arrays and implications for chemotactic signaling. *Elife* **3**, e02151, doi: 10.7554/eLife.02151 (2014).
25. Chang, Y. W. et al. Correlated cryogenic photoactivated localization microscopy and cryo-electron tomography. *Nat Methods* **11**, 737–739, doi: 10.1038/nmeth.2961 (2014).
26. Koning, R. I. et al. Correlative cryo-fluorescence light microscopy and cryo-electron tomography of *Streptomyces*. *Methods Cell Biol* **124**, 217–239, doi: 10.1016/B978-0-12-801075-4.00010-0 (2014).
27. Lucić, V., Rigort, A. & Baumeister, W. Cryo-electron tomography: the challenge of doing structural biology *in situ*. *J Cell Biol* **202**, 407–419, doi: 10.1083/jcb.201304193 (2013).
28. Hoyt, F. H., Hansen, B. T. & Fischer, E. R. Secondary sublimation removes ice contamination for improved visualization of structures by cryo-SEM. *Microsc Microanal (Suppl. S2)* **16**, 976–977, doi: 10.1017/S1431927610057673 (2010).
29. Agronskaia, A. V. et al. Integrated fluorescence and transmission electron microscopy. *J Struct Biol* **164**, 183–189, doi: 10.1016/j.jsb.2008.07.003 (2008).
30. Radolf, J. D., Caimano, M. J., Stevenson, B. & Hu, L. T. Of ticks, mice and men: understanding the dual-host lifestyle of Lyme disease spirochaetes. *Nat Rev Microbiol* **10**, 87–99, doi: 10.1038/nrmicro2714 (2012).
31. Rosa, P. A., Tilly, K. & Stewart P. E. The burgeoning molecular genetics of the Lyme disease spirochaete. *Nat Rev Microbiol* **3**, 129–143 (2005).
32. Dunham-Ems, S. M., Caimano, M. J., Eggers, C. H. & Radolf, J. D. *Borrelia burgdorferi* requires the alternative sigma factor RpoS for dissemination within the vector during tick-to-mammal transmission. *PLoS Pathog* **8**, e1002532, doi: 10.1371/journal.ppat.1002532 (2012).
33. Moriarty, T. J. et al. Real-time high resolution 3D imaging of the Lyme disease spirochaete adhering to and escaping from the vasculature of a living host. *PLoS Pathog* **4**, e1000090, doi: 10.1371/journal.ppat.1000090 (2008).
34. Coburn, J., Leong, J. & Chaconas, G. Illuminating the roles of the *Borrelia burgdorferi* adhesins. *Trends Microbiol* **21**, 372–379, doi: 10.1016/j.tim.2013.06.005 (2013).
35. Chmielewski, T. & Tylewska-Wierzbanska, S. Interactions between *Borrelia burgdorferi* and mouse fibroblasts. *Pol J Microbiol* **59**, 157–160 (2010).
36. Kaufmann, R. et al. Super-resolution microscopy using standard fluorescent proteins in intact cells under cryo-conditions. *Nano Lett* **14**, 4171–4175, doi: 10.1021/nl501870p (2014).

Acknowledgements

This study was supported by the Technology Agency of the Czech Republic (TE01020118), the Czech Academy of Sciences (Z60220518), the Czech Science Foundation projects Nos. P502/11/2116 and GA14-29256S, ANTIGONE (EU-7FP; 278976), ANTIDotE (EU-7FP; 602272–2) and project LO1218, with financial support from the MEYS

of the Czech Republic under the NPU I program. M.S. was funded by the Grant Agency of the University of South Bohemia in České Budějovice. We would like to thank Ruwin Pandithage and Andreas Nowak from Leica Microsystems GmbH for providing Leica EM Cryo-CLEM and for the thorough training in the use of this instrument. Next, we thank Dr. Melissa J. Caimano for providing GFP-expressing strain Bb914 and Prof. Tomáš Eckschlager for providing UKF-NB-4 cells. We would also like to thank Jiří Vaněček for help with SEM images acquisition and general technical support throughout the whole procedure.

Author Contributions

M.S. conceived the study, acquired and analyzed the data, and together with R.O.M.R. wrote the majority of the manuscript. J.S., M.V. and J.N. participated in the experimental design and in the microscopic examination. M.S. and R.O.M.R. carried out the viability assays. J.E. participated in the preparation of cell cultures and in the non-microscopic part of the project. L.G. and J.N. participated in the design and coordination of the study. All authors have given approval to the final version of the manuscript.

Additional Information

Supplementary information accompanies this paper at <http://www.nature.com/srep>

Competing financial interests: The authors declare no competing financial interests.

How to cite this article: Strnad, M. *et al.* Correlative cryo-fluorescence and cryo-scanning electron microscopy as a straightforward tool to study host-pathogen interactions. *Sci. Rep.* **5**, 18029; doi: 10.1038/srep18029 (2015).



This work is licensed under a Creative Commons Attribution 4.0 International License. The images or other third party material in this article are included in the article's Creative Commons license, unless indicated otherwise in the credit line; if the material is not included under the Creative Commons license, users will need to obtain permission from the license holder to reproduce the material. To view a copy of this license, visit <http://creativecommons.org/licenses/by/4.0/>

3.5 Manuscript 5:

Hillman, C., Stewart, P.E., **Strnad, M.**, Stone, H., Starr, T., Carmody, A., Evans, T.J., Carracoi, V., Wachter, J., Rosa, P. (2019) Visualization of spirochetes by labeling membrane proteins with fluorescent biarsenical dyes. *Frontiers in Cellular and Infection Microbiology* 9: 287.

Annotation

In **Manuscript 4**, we have studied the *Borrelia*-cell interactions using green fluorescent protein-expressing spirochetes, which were created by insertion of a *gfp* expression cassette into the cp26 plasmid of the bacteria. Although such mutants are perfectly applicable to a vast majority of infectious studies, the bulkiness of GFP (~30 kDa) fusion protein can lead to interference with a target protein. It may hinder or impede proper folding of the target protein or affect its cellular localization. Additionally, in such an assembly, the fluorescence is not spatially localised as the *gfp* expression cassette is not fused to a particular borrelial protein. As my long-term intention is to study and visualize the underlying binding mechanisms at the borrelia-cell interaction interface, a system that better copes with this goal needs to be established. Here in **Manuscript 5**, we have reported the successful adaptation of FIAsh dye for live-cell imaging of two genera of spirochetes, *Leptospira* and *Borrelia*, by labeling inner or outer membrane proteins tagged with tetracysteine motifs. This protein labeling system circumvents the above mentioned issues with bulkiness of GFP and its derivatives. We have demonstrated by using infectious *Borrelia* that the tetracysteine motif was stably maintained *in vivo* and did not adversely affect infectivity in either the arthropod vector or murine host. The biarsenical-bound proteins could be followed over several days, indicating that this approach can be used in time-course studies of live cells.



Visualization of Spirochetes by Labeling Membrane Proteins With Fluorescent Biarsenical Dyes

Chadwick Hillman¹, Philip E. Stewart¹, Martin Strnad^{1,2,3}, Hunter Stone¹, Tregel Starr¹, Aaron Carmody⁴, Tyler J. Evans¹, Valentina Carracoi¹, Jenny Wachter¹ and Patricia A. Rosa^{1*}

¹ Laboratory of Bacteriology, Rocky Mountain Laboratories, National Institute of Allergy and Infectious Diseases, National Institutes of Health, Hamilton, MT, United States, ² Institute of Parasitology, Biology Centre of the Czech Academy of Sciences, České Budějovice, Czechia, ³ Faculty of Science, University of South Bohemia in České Budějovice, České Budějovice, Czechia, ⁴ Research Technologies Section, Rocky Mountain Laboratories, National Institute of Allergy and Infectious Diseases, National Institutes of Health, Hamilton, MT, United States

OPEN ACCESS

Edited by:

Tao Lin,
Baylor College of Medicine,
United States

Reviewed by:

Janakiram Seshu,
University of Texas at San Antonio,
United States
Robert D. Gilmore,
Centers for Disease Control and
Prevention (CDC), United States
Mathieu Picardeau,
Institut Pasteur, France

*Correspondence:

Patricia A. Rosa
prosa@niaid.nih.gov

Specialty section:

This article was submitted to
Molecular Bacterial Pathogenesis,
a section of the journal
Frontiers in Cellular and Infection
Microbiology

Received: 06 June 2019

Accepted: 24 July 2019

Published: 20 August 2019

Citation:

Hillman C, Stewart PE, Strnad M,
Stone H, Starr T, Carmody A,
Evans TJ, Carracoi V, Wachter J and
Rosa PA (2019) Visualization of
Spirochetes by Labeling Membrane
Proteins With Fluorescent
Biarsenical Dyes.
Front. Cell. Infect. Microbiol. 9:287.
doi: 10.3389/fcimb.2019.00287

Numerous methods exist for fluorescently labeling proteins either as direct fusion proteins (GFP, RFP, YFP, etc.—attached to the protein of interest) or utilizing accessory proteins to produce fluorescence (SNAP-tag, CLIP-tag), but the significant increase in size that these accompanying proteins add may hinder or impede proper protein folding, cellular localization, or oligomerization. Fluorescently labeling proteins with biarsenical dyes, like FIAsH, circumvents this issue by using a short 6-amino acid tetracysteine motif that binds the membrane-permeable dye and allows visualization of living cells. Here, we report the successful adaptation of FIAsH dye for live-cell imaging of two genera of spirochetes, *Leptospira* and *Borrelia*, by labeling inner or outer membrane proteins tagged with tetracysteine motifs. Visualization of labeled spirochetes was possible by fluorescence microscopy and flow cytometry. A subsequent increase in fluorescent signal intensity, including prolonged detection, was achieved by concatenating two copies of the 6-amino acid motif. Overall, we demonstrate several positive attributes of the biarsenical dye system in that the technique is broadly applicable across spirochete genera, the tetracysteine motif is stably retained and does not interfere with protein function throughout the *B. burgdorferi* infectious cycle, and the membrane-permeable nature of the dyes permits fluorescent detection of proteins in different cellular locations without the need for fixation or permeabilization. Using this method, new avenues of investigation into spirochete morphology and motility, previously inaccessible with large fluorescent proteins, can now be explored.

Keywords: spirochetes, *Borrelia*, *Leptospira*, fluorescent protein, tetracysteine tag, biarsenical dye

INTRODUCTION

The phylum *Spirochaetes* contains multiple members of medical and veterinary concern, which include *Borrelia* species (Lyme disease and relapsing fever) and pathogenic *Leptospira* species (leptospirosis). Both genera exhibit distinctive morphologies with periplasmic flagella encompassed between inner and outer membranes, which, combined with their unique shape and structure, allow these pathogens to move quickly through tissues during infection. However, the molecular

techniques available to identify virulence determinants and key cellular factors are rudimentary in spirochetes compared to those available for some members of the *Enterobacteriaceae*. Such limitations have hampered efforts to identify proteins involved in cell shape, spatial localization of proteins, and transport across the periplasmic space while accommodating flagellar rotation. To address some of the molecular mechanisms underpinning these and other cellular processes, fluorescent proteins and dyes have proven to be valuable tools, permitting detection of spirochete-host interactions (Moriarty et al., 2008; Norman et al., 2008; Dunham-Ems et al., 2009; Bockenstedt et al., 2012; Carrasco et al., 2015; Teixeira et al., 2016; Krishnavajhala et al., 2017), localization or transport of proteins within the bacterial cell (Schulze and Zuckert, 2006; Schulze et al., 2010; Xu et al., 2011; Zhang et al., 2015), or as reporter systems for gene expression (Carroll et al., 2003; Bykowski et al., 2006; Clifton et al., 2006; Eggers et al., 2006; Miller et al., 2006; Gautam et al., 2008, 2009; Whetstone et al., 2009; Aviat et al., 2010; Cerqueira et al., 2011; Grove et al., 2017; Matsunaga and Haake, 2018; Takacs et al., 2018). However, the use of fluorescent protein fusions, most commonly with green or red fluorescent protein (GFP or RFP, respectively), has limitations: the bulkiness of these proteins, typically 25–30 kDa, can lead to atypical protein localization and irregular cellular trafficking (Senf et al., 2008), and some FP alleles have specific pH or oxygen requirements that are not always compatible with the targeted location or underlying biological question. More recent adaptations, such as SNAP- and CLIP-tags, are comparable in size (20 kDa) and require an additional extraneous chemical agent that could impact cell growth and viability in order to fluoresce.

In an attempt to subvert size-related problems caused by fluorescent protein fusions, Griffin and Tsien developed a system for intra- and extra-cellular *in vitro* protein labeling using biarsenical dyes that bind specifically to tetracysteine motifs (Griffin et al., 1998). This method uses a synthetic fluorescent biarsenical compound, such as **Fluorescein Arsenical Helix binder (FIAsH)** or **Resorufin Arsenical Helix binder (ReAsH)**, which forms a stable complex with a tetracysteine motif consisting of six amino acids (CCPGCC). The central two amino acids of the spacer (proline plus glycine) create a hairpin that reduces steric hindrance between the arsenical groups and the tetracysteine motif, yielding optimum fluorescence (Adams et al., 2002). Using this technique, fluorescent live cells can be viewed in real-time without the issues typically encountered with GFP and other accessory proteins.

Biarsenical dyes have been widely used to study protein dynamics and interactions in various bacteria, viruses and even prions. In an attempt to view components of the Type II secretion system in *Pseudomonas*, Senf et al. initially used GFP fused to their target protein, but the fusion resulted in a non-functional and unstable protein (Senf et al., 2008). In contrast, the nominal mass added by the tetracysteine motif did not perturb the system and allowed successful visualization of the Type II secretion system. Likewise, groups studying viral kinetics encountered similar obstacles with GFP-fusions of polyproteins, which disrupted normal viral function (Panchal et al., 2003; Arhel et al., 2006). However, both groups successfully employed

the much smaller tetracysteine tags coupled with biarsenical dyes to visualize HIV infection and Ebola virus assembly. Other examples of the successful use of tetracysteine tags include the visualization of flagellar dynamics in *E. coli* communities (Copeland et al., 2010), *Shigella* effector components of the Type III secretion system entering host cells in real time (Enninga et al., 2005), and converted forms of prion proteins (Gaspersic et al., 2010). More recently, biarsenical dyes have been used to gain an understanding of flagellar elongation and decay in *E. coli* (Zhao et al., 2018). The broad application potential of tetracysteine motifs coupled with biarsenical dyes provides an alternative fluorescent method to visualize cells and proteins when fusion to larger fluorescent proteins may produce aberrant results.

Here, our group utilized tetracysteine motifs and biarsenical dyes to successfully label membrane proteins in live cells of the spirochetes *Leptospira biflexa* and *Borrelia burgdorferi*. We found that the biarsenical dyes can diffuse across the outer membranes of these spirochetes, and that concatenating two copies of the 6-amino acid tag increased the intensity and duration of fluorescence. Mouse-tick infection studies of a tetracysteine-tagged *B. burgdorferi* strain demonstrated that the tetracysteine motif was stably maintained *in vivo* and did not adversely affect infectivity in either the arthropod vector or murine host. Finally, biarsenical-bound proteins could be followed over several days, indicating that this approach can be used in time-course studies of live cells.

MATERIALS AND METHODS

Bacterial Strains and Growth Conditions

All strains used in this study are listed in **Table 1**. *Borrelia burgdorferi* strain B31 A3 is an infectious clonal derivative of the type strain B31 (Burgdorfer et al., 1982; Elias et al., 2002). *B. burgdorferi* Δ D109, a previously characterized B31 A3 mutant lacking a wild-type copy of the plasmid-borne gene encoding outer-surface protein (Osp) D, was utilized in this study (Stewart et al., 2008). In addition, strain B31 A34, a non-infectious and more readily transformed clone that lacks restriction modification systems (Jewett et al., 2007), was also used. *Borrelia* cultures were grown at 35°C in liquid Barbour-Stoenner-Kelly (BSK)-II medium supplemented with 6% rabbit serum (Pel Freez Biologicals, Rogers, AZ) or in solid BSK medium under 2.5% CO₂ (Samuels et al., 1994). *Borrelia* growth media were supplemented with antibiotics at the following concentrations when appropriate: gentamicin (40 μ g/mL), kanamycin (200 μ g/mL), and streptomycin (50 μ g/mL).

Leptospira biflexa serovar Patoc (strain Patoc I) was cultured at 30°C in a shaking incubator at 150 RPM in EMJH medium (Fisher Scientific). Solid EMJH media for plating included 1.2% wt/vol Nobel agar (Fisher Scientific), and plates were inverted, sealed with parafilm and incubated at 30°C for up to 1 week. *Leptospira* growth media were supplemented with kanamycin (20 μ g/mL) where appropriate.

Escherichia coli TOP10 cells (Invitrogen, Carlsbad, CA) were used for recombinant DNA cloning purposes unless

TABLE 1 | Strains used in this study.

Designation	Description	Purpose
<i>B. burgdorferi</i> B31 A3	Wild-type infectious (Elias et al., 2002)	Parental strain
<i>B. burgdorferi</i> B31 A34	Non-infectious/high-passage (Jewett et al., 2007)	Parental strain
A34-SV-OspDTC	OspD with a single tetracycline tag expressed from shuttle vector, B31 A34 background (this study). This strain produces both a tagged and wild-type form of OspD	Testing and optimization of FIAsH system in <i>B. burgdorferi</i>
A34-SV-OspD2xTC	OspD with a double tetracycline tag expressed from shuttle vector, B31 A34 background (this study). This strain produces both a tagged and wild-type form of OspD	Evaluating the benefit of concatenating two tetracycline tags to increase fluorescence and prolong detection
A3ΔOspD 109	<i>ospD</i> deletion strain, A3 background (Stewart et al., 2008)	Parental strain lacking <i>ospD</i>
ΔOspD-SV-TC	OspD with a single tetracycline tag expressed from shuttle vector, A3ΔOspD 109 background (this study)	Evaluation of fluorescence and duration of fluorescence in a strain lacking a wild-type version of OspD
ΔOspD-SV-2xTC	OspD with a double tetracycline tag expressed from shuttle vector, A3ΔOspD 109 background (this study)	For comparing a double tetracycline tag to a single tag in a strain lacking a wild-type version of OspD; used for OspD re-labeling experiments
A3-LA7TC	LA7 with a single tetracycline tag created by allelic exchange with the endogenous gene	Used to assess effect of tetracycline motif on a protein that is important in the <i>B. burgdorferi</i> infectious cycle
<i>L. biflexa</i> serovar patoc strain Patoc I (Paris)	Wild-type	Parental strain
OmpATC	OmpA with a tetracycline tag created by integration at the endogenous locus (this study). This strain produces both a tagged and wild-type form of OmpA	Testing FIAsH system in <i>Leptospira</i>

otherwise noted. Final antibiotic concentrations were as follows: gentamicin (5 μg/mL), kanamycin (50 μg/mL), and spectinomycin (100 μg/mL).

Mutant Construction and Transformation

Oligonucleotides used in mutant construction are listed in **Table 2**. All plasmids generated in this study were confirmed by sequencing and are listed in **Table 3**. A tetracycline motif was added to the 3' end of a second copy of *ompA* (Outer Membrane Protein A, UniProt accession #: B0SQ62) in *L. biflexa* by targeted integration of a non-replicating plasmid at the endogenous locus. First, the primer pair A/B was used to amplify the *ompA*-like coding sequence and clone it into pGem-T EZ (Promega Inc., Madison, WI). Next, an inverse PCR reaction was used in conjunction with primer pair C/D to add the tetracycline tag (TC-tag) at the 3' end of *ompA*, which results in an in-frame addition of the motif to the carboxy-terminus of OmpA. Amplicons were digested, self-ligated, and transformed into *E. coli* Top 10 cells. Next, a kanamycin resistance cassette suitable for use in *L. biflexa* (*flgBp aph1*) was cloned into the construct using the available XhoI restriction enzyme site. Lastly, the ampicillin resistance cassette within pGem-T EZ was inactivated by excising part of the coding region with the restriction enzyme AclI; the plasmid was subsequently self-ligated, transformed into *E. coli* Top 10 cells and selected on kanamycin plates. Colonies resistant to kanamycin were replica-plated for susceptibility to carbenicillin to demonstrate inactivation of the ampicillin resistance cassette. The completed targeted integration construct, pGem::OmpA-TC, was transformed into *L. biflexa* using protocols previously established (Louvel and Picardeau, 2007)

and the resulting strain designated OmpATC. Transformants were confirmed by PCR (**Figure 1A**) and Southern blot analysis (data not shown).

The TC-tag was incorporated into the 3' end of the *ospD* coding sequence by PCR amplification using primers G and H, to create *ospDTC*. This amplicon includes the putative promoter 5' of the *ospD* gene (Stewart et al., 2008) and 15 bp homologous to the multiple cloning site of shuttle vector pKFSS1 (Frank et al., 2003). The resulting PCR product was cloned into pKFSS1 using the In-fusion kit (Takara, Mountain View, CA), following the manufacturer's recommendations, and transformed into *E. coli* Stellar cells.

The *ospD-2xTC* cassette was cloned into the *B. burgdorferi* shuttle vector pBSV2G (Elias et al., 2003). An amino acid pocket consisting of GDEG was placed between the dual tetracycline motifs, as described previously (Andresen et al., 2004). Briefly, primer pair I/J was used to PCR-amplify OspD-1xTC and add a second tetracycline motif at the 3' end of the PCR amplicon with primer J. PCR products were digested with SalI and ligated into pBSV2G to form the shuttle vector pBSV2G::OspD2xTC.

The coding region of *la7* was replaced with *la7-TC* by allelic replacement using a construct encoding TC-tagged LA7 cloned into pGEM-T EZ. Briefly, primers L and M were used to PCR-amplify *la7*, including ~500 bp upstream and downstream, of *B. burgdorferi* and clone into pGEM-T EZ. Next, the primer pair N/O was used in an inverse PCR reaction to add the tetracycline motif to the 3' end of *la7*. Amplicons were digested, self-ligated, and transformed into *E. coli* Top 10 cells. A kanamycin resistance cassette suitable for use in

TABLE 2 | Primers used in this study.

Primers			
Name	Sequence	Function	
LEPTOSPIRA			
A	OmpA.SnaBI.For	tacgtaGAGCAG TCCGTTGACAAG	Cloning of <i>ompA</i>
B	OmpA.SnaBI.Rev	tacgtaTCG TCTGGTAAGGAT TGG	Cloning of <i>ompA</i>
C	iPCR.OmpA.XhoI.For	ctcgagGAAATTCATTTTCTTACTAGAGACC	Inverse PCR for addition of tetracycline motif
D	iPCR.OmpA.TC.XhoI.Rev	ctcgagTTAACAAACATCCAGGGCAACATTAGAAACGA CTTGGAAAGTCAC	Genetically encoding the tetracycline motif at the 3' end of <i>ompA</i> before the stop codon (underlined)
E	OmpA.Seq1.For	TAAACTATGGAAACATTAAGGCAGG	Transformant confirmation by PCR
F	Kan.Out.RC	GCAGTTTCATTTGATGCTCG	Transformant confirmation by PCR
BORRELIA			
OspD1xTC			
G	PospD-TC.SV2.F	CGGTACCCGGGGATCGGCCATGGGAAGAAGGAG	Amplifying <i>ospD</i> and cloning into pKFSS1
H	OspD-TC.SV2.RC	ATGCCTGCAGGTGATTAACAACATCCAGGGCAAC AAGTATTTAAACAAGGCCACAACCTTC	Genetically encoding the tetracycline motif at the 3' end of <i>ospD</i> before the stop codon (underlined)
OspD2xTC			
I	OspD.F.Sall	gtcgacCGTCTCTACTGTATTTCTCTGC	Cloning of <i>ospD</i>
J	OspD.2TC.Sall.Rev	gtcgacTTAGCAACAACCTGGGCAGCAACCTTCATCT CCACAACATCCAGGGC	Genetically encoding the double tetracycline motif at the 3' end of <i>ospD</i> before the stop codon (underlined)
K	OspD.For	GCTCTCAATATCTTGTGTTC	Transformant confirmation by PCR
LA7TC			
L	LA7.SnaB1.For	tacgtaGCATCAAGTCTTGGTGAATCTG	Cloning of <i>la7</i>
M	LA7.SnaB1.Rev	tacgtaCTAGAAATAGACTATGGGCAAGG	Cloning of <i>la7</i>
N	iPCR.LA7.XhoI.For	TATtctcgagTTTATATTTTTGATTTATAGGCTTTAATC	Inverse PCR for addition of tetracycline motif
O	iPCR.LA7.TC.XhoI.Rev	ATctcgagTTAACAAACATCCAGGGCAACAATTGG TTAACATAGGTGAAATTTTTCAACG	Genetically encoding the tetracycline motif at the 3' end of <i>la7</i> before the stop codon (underlined)
P	LA7.Seq3.For	GCACGTTTTTCACGCTATG	Transformant confirmation by PCR
Q	Kan736.RC	AAAGCCGTTTCTGTAATGAAGGAG	Transformant confirmation by PCR

All oligos are shown in the 5' to 3' orientation. Restriction enzyme sites are depicted in the primer name and sequences are indicated in lower case. Stop codon sequences are underlined where applicable.

TABLE 3 | Plasmids used in this study.

Plasmids	Function	References
pGem-T EZ	Backbone for <i>ompA</i> integration construct	Promega
pKFSS1	Shuttle vector for <i>B. burgdorferi</i>	Frank et al., 2003
pBSV2G	Shuttle vector for <i>B. burgdorferi</i>	Elias et al., 2003
pGem::OmpA-TC	OmpA-TC suicide vector for <i>L. biflexa</i>	Current study
pKFSS1::OspD1xTC	OspD-TC shuttle vector	Current study
pBSV2G::OspD2xTC	OspD-2xTC shuttle vector	Current study
pGEM::LA7-TC	LA7-TC allelic exchange vector for <i>B. burgdorferi</i>	Current study

B. burgdorferi (*flgBp aph1*) was added to the construct using the available XhoI restriction enzyme site introduced at the previous inverse PCR step. Lastly, ampicillin resistance was inactivated as

described above to generate the completed allelic replacement construct, pGEM::LA7-TC.

Allelic exchange and shuttle vector constructs were transformed into *B. burgdorferi* by electroporation as previously described (Samuels et al., 1994). Strains A34-SV-OspDTC and A34-SV-OspD2xTC were created in the high-passaged, non-infectious strain B31 A34, which has a higher transformation frequency than the parental strain B31 A3 and also carries a wild-type copy of the *ospD* gene. Strains Δ OspD-SV-TC and Δ OspD-SV-2xTC were produced by transforming pKFSS1::OspD1xTC or pBSV2G::OspD2xTC into A3 Δ D109, a B31 A3 derivative lacking a wild-type copy of *ospD* (described by Stewart et al., 2008). Both OspD tetracycline constructs are on shuttle vectors present at multiple copies per cell in *Borrelia*. Note that strain Δ OspD-SV-2xTC produces only an OspD-TC protein, whereas B31 A34-derived strains produce both wild-type OspD (lacking a TC tag) and TC-tagged OspD. In contrast, A3-LA7TC was constructed by an allelic exchange event that replaced the wild-type copy of LA7 on the chromosome in strain B31 A3. All strains were confirmed by restriction enzyme digestion, sequencing, PCR, and immunoblotting. Rabbit anti-OspD antiserum was used at a dilution of 1:1,000

and rabbit anti-LA7 antiserum (kindly provided by Dr. Brian Stevenson) at 1:250.

FIAsh/ReAsH Assays

Spirochetes were grown to mid-exponential phase ($\sim 5 \times 10^7$ cells/mL for *B. burgdorferi* and $\sim 5 \times 10^8$ cells/mL for *L. biflexa*) and harvested by centrifugation (5,800 RCF for *B. burgdorferi* and 4,100 RCF for *L. biflexa*) for 10 min at room temperature. Pelleted spirochetes were then washed with 1 mL FIAsh wash buffer (50 mM MOPS pH 7.2, 67 mM NaCl, 20 mM NH_4Cl). Spirochetes were again pelleted and washed in FIAsh wash buffer with 20 mM DTT. After the second wash, pelleted cells were resuspended in 158 μL of FIAsh solution and incubated in the dark at room temperature for 1 h. The FIAsh or ReAsH solution for staining spirochetes was prepared as follows: 2 mM FIAsh-EDT₂ or 2 mM ReAsH-EDT₂ (ThermoFisher Scientific) was resuspended in FIAsh wash buffer at a final concentration of 4.75 μM , and DTT was added to a final concentration of 2.5 mM. The solution was then passed through a 0.22 μM filter, and 2 M DTT was added at 1/100 v/v to a final concentration of 22.5 mM. After labeling, 1 mL of FIAsh wash buffer was added and cells were pelleted as described above. Lastly, spirochetes were resuspended in $\sim 50 \mu\text{L}$ FIAsh wash buffer for visualization.

Microscopy

All microscopy was done with a Nikon E80i fluorescent microscope. Image files were obtained and analyzed using Nikon Elements version 4.2 and ImageJ software version 2.0.0-rc-69/1.52i. FIAsh dye was observed in the FITC channel while ReAsH was observed in the Texas Red channel. When comparing peak fluorescence, identical settings for exposure and gain were used for all images. Peak fluorescence data were obtained by setting a constant exposure and gain between strains (typically this was an exposure of 1 s with a gain of 9.6x); however, if these settings oversaturated the image sensor, the exposure was lowered for all strains tested. Average peak fluorescence data were obtained by placing a region of interest (ROI) box within a spirochete along an area of uniform fluorescence. The peak fluorescence of that box was calculated with Nikon Elements software and that value represented the peak fluorescence intensity for that spirochete. Approximately 250 spirochetes per group, and 100 measurements of background, pooled from 3 independent biological replicates, were analyzed.

Flow Cytometry

To assess fluorescence intensity of a larger number of spirochetes, cultures were first FIAsh- or ReAsH-stained, incubated with Hoechst 33342 DNA stain (20 μM) (ThermoFisher Scientific) for 30 min at room temperature, and then analyzed with an LSR II BD Flow Cytometer. Spirochetes were gated based on forward scatter (FSC), side scatter (SSC), and FITC. B31 A34 was utilized as a non-fluorescent wild-type control in conjunction with Hoechst 33342 to identify the spirochete populations, while FITC was used to detect the fluorescent spirochete population. B31 A34-derived strains were utilized to avoid introduction of infectious material in the flow cytometer. A34-SV-OspDTC and A34-SV-OspD2xTC were used to determine the effect of

concatenating tetracysteine motifs on OspD. FlowJo version 10.4.2 software was used to analyze data and to calculate geometric means of populations.

Animal Studies

Rocky Mountain Laboratories (RML) is accredited by the International Association for Assessment and Accreditation of Laboratory Animal Care. Protocols for animal experiments were prepared according to the guidelines of the National Institutes of Health and approved by the RML Animal Care and Use Committee. RML mice are an outbred colony of Swiss-Webster mice maintained at Rocky Mountain Laboratories and used exclusively throughout this study. Mice were inoculated with $\sim 5 \times 10^3$ spirochetes intraperitoneally and 1×10^3 spirochetes subcutaneously. Infection was assessed by attempted isolation of spirochetes from ear, bladder, and rear ankle joint tissues at 3 weeks post-inoculation.

Larval *Ixodes scapularis* were reared from egg masses laid by engorged female ticks purchased from Oklahoma State University. All ticks were maintained in a temperature- and humidity-controlled chamber (Caron Model 7000-25) at 22°C with 95% relative humidity. Approximately 100 larvae or 10–20 nymphs per mouse were allowed to feed to repletion. A subset of fed nymphs was crushed and the resulting homogenate serially diluted and plated to determine spirochete burden. Fluorescence of FIAsh-stained organisms was assessed immediately for spirochetes derived from mechanically-disrupted, engorged nymph midguts, and from cultured spirochetes isolated from ticks and mouse tissues.

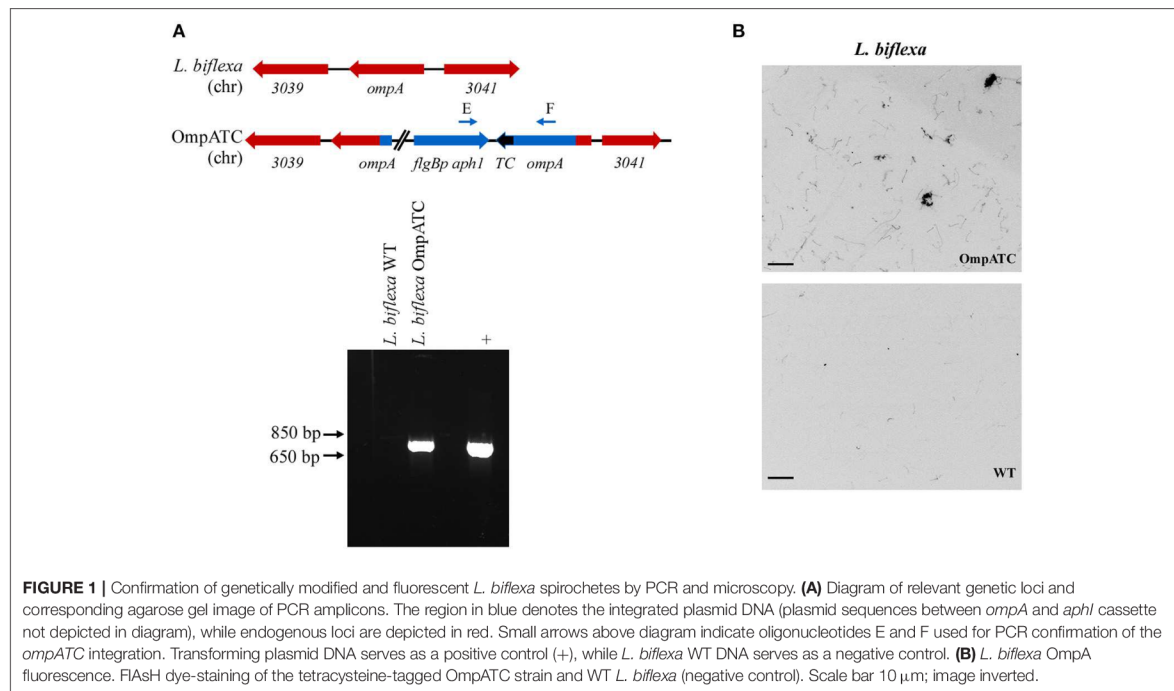
Time-Course of OspD-Biarsenical Dye Fluorescence

To assess the longevity of FIAsh fluorescence during *in vitro* cultivation, *B. burgdorferi* cells were FIAsh-labeled as described above. Strains lacking a tetracysteine tag were used as negative controls for the procedure. For heat-killed cells, samples were placed at 55°C for 15 min post-FIAsh labeling and observed subsequently for absence of motility; these cells served as a control for passive loss of fluorescence over time. Labeled cells were resuspended in 1–2 mL of BSK-H medium (Sigma) with *Borrelia* antibiotics (20 $\mu\text{g}/\text{ml}$ phosphomycin, 50 $\mu\text{g}/\text{ml}$ rifampicin, 2.5 $\mu\text{g}/\text{ml}$ amphotericin B), placed in cryovials (Corning), and incubated at 22°C in the dark. Spirochetes were counted using Petroff-Hauser chambers to monitor growth, and all cultures were imaged every 48 h for 7–8 days. Experiments were performed as 3 biological replicates and the images shown come from a single experiment representative of the trends observed.

Counter-labeling assays were performed in order to assess FIAsh saturation of OspD protein over time. In cells originally stained with FIAsh where cell concentrations and images had already been obtained for comparison, 400 μL aliquots were removed, and a ReAsH assay performed as stated above.

Statistics

Statistical analyses were conducted using GraphPad Prism 7 software. Mann-Whitney statistical analysis was applied when



comparing fluorescence intensity by microscopy, geometric mean variation by flow cytometry, and spirochete burden in nymphs.

RESULTS

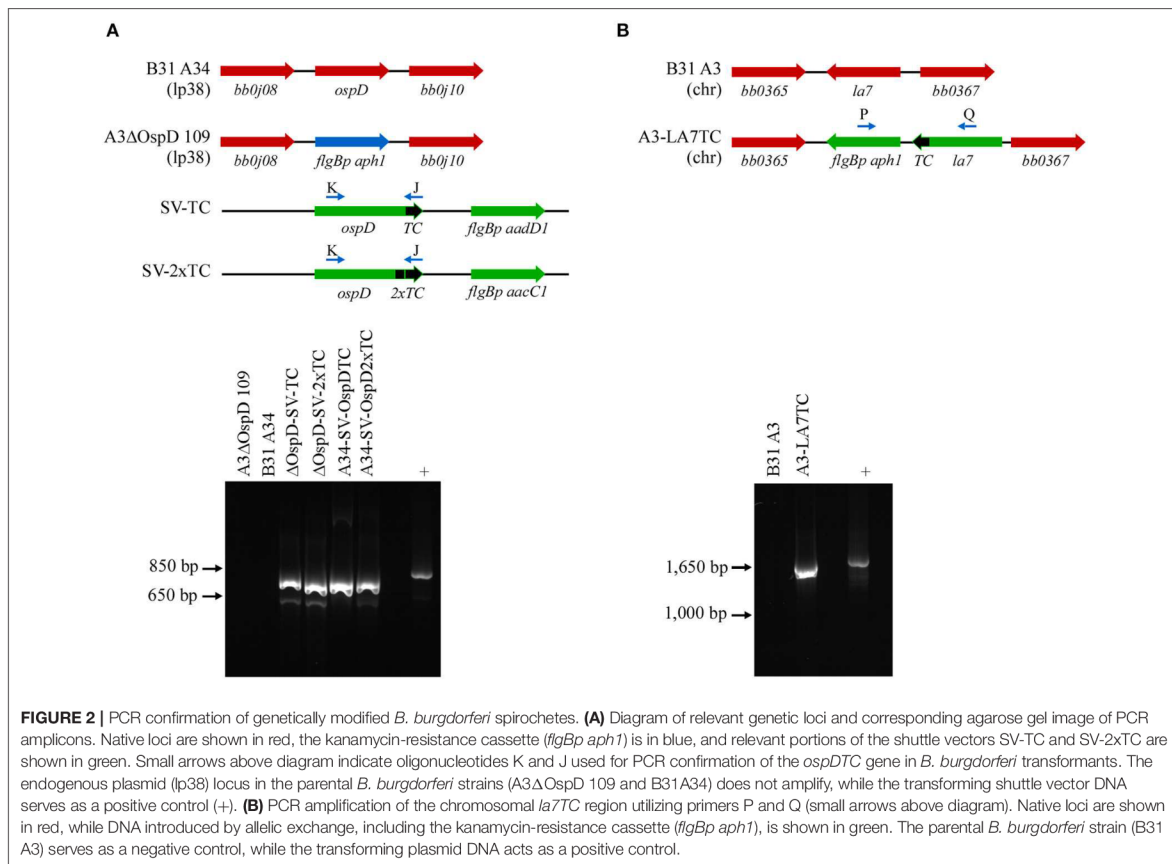
Tetracycline Tags and Biarsenical Dyes to Visualize Spirochetes

As proof of principle, we assessed the use of biarsenical dyes in the model organism *L. biflexa*. Although membrane proteins have not been extensively characterized in this spirochete, a previous study identified a moderately abundant membrane protein, OmpA (Stewart et al., 2016). To assess the functionality of the FIAsh dye technique in *Leptospira*, a tetracycline tag was added to the carboxy-terminus of OmpA encoded by a second copy of the gene integrated at the endogenous locus (Figure 1A). Transformants were confirmed by PCR utilizing a primer pair spanning the region between *ompA* and the kanamycin resistance cassette (Figure 1A), and transformed spirochetes fluoresced when exposed to FIAsh dye, permitting visualization of the helical shape characteristic of *Leptospira* cells (OmpATC in Figure 1B). In contrast, cells that did not contain a tetracycline motif (WT negative control, Figure 1B) did not fluoresce when exposed to the biarsenical dye and only minimal background staining was observed.

To broaden the utility of this technique, we used a similar approach in another spirochete, *B. burgdorferi*, and tagged both outer and inner membrane proteins OspD and

LA7, respectively. These abundant and accessible lipoproteins should be suitable candidates for applying the FIAsh dye technique in *B. burgdorferi*. Spirochetes transformed with a shuttle vector encoding *ospDTC* were confirmed by PCR with primers specific to the *ospD* coding region and the tetracycline motif; wild-type cells that did not contain the motif did not yield an amplicon (Figure 2A, lower panel). Immunoblot analysis of OspD production in all engineered strains indicated an increase in OspD protein in strains transformed with a shuttle vector encoding either a single tetracycline motif, A34-SV-OspDTC, or two tetracycline motifs, A34-SV-OspD2xT (Supplementary Figure 1A). LA7, originally proposed to be an outer membrane lipoprotein (Grewe and Nuske, 1996), but subsequently shown to localize primarily to the inner membrane (von Lackum et al., 2007; Yang et al., 2013), was chosen as a target to assess the ability of biarsenical dyes to freely diffuse across the outer membrane of living *B. burgdorferi* cells. Allelic exchange transformants were screened by PCR using a primer set spanning *la7* and the kanamycin resistance cassette (Figure 2B, lower panel), and spirochetes containing a tetracycline motif engineered on LA7 (strain A3-LA7TC) produced comparable levels of protein as their wild-type counterpart (Supplementary Figure 1B).

After confirming the presence of the tetracycline motif in all strains, we next assessed the FIAsh system in *B. burgdorferi*. Fluorescent spirochetes were observed when the tagged strains A34-SV-OspDTC and A3-LA7TC were exposed to FIAsh or ReAsH dye, whereas WT B31 A34 spirochetes (negative control) displayed only background fluorescence (Figure 3).



This demonstrated successful application of the technique to inner and outer membrane proteins of *B. burgdorferi*, and thus confirms that biarsenical dyes can diffuse across the outer membrane of live spirochetes without the need for fixation or permeabilization procedures.

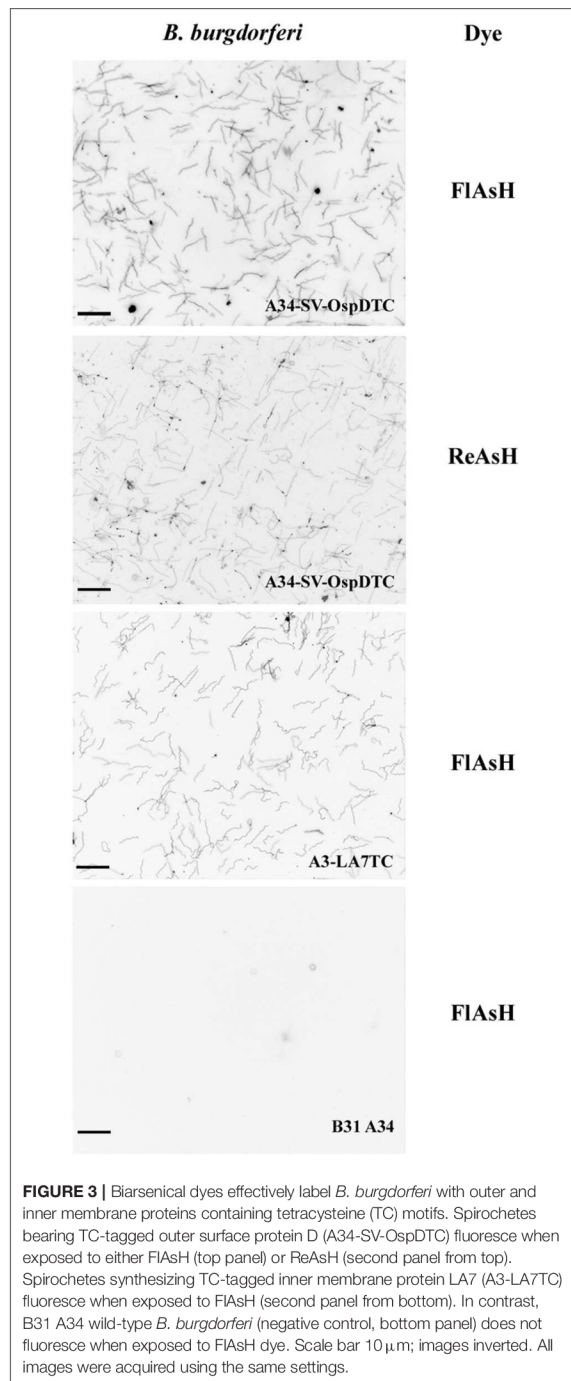
Optimization of the FIAsh Technique

Having ensured that biarsenical dyes could be utilized in spirochetes, we next assessed whether adding a second tetracycline tag would augment fluorescence. Using identical imaging conditions between B31 A34, A34-SV-OspDTC, and A34-SV-OspD2xTC, a significant increase in fluorescence intensity was observed with addition of a second tetracycline motif onto OspD (Figures 4A,B), while the overall OspD protein level appeared similar between strains A34-SV-OspDTC and A34-SV-OspD2xTC (Supplementary Figures 1A–D), indicating the increase in fluorescence was a result of the second tetracycline motif. FIAsh dye-labeled OspD2xTC spirochetes retained motility and grew comparably to unlabeled organisms when incubated at 35 degrees, confirming their viability and the lack of toxicity of the protocol. Also, the addition of a

second tetracycline motif allowed prolonged detection of the fluorescent signal (see Supplementary Figure 2).

FIAsh-labeled spirochetes were also analyzed by flow cytometry to quantify and compare fluorescence of a larger number of cells (Figure 4C). Using this method, we independently validated that two tetracycline tags fused to OspD resulted in a significant increase in mean fluorescence relative to cells containing OspD with a single tag (Figure 4D). Hence the relative mean fluorescence intensity of spirochetes measured by both methods, fluorescence microscopy and flow cytometry, were in agreement for these *B. burgdorferi* strains.

Surprisingly, while optimizing the protocol, we found that FIAsh dye would non-specifically bind to heat-killed *B. burgdorferi* cells in the absence of tetracycline motifs (Supplementary Figure 3). The nature of this non-specific interaction between the dye and spirochetes lacking an engineered tetracycline pocket is not clear. However, this fluorescence requires the FIAsh dye and is only detected in the FITC channel, indicating that it does not reflect general autofluorescence of dead spirochetes. It should be noted that although non-specific staining of heat-killed spirochetes could



be abrogated by increasing the concentration of DTT, there was a concomitant decrease in the fluorescence intensity of viable spirochetes containing tetracycline motifs (data not

shown). Hence there is a balance to be achieved between the concentration of reducing agent and fluorescence intensity. Taking these observations into consideration, 20 mM DTT was chosen as the optimal concentration, and WT spirochetes included as negative controls in all experiments to confirm specificity of labeling.

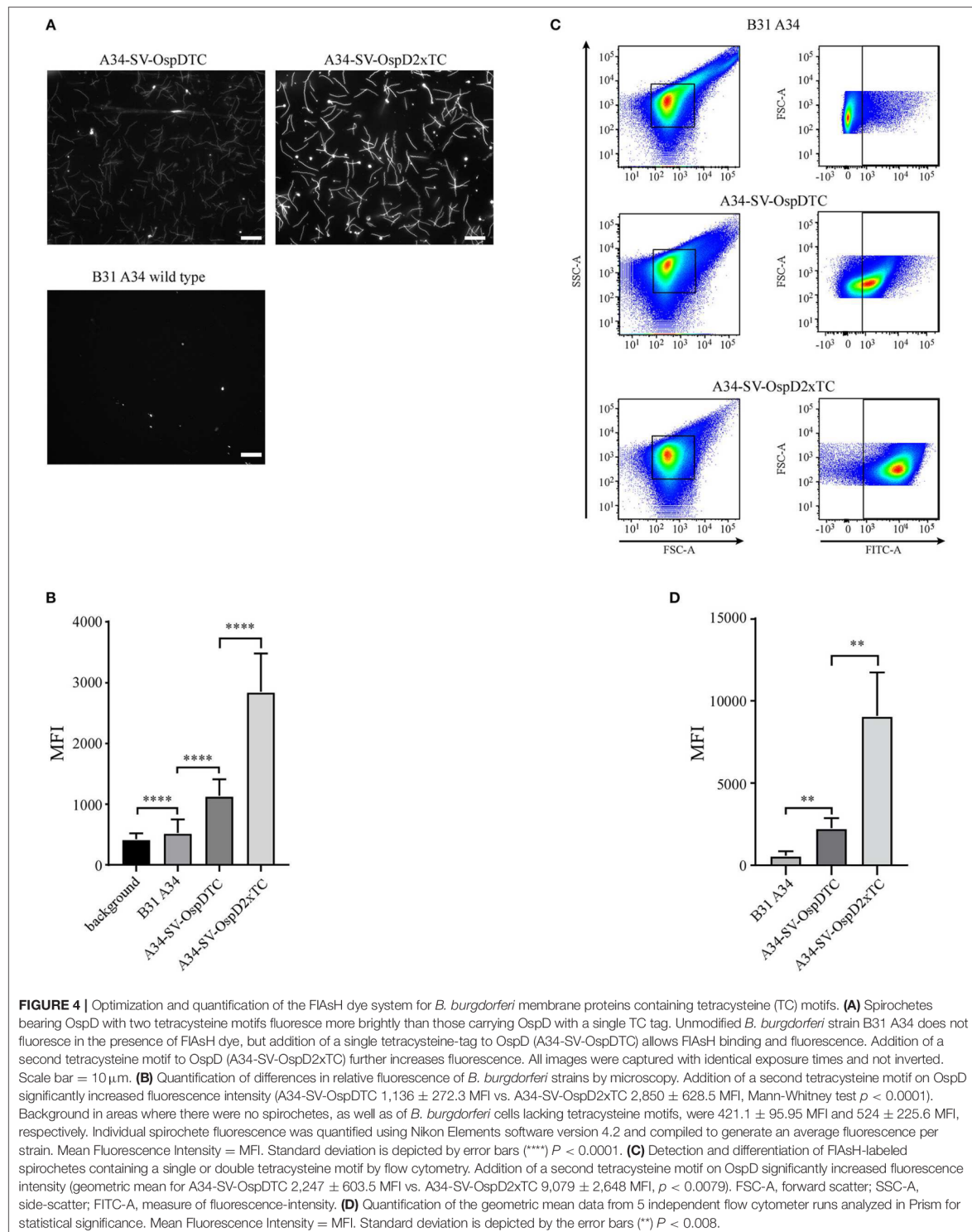
Tetracycline Motifs Are Stable Throughout the Mouse-Tick Infectious Cycle

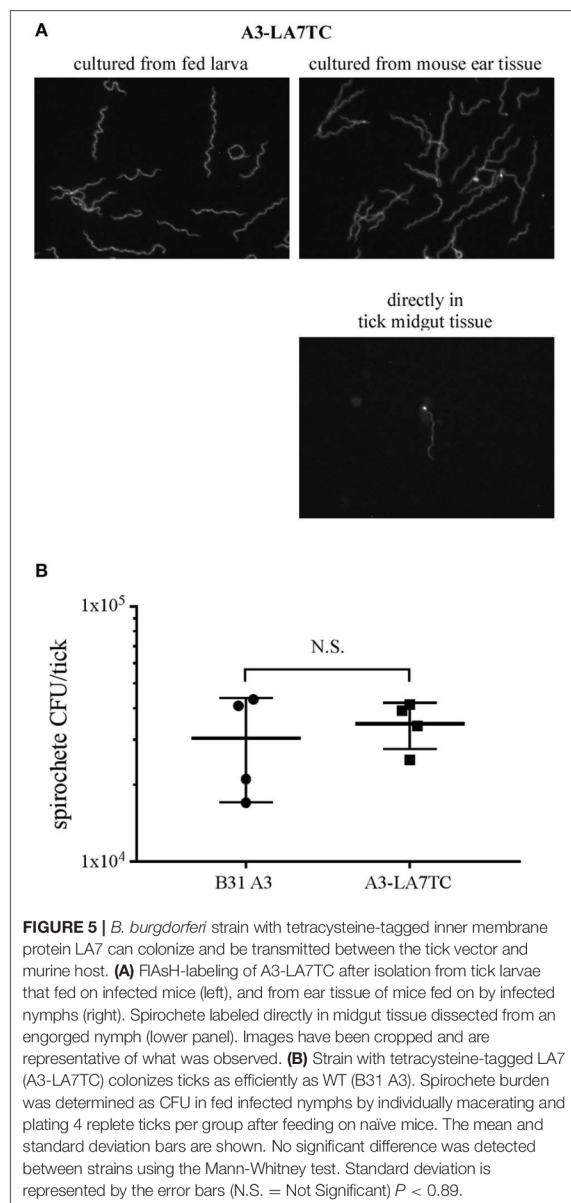
In nature, *B. burgdorferi* cycles between tick vectors and vertebrate hosts. Potentially, addition of the tetracycline tag to a protein such as LA7, which is important during tick acquisition (Pal et al., 2008), might alter infectivity or destabilize the target transcript or protein *in vivo*. To examine this possibility, we needle-inoculated mice with either wild-type A3 or the A3-LA7TC strain. All mice became infected (5 out of 5 mice for each strain), and both strains could subsequently be re-isolated from mouse tissues (ankle joint, bladder, and ear).

Before the A3-LA7TC-infected mice were euthanized for attempted spirochete isolation, they were fed upon by naïve *I. scapularis* larvae. A subset of replete larvae was mechanically disrupted and the resulting homogenates cultured to evaluate acquisition of *B. burgdorferi* and whether spirochetes retained the tetracycline tag. Among larvae that fed on wild-type A3 or A3-LA7TC-infected mice, 4/5 and 5/5 larvae, respectively, acquired spirochetes. Further, upon addition of FIAsh dye, all A3-LA7TC spirochetes isolated from larval ticks fluoresced (Figure 5A, top-left panel), indicating retention of the tetracycline motif, while A3 spirochetes did not fluoresce (Supplementary Figure 4).

After molting to the nymphal stage, a subset of unfed ticks were mechanically disrupted and cultured to gauge the transstadial retention of *B. burgdorferi*. Of these, all of the A3-LA7TC-infected nymphs (5 out of 5) and 80% of the A3-infected nymphs (4 out of 5) maintained *B. burgdorferi* through the molt, and spirochetes cultured from the A3-LA7TC outgrowths were fluorescent when stained with FIAsh dye (data not shown).

Lastly, transmission was assessed by allowing the remaining infected nymphs to feed on naïve mice. All naïve mice fed upon by infected nymphs acquired *B. burgdorferi* (5 out of 5), as verified by the presence of spirochetes in tissue outgrowths; when spirochetes in a subset of those outgrowths were subjected to FIAsh assays, A3-LA7TC spirochetes were fluorescent (Figure 5A top-right panel). In addition, although technically challenging due to the absolute number of spirochetes in fed nymph midguts, it was possible to detect fluorescent spirochetes directly from A3-LA7TC infected, engorged nymphs that had been mechanically-disrupted and FIAsh-labeled (Figure 5A, lower right panel). Replete ticks were collected and a subset (4 per strain) was used to estimate the number of spirochetes per tick. On average, there was no significant difference in spirochete burden between A3- and A3-LA7TC-infected ticks (3.04×10^4 vs. 3.48×10^4 spirochetes per tick, respectively; $p = 0.89$; Figure 5B). Taken together, the overall infection and fluorescence data demonstrate that spirochetes bearing a tetracycline motif





on LA7 exhibit a WT phenotype throughout the mouse-tick-mouse infectious cycle and can be FIAsh-labeled either directly in tick midgut tissue or after *in vitro* cultivation of spirochetes from tick or murine tissues.

FIAsh-labeled Proteins Retain Fluorescence Over Time

We utilized biarsenical dyes to assess the length of time FIAsh-labeled protein could be detected during *in vitro* cultivation.

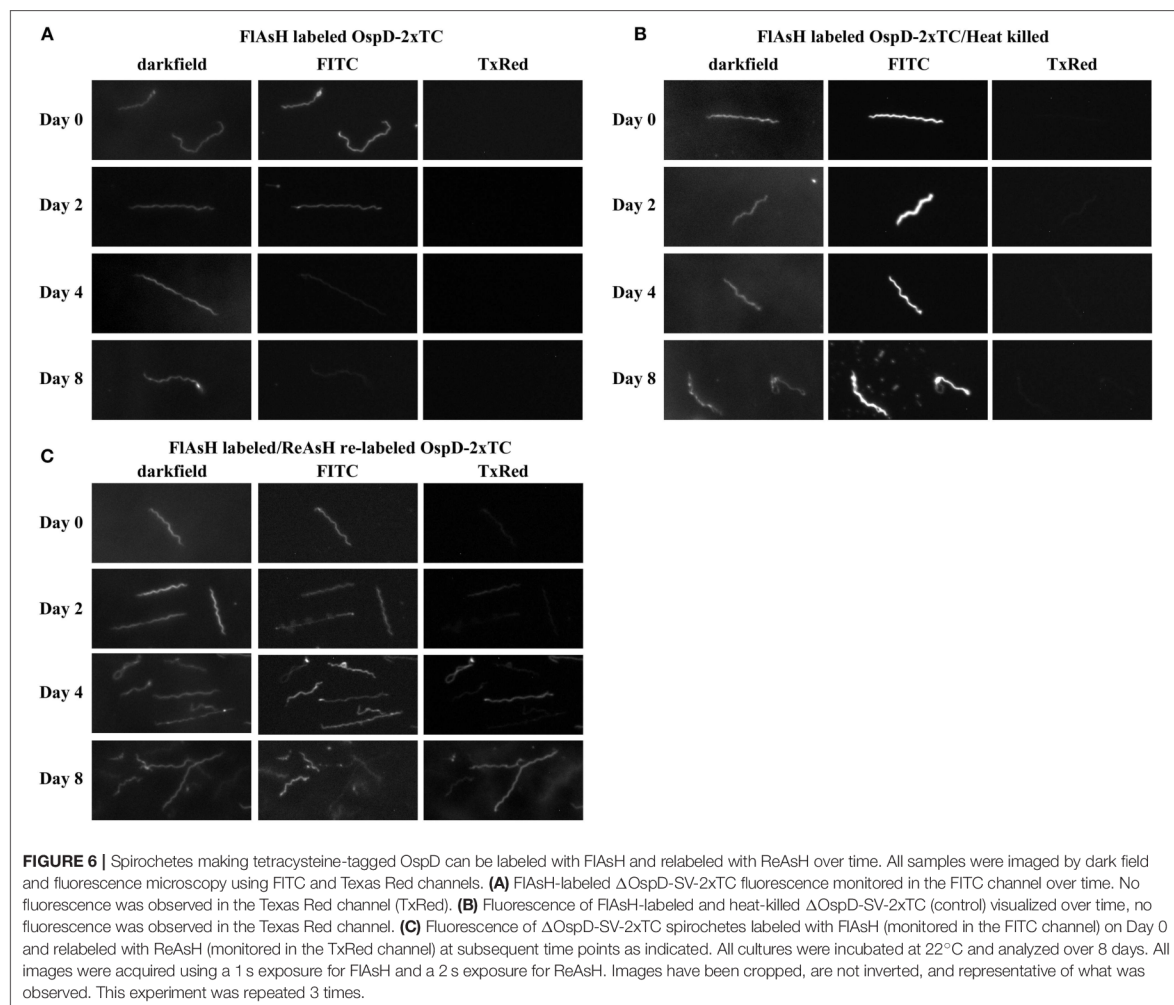
As previously described, we complemented strain A3 Δ OspD in trans with a double tetracycline-tagged copy of *ospD* on a shuttle vector (Δ OspD-SV-2xTC). We used this complemented strain in time-course experiments in order to eliminate potential competition with WT OspD and have only the tetracycline-tagged OspD variant available for processing and insertion into the outer membrane. Δ OspD-SV-2xTC spirochetes were pelleted, labeled with FIAsh dye, and then washed and resuspended in BSK culture medium. When fluorescence was monitored during subsequent *in vitro* growth at 35°C, the signal diminished almost entirely after 24 h (data not shown). Presumably this observed loss of fluorescence was due to dilution of FIAsh-labeled OspD by growth and cell division that occurred within this timeframe (~5 doublings and ~30-fold increase in cell number). Therefore, we performed this experiment at 22°C, a condition in which *Borrelia* grows more slowly, to reduce the dilution of labeled protein resulting from cell growth and division. Fluorescence of the Δ OspD-SV-2xTC strain was monitored over the course of 8 days (Figure 6A). Spirochetes of the same strain that were FIAsh-labeled and then heat-killed were included as a metabolically inert control that does not undergo cell division or have an active mechanism for removing or shedding protein (Figure 6B). Δ OspD-SV-2xTC fluorescence diminished over the time course, compared to day 0, but remained detectable. Passive loss of fluorescence of the FIAsh signal did not appear to be an issue, as fluorescence was relatively stable throughout the time course for the heat-killed samples.

At each time point, we relabeled the cells with ReAsH, a red variant of biarsenical dyes (Figure 6C). This pulse-chase experiment allowed visualization of cells that bound both FIAsh and ReAsH over time. At day 0, very little ReAsH was taken up by cells, whereas the ReAsH signal grew appreciably by days 4 and 8. These data suggest that binding sites for ReAsH became available as FIAsh-labeled OspDTC waned and unlabeled OspDTC increased in the spirochete membrane over time.

Discussion

In this study we describe the application of a new technique in spirochetes for fluorescently labeling specific proteins using tetracycline tags and biarsenical dyes. This technique allowed fluorescent labeling of spirochetes by incorporating a 6 amino acid motif at the C-terminus of both inner or outer membrane proteins, and staining with a membrane-permeable biarsenical dye that binds to this motif. The small increase in protein size conferred by the tetracycline motif minimizes potential negative effects that may occur when targets are fused to larger fluorogenic proteins (e.g., GFP or RFP), such as steric hindrance, causing improper protein folding, trafficking to the incorrect cellular location, or inappropriate oligomerization. We successfully applied the same protocol to the distantly related spirochetes *B. burgdorferi*, a zoonotic human pathogen, and *L. biflexa*, a free-living saprophyte, suggesting that the FIAsh system can be applied broadly across all spirochete species.

This technique worked well for both the outer membrane protein OspD and the inner membrane protein LA7 of *B. burgdorferi*, indicating that the dye is freely diffusible across



the intact outer membrane of living spirochetes without the need for fixation or permeabilization. Although the membrane location of OmpA in *L. biflexa* has not been definitively verified, it is predicted to possess a lipoprotein signal peptide by LipoP 1.0 (<http://www.cbs.dtu.dk/services/LipoP/>) and was identified in the membrane-associated protein fraction of leptospire (Stewart et al., 2016). Further, *ompA-TC* and *la7-TC* constructs were targeted to their respective endogenous loci, while the *ospD-TC* fusions were expressed *in trans* from shuttle vectors, indicating that single copy (endogenous locus) or multicopy (shuttle vector) expression sites are both effective options.

As with any technique, the FIAsh system has limitations and required some optimization. Biarsenical dyes rely on precisely spaced and oriented thiol groups to bind and fluoresce. However, due to the cellular abundance of protein thiols, non-specific binding can occur and occlude proper protein visualization. This can be remedied by reducing protein disulfide bonds in the

cellular environment before labeling with dithiol compounds such as 1,4-dithiothreitol (DTT) or 2,3-dimercaptopropanol (BAL). Unexpectedly, we noticed that heat-killed, wild-type spirochetes will non-specifically bind the FIAsh dye. It does not appear to be general autofluorescence of dead spirochetes because the fluorescent signal is only detectable in the FITC channel, not the Texas Red, or DAPI channels, and requires the FIAsh dye. In an attempt to alleviate this issue, we increased the DTT levels 10-fold, which lowered fluorescence in both viable and dead spirochetes. We speculate that heat-killed spirochetes have exposed di-sulfide bonds that are otherwise inaccessible, resulting in the observed binding of the biarsenical dye.

Biarsenical dyes photo-bleach faster than fluorescent proteins, and the fluorescent signal of a tetracysteine-tagged protein is typically several fold lower than that of a cognate GFP fusion (Adams et al., 2002; Crivat et al., 2011). Also, proteins less abundant than OmpA, OspD, or LA7 have not been tested.

However, these limitations could potentially be mitigated by adding a dual tetracycline motif to the protein of interest, which not only increases signal intensity, but also prolongs fluorescence. HeLa cells transiently transfected with a tetracycline motif on α -tubulin indicated a positive linear relationship between additional tetracycline tags and fluorescence intensity (Van Engelenburg et al., 2010). Our results with OspD-TC in *B. burgdorferi* agree with this finding.

We also noted loss of fluorescence within 24 h when FIAsh-labeled spirochetes were cultured at 35°C, presumably due to cell growth and division, where segregation of labeled protein to daughter cells combined with synthesis of new protein leads to dilution of the signal on individual bacteria. We are not aware of similar studies examining the duration of fluorescent protein fusions in *B. burgdorferi* as a comparator. However, when grown at 22°C, *B. burgdorferi* replication is significantly slower and fluorescence could be monitored over a longer time frame. At this temperature, we were able to follow FIAsh dye-stained OspD on the surface of *B. burgdorferi* for 8 days, albeit with diminishing signal. Re-labeling assays (using the red-variant, ReAsH) indicated that there was very little OspD available to re-label at the onset of the experiment, suggesting that the initial dye labeling was highly efficient. With time, OspD protein became available for re-labeling and we observed increased fluorescence with ReAsH. This is in contrast to spirochetes that were heat-killed and do not lose fluorescence over time. Together, this would suggest that the decrease in FIAsh fluorescence with time in culture is not due to diffusion of the dye into the media, but to cell division and new protein synthesis, leading to dilution of the labeled protein in the daughter cells. However, another possible explanation for loss of fluorescence could be due to shedding of labeled protein into the media via membrane bound vesicles, or active release by an undefined mechanism.

A significant attribute of the biarsenical dye system is the small size of the tetracycline motif, which does not impede critical protein function *in vivo*. Previous work on LA7 indicated a role in tick acquisition, with upregulation of expression of the gene encoding LA7 (*bb0365*) in feeding ticks (Pal et al., 2008). LA7-deficient spirochetes were severely impaired in both tick acquisition and transmission. Here, we show that a strain with an engineered tetracycline motif on LA7 is fully competent in an experimental mouse-tick-mouse infectious cycle. No difference in the spirochete burden per nymphal tick was observed between TC-tagged and WT strains. When subjected to FIAsh assays, TC-tagged spirochetes isolated from mouse tissues or ticks fluoresced, indicating retention of the tetracycline motif on the protein. A further advantage of TC-tagged spirochetes is the ability to directly visualize live spirochetes in dissected tick tissues, allowing assessment of target gene expression without fixation or culturing. Together, these data demonstrate that the gene encoding a TC-tagged protein is stably maintained throughout the infectious cycle and that addition of the TC tag does not interfere with the function of a protein that is important for maintenance in the tick. An additional benefit of this system over other fluorogenic methods includes the freely diffusible nature of biarsenical dyes, allowing labeling of sub-surface proteins in live spirochetes without fixation or permeabilization.

We demonstrate that tetracycline motifs coupled with biarsenical dyes are capable of labeling abundant membrane proteins in both *B. burgdorferi* and *L. biflexa*, and likely can be extended to proteins in other cellular locations in these and other spirochetes. Compared to their fluorescent protein counterparts, the small size of the tetracycline motifs makes them ideal for protein localization and trafficking studies. Genetically encoded tetracycline motifs coupled with biarsenical dyes represent a novel molecular tool for studying spirochetes, and can provide valuable insights into spirochete morphology, protein-protein interactions, and cellular trafficking.

DATA AVAILABILITY

All datasets generated for this study are included in the manuscript/**Supplementary Files**.

AUTHOR CONTRIBUTIONS

PS conceived and supervised the study with input from PR. CH, HS, MS, and TE contributed to the design and conducted the FIAsh dye experiments. VC and JW assisted with the animal study. AC analyzed samples by flow cytometry. TS provided advice and assistance with image analyses. CH took the lead role in manuscript preparation with direction and assistance from PS and PR.

FUNDING

This research was supported by the Intramural Research Program of the National Institute of Allergy and Infectious Diseases, National Institutes of Health, and salary support for MS by the Technology Agency of the Czech Republic (TE01020118).

ACKNOWLEDGMENTS

We would like to thank Dr. Gerry Baron for development of the FIAsh-dye protocol that we employed, Dr. Elsie Wunder for providing the vectors used for conjugation with *Leptospira*, and Dr. Brian Stevenson for the LA7 antibody. In addition, we appreciate the graphical expertise of Anita Mora, Ryan Kissinger, and Austin Athman in figure preparation. We thank Drs. Karin Aistleitner and Paul Beare for critical reading of the manuscript and insightful comments.

SUPPLEMENTARY MATERIAL

The Supplementary Material for this article can be found online at: <https://www.frontiersin.org/articles/10.3389/fcimb.2019.00287/full#supplementary-material>

Supplementary Figure 1 | OspD and LA7 protein levels in B31 strains. **(A)** Immunoblot analysis using antisera recognizing OspD (~28 kDa). OspD protein levels are comparable in strains transformed with SV-OspDTC and SV-OspD2xTC. **(B)** Immunoblot analysis using antisera recognizing LA7 (~22 kDa). LA7 protein level is comparable between strains B31 A3 and A3-LA7TC. **(C,D)** Coomassie brilliant blue-stained polyacrylamide gel indicating relative protein loads of samples used for immunoblots in **(A,B)**, respectively.

Supplementary Figure 2 | Duration of fluorescence increased by the addition of a second tetracycline motif. Fluorescence of strain A34-SV-OspDTC was compared to A34-SV-OspD2xTC over time. Videos were taken with Nikon Elements software and data analyzed in Prism. Measurements were taken of three spirochetes/strain during the same experiment. Fluorescence represents the intensity of spirochetes measured with the Nikon Elements software; time measured in seconds (s).

Supplementary Figure 3 | Non-specific binding of FIAsh dye to heat-killed spirochetes. A3 spirochetes that do not contain a tetracycline motif, but were heat killed prior to FIAsh staining, readily take up the dye and fluoresce (1st row)

similarly to A3-LA7TC spirochetes containing a tetracycline motif (2nd row). Spirochetes that have been heat-killed but not incubated with FIAsh, do not fluoresce (3rd and 4th row). Fluorescent spirochetes are only detected in the FITC channel, not in any other channels (not shown).

Supplementary Figure 4 | *B. burgdorferi* wild-type spirochetes (B31 A3) isolated from tick vectors and murine hosts do not fluoresce after labeling. FIAsh-labeling of spirochetes isolated from larval ticks fed on B31 A3-infected mice (**top**); spirochetes isolated from ear tissue of mice fed on by B31-A3 infected nymphs (**middle**); and spirochete in dissected midgut of an engorged B31 A3-infected nymph (**bottom**). Representative dark field and FITC images are shown.

REFERENCES

- Adams, S. R., Campbell, R. E., Gross, L. A., Martin, B. R., Walkup, G. K., Yao, Y., et al. (2002). New biarsenical ligands and tetracycline motifs for protein labeling *in vitro* and *in vivo*: synthesis and biological applications. *J. Am. Chem. Soc.* 124, 6063–6076. doi: 10.1021/ja017687n
- Andresen, M., Schmitz-Salue, R., and Jakobs, S. (2004). Short tetracycline tags to beta-tubulin demonstrate the significance of small labels for live cell imaging. *Mol. Biol. Cell* 15, 5616–5622. doi: 10.1091/mbc.e04-06-0454
- Arhel, N., Genovesio, A., Kim, K. A., Miko, S., Perret, E., Olivo-Marin, J. C., et al. (2006). Quantitative four-dimensional tracking of cytoplasmic and nuclear HIV-1 complexes. *Nat. Methods* 3, 817–824. doi: 10.1038/nmeth928
- Aviat, F., Slamti, L., Cerqueira, G. M., Lourault, K., and Picardeau, M. (2010). Expanding the genetic toolbox for *Leptospira* species by generation of fluorescent bacteria. *Appl. Environ. Microbiol.* 76, 8135–8142. doi: 10.1128/AEM.02199-10
- Bockenstedt, L. K., Gonzalez, D. G., Haberman, A. M., and Belperron, A. A. (2012). Spirochete antigens persist near cartilage after murine Lyme borreliosis therapy. *J. Clin. Invest.* 122, 2652–2660. doi: 10.1172/JCI58813
- Burgdorfer, W., Barbour, A. G., Hayes, S. F., Benach, J. L., Grunwaldt, E., and Davis, J. P. (1982). Lyme disease—a tick-borne spirochetosis? *Science* 216, 1317–1319.
- Bykowski, T., Babb, K., von Lackum, K., Riley, S. P., Norris, S. J., and Stevenson, B. (2006). Transcriptional regulation of the *Borrelia burgdorferi* antigenically variable VlsE surface protein. *J. Bacteriol.* 188, 4879–4889. doi: 10.1128/JB.00229-06
- Carrasco, S. E., Troxell, B., Yang, Y., Brandt, S. L., Li, H., Sandusky, G. E., et al. (2015). Outer surface protein OspC is an antiphagocytic factor that protects *Borrelia burgdorferi* from phagocytosis by macrophages. *Infect. Immun.* 83, 4848–4860. doi: 10.1128/IAI.01215-15
- Carroll, J. A., Stewart, P. E., Rosa, P., Elias, A. F., and Garon, C. F. (2003). An enhanced GFP reporter system to monitor gene expression in *Borrelia burgdorferi*. *Microbiology* 149(Pt 7), 1819–1828. doi: 10.1099/mic.0.26165-0
- Cerqueira, G. M., Souza, N. M., Araujo, E. R., Barros, A. T., Morais, Z. M., Vasconcelos, S. A., et al. (2011). Development of transcriptional fusions to assess *Leptospira interrogans* promoter activity. *PLoS ONE* 6:e17409. doi: 10.1371/journal.pone.0017409
- Clifton, D. R., Nolder, C. L., Hughes, J. L., Nowalk, A. J., and Carroll, J. A. (2006). Regulation and expression of *bba66* encoding an immunogenic infection-associated lipoprotein in *Borrelia burgdorferi*. *Mol. Microbiol.* 61, 243–258. doi: 10.1111/j.1365-2958.2006.05224.x
- Copeland, M. F., Flickinger, S. T., Tuson, H. H., and Weibel, D. B. (2010). Studying the dynamics of flagella in multicellular communities of *Escherichia coli* by using biarsenical dyes. *Appl. Environ. Microbiol.* 76, 1241–1250. doi: 10.1128/AEM.02153-09
- Crivat, G., Tokumasu, F., Sa, J. M., Hwang, J., and Wellems, T. E. (2011). Tetracycline-based fluorescent tags to study protein localization and trafficking in *Plasmodium falciparum*-infected erythrocytes. *PLoS ONE* 6:e22975. doi: 10.1371/journal.pone.0022975
- Dunham-Ems, S. M., Caimano, M. J., Pal, U., Wolgemuth, C. W., Eggers, C. H., Balic, A., et al. (2009). Live imaging reveals a biphasic mode of dissemination of *Borrelia burgdorferi* within ticks. *J. Clin. Invest.* 119, 3652–3665. doi: 10.1172/JCI39401
- Eggers, C. H., Caimano, M. J., and Radolf, J. D. (2006). Sigma factor selectivity in *Borrelia burgdorferi*: RpoS recognition of the *ospE/ospF/elp* promoters is dependent on the sequence of the -10 region. *Mol. Microbiol.* 59, 1859–1875. doi: 10.1111/j.1365-2958.2006.05066.x
- Elias, A. F., Bono, J. L., Kupko, J. J. III, Stewart, P. E., Krum, J. G., and Rosa, P. A. (2003). New antibiotic resistance cassettes suitable for genetic studies in *Borrelia burgdorferi*. *J. Mol. Microbiol. Biotechnol.* 6, 29–40. doi: 10.1159/000073406
- Elias, A. F., Stewart, P. E., Grimm, D., Caimano, M. J., Eggers, C. H., Tilly, K., et al. (2002). Clonal polymorphism of *Borrelia burgdorferi* strain B31 MI: implications for mutagenesis in an infectious strain background. *Infect. Immun.* 70, 2139–2150. doi: 10.1128/iai.70.4.2139-2150.2002
- Enninga, J., Mounier, J., Sansonetti, P., and Tran Van Nhieu, G. (2005). Secretion of type III effectors into host cells in real time. *Nat. Methods* 2, 959–965. doi: 10.1038/nmeth804
- Frank, K. L., Bundle, S. F., Kresge, M. E., Eggers, C. H., and Samuels, D. S. (2003). *aadA* confers streptomycin resistance in *Borrelia burgdorferi*. *J. Bacteriol.* 185, 6723–6727. doi: 10.1128/jb.185.22.6723-6727.2003
- Gaspersic, J., Hafner-Bratkovic, I., Stephan, M., Veranic, P., Bencina, M., Vorberg, I., et al. (2010). Tetracycline-tagged prion protein allows discrimination between the native and converted forms. *FEBS J.* 277, 2038–2050. doi: 10.1111/j.1742-4658.2010.07619.x
- Gautam, A., Hathaway, M., McClain, N., Ramesh, G., and Ramamoorthy, R. (2008). Analysis of the determinants of *bba64* (P35) gene expression in *Borrelia burgdorferi* using a *gfp* reporter. *Microbiology* 154(Pt 1), 275–285. doi: 10.1099/mic.0.2007/011676-0
- Gautam, A., Hathaway, M., and Ramamoorthy, R. (2009). The *Borrelia burgdorferi* *flaB* promoter has an extended -10 element and includes a T-rich $-35/-10$ spacer sequence that is essential for optimal activity. *FEMS Microbiol. Lett.* 293, 278–284. doi: 10.1111/j.1574-6968.2009.01542.x
- Grewe, C., and Nuske, J. H. (1996). Immunolocalization of a 22 kDa protein (IPLA7, P22) of *Borrelia burgdorferi*. *FEMS Microbiol. Lett.* 138, 215–219. doi: 10.1111/j.1574-6968.1996.tb08160.x
- Griffin, B. A., Adams, S. R., and Tsien, R. Y. (1998). Specific covalent labeling of recombinant protein molecules inside live cells. *Science* 281, 269–272.
- Grove, A. P., Liveris, D., Iyer, R., Petzke, M., Rudman, J., Caimano, M. J., et al. (2017). Two distinct mechanisms govern RpoS-mediated repression of tick-phase genes during mammalian host adaptation by *Borrelia burgdorferi*, the Lyme Disease Spirochete. *MBio* 8:4. doi: 10.1128/mBio.01204-17
- Jewett, M. W., Byram, R., Bestor, A., Tilly, K., Lawrence, K., Burtnick, M. N., et al. (2007). Genetic basis for retention of a critical virulence plasmid of *Borrelia burgdorferi*. *Mol. Microbiol.* 66, 975–990. doi: 10.1111/j.1365-2958.2007.05969.x
- Krishnavajhala, A., Wilder, H. K., Boyle, W. K., Damania, A., Thornton, J. A., Perez de Leon, A. A., et al. (2017). Imaging of *Borrelia turicatae* producing the green fluorescent protein reveals persistent colonization of the *Ornithodoros turicata* midgut and salivary glands from nymphal acquisition through transmission. *Appl. Environ. Microbiol.* 83:5. doi: 10.1128/AEM.02503-16
- Louvel, H., and Picardeau, M. (2007). Genetic manipulation of *Leptospira biflexa*. *Curr. Protoc. Microbiol.* Chapter 12, Unit 12E 14. doi: 10.1002/9780471729259.mc12e04s05
- Matsunaga, J., and Haake, D. A. (2018). Identification of a cis-acting determinant limiting expression of sphingomyelinase gene *sph2* in *Leptospira interrogans* with a *gfp* reporter plasmid. *Appl. Environ. Microbiol.* 84:e02068-18. doi: 10.1128/AEM.02068-18

- Miller, J. C., von Lackum, K., Woodman, M. E., and Stevenson, B. (2006). Detection of *Borrelia burgdorferi* gene expression during mammalian infection using transcriptional fusions that produce green fluorescent protein. *Microb. Pathog.* 41, 43–47. doi: 10.1016/j.micpath.2006.04.004
- Moriarty, T. J., Norman, M. U., Colarusso, P., Bankhead, T., Kubes, P., and Chaconas, G. (2008). Real-time high resolution 3D imaging of the Lyme disease spirochete adhering to and escaping from the vasculature of a living host. *PLoS Pathog.* 4:e1000090. doi: 10.1371/journal.ppat.1000090
- Norman, M. U., Moriarty, T. J., Dresser, A. R., Millen, B., Kubes, P., and Chaconas, G. (2008). Molecular mechanisms involved in vascular interactions of the Lyme disease pathogen in a living host. *PLoS Pathog.* 4:e1000169. doi: 10.1371/journal.ppat.1000169
- Pal, U., Dai, J., Li, X., Neelakanta, G., Luo, P., Kumar, M., et al. (2008). A differential role for BB0365 in the persistence of *Borrelia burgdorferi* in mice and ticks. *J. Infect. Dis.* 197, 148–155. doi: 10.1086/523764
- Panchal, R. G., Ruthel, G., Kenny, T. A., Kallstrom, G. H., Lane, D., Badie, S. S., et al. (2003). *In vivo* oligomerization and raft localization of Ebola virus protein VP40 during vesicular budding. *Proc. Natl. Acad. Sci. U.S.A.* 100, 15936–15941. doi: 10.1073/pnas.2533915100
- Samuels, D. S., Mach, K. E., and Garon, C. F. (1994). Genetic transformation of the Lyme disease agent *Borrelia burgdorferi* with coumarin-resistant *gyrB*. *J. Bacteriol.* 176, 6045–6049.
- Schulze, R. J., Chen, S., Kumru, O. S., and Zuckert, W. R. (2010). Translocation of *Borrelia burgdorferi* surface lipoprotein OspA through the outer membrane requires an unfolded conformation and can initiate at the C-terminus. *Mol. Microbiol.* 76, 1266–1278. doi: 10.1111/j.1365-2958.2010.07172.x
- Schulze, R. J., and Zuckert, W. R. (2006). *Borrelia burgdorferi* lipoproteins are secreted to the outer surface by default. *Mol. Microbiol.* 59, 1473–1484. doi: 10.1111/j.1365-2958.2006.05039.x
- Senf, F., Tommassen, J., and Koster, M. (2008). Polar secretion of proteins via the Xcp type II secretion system in *Pseudomonas aeruginosa*. *Microbiology* 154(Pt. 10), 3025–3032. doi: 10.1099/mic.0.2008/018069-0
- Stewart, P. E., Bestor, A., Cullen, J. N., and Rosa, P. A. (2008). A tightly regulated surface protein of *Borrelia burgdorferi* is not essential to the mouse-tick infectious cycle. *Infect. Immun.* 76, 1970–1978. doi: 10.1128/IAI.00714-07
- Stewart, P. E., Carroll, J. A., Olano, L. R., Sturdevant, D. E., and Rosa, P. A. (2016). Multiple posttranslational modifications of *Leptospira biflexa* proteins as revealed by proteomic analysis. *Appl. Environ. Microbiol.* 82, 1183–1195. doi: 10.1128/AEM.03056-15
- Takacs, C. N., Kloos, Z. A., Scott, M., Rosa, P. A., and Jacobs-Wagner, C. (2018). Characterization of fluorescent proteins, promoters, and selectable markers for applications in the Lyme disease spirochete *Borrelia burgdorferi*. *Appl. Environ. Microbiol.* 84:24. doi: 10.1128/AEM.01824-18
- Teixeira, R. C., Baeta, B. A., Ferreira, J. S., Medeiros, R. C., Maya-Monteiro, C. M., Lara, F. A., et al. (2016). Fluorescent membrane markers elucidate the association of *Borrelia burgdorferi* with tick cell lines. *Braz. J. Med. Biol. Res.* 49:7. doi: 10.1590/1414-431X20165211
- Van Engelenburg, S. B., Nahreini, T., and Palmer, A. E. (2010). FACS-based selection of tandem tetracysteine peptides with improved ReAsH brightness in live cells. *Chembiochem* 11, 489–493. doi: 10.1002/cbic.200900689
- von Lackum, K., Ollison, K. M., Bykowski, T., Nowalk, A. J., Hughes, J. L., Carroll, J. A., et al. (2007). Regulated synthesis of the *Borrelia burgdorferi* inner-membrane lipoprotein IplA7 (P22, P22-A) during the Lyme disease spirochete's mammal-tick infectious cycle. *Microbiology* 153(Pt 5), 1361–1371. doi: 10.1099/mic.0.2006/003350-0
- Whetstone, C. R., Slusser, J. G., and Zuckert, W. R. (2009). Development of a single-plasmid-based regulatable gene expression system for *Borrelia burgdorferi*. *Appl. Environ. Microbiol.* 75, 6553–6558. doi: 10.1128/AEM.02825-08
- Xu, H., Raddi, G., Liu, J., Charon, N. W., and Li, C. (2011). Chemoreceptors and flagellar motors are subterminally located in close proximity at the two cell poles in spirochetes. *J. Bacteriol.* 193, 2652–2656. doi: 10.1128/JB.01530-10
- Yang, X., Hegde, S., Shroder, D. Y., Smith, A. A., Promnares, K., Neelakanta, G., et al. (2013). The lipoprotein La7 contributes to *Borrelia burgdorferi* persistence in ticks and their transmission to naive hosts. *Microbes Infect.* 15, 729–737. doi: 10.1016/j.micinf.2013.06.001
- Zhang, K., Liu, J., Charon, N. W., and Li, C. (2015). Hypothetical protein BB0569 is essential for chemotaxis of the Lyme disease spirochete *Borrelia burgdorferi*. *J. Bacteriol.* 198, 664–672. doi: 10.1128/JB.00877-15
- Zhao, Z., Zhao, Y., Zhuang, X. Y., Lo, W. C., Baker, M. A. B., Lo, C. J., et al. (2018). Frequent pauses in *Escherichia coli* flagella elongation revealed by single cell real-time fluorescence imaging. *Nat. Commun.* 9:1885. doi: 10.1038/s41467-018-04288-4

Conflict of Interest Statement: The authors declare that the research was conducted in the absence of any commercial or financial relationships that could be construed as a potential conflict of interest.

This work is authored by Hillman, Stewart, Strnad, Stone, Starr, Carmody, Evans, Carracoi, Wachter and Rosa on behalf of the U.S. Government and, as regards Hillman, Stewart, Strnad, Stone, Starr, Carmody, Evans, Carracoi, Wachter, Rosa, and the U.S. Government, is not subject to copyright protection in the United States. Foreign and other copyrights may apply. This is an open-access article distributed under the terms of the Creative Commons Attribution License (CC BY). The use, distribution or reproduction in other forums is permitted, provided the original author(s) and the copyright owner(s) are credited and that the original publication in this journal is cited, in accordance with accepted academic practice. No use, distribution or reproduction is permitted which does not comply with these terms.





3.6 Manuscript 6:

Strnad, M., Oh, Y.J., Vancová, M., Hain, L., Salo, J., Grubhoffer, L., Nebesářová, J., Hytönen, J., Hinterdorfer, P., Rego, R. O. M. (2021) Nanomechanical mechanisms of Lyme disease spirochete motility enhancement in extracellular matrix. *Communications Biology* 4: 268.

Annotation

Optical and electron microscopy techniques can provide important insights into the host-pathogen interactions (see **Manuscript 4** and **5**). However, these imaging modalities use lenses that exhibit spherical and chromatic aberrations. These defects prevent achieving the theoretical resolution limits and hinder the use of light and electron microscopy at the molecular level. Single-molecule studies are possible using cryo-electron microscopy investigations by means of averaging over a large ensemble of electron micrographs but only static images can be achieved. Here in **Manuscript 6**, we have employed atomic force microscopy-based system to shed light on the dynamics of the underlying functional mechanisms defining the *Borrelia*-host interactions at the single-molecule level. Designing a system that mimics natural environmental signals, which many spirochetes face during their infectious cycle, we observed that a subset of their surface proteins, particularly DbpA and DbpB, can significantly enhance the translational motion of spirochetes in the extracellular matrix of the host. We have disentangled the mechanistic details of DbpA/B and decorin/laminin interactions and showed that spirochetes are able to leverage a wide variety of adherence-based strategies through force-tuning transient molecular binding to extracellular matrix components, which concertedly enhance spirochetal dissemination through the host.

Nanomechanical mechanisms of Lyme disease spirochete motility enhancement in extracellular matrix

Martin Strnad^{1,2,6}[✉], Yoo Jin Oh^{3,6}[✉], Marie Vancová^{1,2}, Lisa Hain³, Jemiina Salo⁴, Libor Grubhoffer^{1,2}, Jana Nebesářová^{1,2}, Jukka Hytönen^{4,5}, Peter Hinterdorfer³ & Ryan O. M. Rego^{1,2}

As opposed to pathogens passively circulating in the body fluids of their host, pathogenic species within the Spirochetes phylum are able to actively coordinate their movement in the host to cause systemic infections. Based on the unique morphology and high motility of spirochetes, we hypothesized that their surface adhesive molecules might be suitably adapted to aid in their dissemination strategies. Designing a system that mimics natural environmental signals, which many spirochetes face during their infectious cycle, we observed that a subset of their surface proteins, particularly Decorin binding protein (Dbp) A/B, can strongly enhance the motility of spirochetes in the extracellular matrix of the host. Using single-molecule force spectroscopy, we disentangled the mechanistic details of DbpA/B and decorin/laminin interactions. Our results show that spirochetes are able to leverage a wide variety of adhesion strategies through force-tuning transient molecular binding to extracellular matrix components, which concertedly enhance spirochetal dissemination through the host.

¹Biology Centre ASCR, v.v.i., Ceske Budejovice, Czech Republic. ²Faculty of Science, University of South Bohemia, Ceske Budejovice, Czech Republic. ³Institute of Biophysics, Johannes Kepler University Linz, Linz, Austria. ⁴Institute of Biomedicine, University of Turku, Turku, Finland. ⁵Laboratory Division, Clinical Microbiology, Turku University Hospital, Turku, Finland. ⁶These authors contributed equally: Martin Strnad, Yoo Jin Oh. ✉email: martin.strnad.cze@gmail.com; yoo_jin.oh@jku.at

Bacterial adhesins are cell-surface components that facilitate adhesion to other cells or surfaces. The conventional viewpoint on adhesins is that they determine bacterial attachment and enable them to resist physical removal by shear stress caused by hydrodynamic shear forces¹. To maximize their contact with the environment, adhesins are often present on outward hairlike structures such as pili and fimbriae. Spirochetes do not possess such external structures. Additionally, spirochetes differ from most other motile pathogenic bacteria in that the spirochetes miss external appendages that are commonly required for bacterial motility. The unique corkscrew rotational movement is generated by periplasmic flagella hidden beneath the outer membrane, which allows them to swim in highly viscous, gel-like media that slow down or stop most bacteria with external flagella².

A typical representative of pathogenic spirochetes, *Borrelia burgdorferi*, expresses several adhesins that enable contact with its vertebrate hosts³. Decorin-binding proteins (DbpA and DbpB) and fibronectin-binding proteins BBK32 and RevA belong to the most recognized and functionally better characterized adhesins^{4–6}. DbpA and DbpB mutants show significant attenuation in mice, particularly early in infection⁷. Disruption of *dbpA* and *dbpB* decrease recovery of spirochetes from tissues distant to the inoculation site⁸. Similarly, *revA*-deficient spirochetes disseminate significantly less to distal organs⁹. BBK32 mutant exhibits a decrease in mice colonization and a delay in dissemination when compared to the parental strain¹⁰.

The common denominator, for all four adhesins in the context of infection, is delayed dissemination and colonization, particularly of distal tissues. Until now, the reason for this remains largely obscure as it was differently attributed to the effects of acquired immunity⁷, innate immunity⁸, or the inability to adhere properly to host ECM components^{8,10}. Surprisingly, relating the dynamic-binding properties of adhesins to borrelial motility or propagation within the host has never been attempted, possibly due to the absence of a quantitative assay that would allow to reliably mimic the movement of the spirochete through the host tissues. The goal here was to pursue the assumption that adhesins not only provide stationary attachments alone but also temporarily enhance the movement of the spirochetes.

Results

Adhesin expression does not enhance motility in standard in vitro assays. We set out to study the potential influence of selected adhesins on borrelial motility by generating three *Borrelia* adhesin expression mutants. The *revA* and *bbk32* genes were inserted into the shuttle vector pBSV2 and transformed into adhesin-less *B. burgdorferi* B313 to generate B313/RevA and B313/BBK32. B313/DbpAB has been tested already elsewhere⁶. Immunoblotting of bacterial lysates with antiserum raised against recombinant DbpA, RevA, or BBK32 revealed that all adhesin expression mutants produced the respective proteins. The presence of DbpA and DbpB on the surface of B313/DbpAB was shown earlier⁶, and corroborated in this study using a proteinase K (PK) assay. With the same strategy, the surface localization of RevA and BBK32 in B313/RevA and B313/BBK32, respectively, was confirmed (Fig. 1a).

Plate assays are commonly utilized to quantitatively examine bacterial motility on agar plates based on circular turbid zones formed by spirochetes migrating away from the point of cell seeding¹¹. To estimate the effect of adhesin expression on borrelial motility, two standard experimental approaches to characterize the undirected movement were performed. Both growth assay (Fig. 1b) and swarm motility assay (Fig. 1c) showed that motility of all adhesin expression mutants (B313/DbpAB,

B313/RevA, B313/BBK32) was not significantly altered compared to the parental wild-type cells, and compared to each other. These data show that the adhesins expression does not enhance undirected motility in standard in vitro conditions.

Spirochetal motility is enhanced in near-natural conditions by DbpA/B.

The standard methods that are used in studying the specific gene effects on borrelial motility are solely in vitro studies, lacking the vast majority of components and environmental signals which the spirochete faces during its infectious cycle. To bridge the gap between controllable in vitro motility assays and the natural environments that *B. burgdorferi* encounters, we designed a feeding setup mimicking the natural tick feeding on an infected host by using a natural ECM analog (Fig. 2a–c). This system allows us to imitate the migration of *Borrelia* in a host at the time of spirochete acquisition by a tick and reliably assess and quantify the effects of adhesin expression on borrelial motility. Tick feeding was induced by placing *Ixodes ricinus* ticks on fresh rabbit blood for 24 h (Fig. 2a). This time period ensured stable tick feeding as an attachment in membrane-feeding systems is often delayed compared to attachment onto hosts. Next, the spirochetes were embedded in the ECM matrix and overlaid with rabbit serum (RS) (Fig. 2b). As the primary goal of this study was to estimate the effect of adhesins solely on the translational movement of *Borrelia* in the ECM matrix, inactivated RS was used instead of blood during next feeding stages. Blood is known to contain many components with adverse effects on the spirochetes that could reduce their vitality/motility¹². Moreover, *I. ricinus* is known to feed well on blood serum¹³.

Ticks were allowed to feed and samples of RS were collected in duplicates at 1-h intervals, for a total of 4 h (Fig. 2c). Intriguingly, we observed that the surface presence of two studied borrelial adhesins, DbpAB and BBK32 from *B. afzelii* A91, increase significantly the number of spirochetes in RS and, therefore, the motility of the bacteria, as evidenced by quantitative PCR (Fig. 2d). Spirochete burdens of B313/DbpAB in RS were significantly higher (approximately 3 times) than control group B313/pBSV2 already at 1 hr after spirochete placement, indicating the immediate effect of DbpAB on spirochete motility. Presence of BBK32 also significantly enhanced the motility but the effect was not as strong as of DbpAB. RevA had no significant effect on borrelial motility. To determine whether the enhanced translational motion of spirochetes is caused due to certain specific DbpAB-ECM interactions or just due to the sheer presence of DbpAB, an inhibition experiment was performed. Blocking the availability of DbpAB by soluble decorin resulted in a significant reduction of motility in B313/DbpAB (Fig. 2e) and *B. afzelii* A91 (positive control; Fig. 2f) but not in DbpAB-less B313/pBSV2 (negative control; Fig. 2g). Together, these data show that the enhancement of borrelial motility is caused by certain DbpAB-ECM interactions.

DbpA/B show stronger interaction with decorin than with laminin in single-molecule bond analysis.

Borrelial adhesins are known to bind to multiple ECM ligands¹⁴. Therefore, we first confirmed that DbpA and DbpB interact and bind components of the ECM gel (Supplementary Fig. 1a). Further, adherence to a number of highly abundant components of the ECM (laminin, fibronectin, collagen, and decorin) was tested using microtiter plate assay, revealing that the Dbps showed efficient binding to decorin and laminin (Supplementary Fig. 1b). To investigate the underlying interaction characteristics of DbpA and DbpB with decorin and laminin as representatives of the ECM components in detail, we utilized the single-molecule force spectroscopy (SMFS) technique^{15–18}, based on the wide use of atomic force

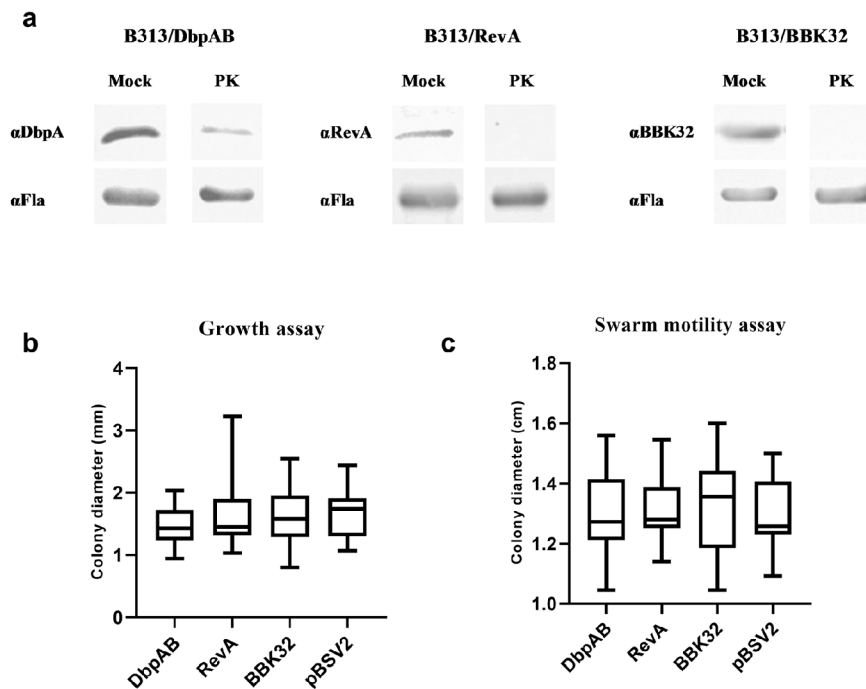


Fig. 1 Expression of adhesins does not enhance undirected motility in standard in vitro conditions. **a** To determine if DbpAB, BBK32, and RevA proteins are present in borrelial lysates and are surface exposed, a proteinase K (PK) assay was employed. PK-treated and -untreated lysates of recombinant *B. burgdorferi* B313 strains (B313/DbpAB, B313/RevA, B313/BBK32) expressing DbpA and DbpB, RevA, and BBK32 were separated by SDS-PAGE and immunoblotted with the indicated antibodies (α , anti). Bands corresponding to specific proteins are absent or faint from PK treated samples. The intensity of subsurface flagellar protein bands are identical between mock and PK treated cells, indicating surface localization of the adhesins. **b, c** The effect of DbpAB, RevA, and BBK32 on the undirected movement of spirochetes was studied using growth and swarm motility assays. Empty shuttle vector pBSV2 was used as the control. Results are expressed as arithmetic mean and were compared by one-way ANOVA. Error bars, standard deviation. In the growth assay, 30 colony diameters were measured for each mutant strain. In the swarm motility assay, 12 diameters for each strain were measured. Differences were not statistically significant ($P > 0.05$).

microscopy (AFM) in microbiology^{19–23}. SMFS directly measures dissociation forces by mechanically pulling on molecular interaction bonds. Borrelial surface proteins were conjugated to AFM tips and ECM analogs to surfaces, respectively, via a 6 nm long flexible PEG linker (Fig. 3a) to equip the molecules with sufficient motional freedom for unconstrained specific binding. We performed consecutive force-distance cycles, during which an AFM tip carrying a borrelial surface protein (DbpA, DbpB) was brought into contact with a surface coated with ECM analogs (decorin, laminin) so that a borrelial surface protein/ECM bond was eventually formed. From subsequently retracting the AFM tip from the surface and pulling on the bond with defined speed, the molecular bond was broken at a characteristic measurable dissociation force (Fig. 3b). In force distributions derived from the collection of dissociation forces (Fig. 3c), we found that binding of DbpA was stronger to decorin than to laminin. DbpB showed larger dissociation forces with decorin than with laminin as well. The superior binding capacity of Dbps to decorin was also evidenced from the binding activity: the binding probability values were generally larger for decorin than for laminin binding (Inset, Fig. 3c).

To decipher molecular dynamic and structural features of the Dbps/ECM bonds, we extended our SMFS studies to dynamic force spectroscopy (DFS) experiments and varied the pulling speed. Dissociation forces were measured and individually plotted vs. their force loading rates (equal to pulling velocity times effective spring constant) (Supplementary Fig. 2). In line with Evan's theory that a single energy barrier is crossed in the

thermally activated regime, a linear rise of the dissociation force with respect to a logarithmically increasing loading rate was found (Fig. 3d). Averaging the data fits using the equation of Bell and Evans^{24,25} (Fig. 3d), yielded the kinetic off-rate constant (K_{off}) extrapolated to zero-force and the length of the force-driven dissociation path (X_{β}) for Dbps binding to decorin and laminin, respectively (see Table 1). Although more sophisticated models are available for complex interactions, the single energy barrier model^{24,25} fitted well with our data. X_{β} was similar for all interactions, indicating comparable dissociation lengths during force-induced bond breakages. In contrast, K_{off} values showed pronounced differences. To account for the temporal stabilities of the bonds, we calculated average bond lifetimes, τ , directly from the kinetic off-rates, K_{off} , using the relation $\tau = 1/K_{off}$ (eq. 1) (Table 1). The lifetime of the DbpB/decorin bond (0.9 s) was slightly larger than that of DbpB/laminin (0.6 s). DbpA/decorin (25.6 s) complexes, however, were strikingly more stable when compared to DbpA/laminin (2.3 s), in line with the ultimately higher dissociation forces required to disrupt this strong bond (Fig. 3c, d).

DbpA/B has faster association kinetics with decorin than with laminin. It should be noted that the Bell–Evans model underlies the assumption of a single sharp and force-independent barrier transversed in the energy landscape along the force-driven bond-dissociation pathway. Thereby, K_{off} and X_{β} , derived from fitting the DFS data, characterize the height and the width of the energy

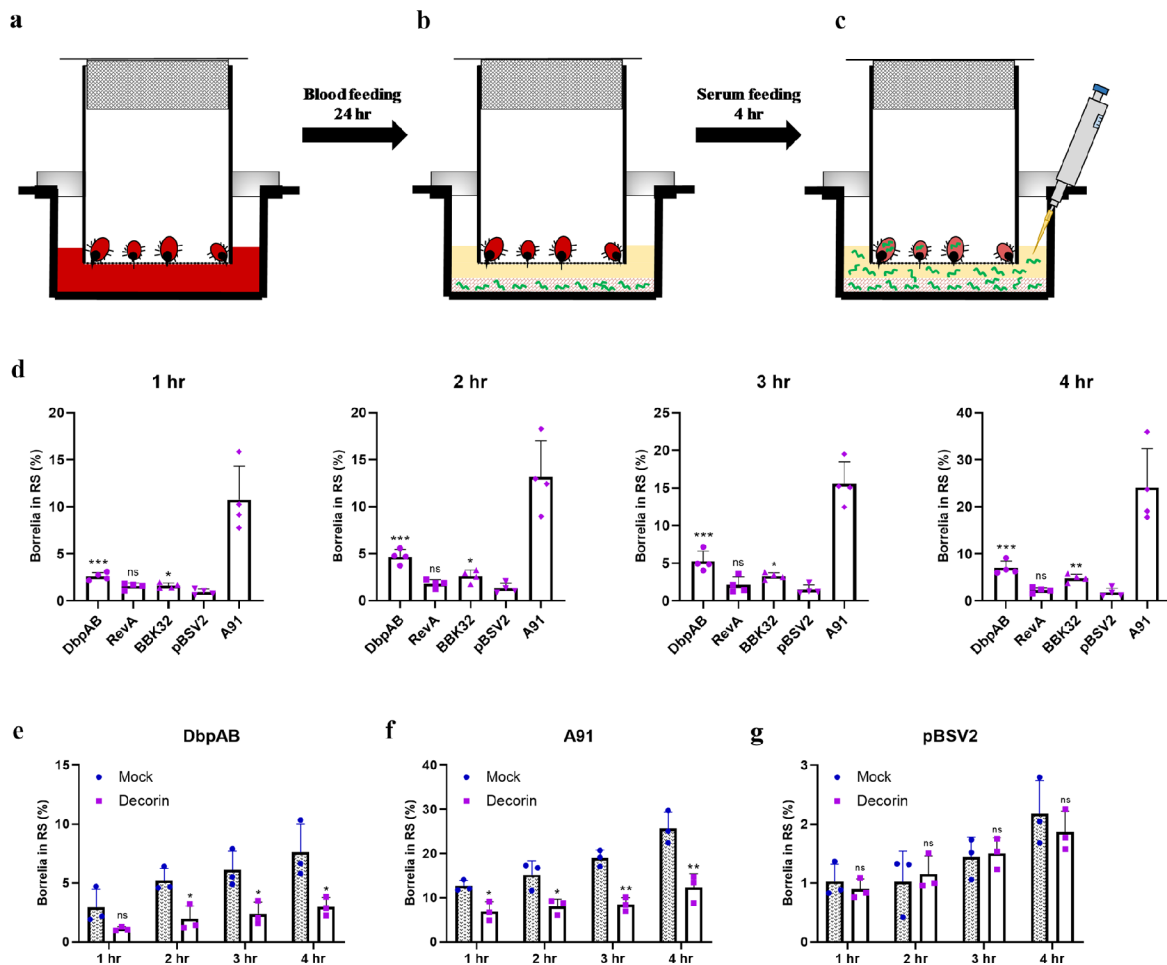


Fig. 2 DbpAB expression strongly enhances the number of spirochetes reaching blood serum upon feeding. **a–c** Schematic design of the ECM motility assay that imitates the period before *B. burgdorferi* acquisition by ticks. Tick feeding was induced by placing the ticks on fresh rabbit blood for 24 h (**a**). *Borrelia* was embedded in the ECM gel and overlaid with rabbit serum (RS) (**b**). Ticks were allowed to feed and samples of RS were collected in duplicates (2 × 200 µL) at 1-h interval, in total for 4 h (**c**). **d** The number of spirochetes that reached RS was monitored over time using qPCR and the influence of adhesin expression was assessed. The values are given as a percentage of the total number of spirochetes seeded to the ECM gel. The results show that addition of *dbpAB* (and also *bbk32*) into the specific adhesin-free *B. burgdorferi* B313 significantly enhances the motility of the bacterium, but does not fully restore the motility to the level of the infectious strain *B. afzelii* A91. pBSV2—*B. burgdorferi* B313 carrying empty shuttle vector was used as the control. Results are expressed as arithmetic mean and were compared by one-way ANOVA with Tukey *post hoc* test with pBSV2 as a control column. Error bars, standard deviation of four experiments. **P* < 0.05; ***P* < 0.01; ****P* < 0.001. The data showed that DbpAB has the most pronounced effect on borrelial motility in ECM. **e–g** To determine the effect of DbpAB-ECM interactions on the translational motion of spirochetes, the DbpAB sites were blocked by binding to soluble decorin. The results of the inhibition assays show that motility is significantly hampered in B313/DbpAB (**e**) and control DbpAB-expressing wild-type *B. afzelii* A91 (**f**), marking the importance DbpAB-ECM interactions for borrelial motility. In the control experiment, *B. burgdorferi* B313 with empty shuttle vector pBSV2 was not significantly affected by soluble decorin (**g**). Results are expressed as arithmetic mean and were compared by unpaired Student’s *t* test. Error bars, standard deviation of three experiments. **P* < 0.05; ***P* < 0.01; ns not statistically significant.

barrier, respectively. Kinetic off-rate constants determined from ensemble average methods such as SPR and QCM^{26,27}, however, may deviate from DFS values, if a different energy well is prominent when no force is applied.

To investigate the binding dynamics with a different approach, we varied the time in which Dbps/ECM bonds may form during force-distance cycles (denoted as dwell time) and monitored the binding probability. Arising from the molecular flexibility provided by the PEG linker, bond formation may occur within a range of about 10 nm (length of the coiled linkers plus attached molecules) above the surface and during tip-surface contact (about 25 nm, see the linear slope in the force curves of Fig. 3b)

for both the approaching and retracting part. Thus, the dwell time *t* is given by the overall sum of these lengths divided by the vertical scanning speed of the tip. Initially, the binding probability increased with the dwell time for all Dbps/ECM combinations (Fig. 3e, f). From this well-known behavior, the kinetic on-rate constant *K*_{on} was retrieved, by approximating with pseudo first-order kinetics according to $dP(t)/dt = K_{on} \cdot C_{eff}(1 - P(t))$ (eq. 2)^{27,28}. The effective concentration *C*_{eff} is the number of binding partners. i.e., effectively one Dbps molecule on the tip, within the effective volume *V*_{eff} accessible for free equilibrium interaction. *V*_{eff} can be described as a half-sphere with radius *r*_{eff}, with the latter being the sum of the equilibrium crosslinker length (3 nm)

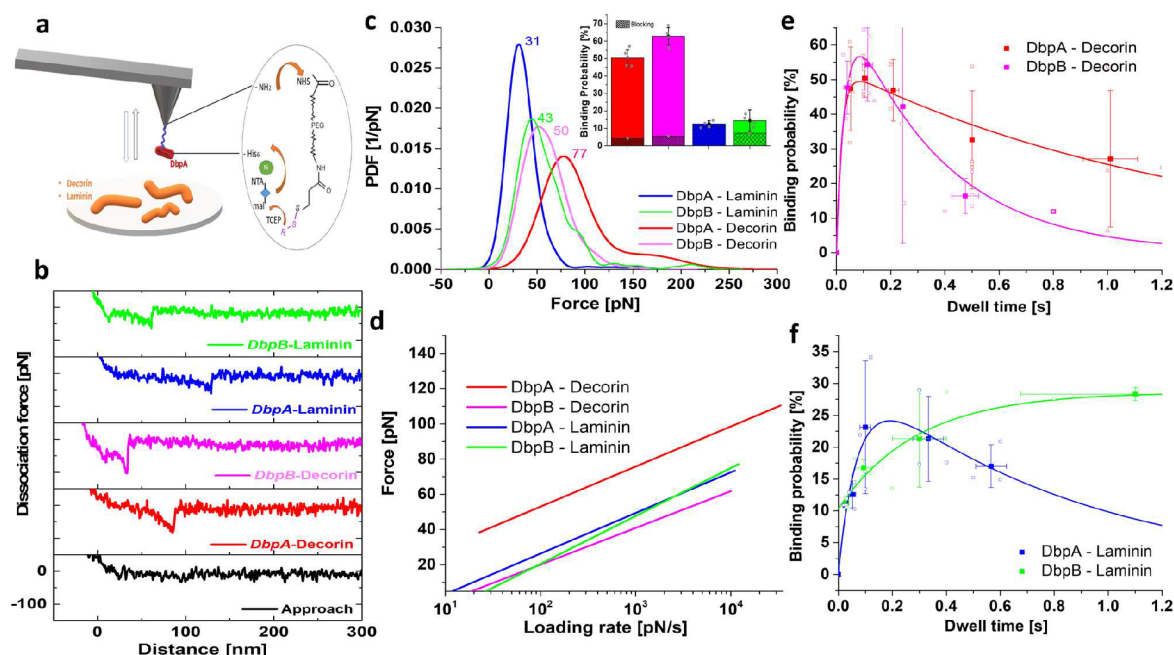


Fig. 3 Single molecular Dbps/ECM bond analysis reveals force-tuned dissociation paths. **a** Scheme of the immobilization strategy of decorin binding protein coupled to an amino-functionalized AFM tip end via a heterobifunctional PEG linker, and attachment of extracellular matrix protein onto a silicon substrate. **b** Typical force-distance curves obtained by SMFS, from which the dissociation forces (visible as spike at about 50–150 nm distance) of individual Dbps/ECM bonds were measured. Dissociation occurred at different distances, reflecting variable stretching lengths of decorin or laminin. **c** Force distributions depicted as experimental probability density functions (PDFs) were constructed from adding dissociation forces represented by Gaussians of unitary area with widths σ representing the measurement noise (cantilever thermal fluctuation). For each PDF at least 1000 force measurements were recorded at a retraction velocity of 1000 nm/s. PDFs are equivalents to continuous histograms with their maxima being the most probable dissociation forces (see indicated numbers in graph) their uncertainties (widths) reflecting the stochastic nature of the dissociation process. Inset. Binding probabilities (from $n = 5000$ force-distance cycles for each condition, 3–5 different tips), calculated as percentages of force-distance cycles monitoring dissociation forces out of the overall force-distance cycles performed, determined at a tip-surface dwell time of ~ 0.05 s. After addition of blocking agents (Dbps) into the bath solution, the binding probability dramatically decreased to around 5%, evidencing that binding was of specific nature. **d** dissociation force vs. force loading rate for single Dbps/ECM bonds, i.e., DbpA/decorin, DbpB/decorin, DbpA/laminin, DbpB/laminin. A maximum likelihood approach was used to fit the data and to extract the kinetic off-rate constant (K_{off}) and the length of the dissociation path (X_p) (see Table 1), using the equation of Bell and Evans^{24,25} (original data and fits are shown in Supplementary Fig. 2). **e, f** binding probability assay (BPA). Dbps/ECM bond formation as a function of the dwell time, **e** DbpA/decorin and DbpB/decorin, **f** DbpA/laminin and DbpB/laminin.

Table 1 Quantification of obtained parameters with dynamic force spectroscopy (DFS) and binding probability assay (BPA) methods.

		DbpA-decorin	DbpB-decorin	DbpA-laminin	DbpB-laminin
DFS	K_{off} [s^{-1}]	0.039 ± 0.03	1.1 ± 0.15	0.436 ± 0.19	1.77 ± 0.39
	X_p [\AA]	4.56 ± 0.37	4.29 ± 0.3	4.53 ± 0.51	3.43 ± 0.06
	τ [s]	25.6	0.91	2.29	0.56
BPA	K_{on} [$M^{-1}s^{-1}$]	5.7×10^4	3.6×10^4	1.7×10^4	4.1×10^3
	K'_{off} [s^{-1}]	1.3	0.35	0.82	-
	τ' [s]	0.7	2.844	1.22	-
	K_D [mM] = K'_{off}/K_{on}	0.023	0.009	0.048	-
	(K'_{off}/K_{on})	(0.0007)	(0.003)	(0.0254)	(0.43)

and the size of the proteins involved in binding (7 nm). In contrast to our earlier work, where the binding probability went into saturation over time²⁷, we here observed a quasi-exponential decrease after a local maximum had been reached (Fig. 3e, f). A similar behavior was also observed for the adhesion of P-selectin to P-selectin glycoprotein-1²⁹, which was interpreted to bear force-dependent rate constants that are important for supporting physiological leukocyte rolling. The decay of the binding probability with time comes from successive dissociation of Dbps

from ECM, before the force detection limit of our SMFS experiments (about 5 pN) in the retraction part of the force-distance cycles has been reached²⁹. Taking the unforced dissociation rate, K_{off} , during this time into account, the overall biomolecular Dbps/ECM reaction kinetics is given by the differential equation $dP(t)/dt = K_{on} \cdot C_{eff}(1 - P(t)) - K_{off}P(t)$ (eq. 3)²⁹.

As a result of the binding probability assay (BPA) (Fig. 3e, f), data fitting using the above equation yielded a kinetic on-rate (K_{on}) of DbpA/decorin binding of $5.7 \times 10^4 M^{-1}s^{-1}$. This value was slightly larger when compared to DbpB/decorin, but considerably exceeded the binding rates of Dbps to laminin (Table 1). The kinetic off-rates, K'_{off} , arising from the decaying part of the binding probability time course $P(t)$ (Fig. 3e, f), were transformed into average bond lifetimes measured at zero-force, τ' , using $\tau' = 1/K'_{off}$ (eq. 4) (Table 1). For the DbpA/decorin bond, τ' taken from this analysis (0.7 s) was dramatically shorter ($\sim 35\times$) than τ determined from DFS experiments. This indicates that the bond becomes greatly stabilized under force load. A similar effect, but much less pronounced, was observed for DbpA/laminin, whereas the behavior for DbpB/decorin (Table 1) was reversed. K_{off} for DbpB/laminin was very slow under equilibrium conditions, as $P(t)$ did not show any decay within the

measurement time (Fig. 3f). The macroscopic thermodynamic equilibrium dissociation constants K_D were measured using an extended microtiter plate assay method and Scatchard plot analysis (Supplementary Fig. 3). By comparing the K_D values carried out with BPA and microtiter plate assay at varying concentrations, we found that both techniques show similar affinity values in the μM range, and that DbpB/decornin shows a slightly higher affinity than DbpA/decornin. From our results it is quite evident that dissociation of the Dbps/ECM complexes in solution do not follow the same dissociation path as when a force is applied to the bonds. The considerably longer bond life time of DbpA/decornin in SMFS experiments clearly indicates that a much higher dissociation energy barrier is involved when the bond is force-loaded. Strikingly different is the behavior of the DbpB/laminin bond, which is governed by a much lower barrier under force than at equilibrium.

Discussion

During its infectious cycle, *B. burgdorferi* migrates through different shear stress environments. After tick transmission, the spirochete interacts with the cells lining the vascular lumen (high shear stress), traverses through the vessel wall (low shear stress), and finally infects target tissues (variable/low shear stress). Thereafter, when a new naive tick starts feeding on an infected host, the spirochete migrates “tick-wards” through the ECM (variable/low shear stress). Whereas some of the molecular interactions that enable efficient dissemination in high shear stress areas have been described^{30,31}, the effects of adhesions on spirochetal motility in low shear stress niches are unknown.

As shown by others³², spirochetes are able to adopt distinct motility states and transition between them in the ECM as they disseminate within the host. Our results reveal that a possible strategy how spirochetes coordinate the transition between these motility states, is by forming various bonds of different mechanical properties that are tuned by external forces. The increased stability of DbpA/decornin when force-loaded is tailored for spirochetes to withstand shear stress, thereby facilitating dissemination within vascular endothelia in blood vessels. Similar bond behavior has been reported to be involved in cellular adhesion, including BBK32 of *B. burgdorferi*^{30,31}, selectin-mediated binding²⁹, or ClfA–fibrinogen interaction³³. In the milieu with absence of significant shear stress, these binding interactions appear to be responsible for the “wriggling” and “lunging” motility states that *Borrelia* establishes for instance during colonization of the mouse dermis³². On the other hand, some of the bonds (as the most striking DbpB/laminin) are better adapted to mediate long-term stationary adhesions in equilibrium and short-term binding under force. This allows the spirochetes to detach easily underflow or during their rotatory movement.

Although certain binding interactions might prevail at a certain motility state, the differing kinetics between the DbpA/B proteins and the various components of the ECM need to work together synchronously as a single strategy to enhance motility through the ECM. It is not probable that spirochetes could actively influence which ECM components they will bind to and therefore the overall net effect of all interactions has to be translocation-enhancing. Additionally, DbpA and DbpB are not known to be downregulated at any phase of mammalian infection, as opposed to other infection-associated borrelial surface proteins such as OspC or VlsE³⁴, therefore it is not probable that some binding interactions are suppressed at any infection stage.

High torque generated by the flagellar motor is the essential player in generating the force needed for spirochetes to migrate³⁵. However, to be able to squeeze through dense, gel-like matrices with pore sizes much smaller than the diameter of their body,

spirochetes need to form transiently stable interactions that facilitate pushing against the adjacent surface³². We show that DbpA/B are multifunctional proteins, which through binding either directly to ECM proteins or their associated glycosaminoglycans side chains³⁶, are capable to propel and coordinate the movement within the ECM. The relatively weak forces between DbpA/B and ECM, when compared with higher binding forces of adhesins in nonmotile pathogenic bacteria^{37–39}, suggest that the spirochetes maintain a very dynamic state in an infected host^{30–32}. Together, these interactions help spirochetes to reach extraordinary high speeds⁴⁰, which enable them to colonize a host and to avoid clearance by the immune system of a host more efficiently. As it is known that bacteria are able to sense and respond to physical stimuli to optimize their function and overall fitness⁴¹, an attractive target of future studies could be to find out whether mechanical stress, experienced by spirochetes for instance as they penetrate the tight gel matrices, leads to upregulation of proteins such as DbpA/B.

In summary, we showed that spirochetes, despite a limited number of adhesive molecules, are able to leverage a wide variety of adhesion strategies in order to streamline their dissemination through the host. This unique mode of motility enhancement in low shear stress environment exploiting transient binding of the spirochete to adjacent surfaces might be common for many pathogenic organisms that are able to effectively migrate through dense, gel-like matrices^{42,43}.

Methods

Ethics statement. All tick and animal experiments were approved by the BC ASCR animal ethical committee (Animal protection laws of the Czech Republic No. 246/1992 Sb., Ethics approval No. 79/2013). All experiments were performed in accordance with relevant guidelines and regulations.

Bacterial strains and culture conditions. *E. coli* strains DH5a (NEB), NEB Express Iq (NEB) and M15 [pREP4] (Qiagen) were grown with aeration in Lysogeny broth at 37 °C under antibiotic selection with ampicillin (100 $\mu\text{g}/\text{mL}$) or kanamycin (50 $\mu\text{g}/\text{mL}$), where appropriate.

Recombinant *B. burgdorferi* B313 strains (B313/DbpAB, B313/BBK32, B313/RevA) expressing DbpA and DbpB, BBK32, and RevA of *B. afzelii* A91 were used in this study. B313/DbpAB together with the control strain containing empty shuttle vector pBSV2 (B313/pBSV2) were prepared elsewhere⁶. These isolates together with *B. burgdorferi* B31, *B. burgdorferi* B313, and *B. afzelii* A91 were cultured in Barbour–Stoenner–Kelly (BSK)-H medium (Sigma-Aldrich) at 34 °C.

Generation of recombinant DbpA, DbpB, RevA, and BBK32 proteins. To generate recombinant histidine-tagged RevA and BBK32 proteins, the *revA* and *bbk32* open reading frames lacking the putative signal sequences from *B. afzelii* A91 were amplified using the primers described in Supplementary Table 1. Amplified fragments were engineered to encode a BamHI site at the 5' end and a HindIII site at the 3' end. Amplified DNA fragments were inserted into TA cloning vector pGEM-T Easy (Promega). The resulting plasmids were then digested with BamHI and HindIII to release the genes, which were then inserted into the pQE30 (Qiagen) predigested with BamHI and HindIII. The resulting plasmids were transformed into *E. coli* NEB Express Iq (NEB) and the plasmid inserts were sequenced. The construction of recombinant strains *E. coli* M15 expressing DbpA and DbpB from *B. afzelii* A91 is described elsewhere⁴⁴.

Large cultures were induced with the use of isopropyl β -D-1-thiogalactopyranoside (final concentration, 0.5 mM) and lysed by sonication. Recombinant soluble proteins were harvested and purified under native conditions using Protino Ni-NTA Agarose (Macherey-Nagel). Bound proteins were eluted with 250 mM imidazole in TRIS buffer (50 mM, pH 8, 300 mM NaCl). The proteins were washed, desalted, and concentrated in Amicon Ultra-15 3000 MWCO (Merck Millipore). Purity was checked using SDS-PAGE and protein concentrations were measured using Bradford assay.

Immunization of rabbit with DbpA, DbpB, RevA, and BBK32. Female New Zealand white rabbits (Velaz, Czech Republic) were immunized by injection subcutaneously with 100 μg recombinant DbpA or DbpB from *B. afzelii* A91 in TRIS buffer (1:1) with complete Freund's adjuvant (Sigma-Aldrich). The rabbit received two boosts of 100 μg recombinant DbpA or DbpB in TRIS buffer (1:1) with incomplete Freund's adjuvant (Sigma-Aldrich) at 14-day intervals. One week after the final boost, the rabbit was bled to obtain serum. The serum was tested qualitatively by Western blotting to determine the specificity of the antiserum for DbpA

and DbpB against recombinant DbpA protein and *B. burgdorferi* lysates. Briefly, proteins were separated by SDS-polyacrylamide gel electrophoresis and transferred to nitrocellulose. Membranes were blocked for 2 h with 5% BSA in TRIS-buffered saline with 0.05% Tween 20 (TBS-T). Membranes were washed with TBS-T and incubated for 2 h at room temperature (RT) with DbpA/DbpB antisera diluted 1:200 in blocking buffer. After washing with TBS-T, membranes were incubated for 1 h at RT with goat anti-rabbit immunoglobulin G conjugated with horseradish peroxidase (HRP) (Vector Laboratories) diluted 1:10,000 in blocking buffer. After a final series of washes with TBS-T, bound antibodies were detected by using Pierce ECL western blotting chemiluminescence substrate (Thermo Scientific).

Generation and characterization of B313/BBK32 and B313/RevA. To generate the shuttle vectors expressing BBK32 and RevA proteins, the respective genes with upstream regions were first PCR amplified with the addition of a HindIII site and a BamHI site at the 5' and 3' ends, respectively, using the primers listed in Supplementary Table 1. Amplified DNA fragments were inserted into TA cloning vector pGEM-T Easy (Promega). The resulting plasmids were then digested with HindIII and BamHI to release the genes, which were then inserted into the shuttle vector pBSV2K predigested with HindIII and BamHI.

B. burgdorferi B313 was transformed by electroporation with 40 µg of each of the shuttle vectors and cultured in BSK-H medium at 34 °C for 24 h. The transformants were selected in BSK1.5× semisolid medium containing 1.7% agarose and 50 µg/mL kanamycin at 34 °C for 2 weeks. *B. burgdorferi* transformants were confirmed by colony PCR using kanamycin specific primers. The presence of RevA/BBK32 was confirmed by Western blot assay using sera from a rabbit immunized with recombinant RevA/BBK32 from *B. afzelii* A91.

Surface localization of the adhesins was performed with proteinase K assay similarly as in the previous studies^{6,45}. Proteinase K was added to the cell suspension at a final concentration of 100 µg/mL, incubated at RT for 3 min, and washed twice with PBS before preparing the samples for Western blot analyzes. Anti-flagellin antibody (Rockland) (1:5000) with anti-rabbit HRP as a secondary antibody (1:10,000) were used. Protein Marker VI (10–245) pre-stained (AppliChem) was used for all Western blots.

Plate growth and swarm motility assays. For growth assay, BSK 1.5× medium for semisolid plating was prepared as described by Samuels⁴⁶ and 100 spirochetes were plated by mixing with BSK 1.5× in a petri dish. Plates were incubated at 34 °C and for 3 weeks in a microaerophilic chamber. Colony images were obtained in a Bio-Rad ChemiDoc Imaging System and colony diameters were measured using ImageJ. Thirty colony diameters were measured for each strain. One-way ANOVA test was used to compare the colony diameters.

Spirochete cell motility was determined by swarm plate assays. Swarm plates were prepared by mixing 50 mL BSK 1.5× medium, 144 mL Dulbecco's Phosphate Buffered Saline (PBS), and 60 mL 1.7% agarose. Approximately 1×10^6 cells in a volume of 5 µL were spotted onto plates. Swarm plates were incubated at 34 °C and for 3 weeks in a microaerophilic chamber. Statistical tests were performed as stated above for growth assay.

In vitro tick feeding assay. Pathogen-free adult females of *I. ricinus* reared in our in-house facility were used for the experiments. The feeding units for membrane feeding of ticks were prepared according to the procedure developed by Kröber and Guerin⁴⁷. Rabbit blood was collected in the animal house facility of the Institute of Parasitology, Biology Center ASCR and manually defibrinated. For feeding, 10 ticks were placed in the feeding unit. To initiate tick feeding, blood was added into the feeding unit and regularly exchanged at intervals of 8 h. After 24 h, unattached females were removed. To study the motility of *Borrelia*, 100 µL of ECM Gel from Engelbreth-Holm-Swarm murine sarcoma (Sigma-Aldrich, E6909) and 600 µL of *Borrelia* cultures (5×10^6 cells) were first mixed on ice and then thoroughly mixed with 500 µL of 2% low melting point agarose (SeaPlaqueTM, Lonza, 50100) heated to 60 °C and placed into the six-well cell culture plate (Corning Costar). Once solidified, 3.5 mL of sterile-filtered rabbit serum (Sigma, R4505) was pipetted onto the gel-embedded bacteria. The feeding units with ticks were submerged into the serum and placed in a water bath heated to 37 °C. Samples of rabbit serum were collected in duplicates (2 × 200 µL) at 1-hr interval, in total 4 h. For inhibition experiments, the spirochetes were preincubated with decorin (10 µg) from bovine articular cartilage (Sigma-Aldrich) at 37 °C for 30 min and the feeding assay was done as described above. The unpaired Student *t* test was used to test the statistical significance.

DNA isolation and real-time quantitative PCR. DNA isolation from rabbit sera was performed using the Nucleospin Blood kit as per manufacturer's instructions (Macherey-Nagel). DNA extracts were examined for *B. burgdorferi* spirochetes by using a real-time quantitative PCR (qPCR) assay with Fast Start Universal SYBR Green Master Kit (Roche) and primers specific for a section of the 16S rRNA gene⁴⁸, listed in Supplementary Table 1. To assess spirochete density per sample, a standard curve was generated in log increments (10–10⁶). The numbers of borrelial genomic copies were calculated by comparing the threshold cycle (*C_T*) values with the values for serial dilutions of known amounts of *B. burgdorferi* genomic DNA, which were used as standards. Samples were analyzed using a LightCycler 480

(Roche). The PCR conditions were as follows: 95 °C for 5 min, followed by 50 cycles of 95 °C for 15 s, 60 °C for 15 s, and 72 °C for 15 s.

Adhesion of recombinant DbpA and DbpB to ECM gel and ECM components.

Specific interactions between borrelial adhesins and ECM gel components were detected using far western blotting. Briefly, 2 µL of ECM gel was separated by SDS-polyacrylamide gel electrophoresis and after blotting and blocking with 2.5% BSA, recombinant DbpA and DbpB (50 µg) were added, followed by incubation with anti-HisTag-HRP labeled antibody (R&D Systems).

The Nunc MaxiSorp ELISA plates (Thermo Scientific) were coated with 1 µg laminin from human fibroblasts (Sigma-Aldrich), recombinant human collagen Type I (Sigma-Aldrich), human fibronectin (R&D Systems), or with decorin from bovine articular cartilage (Sigma-Aldrich) in 100 µL/well coating buffer (100 mM bicarbonate/carbonate buffer [pH 9.6]) overnight at 4 °C, and blocked with 200 µL of 2.5% BSA in TRIS buffer for 1 h at RT. Subsequently, the respective DbpA (0.5 µg/well in 100 µL TRIS buffer) was added, incubated for 1 h at RT, and washed (wash buffer; TRIS plus 0.05% Tween-20), followed by incubation with anti-HisTag-HRP (1:10,000) labeled antibody in 50 µL of blocking buffer for 30 min at RT and five washes. Finally, tetramethylbenzidine substrate (Sigma-Aldrich) was added. The reaction was stopped with 1 M sulfuric acid and the absorbance at 450 nm was determined using the Infinite 200 M Pro microplate reader (Tecan). For the extended microtiter plate assay method we varied the concentration of the ligand and fitted the data using a Scatchard plot by applying the following equation to calculate the dissociation constant K_D , $B/F = 1/K_D(B_{max} - B)$, where *B* equals the bound molecules and *F* the free ligand concentration⁴⁹.

Conjugation of borrelial surface proteins through histidine residues of His-tagged protein.

A maleimide-Poly(ethylene glycol) (PEG) linker was attached to a 3-aminopropyltriethoxysilane (APTES)-coated AFM cantilever by incubating the cantilevers for 2 h in 500 µL of chloroform containing 1 mg of maleimide-PEG-N-hydroxysuccinimide (NHS) (Polypure) and 30 µL of triethylamine. After three times washing with chloroform and drying with nitrogen gas, the cantilevers were immersed for 2 h in a mixture of 100 µL of 2 mM thiol-trisNTA, 2 µL of 100 mM EDTA (pH 7.5), 5 µL of 1 M HEPES (pH 7.5), 2 µL of 100 mM tris(carboxyethyl) phosphine (TCEP) hydrochloride, and 2.5 µL of 1 M HEPES (pH 9.6) buffer, and subsequently washed with HEPES buffer. Thereafter, the cantilevers were incubated for 4 h in a mixture of 4 µL of 5 mM NiCl₂ and 100 µL of 0.2 µM His-tagged borrelial surface proteins (DbpA, DbpB). After washing three times with HEPES-buffer saline (HBS), the cantilevers were store in HBS at 4 °C²¹.

Conjugation of extracellular matrix (decorin, laminin) through lysine residues to the substrate.

$1 \times 1 \text{ cm}^2$ silicon nitride substrates were coated with APTES, before a heterobifunctional acetal-PEG linker was attached via its NHS ester group for coupling of decorin from bovine articular cartilage (Sigma-Aldrich) or laminin from human fibroblasts (Sigma-Aldrich) via one of the lysine residues. The bond was fixed by reduction with NaCNBH₃. The overall procedure was done as described before⁵⁰. Substrates were washed and stored in PBS at 4 °C before measurements.

Single-molecule force spectroscopy (SMFS).

SMFS measurements were performed at RT using borrelial surface protein conjugated tips with 0.01 N/m nominal spring constants (MSCT, Bruker). The deflection sensitivity was calculated from the slope of the force-distance curves recorded on a bare silicon substrate. Force-distance curves were acquired by recording at least 1000 curves with vertical sweep times between 0.5 and 10 s and at a z-range of typically 500 nm, resulting in loading rate from 100 to 10,000 pN/s, using a commercial AFM (Keysight Technologies, USA). The relationship between experimentally measured unbinding forces and the interaction potential is described by kinetic models^{24,25}. Blocking of a specific interaction between borrelial surface protein and extracellular matrix was done by injecting borrelial surface proteins into the bath solution, which resulted in a de-activated ECM on the surface. All SMFS experiments were repeated on at least five different preparations of functionalized AFM cantilevers and sample surfaces.

Statistics and reproducibility.

The details about experimental design and statistics used in different data analyzes performed in this study are given in the respective sections of results, figure legends, and methods. All AFM experiments were performed at least three times independently. Data are presented as mean ± standard error of the mean. The number of experiments, the name of the statistical test, and exact *p* values are provided in each figure legend. Comparisons between groups were determined using Student's *t* test or ANOVA. Differences were considered significant at **P* < 0.05; ***P* < 0.01; ****P* < 0.001.

Reporting summary. Further information on research design is available in the Nature Research Reporting Summary linked to this article.

Data availability

The datasets generated or analyzed during the current study are available from the corresponding author on reasonable request. Source data underlying plots shown in figures are provided in Supplementary Data 1. Uncropped scans of Western blots are shown in Supplementary Fig. 4.

Received: 30 June 2020; Accepted: 1 February 2021;

Published online: 01 March 2021

References

- Klemm, P. & Schembri, M. A. Bacterial adhesins: function and structure. *Int. J. Med. Microbiol.* **290**, 27–35 (2000).
- Charon, N. W. & Goldstein, S. F. Genetics of motility and chemotaxis of a fascinating group of bacteria: the spirochetes. *Annu. Rev. Genet.* **36**, 47–73 (2002).
- Hyde, J. A. *Borrelia burgdorferi* keeps moving and carries on: a review of borrelial dissemination and invasion. *Front. Immunol.* **8**, 114 (2017).
- Brissette, C. A., Bykowski, T., Cooley, A. E., Bowman, A. & Stevenson, B. *Borrelia burgdorferi* RevA antigen binds host fibronectin. *Infect. Immun.* **77**, 2802–2812 (2009).
- Probert, W. S. & Johnson, B. J. Identification of a 47 kDa fibronectin-binding protein expressed by *Borrelia burgdorferi* isolate B31. *Mol. Microbiol.* **30**, 1003–1015 (1998).
- Salo, J., Loimaranta, V., Lahdenne, P., Viljanen, M. K. & Hytönen, J. Decorin binding by DbpA and B of *Borrelia garinii*, *Borrelia afzelii*, and *Borrelia burgdorferi* sensu stricto. *J. Infect. Dis.* **204**, 65–73 (2011).
- Imai, D. M. et al. The early dissemination defect attributed to disruption of decorin-binding proteins Is abolished in chronic murine Lyme borreliosis. *Infect. Immun.* **81**, 1663–1673 (2013).
- Weening, E. H. et al. *Borrelia burgdorferi* lacking DbpBA exhibits an early survival defect during experimental infection. *Infect. Immun.* **76**, 5694–5705 (2008).
- Byram, R. et al. *Borrelia burgdorferi* RevA significantly affects pathogenicity and host response in the mouse model of Lyme Disease. *Infect. Immun.* **83**, 3675–3683 (2015).
- Seshu, J. et al. Inactivation of the fibronectin-binding adhesin gene *bbk32* significantly attenuates the infectivity potential of *Borrelia burgdorferi*. *Mol. Microbiol.* **59**, 1591–1601 (2006).
- Zhang, K. & Li, C. Measuring *Borrelia burgdorferi* motility and chemotaxis. *Methods Mol. Biol.* **1690**, 313–317 (2018).
- Bhide, M. R. et al. Sensitivity of *Borrelia* genospecies to serum complement from different animals and human: a host–pathogen relationship. *FEMS Immunol. Med. Microbiol.* **43**, 165–172 (2005).
- Perner, J. et al. Acquisition of exogenous haem is essential for tick reproduction. *Elife* **5**, e12318 (2016).
- Coburn, J., Leong, J. & Chaconas, G. Illuminating the roles of the *Borrelia burgdorferi* adhesins. *Trends Microbiol.* **21**, 372–379 (2013).
- Florin, E. L., Moy, V. T. & Gaub, H. E. Adhesion forces between individual ligand–receptor pairs. *Science* **264**, 415–417 (1994).
- Hinterdorfer, P., Baumgartner, W., Gruber, H. J., Schilcher, K. & Schindler, H. Detection and localization of individual antibody–antigen recognition events by atomic force microscopy. *Proc. Natl Acad. Sci. USA* **93**, 3477–3481 (1996).
- Lee, G. U., Chrisey, L. A. & Colton, R. J. Direct measurement of the forces between complementary strands of DNA. *Science* **266**, 771–773 (1994).
- Dammer, U. et al. Binding strength between cell adhesion proteoglycans measured by atomic force microscopy. *Science* **267**, 1173–1175 (1995).
- Odermatt, P. D. et al. Overlapping and essential roles for molecular and mechanical mechanisms in mycobacterial cell division. *Nat. Phys.* **16**, 57–62 (2020).
- Doktycz, M. J. et al. AFM imaging of bacteria in liquid media immobilized on gelatin coated mica surfaces. *Ultramicroscopy* **97**, 209–216 (2003).
- Oh, Y. J. et al. Curli mediate bacterial adhesion to fibronectin via tensile multiple bonds. *Sci. Rep.* **6**, 1–8 (2016).
- Dufrène, Y. F. Atomic force microscopy, a powerful tool in microbiology. *J. Bacteriol.* **184**, 5205–5213 (2002).
- Oh, Y. J. et al. Characterization of curli A production on living bacterial surfaces by scanning probe microscopy. *Biophys. J.* **103**, 1666–1671 (2012).
- Bell, G. I. Models for the specific adhesion of cells to cells. *Science* **200**, 618–627 (1978).
- Evans, E. & Ritchie, K. Dynamic strength of molecular adhesion bonds. *Biophys. J.* **72**, 1541–1555 (1997).
- Sieben, C. et al. Influenza virus binds its host cell using multiple dynamic interactions. *Proc. Natl Acad. Sci. USA* **109**, 13626–13631 (2012).
- Rankl, C. et al. Multiple receptors involved in human rhinovirus attachment to live cells. *Proc. Natl Acad. Sci. USA* **105**, 17778–17783 (2008).
- Baumgartner, W., Gruber, H. J., Hinterdorfer, P. & Drenckhahn, D. Affinity of trans-interacting VE-cadherin determined by atomic force microscopy. *Single Mol.* **1**, 119–122 (2000).
- Fritz, J., Katopodis, A. G., Kolbinger, F. & Anselmetti, D. Force-mediated kinetics of single P-selectin/ligand complexes observed by atomic force microscopy. *Proc. Natl Acad. Sci. USA* **95**, 12283–12288 (1998).
- Niddam, A. F. et al. Plasma fibronectin stabilizes *Borrelia burgdorferi*–endothelial interactions under vascular shear stress by a catch-bond mechanism. *Proc. Natl Acad. Sci. USA* **114**, E3490–E3498 (2017).
- Ebady, R. et al. Biomechanics of *Borrelia burgdorferi* vascular interactions. *Cell Rep.* **16**, 2593–2604 (2016).
- Harman, M. W. et al. The heterogeneous motility of the Lyme disease spirochete in gelatin mimics dissemination through tissue. *Proc. Natl Acad. Sci. USA* **109**, 3059–3064 (2012).
- Geoghegan, J. A. & Dufrène, Y. F. Mechanobiology: how mechanical forces activate *Staphylococcus aureus* adhesion. *Trends Microbiol.* **26**, 645–648 (2018).
- Tilly, K., Bestor, A. & Rosa, P. A. Lipoprotein succession in *Borrelia burgdorferi*: similar but distinct roles for OspC and VlsE at different stages of mammalian infection. *Mol. Microbiol.* **89**, 216–227 (2013).
- Beeby, M. et al. Diverse high-torque bacterial flagellar motors assemble wider stator rings using a conserved protein scaffold. *Proc. Natl Acad. Sci. USA* **113**, E1917–E1926 (2016).
- Benoit, V. M., Fischer, J. R., Lin, Y.-P., Parveen, N. & Leong, J. M. Allelic variation of the Lyme disease spirochete adhesin DbpA influences spirochetal binding to decorin, dermatan sulfate, and mammalian cells. *Infect. Immun.* **79**, 3501–3509 (2011).
- Herman-Bausier, P., El-Kirat-Chatel, S., Foster, T. J., Geoghegan, J. A. & Dufrène, Y. F. *Staphylococcus aureus* fibronectin-binding protein A mediates cell–cell adhesion through low-affinity homophilic bonds. *mBio* **6**, e00413–e00415 (2015).
- Milles, L. F., Schulten, K., Gaub, H. E. & Bernardi, R. C. Molecular mechanism of extreme mechanostability in a pathogen adhesin. *Science* **359**, 1527–1533 (2018).
- Herman-Bausier, P. et al. *Staphylococcus aureus* clumping factor A is a force-sensitive molecular switch that activates bacterial adhesion. *Proc. Natl Acad. Sci. USA* **115**, 5564–5569 (2018).
- Malawista, S. E. & de Boisfleury Chevance, A. Clocking the Lyme spirochete. *PLoS ONE* **3**, e1633 (2008).
- Dufrène, Y. F. & Persat, A. Mechanobiology: how bacteria sense and respond to forces. *Nat. Rev. Microbiol.* **18**, 227–240 (2020).
- Sycuro, L. K. et al. Relaxation of peptidoglycan cross-linking promotes *Helicobacter pylori*'s helical shape and stomach colonization. *Cell* **141**, 822–833 (2010).
- Goldstein, S. F. & Charon, N. W. Motility of the spirochete *Leptospira*. *Cell Motil. Cytoskeleton* **9**, 101–110 (1988).
- Heikkilä, T. et al. Species-specific serodiagnosis of Lyme arthritis and neuroborreliosis due to *Borrelia burgdorferi* sensu stricto, *B. afzelii*, and *B. garinii* by using decorin binding protein A. *J. Clin. Microbiol.* **40**, 453–460 (2002).
- Fischer, J. R., LeBlanc, K. T. & Leong, J. M. Fibronectin binding protein BBK32 of the Lyme disease spirochete promotes bacterial attachment to glycosaminoglycans. *Infect. Immun.* **74**, 435–441 (2006).
- Samuels, D. S. Electrotransformation of the Spirochete *Borrelia burgdorferi*. *Methods Mol. Biol.* **47**, 253–259 (1995).
- Kröber, T. & Guerin, P. M. In vitro feeding assays for hard ticks. *Trends Parasitol.* **23**, 445–449 (2007).
- Tsao, J. I. et al. An ecological approach to preventing human infection: vaccinating wild mouse reservoirs intervenes in the Lyme disease cycle. *Proc. Natl Acad. Sci. USA* **101**, 18159–18164 (2004).
- Indexing, I. A new method for the determination of dissociation constant (Kd) on the binding of CA19-9 to its antibody in type 2 diabetic patients by enzyme linked immunosorbent assay (ELISA) with some modifications.
- Wildling, L. et al. Linking of sensor molecules with amino groups to amino-functionalized AFM tips. *Bioconjug. Chem.* **22**, 1239–1248 (2011).

Acknowledgements

This study was supported by the WTZ programme from the Austrian Federal Ministry of Education, Science and Research and Czech Ministry of Education, Youth and Sports (8J19AT009). Y.J.O. acknowledges the financial support from the Austrian Science Fund FWF project I 3173, V584-BBL and the Austrian National Foundation for Research, Technology, and Development and Research Department of the State of Upper Austria. M.S. and R.O.M.R. acknowledge the support from the Czech Science Foundation grant

No. 17-21244S funded to R.O.M.R. and Czechoslovak Microscopy Society stipend funded to M.S. M.V. and J.N. acknowledge the support from the MEYS CR (Czech BioImaging LM2015062 and CZ.02.1.01/0.0/0.0/16_013/0001775). L.H. acknowledges the ĀAW fellowship STIP13202002. We thank J. Grammer and F. Kaser for their assistance in force-distance curves analysis.

Author contributions

M.S. and Y.J.O. conceived and coordinated the project. M.S., J.S., J.H., and R.O.M.R. prepared *Borrelia* mutants and recombinant adhesins. M.S. and M.V. performed tick feeding and in vitro motility assays. J.N. and L.G. provided reagents and contributed to tick feeding experiments. Y.J.O. performed force spectroscopy measurements and data analysis. L.H. analyzed ELISA data. M.S., Y.J.O., and P.H. wrote the original draft of this manuscript with guidance and edits from R.O.M.R. Critical reading, supervision, and further edits were also provided by M.V. and J.S.

Competing interests

The authors declare no competing interests.

Additional information

Supplementary information The online version contains supplementary material available at <https://doi.org/10.1038/s42003-021-01783-1>.

Correspondence and requests for materials should be addressed to M.S. or Y.J.O.

Reprints and permission information is available at <http://www.nature.com/reprints>

Publisher's note Springer Nature remains neutral with regard to jurisdictional claims in published maps and institutional affiliations.



Open Access This article is licensed under a Creative Commons Attribution 4.0 International License, which permits use, sharing, adaptation, distribution and reproduction in any medium or format, as long as you give appropriate credit to the original author(s) and the source, provide a link to the Creative Commons license, and indicate if changes were made. The images or other third party material in this article are included in the article's Creative Commons license, unless indicated otherwise in a credit line to the material. If material is not included in the article's Creative Commons license and your intended use is not permitted by statutory regulation or exceeds the permitted use, you will need to obtain permission directly from the copyright holder. To view a copy of this license, visit <http://creativecommons.org/licenses/by/4.0/>.

© The Author(s) 2021

3.7 Manuscript 7:

Hejduk, L., Rathner, P., **Strnad, M.**, Grubhoffer, L., Sterba, J., Rego, R. O. M., Müller, N., Rathner, A. (accepted with minor revisions) Resonance assignment and secondary structure of DbpA protein from the European species, *Borrelia afzelii*. *Biomol NMR Assign.*

Annotation

In **Manuscript 6**, we revealed that DbpA and DbpB from *B. afzelii* have the most pronounced effects on the dissemination and motility of *Borrelia* in the host extracellular matrix. Specifically, we have studied the pathogenic dissemination mechanisms at the single-molecular level. As our aim is to go even deeper in our understanding of the underlying interactions, in **Manuscript 7**, we have performed backbone and side chain resonance assignment, and predicted secondary structure of DbpA from *B. afzelii* by solution NMR spectroscopy. Characterization of backbone dynamics is crucial for proper understanding of the key interactions at sub-molecular level. It allows one to examine the importance of individual amino acid residues in DbpA. Structural and dynamics comparison of DbpA from various *B. burgdorferi* sensu lato will help to establish a starting point in deciphering exact interaction schemes between DbpA of *B. afzelii* and of other species. This may ultimately help to elucidate the species-to-species variation in clinical manifestations of the Lyme disease.

Resonance assignment and secondary structure of DbpA protein from the European species, *Borrelia afzelii*

Libor Hejduk^{1,2}, Petr Rathner^{3†}, Martin Strnad^{1,2}, Libor Grubhoffer^{1,2}, Jan Sterba¹, Ryan O. M. Rego^{1,2}, Norbert Müller^{1,4}, Adriana Rathner^{3*}

¹Faculty of Science, University of South Bohemia, Branišovská 1760, 370 05, České Budějovice, Czech Republic

²Institute of Parasitology, Biology Centre, Czech Academy of Sciences, Branišovská 31, 370 05, České Budějovice, Czech Republic

³Institute of Inorganic Chemistry, Johannes Kepler University, Altenbergerstraße 69, 4040, Linz, Austria

⁴Institute of Organic Chemistry, Johannes Kepler University, Altenbergerstraße 69, 4040, Linz, Austria

†Present address: Institute of Analytical Chemistry, University of Vienna, Währingerstraße 38, 1090, Vienna, Austria

Abstract

Decorin binding proteins (Dbps) mediate attachment of spirochetes in host organisms during the early stages of Lyme disease infection. Previously, different binding mechanisms of Dbps to glycosaminoglycans have been elucidated for the pathogenic species *Borrelia burgdorferi* sensu stricto and *B. afzelii*. We are investigating various European *borrelia* spirochetes and their interactions at the atomic level using NMR. We report preparative scale recombinant expression of uniformly stable isotope enriched *B. afzelii* DbpA in *Escherichia coli*, its chromatographic purification, and solution NMR assignments of its backbone and sidechain ¹H, ¹³C, and ¹⁵N atoms. This data was used to predict secondary structure propensity, which we compared to the North American *B. burgdorferi* sensu stricto and European *B. garinii* DbpA for which solution NMR structures had been determined previously. Backbone dynamics of DbpA from *B. afzelii* were elucidated from spin relaxation and heteronuclear NOE experiments. NMR-based secondary structure analysis together with the backbone dynamics characterization provided a first look into structural differences of *B. afzelii* DbpA compared to the North American species and will serve as the basis for further investigation of how these changes affect interactions with host components.

Keywords: NMR resonance assignment, decorin-binding proteins, *Borrelia afzelii*

***Corresponding author:** Adriana Rathner, adriana.rathner@jku.at, ORCID: <https://orcid.org/0000-0003-2919-9407>

Acknowledgments

We greatly acknowledge financial support through Ministry of Education, Youth and Sports of the Czech Republic; Grant Agency of the Czech Republic and the European Union.

Biological context

Borrelia burgdorferi sensu lato (s.l.) complex of genospecies is the causative agent of Lyme disease, the most common tick-borne disease in Europe and North America. The Lyme disease manifestation includes tissue tropism related to colonisation by particular *borrelia* genospecies. For instance, *B. burgdorferi* sensu stricto (s.s.) preferentially colonises joints while *B. garinii*, whose infection leads to neuroborreliosis, prefers neural tissues (Wang et al., 1999). The development of Lyme disease, primarily during the early phase, proceeds by invasion and adhesion of bacteria to different structures in the host organism. The outer surface of *borrelia* is coated with various proteins including adhesins, which mediate attachment to cell surface proteins or other molecules in the extracellular matrix.

Decorin binding proteins (Dbps) are important adhesins exposed on the surface of bacteria from the *B. burgdorferi* s.l. complex. Dbps bind collagen-associated protein decorin through glycosaminoglycan (GAG) chain attached to the decorin (Fischer et al., 2003). Decorin is a glycoprotein highly abundant in the connective tissues associated with collagen fibres. Decorin is modified with various GAG chains depending on its presence in different tissues. DbpA and DbpB, two homologous Dbps, have been described as important factors for *borrelia* virulence

and host colonization. According to previous research (Shi et al., 2008), cooperation of both homologues in binding to decorin is necessary for tissue colonisation. DbpA is species variable in its amino acid sequence, whereas DbpB is more conserved. The sequence similarity of DbpA across the genospecies is above 58 % in contrast to DbpB which lies above 96% (Roberts et al., 1998; Fig. 3). Based on the sequence identity, DbpA variants also differ in their binding affinity to different GAGs attached to decorin (Lin et al., 2014). Combining these aspects – tissue tropism of bacteria and structural variability of adhesins including Dbps, DbpA-GAG interaction variations are acknowledged to have a considerable effect on the pathogenicity of *borrelia* genospecies. Characterization of DbpA from various *B. burgdorferi* s.l. by solution NMR spectroscopy, i.e. under near-native conditions will help to establish a starting point in deciphering exact interaction schemes between DbpA of *B. afzelii* and of other species and small GAGs which have been studied only in North American *borrelia* strains so far. For comprehensive understanding of these relatively weak interactions assessment of the protein backbone dynamics is crucial.

Methods and Experiments

Cloning, expression, and purification of DbpA

The gene coding sequence for DbpA from *B. afzelii* (strain A91) without the transmembrane part of the protein was cloned into pQE30 plasmid, which includes the sequence for His₆ tag directly attached to N-terminus of the protein. The construct was transformed into *E. coli* M15 (pREP4) strain. 20 ml Lysogeny Broth (LB) media was inoculated by the cells and grown for 12 h at 37 °C as an overnight culture. The culture was used in dilution 1:100 for inoculation of fresh LB medium in volume of 250 ml. The cell culture was cultivated at 37 °C with shaking at 200 rpm and after the optical density (OD 600 nm) reached 0.7, the cells were centrifuged at 3000 x g for 30 min. The pelleted cells were resuspended in the same volume of M9 minimal media supplemented with ¹⁵N (>98%, Cambridge

Isotope Laboratories, Inc.) ammonium sulphate (1.5 g/l) and uniformly ^{13}C (>99%, Cambridge Isotope Laboratories, Inc.) labelled glucose (2 g/l). The temperature was lowered to 25°C, after 1 h the cells were induced by 1 mM IPTG and incubated for 18 h at 25 °C with shaking at 200 rpm. The cells were harvested and resuspended in 10 ml of buffer A (buffer A: 20 mM Tris, 200 mM NaCl, pH 7.2; buffer B: 20 mM Tris, 200 mM NaCl, 500 mM imidazole, pH 7.2) with Halt Protease inhibitor mix (Thermo Fisher Scientific). Cells were disrupted using French press (Stansted Fluid Power Ltd.) at approx. 120 MPa and lysate was centrifuged in an ultracentrifuge at 70000 x g for 1 h. The first purification step was Ni^{2+} affinity chromatography performed on 5 ml HisTrap HP column (Cytiva). The lysate was directly applied to the column equilibrated with Buffer A. Non-specifically bound proteins were washed out by step of 12% buffer B. DbpA was received within the gradient elution of 12% – 100% of buffer B. The fractions containing DbpA were concentrated by Amicon Ultra 10K filter columns. In the second step, the concentrated sample was purified with size exclusion chromatography on SuperDex 75 10/300 GL (Cytiva) using a constant flow of 0.2 ml/min of running buffer (50 mM KH_2PO_4 , 200 mM NaCl, pH 7.2).

Nuclear magnetic resonance spectroscopy

All NMR experiments were recorded on a 700 MHz Avance III spectrometer with an Ascend magnet and TCI cryoprobe (manufactured in 2011 by Bruker). Uniformly ^{15}N , ^{13}C labelled DbpA was measured in 20 mM KH_2PO_4 , pH 6.0, 10% D_2O at 470 μM concentration enriched with 1/7 of the sample volume of stock solution of Protease cOmplete[®] Mini inhibitors cocktail, EDTA free (stock solution contained 1 tablet/1.5 ml; Roche).

To determine the ideal temperature for further measurements, a set of ^{15}N TROSY HSQC experiments in thermal gradient was performed at temperatures ranging from 288 K to 315 K and back (3 K steps). Best signal-to-noise ratio and peak dispersion were observed at 313 K.

Spectra recorded for backbone assignment comprised: ^1H , ^{15}N HSQC, ^1H , ^{13}C HSQC, ^{15}N TOCSY-HSQC, ^1H , ^{15}N TROSY-HSQC, HNC0, HNCA, HNHA, HNCACB, CBCA(CO)NH. In addition to mentioned experiments, H(CCO)NH, CC(CO)NH, (H)CCH-TOCSY and HCCH-COSY were recorded to assign the sidechain atoms. (Sattler et al., 1999; Grzesiek et al., 1993; Vuister et al., 1993) All spectra were processed using Topspin 3.6.1 (Bruker). The resonance assignment of backbone and side chain resonances of DbpA was accomplished manually in CARA program (Keller, 2004). Secondary structure propensity was analysed by online prediction service TALOS-N based on calculations of backbone torsion angles ϕ , ψ and sidechain torsion angle χ from experimentally measured chemical shifts (Shen and Bax, 2013).

Local dynamics was assessed with T_1 , T_2 and heteronuclear ^{15}N $\{^1\text{H}\}$ NOEs values. For ^{15}N T_1 relaxation times, 2D phase sensitive ^1H , ^{15}N HSQC using inversion recovery with PEP (Preservation of Equivalent Pathways) sensitivity improvement was recorded using the pulse program `hsqct1etf3gpsi` (inversion recovery delays were following: 10, 50, 100, 200, 300, 400, 500, 600, 700, 800, 900, 1000, 1100 and 1200 ms) (Canavagh et al., 2007). ^{15}N T_2 relaxation times were determined in an analogous way to T_1 times using a version of the previously mentioned 2D experiment specific to T_2 relaxation times, `hsqct2etf3gpsi` (delays of 5, 10, 15, 20, 25, 30, 35, 40, 50, 60, 70, 80, 90, 100 and 120 ms). After optimization, relaxation delay parameter (d1) of 1s duration was used for both experiments. Backbone heteronuclear NOEs were obtained from the phase sensitive gradient-enhanced 2D ^1H - ^{15}N HSQC using PEP sensitivity improvement (`hsqcnoef3gpsi` pulse program). All spectra were processed equally (with the same intensity scaling factor) and analyzed in NMRFAM-Sparky (Lee et al., 2015).

Extent of assignments and data deposition

The whole recombinant construct (including the N-terminal His₆ tag and linker sequence) contains 157 residues from which 135 amino acids were at least partially assigned sequence specifically (Fig. 1). Assignments were deposited in BMRB under ID 50751. Unassigned remain the His₆ tag, GS-linker and 14 residues from across the protein which makes the total extent of 90.6 % assignment of the DbpA sequence (86 % of all amino acids in the construct). We have assigned 91.1 % of the backbone, 75.4 % of side chains and 90.7 % of ¹H, ¹⁵N, ¹³Ca, ¹³Cb, ¹³CO, respectively (not taking into account the tag and linker residues). From the total of 22 unassigned residues in the protein (14 within the original DbpA sequence), 8 were located in ¹⁵N HSQC spectra but could not be assigned unequivocally due to severe overlap in the center of the ¹⁵N HSQC spectrum as well as lack of intensity for these systems in 3D spectra (e.g. ¹⁵N TOCSY HSQC). Systems which were assigned with amino acid type and position in sequence also have most of the side chain atoms assigned.

Results from TALOS-N secondary structure propensity prediction tool reveal that the secondary structure profile of European *B. afzelii* DbpA is generally similar to the DbpA solution NMR structures of two *borrelia* species – *B. burgdorferi* s.s. (North America) and *B. garinii* (Europe) DbpAs (Fig. 2B, BD). The longest loop (res. G38 – G55) of *B. afzelii* DbpA contains a small approx. one-turn alpha helix just like DbpA from *B. burgdorferi* s.s., whereas in the more sequentially related *B. garinii* DbpA one found a long alpha helix in the same place. The second substantial difference we find in the short loop (E85 – G89) region: in *B. garinii* DbpA there is an extended helix while in *B. burgdorferi* DbpA the disordered regions extend from T104 - S112. The secondary structure similarity of *B. burgdorferi* s.s. and *B. afzelii* DbpAs appears to be bigger than the one to *B. garinii* DbpA, although the sequence similarity behaves in the opposite way. These structural differences within DbpAs of different *borrelia* species most likely mirror the difference in species specificity for various host tissues. It is also to be

expected that these structural characteristics will be responsible for different affinities of DbpAs to various GAG chains across *borrelia* species.

Sequence specific backbone dynamics of *B. afzelii* DbpA correlates with TALOS-N prediction and shows 5 ordered regions corresponding to alpha helical regions (Fig. 2C). The most dynamic part of the assigned backbone resonances is the longest loop (G38 – G55) which also contains a small helix. A fraction of 32 % of dynamic parts was estimated from values of R_2/R_1 ratios in *B. afzelii* DbpA protein. This is in good agreement with 34 % of dynamic regions found in *B. burgdorferi* s.s. DbpA (PDB: 2MTC; Morgan and Wang, 2015) and slightly higher than 24 % of intrinsically disordered parts of *B. garinii* DbpA (PDB: 2MTD; Morgan and Wang, 2015). These difference in dynamics are most likely linked to differences in binding mechanisms to GAGs.

In summary, we report the first characterization of DbpA from European *B. afzelii* by solution NMR spectroscopy. Backbone and side chain resonance assignments provide a crucial starting point for the comparative study of interactions between this DbpA variant and various GAG chains. Secondary structure estimates provide important first insight into structural differences among DbpA homologues that are most probably linked to their varied dissemination strategies. Backbone dynamics (and its changes) can be correlated to differential interaction mechanisms between GAG ligands and *borrelia* DbpA variants.

Declarations

Funding

This study was supported by the Ministry of Education, Youth and Sports of the Czech Republic INTER-ACTION projects LTARF18021 and LTAUSA18040, and the Grant Agency of the Czech Republic (18-27204S). NMR experiments were recorded at the Austro-Czech RERI-uasb NMR Centre (co-funded by the European Union, program EFRE INTERREG IV ETC-AT-CZ, project M00146 "RERI- uasb").

Conflict of interest

The authors declare no conflict of interest.

Author contributions

LG, JS, RR, and NM conceived the study. MS prepared and transformed plasmids. LH and PR planned and carried out expression and purification protocol of the protein. AR planned and carried out NMR experiments. LH analyzed NMR data under supervision of AR and PR. All authors contributed to writing of the manuscript and approved the final version.

Data availability

Set of assigned resonances is available at the Biological Magnetic Resonance Databank under accession number of 50751.

References

Lee W, Tonelli M, Markley JL. (2015) NMRFAM-SPARKY: enhanced software for biomolecular NMR spectroscopy. *Bioinformatics*. 31(8):1325-7.

Cavanagh, J., Fairbrother, W. J., Palmer III, A. G., & Skelton, N. J. (2007). *Protein NMR spectroscopy: principles and practice*. Second edition. Elsevier.

Shen, Y., Bax, A. (2013) Protein backbone and sidechain torsion angles predicted from NMR chemical shifts using artificial neural networks. *J Biomol NMR* 56, 227–241.

Lin, Y. P., Benoit, V., Yang, X., Martínez-Herranz, R., Pal, U., & Leong, J. M. (2014). Strain-specific variation of the decorin-binding adhesin DbpA influences the tissue tropism of the Lyme disease spirochete. *PLoS pathogens*, 10(7), e1004238.

Roberts, W. C., Mullikin, B. A., Lathigra, R., & Hanson, M. S. (1998). Molecular analysis of sequence heterogeneity among genes encoding decorin binding proteins A and B of *borrelia burgdorferi sensu lato*. *Infection and immunity*, 66(11), 5275–5285.

Shi, Y., Xu, Q., McShan, K., & Liang, F. T. (2008). Both decorin-binding proteins A and B are critical for the overall virulence of *borrelia burgdorferi*. *Infection and immunity*, 76(3), 1239–1246.

Fischer, J. R., Parveen, N., Magoun, L., & Leong, J. M. (2003). Decorin-binding proteins A and B confer distinct mammalian cell type-specific attachment by *borrelia burgdorferi*, the Lyme disease spirochete. *Proceedings of the National Academy of Sciences of the United States of America*, 100(12), 7307–7312.

Wang, G., van Dam, A. P., Schwartz, I., & Dankert, J. (1999). Molecular typing of *borrelia burgdorferi sensu lato*: taxonomic, epidemiological, and clinical implications. *Clinical microbiology reviews*, 12(4), 633–653.

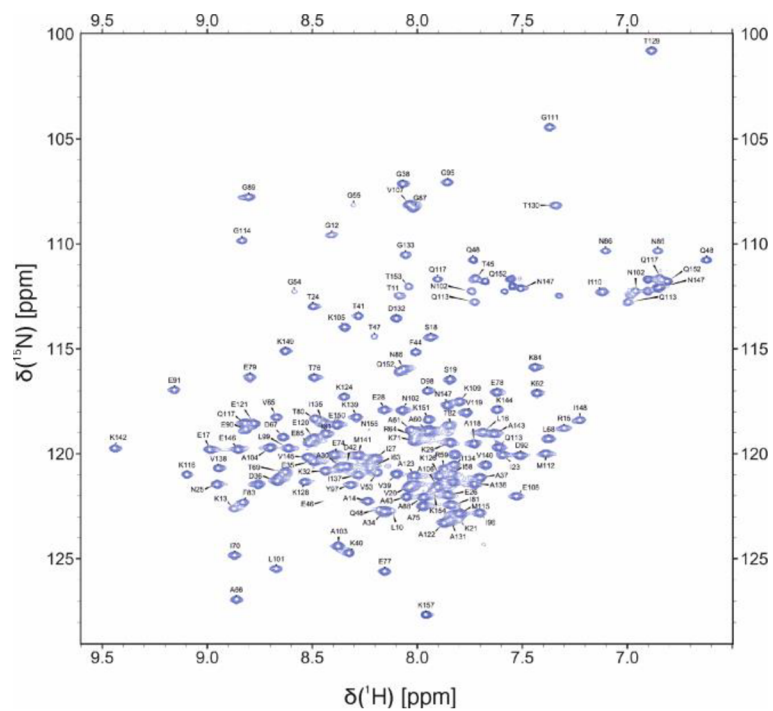
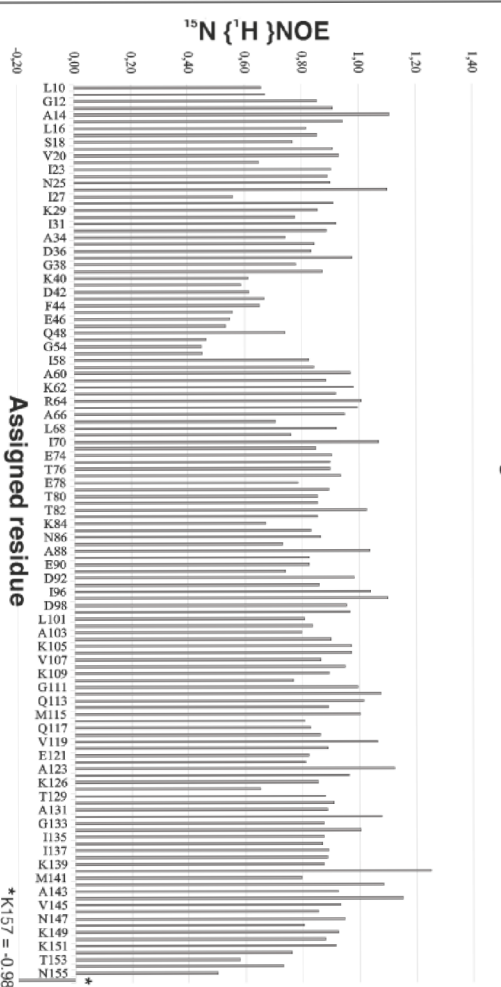
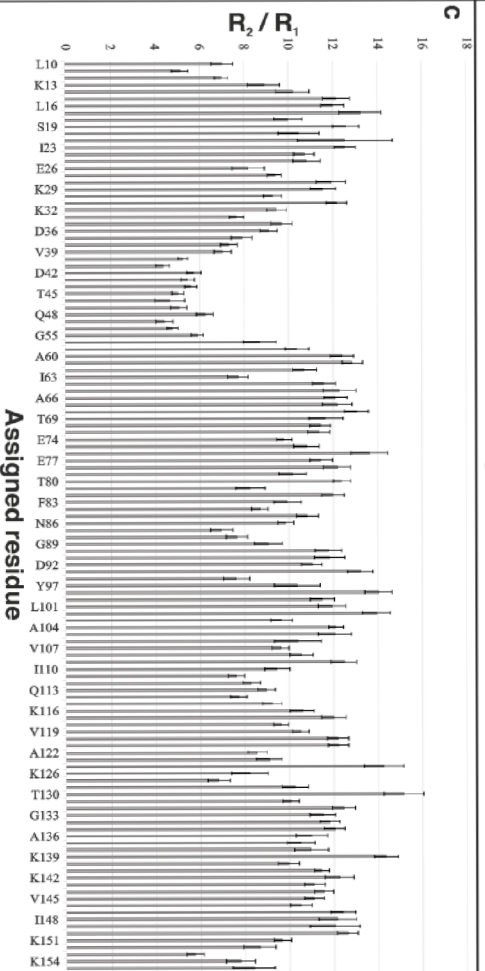
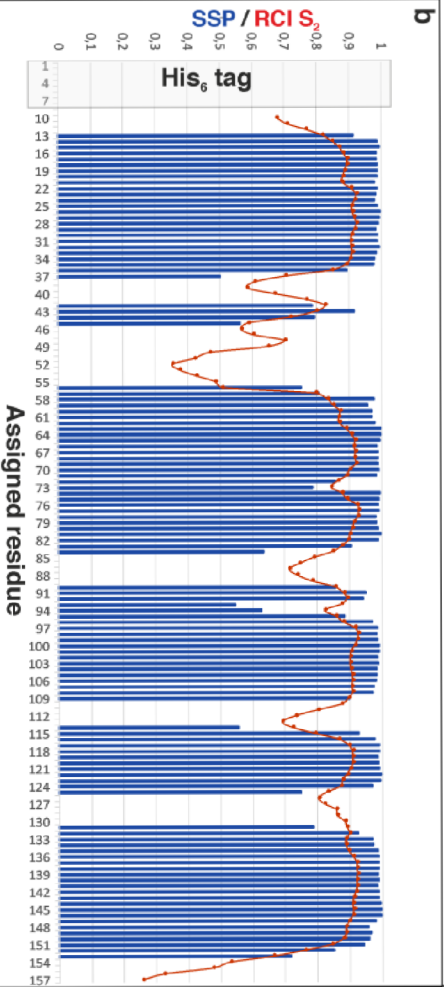


Fig. 1: ^1H – ^{15}N HSQC spectrum of DbpA from *B. afzelii*. Peaks are labelled by a one letter code denoted with position of residue in the recombinant protein sequence. Figure was created using CARRA (Keller, 2004)

a

10 20 30 40 50 60 70 80
 HHHHHHSSSL TGRARLESSV KDIITNEIEKA IKEAEADAGVK TDAFTETOTG GRVGGSSQIRA AKIRVADLTI KFLATEEETI
 90 100 110 120 130 140 150
 ITFKENGAGE EDFSGIYDILI LMAAKAVKEKI GNQGMKQAVE EAAREKPKTT ADGIITAIYKV MKAQVENEIKE KQTKNK



B. burgdorferi s.s.

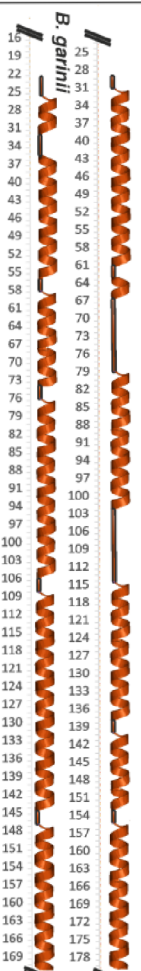


Fig. 2: Secondary structure propensity and backbone dynamics of DbpA. **a:** Complete amino acid sequence of DbpA from *B. afzelii* including the N-terminal His₆tag. **b:** TALOS-N secondary structure propensity (SSP) of DbpA from backbone chemical shifts of all assigned residues. Blue bars represent propensity of given amino acid to form alpha helix, no beta sheets were predicted for DbpA. Residues with no value shown in the plot were predicted to be random coil. Red line indicates random coil index order parameter. **c:** R₂/R₁ spin relaxation rates ratio for backbone amides of all assigned residues (upper graph) and heteronuclear steady state ¹⁵N {¹H} NOE values for all assigned amino acids (lower graph). **d:** Secondary structures of two DbpA protein homologs from North American *borrelia* are plotted for comparison (DbpA from *B. burgdorferi* s.s. - PDB ID: 2MTC; DbpA from *B. garinii* – PDB ID: 2MTD; both in Morgan and Wang, 2015). Alignment of all data of DbpA and the secondary structures of other DbpAs in this graph is based on their sequential alignment using Clustal Omega (<https://www.ebi.ac.uk/Tools/msa/clustalo/>) which can be found in Fig. 3.

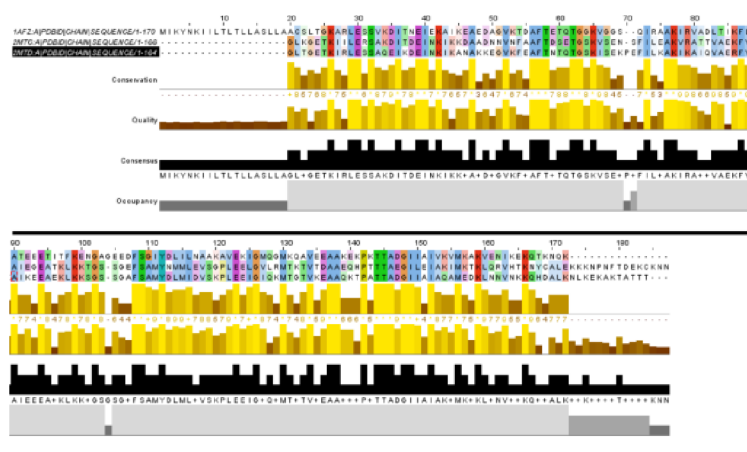


Fig. 3: Sequence alignment of DbpA from *B. afzelii*. Comparison of sequences of *B. afzelii* DbpA (1AFZ) with homologous proteins from *B. burgdorferi* s.s. (PDB: 2MTC; Morgan and Wang, 2015) and *B. garinii* (PDB: 2MTD; Morgan and Wang, 2015).

4 Conclusion and future perspectives

The thesis aims to point to and define the status of *Borrelia* complexity and to tackle the resulting issues arising from this matter. The studies have focused mainly on the most common European *Borrelia* species with human pathogenic potential and on their virulence-associated proteins, especially decorin binding proteins A and B. As nearly all the studies that described the biological functions of DbpA and DbpB (and many other proteins) have been carried out on North American strains of a single species ie., *B. burgdorferi* s.s., an opportunity was taken to rationalize the need to undertake similar studies on European species. Since recent whole-genome sequences of several European species/strains makes adaptation and use of genetic techniques feasible in studying inherent differences between them, a manuscript that proposes to perform independent studies of genospecies within Europe given the varying genetic content, pathogenic potential, and differences in clinical manifestation was prepared [65] (**Manuscript 3**).

Alongside the question of *Borrelia* complexity, the central theme of the thesis is the application of cutting-edge imaging techniques in spirochete research to reveal how structure translates itself into function. Imaging has become one of the key tools for the analysis of *Borrelia*-host/vector interactions and it has made a large contribution to our knowledge of *Borrelia* pathogenesis [66]. A significant amount of information about the pathogen and its virulence mechanisms can be extracted from the equilibrium constants, bands on the gel, or amplification curves, but setting these data within a proper context is equally important. Being able to visualize the pathogen at a site of interaction with a host brings an informative picture on the characteristics of the pathogen, its modes of transmission, and mechanisms of infection.

The adhesion mechanisms of LD *Borrelia* were studied using the correlative light electron microscopy at the cellular resolution. In order to understand the underlying mechanisms and virulence processes at the single-molecule and amino acid resolution, atomic force microscopy-based single-molecule force spectroscopy and nuclear magnetic resonance, respectively, have been utilized to study the Dbps of human pathogenic European species. Some of the results, mainly the data on *B. afzelii*, were already published and are part of the thesis. For instance, we have shown that DbpA/B can strongly enhance the translational motion of spirochetes in the extracellular matrix, enabling the bacteria to relocate faster inside their hosts. Thus, we have clearly demonstrated that adhesins not only provide stationary/anchoring attachments but might also temporarily enhance the movement of the spirochetes. The studies on Dbps of other human pathogenic species, especially *B. garinii* and *B. bavariensis*, are currently in progress but the incomplete results are not disclosed in the thesis. Since the motility-enhancing effects were shown on the non-infectious B313/DbpAB mutants, the next goal is to confirm the data by using a fully infectious strain.

Notably, not only the high gene heterogeneity, but the different surface distribution of the DbpA adhesin might be a significant factor responsible for the differences in the pathogenicity. In our experiments (unpublished data), we have visualized the surface distribution of DbpA in virulent *B. afzelii* A91 and recombinant *B. burgdorferi* B313/DbpAB, a strain complemented with decorin binding proteins from *B. afzelii* A91 using DbpA-specific antibodies with high-resolution SEM (Fig. 3). The frequency of labeling was diametrically different from the results obtained by Hanson and colleagues [67], who showed much lower labeling density

when working with the North American strain *B. burgdorferi* B31. We aim to probe whether different species display different distribution patterns [68] of their adhesive molecules, which could be one of the factors that contribute to differences in LD progression.

In addition, elucidation of the organization of the surface proteins and possible uneven distribution of the proteins during the

adhesion stage could bring up questions on possible “functional fragmentation” along the borrelia cell.

Adhesins are generally perceived as molecules only responsible for mediating interactions with surrounding cells and structures. DbpA and DbpB are stably anchored in the outer borrelial membrane and constitute an important functional but also structural component. A recent study has shown that outer membrane of bacteria is an essential load-bearing element and the proteins present in the membrane constitute critical determinants for the mechanical properties of the bacterial cell [69]. The study overturns the prevailing dogma that the cell wall is the dominant mechanical element

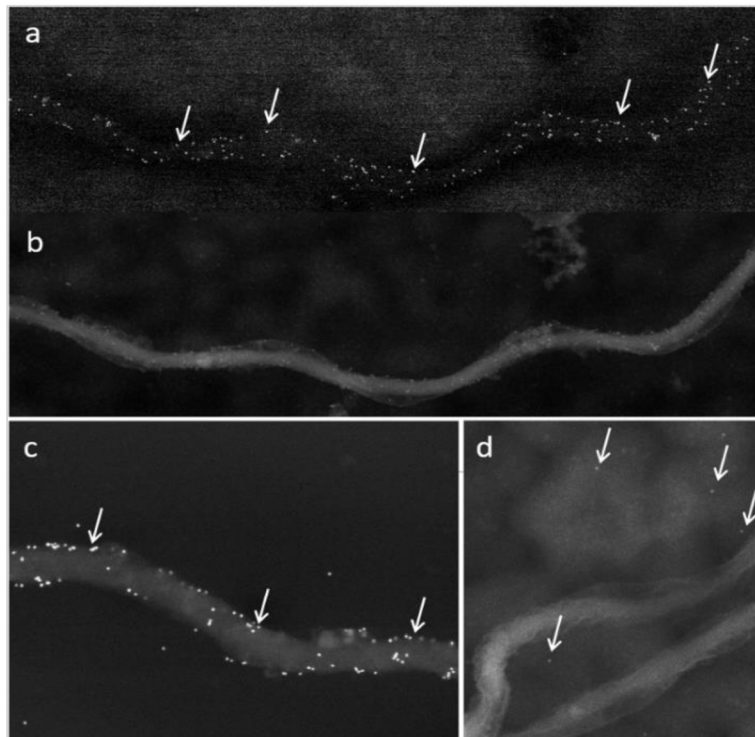


Figure 3. Immunogold distribution of DbpA on the surface of *B. burgdorferi* showing a similar pattern and expression levels in both the strain *B. burgdorferi* B313 complemented with DbpAB on a shuttle vector (a-b) and wild type, *B. afzelii* A91 (c). (d) Negative control, B313. 15 nm gold nanoparticles. The backscatter mode (a, c, d), Everhart-Thornley detector (b). SEM FE-JEOL 7401.

within bacteria possessing both an inner and outer membrane (Gram-negative bacteria), instead demonstrating that the outer membrane can be stiffer than the cell wall. As cell stiffness affects the swimming speed of *Borrelia* [70] and at the same time the motility is crucial to the pathogenic potential of the spirochete [71], the presence and abundance of DbpA and DbpB might have a substantial effect on the swim speed and dissemination of *Borrelia* via modulation of the mechanical properties of the cell.

Biological-atomic force microscopy (Bio-AFM) allows resolving surface biological structures in physiological environments with nanometer resolution [72]. It has been utilized for probing biological surfaces such as proteins, membranes, cells, and bacteria [73–75]. Force mapping-based AFM is additionally capable of quantifying local elasticity and adhesion, as it has also been evidenced on the surface of bacterial cells [76]. Using Bio-AFM, we have started to visualize the structure of borrelial surfaces expressing adhesins at the nano-scale (Fig. 4). Additionally, their mechanical properties (adhesion, elasticity, Young's modulus) are investigated to understand how mechanical parameters might be influenced by Dbps and how it concertedly affects the cellular adhesion behaviour at the nano-scale. We aim to examine whether the expression of adhesins significantly changes the physical parameters of the bacteria in order to determine whether there is a correlation between virulence and mechanical characteristics of the spirochete.

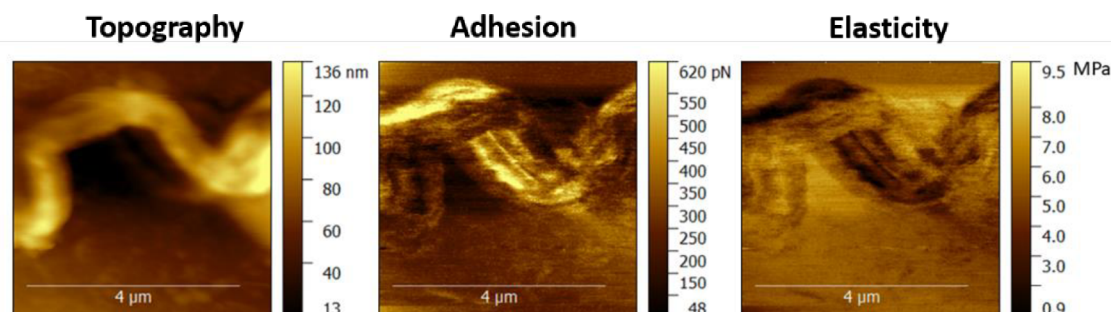


Figure 4. Bio-AFM images of the living *B. burgdorferi* B313 complemented with DbpAB from *B. afzelii*. Adhesion and elasticity maps were obtained simultaneously with topography.

5 References

- 1 Radolf JD, Deka RK, Anand A, Šmajš D, Norgard MV, Yang XF. *Treponema pallidum*, the syphilis spirochete: making a living as a stealth pathogen. *Nat. Rev. Microbiol.* 14(12), 744–759 (2016).
- 2 Evangelista KV, Coburn J. *Leptospira* as an emerging pathogen: a review of its biology, pathogenesis and host immune responses. *Future Microbiol.* 5(9), 1413–1425 (2010).
- 3 Fraser CM, Casjens S, Huang WM *et al.* Genomic sequence of a Lyme disease spirochaete, *Borrelia burgdorferi*. *Nature* 390(6660), 580–586 (1997).
- 4 Fraser CM, Norris SJ, Weinstock GM *et al.* Complete genome sequence of *Treponema pallidum*, the syphilis spirochete. *Science* 281(5375), 375–388 (1998).
- 5 Bergström S, Normark J. Microbiological features distinguishing Lyme disease and relapsing fever spirochetes. *Wien. Klin. Wochenschr.* 130(15), 484–490 (2018).
- 6 Bierque E, Thibeaux R, Girault D, Soupé-Gilbert M-E, Goarant C. A systematic review of *Leptospira* in water and soil environments. *PLoS ONE* 15(1) (2020).
- 7 Tilly K, Rosa PA, Stewart PE. Biology of Infection with *Borrelia burgdorferi*. *Infect. Dis. Clin. North Am.* 22(2), 217–234 (2008).
- 8 Margos G, Fingerle V, Reynolds S. *Borrelia bavariensis*: Vector Switch, Niche Invasion, and Geographical Spread of a Tick-Borne Bacterial Parasite. *Front. Ecol. Evol.* 7 (2019).
- 9 Strnad M, Hönig V, Růžek D, Grubhoffer L, Rego ROM. Europe-Wide Meta-Analysis of *Borrelia burgdorferi* Sensu Lato Prevalence in Questing *Ixodes ricinus* Ticks. *Appl. Environ. Microbiol.* 83(15) (2017).
- 10 Mannelli A, Bertolotti L, Gern L, Gray J. Ecology of *Borrelia burgdorferi* sensu lato in Europe: transmission dynamics in multi-host systems, influence of molecular processes and effects of climate change. *FEMS Microbiol. Rev.* 36(4), 837–861 (2012).
- 11 Rudenko N, Golovchenko M, Růžek D, Piskunova N, Mallátová N, Grubhoffer L. Molecular detection of *Borrelia bissettii* DNA in serum

- samples from patients in the Czech Republic with suspected borreliosis. *FEMS Microbiol. Lett.* 292(2), 274–281 (2009).
- 12 Collares-Pereira M, Couceiro S, Franca I *et al.* First isolation of *Borrelia lusitaniae* from a human patient. *J. Clin. Microbiol.* 42(3), 1316–1318 (2004).
- 13 Margos G, Sing A, Fingerle V. Published data do not support the notion that *Borrelia valaisiana* is human pathogenic. *Infection* 45(4), 567–569 (2017).
- 14 Stanek G, Wormser GP, Gray J, Strle F. Lyme borreliosis. *Lancet Lond. Engl.* 379(9814), 461–473 (2012).
- 15 Ogrinc K, Wormser GP, Visintainer P *et al.* Pathogenetic implications of the age at time of diagnosis and skin location for acrodermatitis chronica atrophicans. *Ticks Tick-Borne Dis.* 8(2), 266–269 (2017).
- 16 van Dam AP, Kuiper H, Vos K *et al.* Different genospecies of *Borrelia burgdorferi* are associated with distinct clinical manifestations of Lyme borreliosis. *Clin. Infect. Dis. Off. Publ. Infect. Dis. Soc. Am.* 17(4), 708–717 (1993).
- 17 Wormser GP, McKenna D, Carlin J *et al.* Brief communication: hematogenous dissemination in early Lyme disease. *Ann. Intern. Med.* 142(9), 751–755 (2005).
- 18 Steere AC. Posttreatment Lyme disease syndromes: distinct pathogenesis caused by maladaptive host responses. *J. Clin. Invest.* 130(5), 2148–2151 (2020).
- 19 Tjisse-Klasen E, Pandak N, Hengeveld P, Takumi K, Koopmans MP, Sprong H. Ability to cause erythema migrans differs between *Borrelia burgdorferi* sensu lato isolates. *Parasit. Vectors* 6(1), 23 (2013).
- 20 Hyde JA, Weening EH, Chang M *et al.* Bioluminescent imaging of *Borrelia burgdorferi* in vivo demonstrates that the fibronectin-binding protein BBK32 is required for optimal infectivity. *Mol. Microbiol.* 82(1), 99–113 (2011).
- 21 Moriarty TJ, Norman MU, Colarusso P, Bankhead T, Kubes P, Chaconas G. Real-time high resolution 3D imaging of the lyme disease spirochete adhering to and escaping from the vasculature of a living host. *PLoS Pathog.* 4(6), e1000090 (2008).

- 22 Sigal YM, Zhou R, Zhuang X. Visualizing and discovering cellular structures with super-resolution microscopy. *Science* 361(6405), 880–887 (2018).
- 23 Wang ZL, Lee JL. Chapter 9 - Electron Microscopy Techniques for Imaging and Analysis of Nanoparticles. In: *Developments in Surface Contamination and Cleaning (Second Edition)*. Kohli R, Mittal KL (Ed.), William Andrew Publishing, Oxford, 395–443 (2008).
- 24 Loussert C, Forestier C-L, Humbel BM. Correlative light and electron microscopy in parasite research. *Methods Cell Biol.* 111, 59–73 (2012).
- 25 de Boer P, Hoogenboom JP, Giepmans BNG. Correlated light and electron microscopy: ultrastructure lights up! *Nat. Methods* 12(6), 503–513 (2015).
- 26 Wu J, Weening EH, Faske JB, Höök M, Skare JT. Invasion of Eukaryotic Cells by *Borrelia burgdorferi* Requires β 1 Integrins and Src Kinase Activity. *Infect. Immun.* 79(3), 1338–1348 (2011).
- 27 Klempner MS, Noring R, Rogers RA. Invasion of human skin fibroblasts by the Lyme disease spirochete, *Borrelia burgdorferi*. *J. Infect. Dis.* 167(5), 1074–1081 (1993).
- 28 Aberer E, Surtov-Pudar M, Wilfinger D, Deutsch A, Leitinger G, Schaidler H. Co-culture of human fibroblasts and *Borrelia burgdorferi* enhances collagen and growth factor mRNA. *Arch. Dermatol. Res.* 310(2), 117–126 (2018).
- 29 Livengood JA, Gilmore RD. Invasion of human neuronal and glial cells by an infectious strain of *Borrelia burgdorferi*. *Microbes Infect.* 8(14–15), 2832–2840 (2006).
- 30 Chmielewski T, Tylewska-Wierzbanowska S. Interactions between *Borrelia burgdorferi* and mouse fibroblasts. *Pol. J. Microbiol.* 59(3), 157–160 (2010).
- 31 Kim D, Deerinck TJ, Sigal YM, Babcock HP, Ellisman MH, Zhuang X. Correlative Stochastic Optical Reconstruction Microscopy and Electron Microscopy. *PLOS ONE* 10(4), e0124581 (2015).
- 32 Monosov EZ, Wenzel TJ, Lüers GH, Heyman JA, Subramani S. Labeling of peroxisomes with green fluorescent protein in living P.

- pastoris cells. *J. Histochem. Cytochem. Off. J. Histochem. Soc.* 44(6), 581–589 (1996).
- 33 Ellisman MH, Deerinck TJ, Shu X, Sosinsky GE. Picking faces out of a crowd: Genetic labels for identification of proteins in correlated light and electron microscopy imaging. *Methods Cell Biol.* 111, 139–155 (2012).
- 34 Grabenbauer M, Geerts WJC, Fernandez-Rodriguez J, Hoenger A, Koster AJ, Nilsson T. Correlative microscopy and electron tomography of GFP through photooxidation. *Nat. Methods* 2(11), 857–862 (2005).
- 35 Griffin BA, Adams SR, Tsien RY. Specific covalent labeling of recombinant protein molecules inside live cells. *Science* 281(5374), 269–272 (1998).
- 36 Adams SR, Tsien RY. Preparation of the membrane-permeant biarsenicals, FIAsh-EDT2 and ReAsH-EDT2 for fluorescent labeling of tetracysteine-tagged proteins. *Nat. Protoc.* 3(9), 1527–1534 (2008).
- 37 Rudner L, Nydegger S, Coren LV, Nagashima K, Thali M, Ott DE. Dynamic Fluorescent Imaging of Human Immunodeficiency Virus Type 1 Gag in Live Cells by Biarsenical Labeling. *J. Virol.* 79(7), 4055–4065 (2005).
- 38 Hillman C, Stewart PE, Strnad M *et al.* Visualization of Spirochetes by Labeling Membrane Proteins With Fluorescent Biarsenical Dyes. *Front. Cell. Infect. Microbiol.* 9 (2019).
- 39 Lin Y-P, Benoit V, Yang X, Martínez-Herranz R, Pal U, Leong JM. Strain-specific variation of the decorin-binding adhesin DbpA influences the tissue tropism of the lyme disease spirochete. *PLoS Pathog.* 10(7), e1004238 (2014).
- 40 Lin Y-P, Tan X, Caine JA *et al.* Strain-specific joint invasion and colonization by Lyme disease spirochetes is promoted by outer surface protein C. *PLoS Pathog.* 16(5) (2020).
- 41 Salo J, Loimaranta V, Lahdenne P, Viljanen MK, Hytönen J. Decorin binding by DbpA and B of *Borrelia garinii*, *Borrelia afzelii*, and *Borrelia burgdorferi sensu stricto*. *J. Infect. Dis.* 204(1), 65–73 (2011).
- 42 Benoit VM, Fischer JR, Lin Y-P, Parveen N, Leong JM. Allelic Variation of the Lyme Disease Spirochete Adhesin DbpA Influences

- Spirochetal Binding to Decorin, Dermatan Sulfate, and Mammalian Cells ∇ . *Infect. Immun.* 79(9), 3501–3509 (2011).
- 43 Shi Y, Xu Q, McShan K, Liang FT. Both Decorin-Binding Proteins A and B Are Critical for the Overall Virulence of *Borrelia burgdorferi*. *Infect. Immun.* 76(3), 1239–1246 (2008).
- 44 Byram R, Gaultney RA, Floden AM *et al.* *Borrelia burgdorferi* RevA Significantly Affects Pathogenicity and Host Response in the Mouse Model of Lyme Disease. *Infect. Immun.* 83(9), 3675–3683 (2015).
- 45 Cassatt DR, Patel NK, Ulbrandt ND, Hanson MS. DbpA, but not OspA, is expressed by *Borrelia burgdorferi* during spirochetemia and is a target for protective antibodies. *Infect. Immun.* 66(11), 5379–5387 (1998).
- 46 Salo J, Jaatinen A, Söderström M, Viljanen MK, Hytönen J. Decorin Binding Proteins of *Borrelia burgdorferi* Promote Arthritis Development and Joint Specific Post-Treatment DNA Persistence in Mice. *PLOS ONE* 10(3), e0121512 (2015).
- 47 Seshu J, Esteve-Gassent MD, Labandeira-Rey M *et al.* Inactivation of the fibronectin-binding adhesin gene *bbk32* significantly attenuates the infectivity potential of *Borrelia burgdorferi*. *Mol. Microbiol.* 59(5), 1591–1601 (2006).
- 48 Shi Y, Xu Q, McShan K, Liang FT. Both Decorin-Binding Proteins A and B Are Critical for the Overall Virulence of *Borrelia burgdorferi*. *Infect. Immun.* 76(3), 1239–1246 (2008).
- 49 Imai DM, Samuels DS, Feng S, Hodzic E, Olsen K, Barthold SW. The Early Dissemination Defect Attributed to Disruption of Decorin-Binding Proteins Is Abolished in Chronic Murine Lyme Borreliosis. *Infect. Immun.* 81(5), 1663–1673 (2013).
- 50 Weening EH, Parveen N, Trzeciakowski JP, Leong JM, Höök M, Skare JT. *Borrelia burgdorferi* lacking DbpBA exhibits an early survival defect during experimental infection. *Infect. Immun.* 76(12), 5694–5705 (2008).
- 51 Fortune DE, Lin Y-P, Deka RK *et al.* Identification of lysine residues in the *Borrelia burgdorferi* DbpA adhesin required for murine infection. *Infect. Immun.* 82(8), 3186–3198 (2014).

- 52 Brown EL, Wooten RM, Johnson BJ *et al.* Resistance to Lyme disease in decorin-deficient mice. *J. Clin. Invest.* 107(7), 845–852 (2001).
- 53 Strnad M, Oh YJ, Vancová M *et al.* Nanomechanical mechanisms of Lyme disease spirochete motility enhancement in extracellular matrix. *Commun. Biol.* 4(1), 1–9 (2021).
- 54 Milles LF, Schulten K, Gaub HE, Bernardi RC. Molecular mechanism of extreme mechanostability in a pathogen adhesin. *Science* 359(6383), 1527–1533 (2018).
- 55 Yang B, Liu Z, Liu H, Nash MA. Next Generation Methods for Single-Molecule Force Spectroscopy on Polyproteins and Receptor-Ligand Complexes. *Front. Mol. Biosci.* 7 (2020).
- 56 Deniz AA, Mukhopadhyay S, Lemke EA. Single-molecule biophysics: at the interface of biology, physics and chemistry. *J. R. Soc. Interface* 5(18), 15–45 (2008).
- 57 Sapienza PJ, Lee AL. Using NMR to study fast dynamics in proteins: methods and applications. *Curr. Opin. Pharmacol.* 10(6), 723–730 (2010).
- 58 Williamson MP. Using chemical shift perturbation to characterise ligand binding. *Prog. Nucl. Magn. Reson. Spectrosc.* 73, 1–16 (2013).
- 59 Wang X. Solution Structure of Decorin-Binding Protein A from *Borrelia burgdorferi*. *Biochemistry* 51(42), 8353–8362 (2012).
- 60 Morgan AM, Wang X. Structural mechanisms underlying sequence-dependent variations in GAG affinities of decorin binding protein A, a *Borrelia burgdorferi* adhesin. *Biochem. J.* 467(3), 439–451 (2015).
- 61 Feng W, Wang X. Structure of Decorin Binding Protein B from *Borrelia burgdorferi* and Its Interactions with Glycosaminoglycans. *Biochim. Biophys. Acta* 1854(12), 1823–1832 (2015).
- 62 Aquino RS, Lee ES, Park PW. Diverse functions of glycosaminoglycans in infectious diseases. *Prog. Mol. Biol. Transl. Sci.* 93, 373–394 (2010).
- 63 Fischer JR, LeBlanc KT, Leong JM. Fibronectin binding protein BBK32 of the Lyme disease spirochete promotes bacterial attachment to glycosaminoglycans. *Infect. Immun.* 74(1), 435–441 (2006).

- 64 Parveen N, Robbins D, Leong JM. Strain variation in glycosaminoglycan recognition influences cell-type-specific binding by Lyme disease spirochetes. *Infect. Immun.* 67(4), 1743–1749 (1999).
- 65 Strnad M, Rego ROM. The need to unravel the twisted nature of the *Borrelia burgdorferi* sensu lato complex across Europe. *Microbiology* (2020).
- 66 Chaconas G, Moriarty TJ, Skare J, Hyde JA. Live Imaging. *Curr. Issues Mol. Biol.* 42, 385–408 (2021).
- 67 Hanson MS, Cassatt DR, Guo BP *et al.* Active and Passive Immunity against *Borrelia burgdorferi* Decorin Binding Protein A (DbpA) Protects against Infection. *Infect. Immun.* 66(5), 2143–2153 (1998).
- 68 Lemgruber L, Sant’Anna C, Griffiths C *et al.* Nanoscopic Localization of Surface-Exposed Antigens of *Borrelia burgdorferi*. *Microsc. Microanal. Off. J. Microsc. Soc. Am. Microbeam Anal. Soc. Microsc. Soc. Can.* 21(3), 680–688 (2015).
- 69 Rojas ER, Billings G, Odermatt PD *et al.* The outer membrane is an essential load-bearing element in Gram-negative bacteria. *Nature* 559(7715), 617–621 (2018).
- 70 Harman MW, Hamby AE, Boltyanskiy R *et al.* Vancomycin Reduces Cell Wall Stiffness and Slows Swim Speed of the Lyme Disease Bacterium. *Biophys. J.* 112(4), 746–754 (2017).
- 71 Sultan SZ, Manne A, Stewart PE *et al.* Motility Is Crucial for the Infectious Life Cycle of *Borrelia burgdorferi*. *Infect. Immun.* 81(6), 2012–2021 (2013).
- 72 Dufrêne YF, Ando T, Garcia R *et al.* Imaging modes of atomic force microscopy for application in molecular and cell biology. *Nat. Nanotechnol.* 12(4), 295–307 (2017).
- 73 Dupres V, Alsteens D, Andre G, Dufrêne YF. Microbial nanoscopy: a closer look at microbial cell surfaces. *Trends Microbiol.* 18(9), 397–405 (2010).
- 74 Fantner GE, Barbero RJ, Gray DS, Belcher AM. Kinetics of antimicrobial peptide activity measured on individual bacterial cells using high-speed atomic force microscopy. *Nat. Nanotechnol.* 5(4), 280–285 (2010).

- 75 Francius G, Lebeer S, Alsteens D *et al.* Detection, localization, and conformational analysis of single polysaccharide molecules on live bacteria. *ACS Nano* 2(9), 1921–1929 (2008).
- 76 Dufrêne YF. Sticky microbes: forces in microbial cell adhesion. *Trends Microbiol.* 23(6), 376–382 (2015).

6 List of abbreviations

AFM-SMFS	atomic force microscope-based single-molecule force spectroscopy
CLEM	correlative light and electron microscopy
CSP	chemical shift perturbation
DAB	diaminobenzidine
DbpA, DbpB	decorin binding proteins A and B
ECM	extracellular matrix
EM	electron microscopy
FM	fluorescence microscopy
GAG	glycosaminoglycan
GFP	green fluorescent protein
LD	Lyme disease
LM	light microscopy
NMR	nuclear magnetic resonance
PTLDS	post-treatment Lyme disease syndrome
SEM	scanning electron microscopy
TEM	transmission electron microscopy

7 Curriculum vitae

Martin Strnad, MSc.

Institute of Parasitology

Biology Centre CAS, České Budějovice, Czech Republic

ResearcherID: [AAB-1914-2020](https://orcid.org/0000-0001-9141-2020)

e-mail: martin.strnad.cze@gmail.com

Date & Place of Birth: 17.9.1987, České Budějovice, Czech Republic

Education:

2007-2010: Bc., Biological Chemistry program, Faculty of Science, University of South Bohemia, České Budějovice, Czech Republic

2007-2010: BSc., Biological Chemistry program, Faculty of Engineering & Natural Sciences, Johannes Kepler University Linz, Austria

2007-2013: Mgr./MSc., Biological Chemistry program, University of South Bohemia / Johannes Kepler University, České Budějovice/Linz, CZE/AUT

2013-: PhD study, Molecular and Cell Biology and Genetics program, Faculty of Science, University of South Bohemia, České Budějovice, Czech Republic

Employment History:

2013-: Junior Research Scientist, Laboratory of Molecular Ecology of Vectors and Pathogens & Laboratory of Electron Microscopy, Biology Centre CAS, Czech Republic

Research Stays:

2016 (3 months): Laboratory of zoonotic pathogens (PI Patricia Ann Rosa), Rocky Mountain Laboratories - NIAID - National Institutes of Health (MT, USA)

2016 (2 months): Department of Natural Sciences (PI Vivian Kjelland), University of Agder, Norway

Awards:

Diploma (master) thesis was awarded **Dean's prize for Outstanding thesis.**

Winner of the **Czechoslovak Microscopy Society** award (2019-2020) – 2 years stipend (annual award granted to one scientist under 35 years)

Attended Practical Courses (selection):

2013: Advanced Techniques in Electron Microscopy, Prague, Czech Republic

2013: Microscopy Methods in Biomedicine, Prague, Czech Republic

2014: EMBO Practical Course on Correlative light electron microscopy, Bristol, UK

2015: Advanced techniques in fluorescence microscopy, Prague, Czech Republic

2017: Linz Winter School on AFM, Linz, Austria

Research Projects as PI:

2015-2016: GAJU (South Bohemia University grant): Delineating the genetic requirements of the major European Lyme disease spirochete *Borrelia afzelii* for persistence/migration of the bacterium within the tick vector

Recent Scientific Focus:

molecular biology, light and electron microscopy, virulence studies on tick transmitted *Borrelia burgdorferi* s.l

Impacted Publications (12):

Strnad M., Oh Y.J., Vancová M., Hain L., Salo J., Grubhoffer L., Nebesářová J., Hytönen J., Hinterdorfer P., Rego R. O. M. (2021) Nanomechanical mechanisms of Lyme disease spirochete motility enhancement in extracellular matrix. *Communications Biology* 4: 268.

Strnad M., Grubhoffer L., Rego R. O. M. (2020) Novel targets and strategies to combat borreliosis. *Applied Microbiology and Biotechnology* 104 : 1915-1925.

Strnad M., Rego R. O. M. (2020) The need to unravel the twisted nature of the *Borrelia burgdorferi* sensu lato complex across Europe. *Microbiology* 166 : 428–435.

Vancová M., Bílý T., Šimo L., Touš J., Horodyský P., Růžek D., Novobilský A., Salat J., **Strnad M.**, et al. (2020) Three-dimensional reconstruction of the feeding apparatus of the tick *Ixodes ricinus* (Acari: Ixodidae): a new insight into the mechanism of blood-feeding. *Scientific Reports* 10 : 165.

Hillman C., Stewart P.E., **Strnad M.**, Stone H., Starr T., Carmody A., Evans T.J., Carracoi V., Wachter J., Rosa P. (2019) Visualization of spirochetes by labeling membrane proteins with fluorescent biarsenical dyes. *Frontiers in Cellular and Infection Microbiology* 9: 287.

Rego R. O. M., Trentelman J.J., Anguita J., Nijhof A., Sprong H., Klempa B., Hajdušek O., Tomás-Corázar J., Azagi T., **Strnad M.**, et al. (2019) Counterattacking the tick bite: towards a rational design of anti-tick vaccines targeting pathogen transmission. *Parasites & Vectors* 12: 229.

Strnad M., Oh Y., Vancová M., Hinterdorfer P., Grubhoffer L., Rego R. O. M. (2018) Interaction forces between the extracellular matrix

and variants of borellial decorin binding protein A probed by atomic force microscopy. FEBS OPEN BIO, 8 (Suppl.1) p.203.

Vechtova P., Sterbova J., Sterba J., Vancová M., Rego R. O. M., Selinger M, **Strnad M.**, Golovchenko M., Rudenko N., Grubhoffer L. (2018) A bite so sweet: the glycobiology interface of tick-host-pathogen interactions. Parasites & Vectors 11: 594.

Strnad, M., Hönig, V., Růžek, D., Grubhoffer, L., Rego, R. O. M. (2017) Europe-wide meta-analysis of *Borrelia burgdorferi* sensu lato prevalence in questing Ixodes ricinus ticks. Applied and Environmental Microbiology 83: e00609-17.

Vancová, M., Rudenko, N., Vaněček, J., Golovchenko, M., **Strnad, M.**, Rego, R. O. M., Tichá, L., Grubhoffer, L., Nebesářová, J. (2017) Pleomorphism and viability of the Lyme disease pathogen *Borrelia burgdorferi* exposed to physiological stress conditions: a correlative cryo-fluorescence and cryo-scanning electron microscopy study. Frontiers in Microbiology 8: 596.

Strnad, M., Elsterová, J., Schrenková, J., Vancová, M., Rego, R. O. M., Grubhoffer, L., Nebesářová, J. Correlative cryo-fluorescence and cryo-scanning electron microscopy as a straightforward tool to study host-pathogen interactions. Sci. Rep. 5, 18029; doi: 10.1038/srep18029 (2015).

Tonk, M., Cabezas-Cruz, A., Valdés, J. J., Rego, R. O. M., Chrudimská, T., **Strnad, M.**, Šíma, R., Bell-Sakyi, L., Franta, Z., Vilcinskas, A., Grubhoffer, L., Rahnamaeian, M. (2014) Defensins from the tick *Ixodes scapularis* are effective against phytopathogenic fungi and the human bacterial pathogen *Listeria grayi*. Parasit Vectors. 7: 554.

Number of publications in WOS: 12

H-index: 6

Total citations without self-citations: 145